UNIVERSIDADE FEDERAL DE UBERLÂNDIA
INSTITUTO DE CIÊNCIAS BIOMÉDICAS
PROGRAMA DE PÓS-GRADUAÇÃO EM IMUNOLOGIA
E PARASITOLOGIA APLICADAS

MIKAELA DOS SANTOS MARINHO

DESENVOLVIMENTO E VALIDAÇÃO DE CONSTRUÇÕES DO VÍRUS MAYARO COM GENES DE LUCIFERASE COMO FERRAMENTAS PARA ENSAIOS ANTIVIRAIS

UBERLÂNDIA

2024

Mikaela dos Santos Marinho

DESENVOLVIMENTO E VALIDAÇÃO DE CONSTRUÇÕES DO VÍRUS MAYARO COM GENES DE LUCIFERASE COMO FERRAMENTAS PARA ENSAIOS ANTIVIRAIS

Dissertação apresentada ao colegiado do Programa de Pós-Graduação em Imunologia e Parasitologia Aplicadas como requisito parcial para obtenção do título de mestre.

Orientadora: Profa. Dra. Ana Carolina Gomes Jardim

UBERLÂNDIA

Julho – 2024

Dados Internacionais de Catalogação na Publicação (CIP) Sistema de Bibliotecas da UFU, MG, Brasil.

M338d 2024

Marinho, Mikaela dos Santos, 1999-
Desenvolvimento e validação de construções do vírus mayaro com genes de luciferase como ferramentas para ensaios antivirais [recurso eletrônico] / Mikaela dos Santos Marinho. - 2024.

Orientadora: Ana Carolina Gomes Jardim.
Dissertação (Mestrado) - Universidade Federal de Uberlândia, Programa de Pós-graduação em Imunologia e Parasitologia Aplicadas.
Modo de acesso: Internet.
Disponível em: http://doi.org/10.14393/ufu.di.2025.5528
Inclui bibliografia.
Inclui ilustrações.

1. Imunologia. I. Jardim, Ana Carolina Gomes, 1981-, (Orient.). II. Universidade Federal de Uberlândia. Programa de Pós-graduação em Imunologia e Parasitologia Aplicadas. III. Título.

CDU: 612.017

Rejâne Maria da Silva
Bibliotecária-Documentalista – CRB6/1925

UNIVERSIDADE FEDERAL DE UBERLÂNDIA
Coordenação do Programa de Pós-Graduação em Imunologia e Parasitologia Aplicada
Av. Amazonas, s/n, Bloco 4C, Sala 4C218 - Bairro Umuarama, Uberlândia-MG, CEP 38400-902
Telefone: (34) 3225-8672 - www.imunoparasito.ufu.br - coipa@ufu.br

ATA DE DEFESA - PÓS-GRADUAÇÃO

Programa de Pós-Graduação em:	Imunologia e Parasitologia Aplicadas				
Defesa de:	Dissertação de Mestrado Acadêmico nº 300				
Data:	23/08/2024	Hora de início:	13 h e 30 min	Hora de encerramento:	16 h 04 min
Matrícula do Discente:	12222IPA008				
Nome do Discente:	Mikaela dos Santos Marinho				
Título do Trabalho:	“Desenvolvimento e validação de construções do vírus Mayaro com genes de luciferase como ferramentas para ensaios antivirais”				
Área de concentração:	Imunologia e Parasitologia Aplicadas				
Linha de pesquisa:	Biologia das interações entre patógenos e seus hospedeiros e Biotecnologia empregada no diagnóstico e controle de doenças				
Projeto de Pesquisa de vinculação:	Atividade antiviral de compostos naturais, sintéticos e complexos metálicos contra vírus emergentes				

Reuniu-se, em 23 de agosto 2024, ás 13 h e 30 min, por vídeo conferência, a Banca Examinadora designada pelo Colegiado do Programa de Pós-graduação em Imunologia e Parasitologia Aplicadas, assim composta pelos titulares: Presidente: Profa. Dra. Ana Carolina Gomes Jardim - ICBIM/UFU (orientadora da candidata); Profa. Dra. Jaquelline Germano de Oliveira, Instituto René Rachou - Fiocruz Minas; Dr. Rafael Borges Rosa, Fiocruz.

Iniciando os trabalhos o(a) presidente da mesa Profa. Ana Carolina Gomes Jardim, apresentou a Comissão Examinadora e o(a) candidato(a), agradeceu a presença do público, e concedeu ao(à) Discente a palavra para a exposição do seu trabalho. A duração da apresentação do(a) Discente, o tempo de arguição e resposta foram conforme as normas do Programa.

A seguir, o(a) senhor(a) presidente concedeu a palavra, pela ordem sucessivamente, aos(às) examinadores(as), que passaram a arguir o(a) candidato(a). Ultimada a arguição, que se desenvolveu dentro dos termos regimentais, a Banca, em sessão secreta, atribuiu o resultado final, considerando o(a) candidato(a):

APROVADA

Esta defesa faz parte dos requisitos necessários à obtenção do título de Mestre. O competente diploma será expedido após cumprimento dos demais requisitos, conforme as normas do Programa, a legislação pertinente e a regulamentação interna da UFU.

Nada mais havendo a tratar foram encerrados os trabalhos. Foi lavrada a presente ata, que após lida e achada conforme, foi assinada pela Banca Examinadora.

Documento assinado eletronicamente por **Ana Carolina Gomes Jardim**, **Professor(a) do Magistério Superior**, em 23/08/2024, às 16:04, conforme horário oficial de Brasília, com fundamento no art. 6º, § 1º, do Decreto nº 8.539, de 8 de outubro de 2015.

Documento assinado eletronicamente por **Rafael Borges Rosa**, **Usuário Externo**, em 23/08/2024, às 16:05, conforme horário oficial de Brasília, com fundamento no art. 6º, § 1º, do Decreto nº 8.539, de 8 de outubro de 2015.

Documento assinado eletronicamente por **Jaquelline Germano de Oliveira**, **Usuário Externo**, em 26/08/2024, às 13:52, conforme horário oficial de Brasília, com fundamento no art. 6º, § 1º, do Decreto nº 8.539, de 8 de outubro de 2015.

A autenticidade deste documento pode ser conferida no site https://www.sei.ufu.br/sei/controlador_externo.php?acao=documento_conferir&id_orgao_acesso_externo=0, informando o código verificador **5616490** e o código CRC **261E117F**.

Referência: Processo nº 23117.051057/2024-41 SEI nº 5616490

AGRADECIMENTOS

Agradeço primeiramente à minha orientadora, Prof. Dra. Ana Carolina Gomes Jardim, por todos os ensinamentos, pela confiança no meu potencial e por sempre me impulsionar a alcançar meus objetivos.

Além disso, agradeço também à Natasha Cassani, sempre presente no dia a dia do laboratório, ensinando com todo carinho e paciência do mundo, além da assistência com inúmeros ensaios realizados neste trabalho.

Também sou muito grata pela minha "parceira" de mestrado, Shiraz Leite, que sempre foi uma excelente amiga nos melhores e piores dias. Gratidão também por minhas queridas amigas e companheiras de congresso Giulia, Victória, Natasha, Shiraz e Júlia, que são excelentes companhias para todas as horas.

Muita gratidão também às brilhantes alunas de IC e também aos meninos do lab, Igor e Dani, que me ensinaram muito sobre ciência e sobre a vida.

Muita gratidão também pelo meu pai e minha mãe, que vêm apoiando toda minha jornada acadêmica desde a infância. Tudo é graças à determinação, coragem e esforço de vocês para que eu pudesse alcançar sonhos cada vez maiores.

Por fim, agradeço meu marido Victor Hugo, a pessoa mais forte que conheço. Muito obrigada por sempre me apoiar, sem hesitação, mesmo sabendo que não seria fácil.

"A vida não é fácil para nenhum de nós. Temos que ter persistência e, acima de tudo, confiança em nós mesmos."

Marie Curie

LISTA DE ABREVIATURAS E SIGLAS

6K	*6K transmembrane protein/viroporin*, Proteína transmembrana 6K/ viroporina
C	Proteína de Capsídeo
CC_{50}	Concentração citotóxica em 50%
cDNA	*Complementary deoxyribonucleic acid*, Ácido desoxirribonucleico complementar
CHIKV	Vírus da chikungunya
CMV	Citomegalovírus
DNA	*Deoxyribonucleic acid*, Ácido desoxirribonucleico
E1	*Envelope glycoprotein 1*, Glicoproteína de envelope 1
E2	*Envelope glycoprotein 2,* Glicoproteína de envelope 2
E3	*Envelope glycoprotein 3,* Glicoproteína de envelope 3
EC_{50}	Concentração efetiva de 50%
eGFP	*Enhanced green fluorescent protein*, Proteína verde fluorescente melhorada
EIDD-2749	*Emory Institute for Drug Development 2749: 4'-Fluorouridine,* Instituto Emory para desenvolvimento de fármacos 2749: 4'-Fluorouridina
ELISA	*Enzyme Linked Immuno Sorbent Assay*, Imunoensaio enzimático
GO	Estado de Goiás
HTS	*High Throughput Screening,* Triagem de Alto Rendimento
IFA	*Indirect immunofluorescence assay*, Ensaio de imunofluorescência indireta (IFA)
IFIT	*Interferon induced protein with tetratricopeptide repeats*, Interferon com repetições de tetratricopeptídeo
IS	Índice de seletividade
Kb	Kilobases
kDa	Kilodalton
M2	Proteína de membrana 2
MAYV	Vírus Mayaro
MAYV $E2^{nLuc}$	Vírus Mayaro expressando a proteína *nanoluciferase*, com inserção do gene *nanoluciferase* na proteína E2

MAYV eGFP	Vírus Mayaro expressando eGFP
MAYV-*firefly*	Vírus Mayaro expressando a proteína *firefly luciferase*
MAYV-*nanoluc*	Vírus Mayaro expressando a proteína *nanoluciferase*
MT	Estado do Mato Grosso
MXRA8	*Matrix Remodeling Associated 8,* Proteína de remodelação da matriz associada 8
PCR	*Polymerase chain reaction*, Reação da polimerase em cadeia
pE2	Proteína precursora de E2 e E3
nsP1	*Nonstructural protein 1*, Proteína não estrutural 1
nsP2	*Nonstructural protein 2*, Proteína não estrutural 2
nsP2pro	Protease de cisteína contida em nsP2
nsP3	*Nonstructural protein 3,* Proteína não estrutural 3
nsP4	*Nonstructural protein 4,* Proteína não estrutural 4
ORF	*Open reading frame*, Região aberta de leitura
RNA	*Ribonucleic acid*, Ácido ribonucleico
RtdH	Hidrocloreto de rimantadina
SARS-CoV-2	Coronavírus da síndrome respiratória aguda grave 2
SP6	*SP6 RNA Polymerase*, RNA Polimerase do bacteriófago SP6
ssRNA+	*Simple strand positive sense ribonucleic acid*, Ácido ribonucleico de fita simples polaridade positiva
T7	T7 *RNA Polymerase*, RNA Polimerase do bacteriófago T7
TF	Proteína *Transframe*
UTR	*Untranslated region,* Região não codificante
VLP	*Virus Like Particles*, partículas semelhantes a vírus

LISTA DE FIGURAS

RESUMO

O vírus Mayaro (MAYV), um arbovírus do gênero *Alphavirus* e da família *Togaviridae*, é o agente etiológico da febre Mayaro. Endêmico nas Américas do Sul e Central, é mantido em reservatórios animais dentro de um ciclo silvestre. No entanto, o vírus tem alta adaptabilidade a novos hospedeiros e vetores, podendo estabelecer um ciclo urbano. A febre Mayaro apresenta sintomas similares aos de outras arboviroses, podendo resultar em poliartrite e poliartralgia de longa duração. Atualmente, não há vacina ou tratamento antiviral licenciados contra o MAYV, o que contribui para a disseminação da doença. Nesse sentido, o objetivo deste trabalho foi desenvolver construções virais para uso em pesquisa de antivirais de alto desempenho. Os plasmídeos foram produzidos a partir de genética reversa, com base na cepa MAYV BeAr 20290, contendo promotor de citomegalovírus humano e genes repórteres *nanoluciferase* (CMV-MAYV-*nanoluc*) e *firefly luciferase* (CMV-MAYV-*firefly*). Os genes de luminescência foram inseridos no genoma viral, entre o final da nsP4 e o terminal 5' dos genes estruturais. Subsequentemente, esse segmento do genoma viral foi combinado com um promotor CMV obtido por meio de reação em cadeia da polimerase (PCR). Após sequenciamento, os plasmídeos foram amplificados através do uso de bactérias DH5-α competentes. Posteriormente, CMV-MAYV-*nanoluc* e CMV-MAYV-*firefly* foram transfectados em células Vero E6, resultando na geração de partículas infecciosas de MAYV-*nanoluc* e MAYV-*firefly*, respectivamente. Os vírus replicaram eficientemente com propriedades semelhantes ao MAYV selvagem parental e a expressão dos genes repórteres refletiu as taxas de replicação viral. Além disso, empregando MAYV-*nanoluc,* analisamos o potencial de reposicionamento do hidrocloreto de rimantadina (rtdH), fármaco licenciado para o tratamento de Influenza, como um agente anti-MAYV. O fármaco inibiu MAYV com um SI de 2.3, apresentando também atividade contra o vírus Zika (ZIKV), com um SI de 2.4. Adicionalmente, o composto EIDD-2749, descrito como inibidor de RNA polimerase dependente de RNA com potente ação antiviral contra alfavírus, foi utilizado para validar o MAYV-*nanoluc* com ferramenta para ensaios antivirais, demonstrando um SI de 1.8×10^7. Nossos dados demonstraram que o clone MAYV-*nanoluc* é uma ferramenta aplicável para ensaios antivirais, otimizando a triagem de novos agentes anti-MAYV. Adicionalmente, rtdH apresentou atividade de amplo espectro antiviral contra MAYV e ZIKV.

Palavras-chave: Vírus Mayaro; Vírus repórter; Antiviral; Hidrocloreto de rimantadina.

ABSTRACT

The Mayaro virus (MAYV), an arbovirus from the *Alphavirus* genus and *Togaviridae* family, is the etiologic agent of Mayaro fever. Endemic in South and Central Americas, it is maintained in animal reservoirs within a sylvatic cycle. However, the virus exhibits high adaptability to new hosts and vectors, establishing an urban cycle. Mayaro fever presents symptoms similar to other arboviruses, potentially resulting in long-term polyarthritis and polyarthralgia. Currently, there is no licensed vaccine or antiviral treatment against MAYV, which contributes to virus dissemination. In this context, this work aimed to develop viral constructs for use in high-throughput antiviral research. The plasmids were produced by reverse genetics, based on the MAYV BeAr 20290 strain, containing human cytomegalovirus promoter and *nanoluciferase* (CMV-MAYV-*nanoluc*) and *firefly luciferase* (CMV-MAYV-*firefly*) reporter genes. The luminescence genes were inserted into the viral genome between the end of nsP4 and the 5' terminus of the structural genes. Subsequently, this viral genome segment was combined with a CMV promoter obtained through polymerase chain reaction (PCR). After sequencing, the plasmids were amplified using competent DH5-α bacteria. Subsequently, CMV-MAYV-*nanoluc* and CMV-MAYV-*firefly* were transfected into Vero E6 cells, generating infectious MAYV-*nanoluc* and MAYV-*firefly* particles, respectively. The viruses replicated efficiently with properties similar to the parental wild-type MAYV, and the expression of the reporter genes reflected viral replication rates. Additionally, using MAYV-*nanoluc*, we analyzed the repositioning potential of rimantadine hydrochloride (rtdH), licensed drug for the treatment of Influenza, as an anti-MAYV agent. The drug inhibited MAYV with an SI of 2.3 and also showed activity against Zika virus (ZIKV) with an SI of 2.4. Additionally, the compound EIDD-2749, described as an inhibitor of RNA-dependent RNA polymerase with potent antiviral activity against alphavirus, was used to validate the MAYV-*nanoluc* tool for antiviral trials, with an SI of 1.8×10^7. Our data demonstrated that the MAYV-*nanoluc* clone is a valuable tool for antiviral assays, enhancing the screening of new anti-MAYV agents. Furthermore, rtdH showed a broad-spectrum antiviral activity against MAYV and ZIKV.

Keywords: Mayaro virus, Reporter virus, Antiviral, Rimantadine hydrochloride.

SUMÁRIO

CAPÍTULO I

Fundamentação Teórica

INTRODUÇÃO

Histórico, epidemiologia e genótipos virais

O vírus Mayaro (MAYV) é um arbovírus pertencente ao gênero *Alphavirus e* família *Togaviridae,* sendo agente etiológico da febre Mayaro (DIAGNE et al., 2020). Devido ao seu caráter enzoótico é mantido de forma estável em reservatórios animais, associado a um ciclo silvestre (MACKAY; ARDEN, 2016). Foi identificado primeiramente em 1954 no distrito de Mayaro, em Trinidad e Tobago (**Figura 1**), no soro de quatro trabalhadores florestais que apresentavam uma doença febril (ANDERSON et al., 1957). Além disso, no mesmo período e região, um quinto caso foi identificado em uma residente da área urbana (ANDERSON et al., 1957). Entretanto, um estudo retrospectivo sugere a circulação anterior do patógeno a partir de isolados de MAYV encontrados em soros coletados durante a construção de canais no Panamá e na Colômbia ocorrida entre 1904 e 1914 (ACOSTA-AMPUDIA et al., 2018).

Figura 1: Casos de MAYV no mundo. O vírus é endêmico no Brasil e em alguns países das Américas do Sul e Central, tendo sido descritos casos importados nos EUA e Europa.

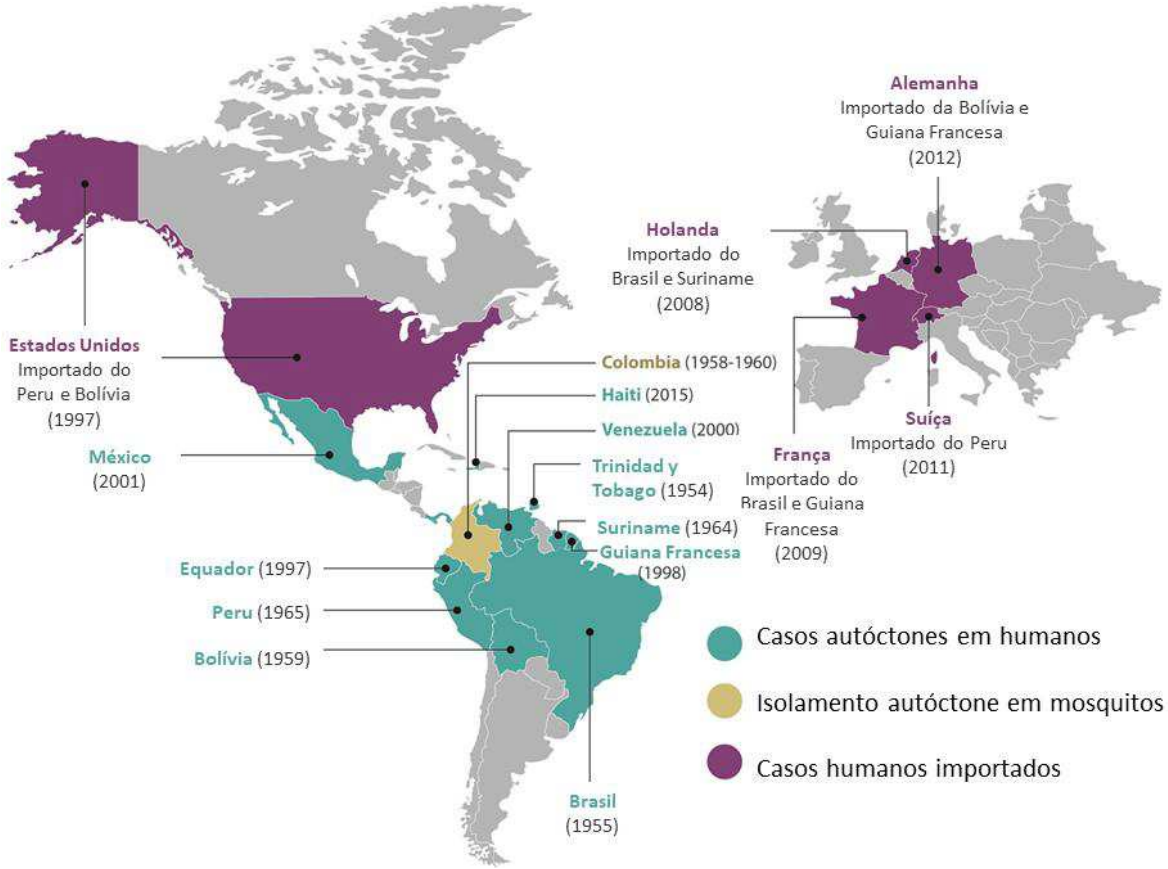

Adaptado de *Mayaro: an emerging viral threat.* | Acosta-Ampudia et al., 2018.

Nos anos seguintes aos primeiros relatos de casos de infecção por MAYV, diversas epidemias e surtos foram identificados em países da América do Sul e Central (**Figura 1**), majoritariamente a partir de transbordamentos do ciclo silvestre (MACKAY; ARDEN, 2016). Atualmente, os casos da Febre Mayaro em humanos são concentrados na região da bacia Amazônica, incluindo Brasil, Bolívia, Equador, Guiana Francesa, Haiti, México, Panamá, Peru e Venezuela, principalmente em regiões próximas a áreas florestais (GANJIAN; RIVIERE-CINNAMOND, 2020). Além disso, também há relatos de casos importados da infecção por MAYV na América do Norte e Europa (**Figura 1**), reportados em indivíduos que foram infectados em regiões que possuíam circulação do vírus (GONZALEZ-ESCOBAR et al., 2021). A primeira identificação da febre do Mayaro no Brasil ocorreu em 1955, em regiões próximas ao rio Guamáia estado do Pará, tendo causado um surto da doença na região (ESPOSITO; FONSECA, 2017). Posteriormente, foram observados diversos surtos nos estados do Pará (1978,1981, 1991, 2008), Tocantins (1991 e 2008), Amazonas (2007 e 2008), Mato Grosso (2000, 2011-2012, 2015-2016) e Goiás (2014-2016) (PEZZI et al., 2019). No Brasil, o MAYV é considerado endêmico na região Amazônica, entre os estados da região Norte e Centro-Oeste, em áreas de mata, rural ou silvestre (ACOSTA-AMPUDIA et al., 2018). Neste sentido, a vigilância epidemiológica do vírus é direcionada a indivíduos sintomáticos que tenham adentrado áreas silvestres, rurais ou de mata, em um período de 15 dias, em todo o território nacional (BRASIL, 2024). A detecção do MAYV é de notificação compulsória imediata, sendo realizada através da detecção do genoma viral e/ou anticorpos contra o vírus (BRASIL, 2024). Entretanto, foram relatados casos da febre do Mayaro e isolamento do agente etiológico fora da área endêmica, nas áreas urbanas do estado de Goiás (DE CURCIO et al., 2022). Até o momento, não há dados epidemiológicos do Ministério da Saúde que contenham informações atualizadas sobre o grau de disseminação de MAYV no Brasil (BRASIL, 2024).

O vírus Mayaro apresenta três genótipos distintos, com diferentes padrões de disseminação e divergência de nucleotídeos entre eles de aproximadamente 17% (PEZZI et al., 2019). O genótipo D (disseminado) foi isolado pela primeira vez em 1954 em Trinidad e Tobago e atualmente é amplamente distribuído na América do Sul, sendo o genótipo predominante de MAYV (ANDERSON et al., 1957). O genótipo L (limitado), identificado em 1955 no Brasil, circulou exclusivamente no país até 2014, quando foi detectado no Haiti, tendo sua distribuição restringida ao norte do Brasil e Haiti (BLOHM et al., 2019; WHITE et al., 2018). O genótipo N (novo), considerado novo, foi isolado a partir de uma única amostra no Peru em 2010, e atualmente não há informações sobre seu grau de disseminação (AUGUSTE et al., 2015) (**Figura 2**). Além disso, foram identificados híbridos heterólogos entre os genótipos L e D e

um híbrido homólogo entre isolados do genótipo D, indicando a circulação de diferentes linhagens do vírus nas mesmas regiões (MARINHO et al., 2024; MAVIAN et al., 2017; WHITE et al., 2018) (**Figura 2**). Estudos *in silico* indicam alta pressão evolutiva no genoma do vírus que, assim como a recombinação genética, atua como mecanismo de evolução para os vírus de RNA e favorece o surgimento de novas linhagens do patógeno (MARINHO et al., 2024; MAVIAN et al., 2017).

Figura 2: Árvore filogenética de máxima verossimilhança reconstruída a partir de sequências de genoma completo de MAYV de amostras coletadas nas Américas. O vírus é classificado em genótipos D (distribuído), L (limitado) e N (novo), apresentando híbridos heterólogos entre os genótipos L e D.

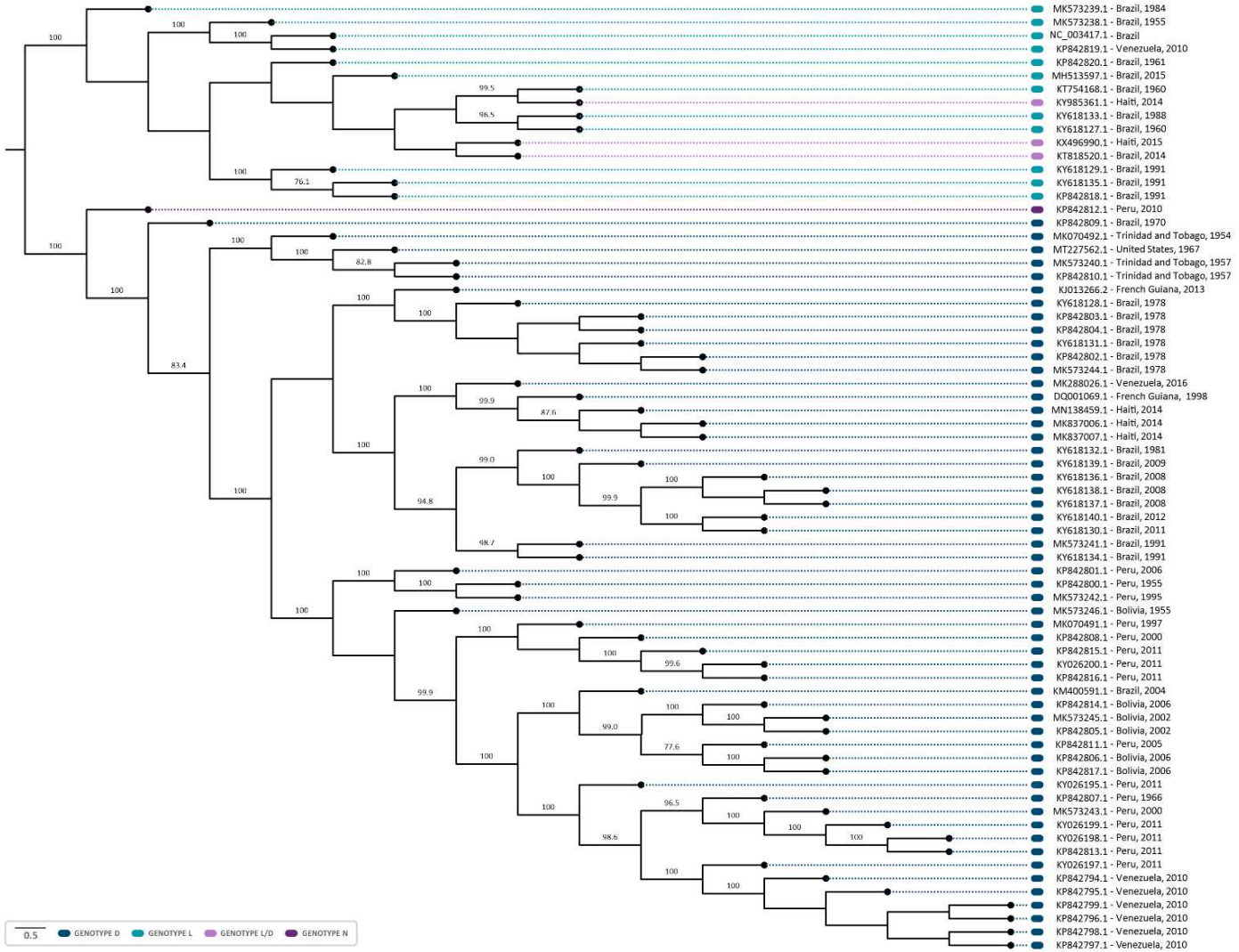

Fonte: *Evolutionary Profile of Mayaro Virus in the Americas: An Update into Genome Variability*. | Marinho et al., 2024.

Partícula viral e ciclo replicativo

O MAYV pertence ao complexo de vírus da floresta de Semliki (BENGUE et al., 2021), que consiste em alfavírus com alta similaridade filogenética e antigênica, associados a doenças febris e articulares em humanos, incluindo os vírus Chikungunya (CHIKV), Sindbis, o'nyong-nyong e Ross river (DIAGNE et al., 2020). O vírion é composto por um RNA de fita simples polaridade positiva (ssRNA+) de aproximadamente 11,5 kb, envolvido pela proteína de capsídeo e por um envelope de membrana lipídica, onde estão inseridas as glicoproteínas E1 e E2 (DIAGNE et al., 2020) (**Figuras 3A e 3B**).

Figura 3: Estrutura do vírion de MAYV e organização genômica do vírus. A partícula viral é constituída a partir das proteínas de capsídeo, trímero E1-E2, membrana lipídica e ssRNA+ (A, B). O genoma viral codifica as proteínas não estruturais (nsP1-nsP4) e estruturais do vírus, além de possuir as regiões 5´ e 3´ UTR (C).

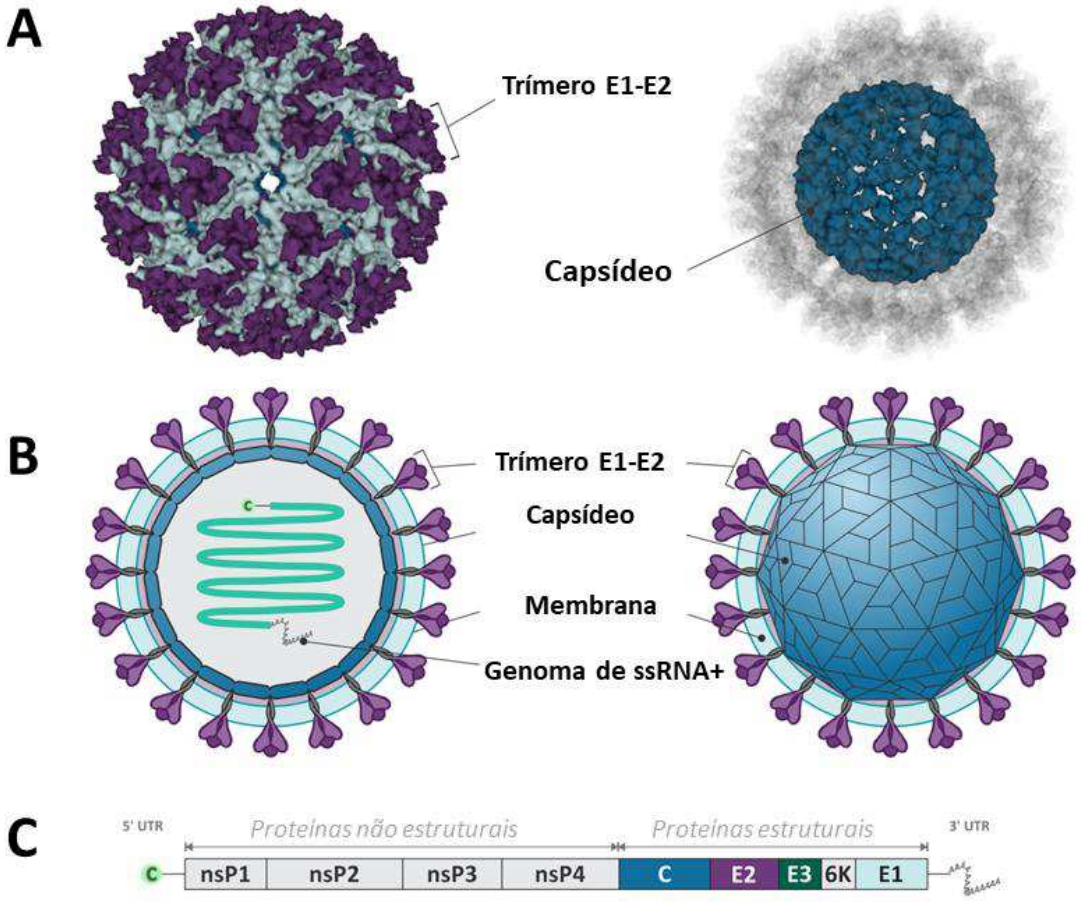

Adaptado de *Evolutionary Profile of Mayaro Virus in the Americas: An Update into Genome Variability*. | Marinho et al., 2024.

O genoma viral é constituído por duas regiões de leitura aberta (*open Reading frames,* ORFs), sendo a primeira responsável por codificar as proteínas não estruturais (nsP1, nsP2, nsP3 e nsP4), e a segunda por codificar as proteínas estruturais (C, E3, E2, TF/ 6K, E1) (LI et

al., 2019; SNYDER et al., 2013). Adicionalmente, assim como outros vírus de RNA, o genoma também apresenta regiões não codificantes (*untranslated regions*, UTR), localizadas nas extremidades 5' e 3' do genoma, que são denominadas como 5'UTR e 3'UTR, respectivamente (LELLO et al., 2021) (**Figura 3C**). Os elementos estruturais localizados na região 5'UTR de alfavírus patogênicos alteram a ligação e o funcionamento de proteínas induzidas por interferon com repetições de tetratricopeptídeo (IFIT), um fator inibitório para a tradução do RNA viral, o que favorece a replicação viral e evasão do sistema imune (LELLO et al., 2021). Além disso, a região 3'UTR tem um papel importante na replicação viral e adaptação a novos transmissores e hospedeiros (CARRASCO; SANZ; GONZÁLEZ-ALMELA, 2018).

O ciclo replicativo do MAYV inicia-se a partir da fusão do envelope viral com a membrana plasmática das células-alvo, mediada pela interação do trímero de glicoproteínas E1-E2 com receptores específicos na superfície celular, como a proteína de remodelação da matriz associada 8 (*Matrix Remodeling Associated 8,* MXRA8), conhecida por ser um receptor de vários alfavírus artritogênicos (ZHANG et al., 2019). Posteriormente, o vírus entra na célula através da endocitose mediada por receptor, associada com a formação de cavidades revestidas por clatrina ou, alternativamente, por caveolina (CARVALHO et al., 2017). Após a endocitose, ocorre a acidificação do pH no interior dos endossomos, que resulta em mudanças conformacionais no envelope viral, resultando na fusão deste com a membrana endossomal e na liberação do RNA no citoplasma (MOTA et al., 2015). O RNA genômico é então traduzido em uma poliproteína precursora a partir da ORF 1, que inclui as proteínas não estruturais nsP1, nsP2, nsP3 e nsP4. A protease de cisteína contida em nsP2 (nsP2pro), cliva a poliproteína em suas proteínas constituintes (LELLO et al., 2021). As proteínas não estruturais liberadas se associam e formam o complexo replicativo viral, essencial para a replicação do RNA viral (DIAGNE et al., 2020). Este complexo sintetiza um RNA de fita simples polaridade negativa intermediário, e o utiliza como molde para a produção de RNA genômico e subgenômico (ACOSTA-AMPUDIA et al., 2018). A partir do RNA subgenômico, a ORF 2 é traduzida em uma poliproteína, clivada por uma serina protease auto-proteolítica, codificada na proteína C, resultando na liberação da proteína C e uma poliproteína contendo E1, 6K (viroporina) e pE2 (precursora de E2 e E3) (DIAGNE et al., 2020). Além disso, durante a tradução do gene 6K, ocorre um evento de *frameshift* que resulta na produção da proteína *Transframe* (TF), associada à montagem e liberação dos alfavírus (FIRTH et al., 2008; SNYDER et al., 2013). A poliproteína contendo pE2, 6K e E1 é processada no retículo endoplasmático por uma peptidase de sinal do hospedeiro, liberando suas proteínas constituintes (KIM; DIAMOND, 2023). Posteriormente, pE2 e E1 formam heterodímeros iniciais, que se organizam em trímeros durante

o tráfego para a membrana plasmática (SNYDER et al., 2013). Durante a maturação das glicoproteínas, pE2 é clivada por uma protease semelhante à furina, resultando nasgu proteínas E2 e E3, sendo esta última liberada (KIM; DIAMOND, 2023). A partir do empacotamento do RNA genômico e montagem do nucleocapsídeo, ocorre a formação dos novos vírions na membrana plasmática, onde são encontradas glicoproteínas virais maduras, levando à liberação das partículas virais por brotamento (DIAGNE et al., 2020). As partículas liberadas então infectam novas células, dando continuidade ao ciclo (**Figura 4**).

Figura 4: Representação gráfica do ciclo replicativo do MAYV.

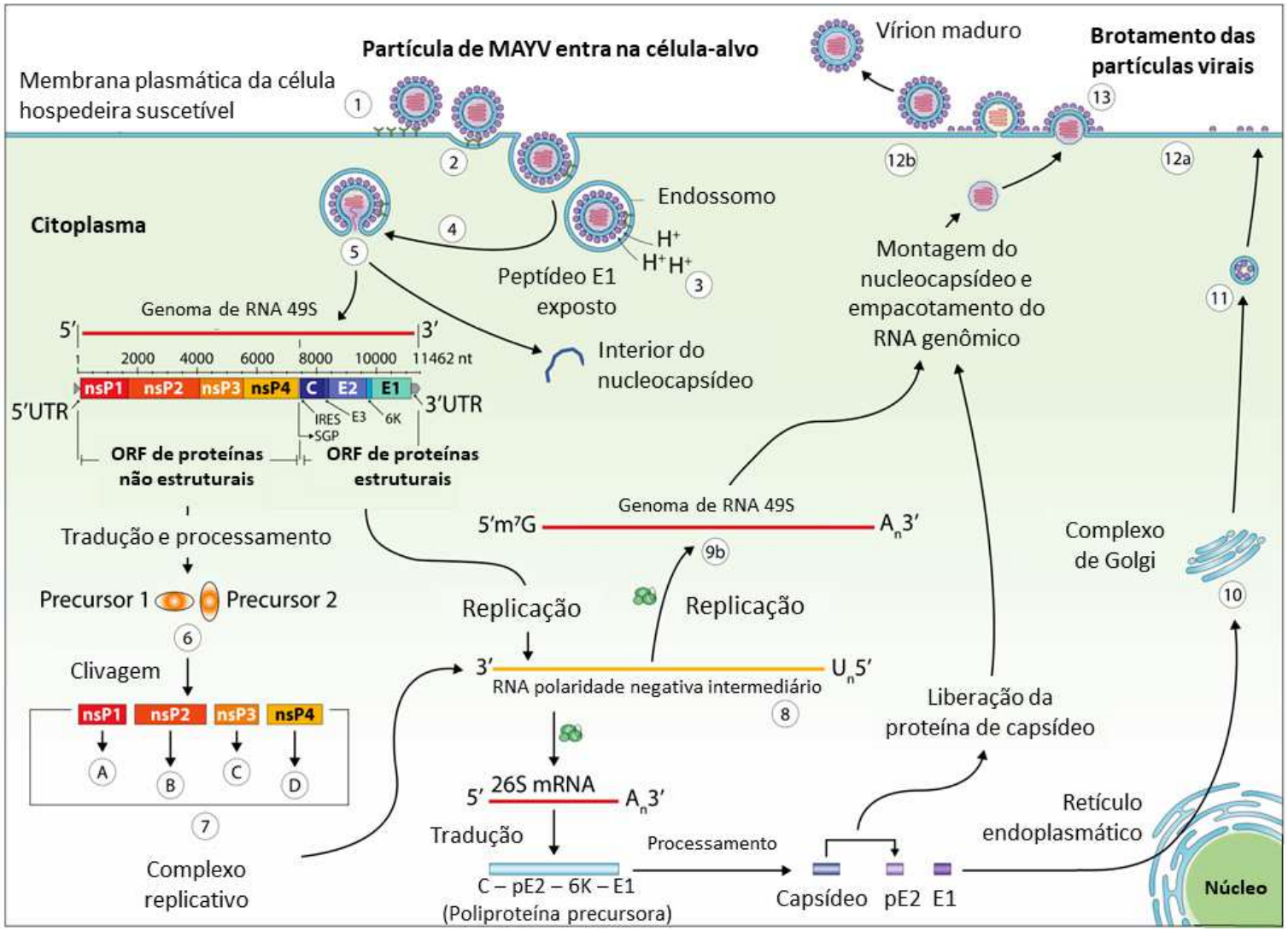

Adaptado a partir de *Mayaro virus Pathogenisis and Transmission Mechanisms.* | Diagne et al., 2020

As proteínas virais desempenham papéis cruciais em todas as etapas do ciclo replicativo do MAYV. A proteína nsP1 atua na síntese do RNA viral como guanililtransferase e metiltransferase, favorecendo a formação da estrutura de cap 5' no RNA genômico e subgenômico, essencial para a replicação e transcrição do RNA (RUPP et al., 2015). A nsP2 apresenta atividades de helicase, protease e trifosfatase, sendo fundamental para a clivagem e processamento das poliproteínas não estruturais (RUPP et al., 2015). Adicionalmente, a proteína também atua na regulação da resposta imune, através do desligamento transcricional e translacional do hospedeiro e inibição de respostas antivirais mediadas por interferon (WARRIER et al., 2008). De maneira similar, a nsP3 modula a resposta imune do hospedeiro e interage com fatores celulares para facilitar a replicação viral, sendo essencial para a formação do complexo replicativo (RUPP et al., 2015). A nsP4 funciona como RNA polimerase dependente de RNA (RdRp), sendo responsável pela síntese de RNA de fita negativa complementar ao genoma viral, do RNA genômico por meio de um RNA de fita negativa e transcrição do RNA subgenômico (WARRIER et al., 2008).

Alternativamente, as proteínas estruturais do MAYV atuam diretamente na estrutura dos vírions. A proteína C forma o capsídeo, que envolve o RNA genômico, além de atuar de maneira autocatalítica na sua clivagem a partir da poliproteína estrutural (WARRIER et al., 2008). As proteínas E1 e E2, consideradas fatores de infectividade e tropismo do vírus, medeiam a fusão do envelope viral com a membrana da célula hospedeira e permitem a liberação do genoma viral no interior da célula (ACOSTA-AMPUDIA et al., 2018). Neste sentido, E1 facilita a fusão de membranas ao interagir com membranas alvo por meio de um peptídeo de fusão hidrofóbico, enquanto E2 auxilia no dobramento e transporte de E1, além de se ligar ao receptor na membrana plasmática (KIM; DIAMOND, 2023). A proteína E3, removida durante a maturação viral, atua como chaperona no dobramento de outras proteínas estruturais e previne mudanças conformacionais prematuras do heterodímero E2–E1 durante o trânsito através do ambiente ácido da via secretora (KIM; DIAMOND, 2023). A proteína 6K está associada à montagem e brotamento do vírion e está envolvida na permeabilização da membrana do hospedeiro através da formação de canais iônicos (MELTON et al., 2002). A proteína TF, produzida a partir de um evento de *frameshift*, contribui para a eficiência na montagem e liberação das partículas virais infecciosas (FIRTH et al., 2008; SNYDER et al., 2013) .

Febre do Mayaro

Após a inoculação subcutânea pela picada de mosquitos, os alfavírus se disseminam no hospedeiro através dos vasos linfáticos e da microvasculatura, sendo transportados como

vírions livres ou em monócitos infectados até os órgãos-alvo (DIAGNE et al., 2020). A replicação viral inicial ocorre principalmente no fígado e no baço, com posterior disseminação para ossos, músculos e tecidos articulares, desencadeando a fase aguda da doença, que está associada ao processo inflamatório local (WEBER et al., 2023) (**Figura 5**).

Figura 5: Representação gráfica da sintomatologia da febre do Mayaro.

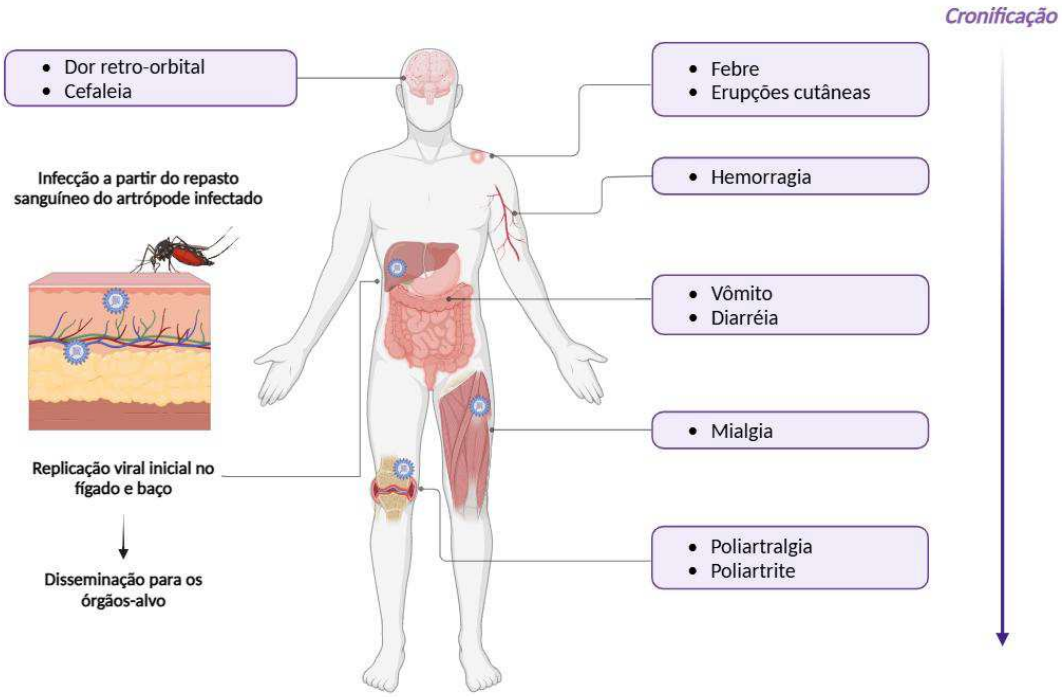

Fonte: BioRender | Marinho, M. d. S. (2025).

Neste sentido, o MAYV pode desencadear a febre do Mayaro em hospedeiro humano, doença caracterizada por sintomas similares aos de outras arboviroses, que se tornam mais evidentes após o período de incubação de cerca de 7 dias (ACOSTA-AMPUDIA et al., 2018). A sintomatologia da doença é moderada na maioria dos infectados, incluindo febre, cefaleia, dor retro-orbital, distúrbios gastrointestinais, mialgia, erupções cutâneas e artralgia (DIOP et al., 2019). Além disso, a infecção pode se tornar crônica, resultando em poliartrite e poliartralgia de longa duração (GONZALEZ-ESCOBAR et al., 2021). Em alguns casos são observadas complicações graves em decorrência da doença, como hemorragia, danos neurológicos, miocardite e, em situações mais raras, óbito (DIAGNE et al., 2020) (**Figura 5**).

Ciclos de transmissão

O principal vetor transmissor de MAYV são mosquitos do gênero *Haemagogus*, que participam de um ciclo de transmissão enzoótico, tendo primatas não humanos como

hospedeiros primários (GANJIAN; RIVIERE-CINNAMOND, 2020). Entretanto, devido à alta capacidade evolutiva do patógeno, outras espécies também atuam como hospedeiros e amplificadores do vírus, dentre elas, roedores, aves, répteis escamosos e outros animais (CELONE et al., 2021). Assim, no ciclo silvestre, os humanos são infectados quando estão dentro ou nas proximidades de áreas rurais ou florestais, sendo caracterizados como hospedeiros acidentais (MACKAY; ARDEN, 2016) (**Figura 6**).

Contudo, estudos indicam adaptabilidade do MAYV a novos possíveis vetores, tendo sido isolado em artrópodes dos gêneros *Culex, Mansonia, Aedes, Psorophora e Sabethes* (GANJIAN; RIVIERE-CINNAMOND, 2020). Adicionalmente, os mosquitos *Aedes albopictus* e *Aedes aegypti*, amplamente distribuídos mundialmente, também demonstraram susceptibilidade e competência vetorial para a transmissão de MAYV (DIOP et al., 2019; MAIA et al., 2019) (**Figura 6**). Estudos recentes demonstraram detecção de MAYV em larvas e mosquitos da espécie *Aedes aegypti* em Goiânia – GO, e de *A. aegypti* e *A. albopictus* em Cuiabá – MT (DE CURCIO et al., 2022; MAIA et al., 2019). Adicionalmente, foi observada a ocorrência de transmissão vertical do vírus nestas espécies de vetor, o que favorece a persistência do vírus na ausência de hospedeiros vertebrados suscetíveis (DE CURCIO et al., 2022; MAIA et al., 2019). Como fator agravante, estudos *in vivo* sugerem que *Aedes aegypti* apresenta capacidade de realizar o ciclo de transmissão completo de MAYV, apresentando acima de 60% de competência para a disseminação do patógeno entre os dias 3 e 14 da infecção em roedores (KROKOVSKY, et al., 2023). A partir de *A. aegypti* e *A. albopictus*, o vírus pode estabelecer um ciclo urbano, tendo os humanos como principal hospedeiro. Embora não existam dados sobre a transmissão de MAYV de humano para humano (por via sexual, vertical ou fluidos corporais), há um relato de infecção acidental por aerossóis do vírus em ambiente laboratorial, sem a participação de um agente transmissor (DIAGNE et al., 2020; JUNT et al., 1999).

Figura 6: Ciclos de transmissão do MAYV. O vírus apresenta dois tipos de ciclo: o silvestre ou rural e o ciclo urbano, possuindo variados hospedeiros e vetores.

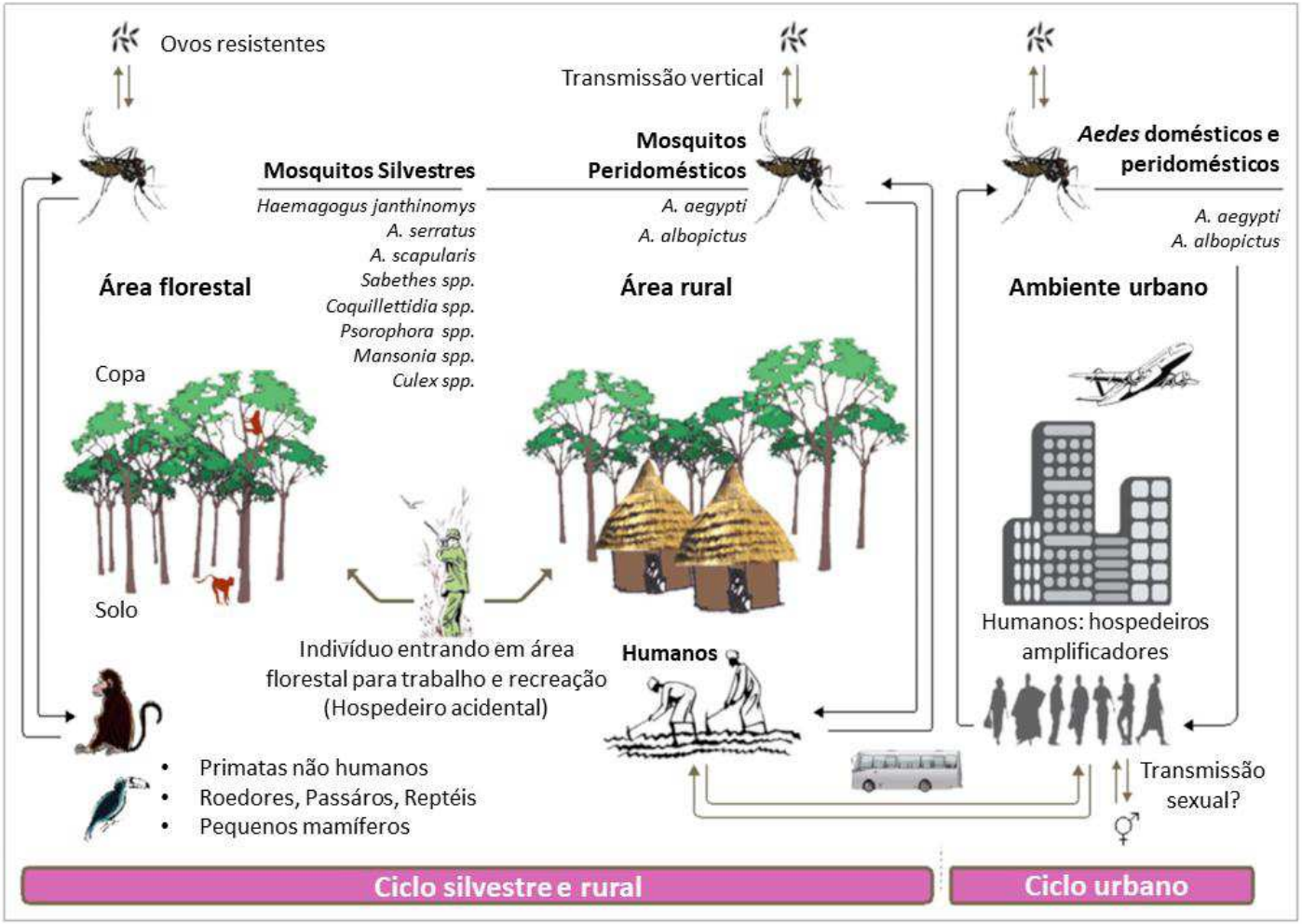

Adaptado de *Mayaro virus Pathogenisis and Transmission Mechanisms.* | Diagne et al., 2020

Diagnóstico Laboratorial

O perfil hematológico e bioquímico observado em pacientes com infecção por MAYV é diverso, sendo que mais de 80% dos pacientes mantêm esses parâmetros dentro dos limites normais (SILVA-RAMOS et al., 2023). Neste sentido, a identificação da infecção baseia-se predominantemente na avaliação dos sintomas apresentados pelos pacientes associados ao diagnóstico laboratorial antigênico ou sorológico (BRASIL, 2024).

Entretanto, a identificação de MAYV é dificultada pela similaridade de sintomas e sobreposição das áreas endêmicas com outras arboviroses, além da reatividade cruzada antigênica entre os vírus do complexo da floresta de Semliki, especialmente o CHIKV (DIOP et al., 2019). Aliado a isso, o diagnóstico diferencial de MAYV também é dificultado pela ocorrência de coinfecção natural do vírus com outros arbovírus, como a Dengue (DENV), ZIKV e CHIKV (DE PAULA SILVEIRA-LACERDA et al., 2021; DOS SANTOS SOUZA MARINHO et al., 2022). Adicionalmente, múltiplas exposições a diferentes alfavírus reduzem a especificidade dos ensaios sorológicos, contribuindo para a subnotificação dos casos de febre do Mayaro (PEZZI et al., 2019).

A partir da sorologia é possível identificar a presença de anticorpos após o período de viremia, sendo uma ferramenta para a identificação de infecções passadas e estudos de soroprevalência. Neste sentido, as metodologias mais utilizadas são o imunoensaio enzimático (*enzyme-linked immunosorbent assay*, ELISA) e ensaio de imunofluorescência indireta (*immunofluorescence assay*, IFA) (DIAGNE et al., 2020) (**Figura 7**). Alternativamente, o MAYV também pode ser identificado a partir de isolamento em cultura celular em laboratórios que possuam infraestrutura, certificação e equipe qualificada (SILVA-RAMOS et al., 2023).

Figura 7: Relação entre sintomatologia da Febre do Mayaro e marcadores utilizados para diagnóstico laboratorial.

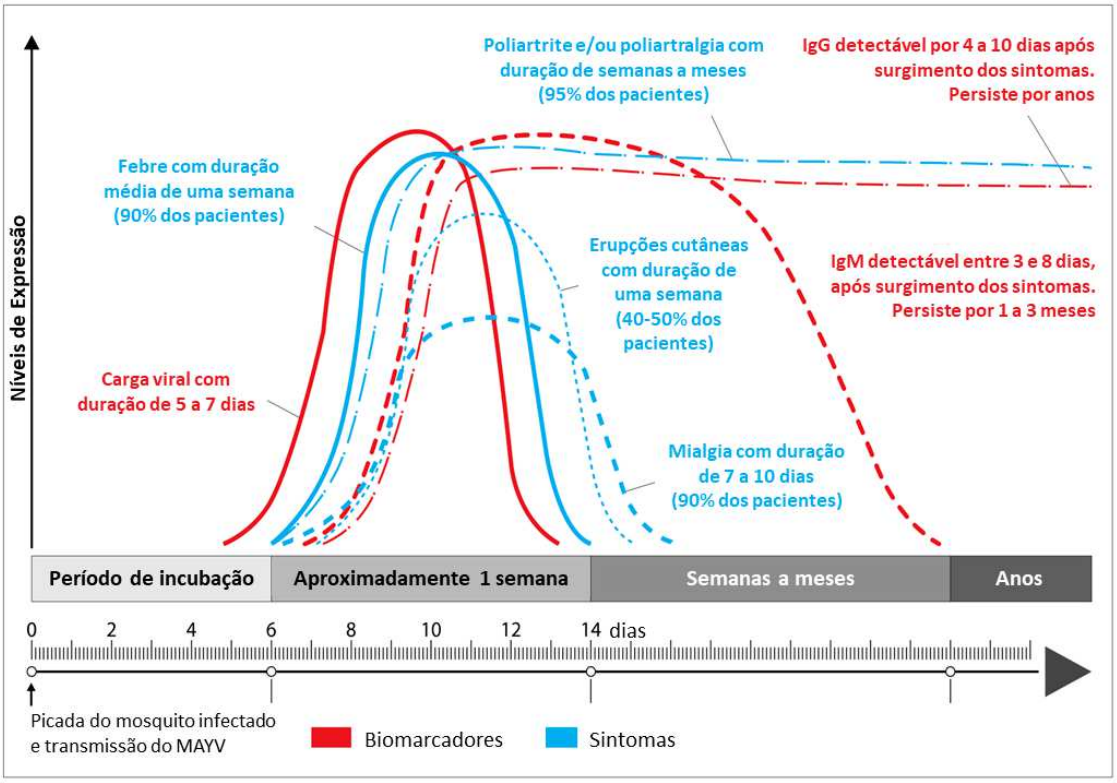

Adaptado a partir de *Mayaro virus Pathogenisis and Transmission Mechanisms*. | Diagne et al., 2020

As metodologias moleculares, em sua maioria baseadas em reação em cadeia da polimerase (*polimerase chain reaction,* PCR), são o padrão ouro para a identificação antigênica (SILVA-RAMOS et al., 2023). Estas técnicas possuem elevada especificidade e sensibilidade na fase virêmica da doença, detectando os ácidos nucleicos virais presentes no sangue de 2 a 6 dias após o início da infecção (ACOSTA-AMPUDIA et al., 2018) **(Figura 7)**. Adicionalmente, o monitoramento genômico permite controlar e/ou prever o surgimento de variantes com características distintas, como maior transmissibilidade, virulência, escape da resposta imune e adaptação a novos hospedeiros e vetores. A análise molecular favorece o diagnóstico diferencial de MAYV, além de identificar a introdução e disseminação de linhagens virais em novos hospedeiros, vetores e localidades, sendo essencial para o controle do vírus (MARINHO et al., 2024).

Prevenção e tratamento da febre do Mayaro

A subnotificação dos casos de Febre do Mayaro, a expansão global de áreas endêmicas, a alta adaptabilidade viral, o desmatamento e as mudanças climáticas, e a inexistência de vacinas e antivirais licenciados contra MAYV são fatores que favorecem a disseminação da doença. Neste contexto, o controle e a prevenção contra este vírus dependem atualmente do

manejo dos vetores e da vigilância epidemiológica e molecular do patógeno (DIAGNE et al., 2020).

Diversos métodos para a contenção de vetores transmissores de arbovírus estão em estudo, incluindo modificações genéticas com CRISPR-Cas9, liberação de mosquitos machos estéreis, uso de inseticidas e inibição da infecção por arbovírus através o uso de outros microrganismos (ACHEE et al., 2019). A bactéria *Wolbachia* foi descrita como capaz de reduzir a competência de *Aedes aegypti* na transmissão de MAYV (PEREIRA et al., 2018). Entretanto, diversos fatores dificultam o controle da disseminação de MAYV por vetores, incluindo a alta adaptabilidade viral a diversas espécies de vetores, altas taxas de disseminação destes artrópodes e emergência de mosquitos resistentes (ACHEE et al., 2019).

Até o momento, não há vacinas específicas para a prevenção da infecção por MAYV. No entanto, estudos pré-clínicos têm explorado diversas abordagens promissoras. Dentre elas estão as vacinas de DNA baseadas em proteínas do envelope do MAYV, de vírus vivo atenuado, com vetor de adenovírus, e de partículas semelhantes a vírus (*Virus like particles,* VLP) (ABBO et al., 2023; ROSA et al., 2023). Como fator agravante, não há tratamento antiviral licenciado para a doença, e o tratamento atual para a Febre do Mayaro é principalmente sintomático, a partir de analgésicos, anti-inflamatórios e antitérmicos (GANJIAN; RIVIERE-CINNAMOND, 2020). Portanto, o desenvolvimento de novas abordagens terapêuticas para o tratamento de indivíduos infectados pelo MAYV se tornou emergencial.

Aminoadamantanos e suas propriedades antivirais

Os aminoadamantanos são uma classe de compostos orgânicos derivados do adamanto, possuindo uma estrutura contendo hidrocarbonetos policíclicos com grupos amino adicionados, o que altera suas propriedades e funções biológicas (POPIOŁEK et al., 2024) **(Figura 8)**. Esses compostos têm atraído interesse significativo na clínica médica, devido às suas propriedades antivirais, associadas à capacidade de sua estrutura em interagir de maneira eficaz com a membrana viral, reduzindo a capacidade do vírus de interagir e infectar novas células (KINNUN et al., 2024).

Figura 8: Representação das estruturas químicas do 2-aminoadamantano e do hidrocloreto de rimantadina.

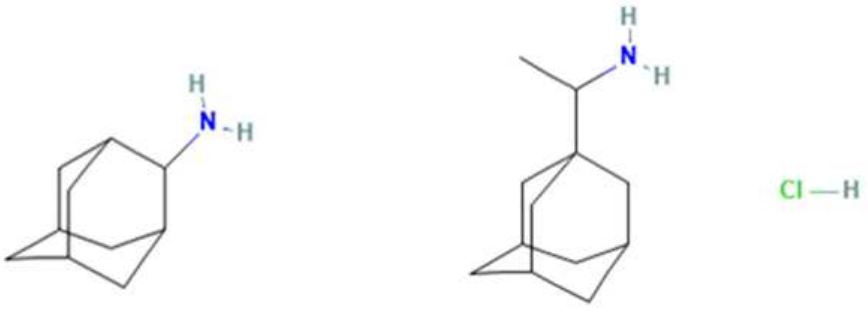

2-Aminoadamantatina Hidrocloreto de rimantadina

Fonte: Estruturas adaptadas a partir do banco de dados Pubchem | KIM et al., 2023

O hidrocloreto de rimantadina (rtdH) **(Figura 8)**, um derivado de aminoadamantano, apresenta propriedades farmacológicas bem descritas e aplicabilidade clínica diversa, sendo um fármaco licenciado para o tratamento da gripe causada pelo vírus Influenza A (GARCIA et al., 2010). A ação antiviral de rtdH está associada com a inibição de canais de íons presentes na membrana do vírus que é constituído pela proteína M2 (GARCIA et al., 2010). Esse fármaco possui estabilidade estrutural, térmica e oxidativa, além de alta lipofilicidade e baixo consumo de energia (SPILOVSKA et al., 2016). Além de seu uso terapêutico contra a influenza, o rtdH tem mostrado atividade antiviral de amplo espectro, sendo eficaz contra CHIKV, SARS-CoV-2 e vírus da hepatite A (LIM et al., 2022; SANTOS et al., 2022; SASAKI-TANAKA et al., 2022). Neste sentido, Santos e colaboradores descreveram a atividade de rtdH contra o CHIKV, pertencente ao gênero *Alphavirus,* tendo sugerido a ação do composto como inibidor de viroporina 6K (SANTOS et al., 2022). O composto demonstrou eficácia de 57% em estágios iniciais da infecção e de 60% como tratamento pós-entrada do vírus, apresentando um SI de 8.4 (SANTOS et al., 2022).

O reposicionamento de medicamentos consiste em utilizar medicamentos já aprovados para tratar diferentes doenças, explorando seus mecanismos de ação conhecidos para novas aplicações. Nesse contexto, a reutilização terapêutica é uma estratégia eficaz e rápida para identificar novas indicações de fármacos existentes para controlar a disseminação de vírus (LANGENDRIES et al., 2021). Esta abordagem permite que esses medicamentos sejam aplicados de forma mais rápida do que novos antivirais, devido ao perfil farmacológico já conhecido e estabelecido, o que reduz significativamente o tempo e os custos envolvidos no processo de desenvolvimento e aprovação (SANTOS et al., 2022). Desta forma, o rtdH pode apresentar potencial para o reposicionamento contra outras viroses, incluindo o MAYV. Adicionalmente, fármacos licenciados, como o rtdH, podem servir como modelo para o

desenvolvimento de novos medicamentos, proporcionando uma base estrutural e funcional para a criação de terapias antivirais de maior eficácia.

Uso de vírus geneticamente modificados para pesquisa

O caráter negligenciado e emergente do MAYV indica a necessidade do desenvolvimento de estudos que impulsionem a compreensão do vírus, além do desenvolvimento de vacinas e antivirais para prevenir e tratar a doença. Neste sentido, os vírus geneticamente modificados representam uma abordagem científica relevante que possibilita a identificação da presença do agente infeccioso a partir da expressão de genes repórteres (CHERKASHCHENKO et al., 2023). Adicionalmente, o desenvolvimento destas tecnologias favorece a padronização de ensaios em larga escala e de maior rendimento (*High Throughput Screening*, HTS), amplamente utilizados na pesquisa de antivirais (KATO; HISHIKI, 2016).

A produção deste tipo de vírus geralmente é feita a partir de clonagem molecular, utilizando-se de plasmídeos bacterianos contendo o genoma de interesse, e/ou por PCR, em que os fragmentos podem ser amplificados sem o uso de bactérias **(Figura 9 A-C).** Neste sentido, a partir da junção de fragmentos sintéticos e/ou extraídos a partir de organismos, são obtidos genomas completos contendo as sequências de interesse que são utilizadas para infectar a célula hospedeira (SUN et al., 2014) **(Figura 9 D, E).** Posteriormente, a partir da obtenção dos vírus modificados, é necessário mensurar as taxas de replicação e a estabilidade do gene repórter, a fim de verificar a viabilidade do vírus para uso nos ensaios de interesse (CHERKASHCHENKO et al., 2023).

Dentre os genes repórter mais utilizados, estão a *nanoluciferase* (*nanoluc*) e *firefly luciferase* (*fluc*), baseados nos genes de bioluminescência de *Oplophorus gracilirostris* e *Photinus pyralis*, respectivamente (ENGLAND; EHLERDING; CAI, 2016). Ao ser transcrito, o gene de *fluc* codifica uma proteína de 61 kDa, que, ao reagir com o substrato D-luciferrina na presença oxigênio, produz luminescência. Alternativamente, a *nanoluc*, que possui 19 kDa, reage com a furimazina para produzir o mesmo efeito (ENGLAND; EHLERDING; CAI, 2016). A partir da inserção do gene de *nanoluc* ou *fluc* no genoma viral, é possível quantificar as taxas de replicação viral com base na mensuração de luminescência, ao reagir as proteínas expressas durante o ciclo replicativo com os seus respectivos substratos (GUO et al., 2023) **(Figura 9 D, E)**. Estudos anteriores descreveram a criação de tecnologias similares, como o MAYV expressando proteína verde fluorescente melhorada (MAYV eGFP) e MAYV com inserção do gene de *nanoluc* na proteína E2 (MAYV $E2^{nLuc}$), ambos baseados em promotores de bacteriófagos (SP6 e T7) (LI et al., 2019; RAMJAG et al., 2022). Entretanto, nessas tecnologias,

para a produção de vírions infecciosos em células eucarióticas é necessário realizar a transcrição do plasmídeo em RNA viral anteriormente à transfecção deste RNA nas células hospedeiras (ÁVILA-PÉREZ et al., 2018), representando uma tecnologia com maior número de processos até a obtenção das partículas virais infecciosas. Em contraste, os sistemas baseados no promotor de citomegalovírus (CMV) permitem a transcrição direta do plasmídeo em RNA viral em células eucarióticas pela ação da RNA polimerase II (ÁVILA-PÉREZ et al., 2018). Neste sentido, o DNA oferece maior estabilidade e eficiência de transfecção em comparação ao RNA, além de tornar o processo menos trabalhoso e mais econômico. Partindo desse pressuposto, o presente estudo apresenta a criação e validação de clones infecciosos de MAYV que expressam genes repórteres, utilizando genética reversa a partir de um promotor CMV **(Figura 9 A-E).**

Figura 9: Representação da produção de plasmídeos CMV-MAYV-*nanoluc* e CMV-MAYV-*firefly* contendo genoma viral a partir de enzimas de restrição e PCR. A) Geração do plasmídeo T7-MAYV-*nanoluc* a partir de T7-MAYV-eGFP; B) Produção do plasmídeo CMV-MAYV-*nanoluc* a partir de T7-MAYV-*nanoluc*. C) Produção do plasmídeo CMV-MAYV-*firefly* a partir de T7-MAYV-*nanoluc*. D) Estrutura do RNA viral e nanoluciferase originados a partir da transfecção do plasmídeo CMV-MAYV-*nanoluc* em células eucariotas. Reação da proteína nanoluciferase usada na identificação da replicação viral a partir de luminescência. E) Estrutura do RNA viral e firefly luciferase originados a partir da transfecção do plasmídeo CMV-MAYV-*firefly* em células eucariotas. Reação da proteína firefly luciferase usada na identificação da replicação viral a partir de luminescência.

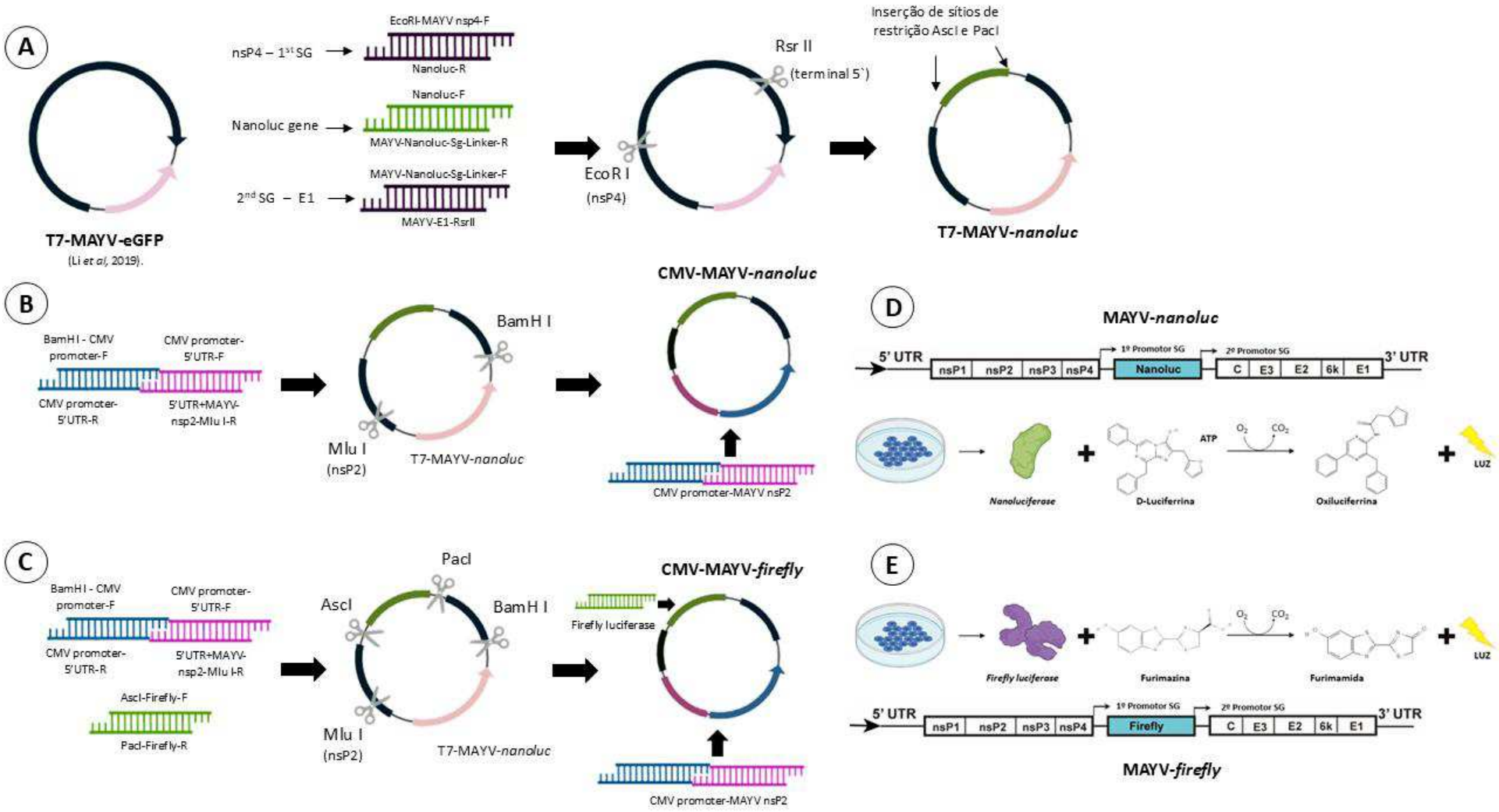

Fonte: BioRender | Marinho, M. d. S. (2025).

OBJETIVOS

O presente trabalho teve como objetivo desenvolver, avaliar e validar os vírus geneticamente modificados MAYV-*nanoluc* e -*firefly* como potenciais abordagens metodológicas para ensaios antivirais.

Objetivos específicos

- Desenvolver os clones infecciosos MAYV-*nanoluc* e -*firefly*, a partir do plasmídeo sob promotor de CMV, contendo o genoma viral com inserção dos genes repórteres;
- Comparar as taxas de replicação do MAYV-*nanoluc* e -*firefly* com as do vírus selvagem;
- Caracterizar e relacionar a estabilidade dos genes *nanoluc e fluc* durante os ciclos de infecção de MAYV-*nanoluc* e -*firefly*;
- Utilizar o MAYV-*nanoluc* para avaliar a atividade anti-MAYV do rtdH;
- Determinar a concentração efetiva de 50% (EC_{50}), concentração citotóxica em 50% (CC_{50}) e índice de seletividade ($IS = CC_{50}/EC_{50}$) de rtdH para obter os valores ótimos de concentração para o tratamento celular.
- Validar o potencial do MAYV-*nanoluc* como ferramenta metodológica em ensaios antivirais, pelo uso de controle positivo EIDD-2749 (4'-Fluorouridina), um composto de amplo-espectro antiviral.

REFERÊNCIAS

ABBO, S. R. et al. Comparative Efficacy of Mayaro Virus-Like Particle Vaccines Produced in Insect or Mammalian Cells. **Journal of Virology**, v. 97, n. 3, 30 mar. 2023.

ACHEE, N. L. et al. Alternative strategies for mosquito-borne arbovirus control. **PLOS Neglected Tropical Diseases**, v. 13, n. 3, p. e0007275, 26 mar. 2019.

ACOSTA-AMPUDIA, Y. et al. Mayaro: an emerging viral threat? **Emerging Microbes & Infections**, v. 7, n. 1, p. 1–11, 1 dez. 2018.

ANDERSON, C. R. et al. Mayaro Virus: A New Human Disease Agent. **The American Journal of Tropical Medicine and Hygiene**, v. 6, n. 6, p. 1012–1016, 1 nov. 1957.

AUGUSTE, A. J. et al. Evolutionary and Ecological Characterization of Mayaro Virus Strains Isolated during an Outbreak, Venezuela, 2010. **Emerging Infectious Diseases**, v. 21, n. 10, p. 1742–1750, out. 2015.

ÁVILA-PÉREZ, G. et al. Reverse Genetic Approaches for the Generation of Recombinant Zika Virus. **Viruses**, v. 10, n. 11, 31 out. 2018.

BENGUE, M. et al. Mayaro Virus Infects Human Brain Cells and Induces a Potent Antiviral Response in Human Astrocytes. **Viruses**, v. 13, n. 3, p. 465, 11 mar. 2021.

BLOHM, G. et al. Mayaro as a Caribbean traveler: Evidence for multiple introductions and transmission of the virus into Haiti. **International Journal of Infectious Diseases**, v. 87, p. 151–153, out. 2019.

CARRASCO, L.; SANZ, M.; GONZÁLEZ-ALMELA, E. The Regulation of Translation in Alphavirus-Infected Cells. **Viruses**, v. 10, n. 2, p. 70, 8 fev. 2018.

CARVALHO, C. A. M. et al. On the entry of an emerging arbovirus into host cells: Mayaro virus takes the highway to the cytoplasm through fusion with early endosomes and caveolae-derived vesicles. **PeerJ**, v. 5, p. e3245, 27 abr. 2017.

CELONE, M. et al. A systematic review and meta-analysis of the potential non-human animal reservoirs and arthropod vectors of the Mayaro virus. **PLOS Neglected Tropical Diseases**, v. 15, n. 12, p. e0010016, 13 dez. 2021.

CHERKASHCHENKO, L. et al. Validation of flavivirus infectious clones carrying fluorescent markers for antiviral drug screening and replication studies. **Frontiers in Microbiology**, v. 14, 15 set. 2023.

DE CURCIO, J. S. et al. Detection of Mayaro virus in Aedes aegypti mosquitoes circulating in Goiânia-Goiás-Brazil. **Microbes and Infection**, v. 24, n. 4, p. 104948, jun. 2022.

DE PAULA SILVEIRA-LACERDA, E. et al. Molecular epidemiological investigation of Mayaro virus in febrile patients from Goiania City, 2017–2018. **Infection, Genetics and Evolution**, v. 95, p. 104981, nov. 2021.

DIAGNE, C. T. et al. Mayaro Virus Pathogenesis and Transmission Mechanisms. **Pathogens**, v. 9, n. 9, p. 738, 8 set. 2020.

DIOP et al. Differential Susceptibility and Innate Immune Response of Aedes aegypti and Aedes albopictus to the Haitian Strain of the Mayaro Virus. **Viruses**, v. 11, n. 10, p. 924, 9 out. 2019.

DOS SANTOS SOUZA MARINHO, R. et al. Re-emergence of mayaro virus and coinfection with chikungunya during an outbreak in the state of Tocantins/Brazil. **BMC Research Notes**, v. 15, n. 1, p. 271, 3 dez. 2022.

ENGLAND, C. G.; EHLERDING, E. B.; CAI, W. NanoLuc: A Small Luciferase Is Brightening Up the Field of Bioluminescence. **Bioconjugate Chemistry**, v. 27, n. 5, p. 1175–1187, 18 maio 2016.

ESPOSITO, D. L. A.; FONSECA, B. A. L. DA. Will Mayaro virus be responsible for the next outbreak of an arthropod-borne virus in Brazil? **The Brazilian Journal of Infectious Diseases**, v. 21, n. 5, p. 540–544, set. 2017.

FIRTH, A. E. et al. Discovery of frameshifting in Alphavirus 6K resolves a 20-year enigma. **Virology Journal**, v. 5, n. 1, p. 108, 2008.

GANJIAN, N.; RIVIERE-CINNAMOND, A. Mayaro virus in Latin America and the Caribbean. **Revista Panamericana de Salud Pública**, v. 44, p. 1, 11 fev. 2020.

GARCIA, J. C. et al. Structural, Electronic, and Vibrational Properties of Amino-adamantane and Rimantadine Isomers. **The Journal of Physical Chemistry A**, v. 114, n. 44, p. 11977–11983, 11 nov. 2010.

GONZALEZ-ESCOBAR, G. et al. Mayaro virus detection in patients from rural and urban areas in Trinidad and Tobago during the Chikungunya and Zika virus outbreaks. **Pathogens and Global Health**, v. 115, n. 3, p. 188–195, 3 abr. 2021.

GUO, S. et al. Construction of coxsackievirus B5 viruses with luciferase reporters and their applications in vitro and in vivo. **Virologica Sinica**, v. 38, n. 4, p. 549–558, ago. 2023.

JUNT, T. et al. Determination of natural versus laboratory human infection with Mayaro virus by molecular analysis. **Epidemiology and Infection**, v. 123, n. 3, p. 511–513, 1 dez. 1999.

KATO, F.; HISHIKI, T. Dengue Virus Reporter Replicon is a Valuable Tool for Antiviral Drug Discovery and Analysis of Virus Replication Mechanisms. **Viruses 2016, Vol. 8, Page 122**, v. 8, n. 5, p. 122, 5 maio 2016.

KIM, A. S.; DIAMOND, M. S. A molecular understanding of alphavirus entry and antibody protection. **Nature Reviews Microbiology**, v. 21, n. 6, p. 396–407, 6 jun. 2023.

KIM, S. et al. PubChem 2023 update. **Nucleic Acids Research**, v. 51, n. D1, p. D1373–D1380, 6 jan. 2023.

KINNUN, J. J. et al. Amantadine interactions with phase separated lipid membranes. **Chemistry and Physics of Lipids**, v. 262, p. 105397, ago. 2024.

KROKOVSKY, L. et al. Dynamic of Mayaro Virus Transmission in Aedes aegypti, Culex quinquefasciatus Mosquitoes, and a Mice Model. Viruses, Basel, v. 15, n. 3, p. 799, mar. 2023.

LANGENDRIES, L. et al. Repurposing Drugs for Mayaro Virus: Identification of EIDD-1931, Favipiravir and Suramin as Mayaro Virus Inhibitors. **Microorganisms**, v. 9, n. 4, p. 734, 31 mar. 2021.

LELLO, L. S. et al. nsP4 Is a Major Determinant of Alphavirus Replicase Activity and Template Selectivity. **Journal of Virology**, v. 95, n. 20, 27 set. 2021.

LI, X. et al. Development of a rapid antiviral screening assay based on eGFP reporter virus of Mayaro virus. **Antiviral Research**, v. 168, p. 82–90, ago. 2019.

LIM, S.-Y. et al. Anti-SARS-CoV-2 Activity of Adamantanes In Vitro and in Animal Models of Infection. **COVID**, v. 2, n. 11, p. 1551–1563, 28 out. 2022.

MACKAY, I. M.; ARDEN, K. E. Mayaro virus: a forest virus primed for a trip to the city? **Microbes and Infection**, v. 18, n. 12, p. 724–734, dez. 2016.

MAIA, L. M. S. et al. Natural vertical infection by dengue virus serotype 4, Zika virus and Mayaro virus in *Aedes* (*Stegomyia*) *aegypti* and *Aedes* (*Stegomyia*) *albopictus*. **Medical and Veterinary Entomology**, v. 33, n. 3, p. 437–442, 18 set. 2019.

MARINHO, M. DOS S. et al. Evolutionary Profile of Mayaro Virus in the Americas: An Update into Genome Variability. **Viruses**, v. 16, n. 5, p. 809, 20 maio 2024.

MAVIAN, C. et al. Emergence of recombinant Mayaro virus strains from the Amazon basin. **Scientific Reports**, v. 7, n. 1, p. 8718, 18 ago. 2017.

MELTON, J. V. et al. Alphavirus 6K Proteins Form Ion Channels. **Journal of Biological Chemistry**, v. 277, n. 49, p. 46923–46931, dez. 2002.

MOTA, M. T. DE O. et al. Mayaro virus: a neglected arbovirus of the Americas. **Future Virology**, v. 10, n. 9, p. 1109–1122, set. 2015.

PEREIRA, T. N. et al. Wolbachia significantly impacts the vector competence of Aedes aegypti for Mayaro virus. **Scientific Reports**, v. 8, n. 1, p. 6889, 2 maio 2018.

PEZZI, L. et al. GloPID-R report on chikungunya, o'nyong-nyong and Mayaro virus, part 3: Epidemiological distribution of Mayaro virus. **Antiviral Research**, v. 172, p. 104610, dez. 2019.

POPIOŁEK, Ł. et al. Novel Adamantane Derivatives: Synthesis, Cytotoxicity and Antimicrobial Properties. **Applied Sciences**, v. 14, n. 9, p. 3700, 26 abr. 2024.

RAMJAG, A. et al. A high-throughput screening assay to identify inhibitory antibodies targeting alphavirus release. **Virology Journal**, v. 19, n. 1, p. 170, 29 out. 2022.

ROSA, R. B. et al. Mouse Models of Mayaro Virus. **Viruses**, v. 15, n. 9, p. 1803, 24 ago. 2023.

RUPP, J. C. et al. Alphavirus RNA synthesis and non-structural protein functions. **The Journal of general virology**, v. 96, n. 9, p. 2483–2500, set. 2015.

SANTOS, I. A. et al. Repurposing potential of rimantadine hydrochloride and development of a promising platinum(II)-rimantadine metallodrug for the treatment of Chikungunya virus infection. **Acta Tropica**, v. 227, p. 106300, mar. 2022.

SASAKI-TANAKA, R. et al. Amantadine and Rimantadine Inhibit Hepatitis A Virus Replication through the Induction of Autophagy. **Journal of Virology**, v. 96, n. 18, 28 set. 2022.

SILVA-RAMOS, C. R. et al. Clinical, Epidemiological, and Laboratory Features of Mayaro Virus Infection: a Systematic Review. **Current Tropical Medicine Reports**, v. 10, n. 4, p. 309–319, 27 nov. 2023.

SNYDER, J. E. et al. Functional Characterization of the Alphavirus TF Protein. **Journal of Virology**, v. 87, n. 15, p. 8511–8523, ago. 2013.

SPILOVSKA, K. et al. Adamantane – A Lead Structure for Drugs in Clinical Practice. **Current Medicinal Chemistry**, v. 23, n. 29, p. 3245–3266, 17 out. 2016.

SUN, C. et al. Stable, High-Level Expression of Reporter Proteins from Improved Alphavirus Expression Vectors To Track Replication and Dissemination during Encephalitic and Arthritogenic Disease. **Journal of Virology**, v. 88, n. 4, p. 2035–2046, 15 fev. 2014.

WARRIER, R. et al. Role of Sindbis Virus Capsid Protein Region II in Nucleocapsid Core Assembly and Encapsidation of Genomic RNA. **Journal of Virology**, v. 82, n. 9, p. 4461–4470, maio 2008.

WEBER, W. C. et al. Mayaro virus pathogenesis and immunity in rhesus macaques. **PLOS Neglected Tropical Diseases**, v. 17, n. 11, p. e0011742, 20 nov. 2023.

WHITE, S. K. et al. Detection and phylogenetic characterization of arbovirus dual-infections among persons during a chikungunya fever outbreak, Haiti 2014. **PLoS neglected tropical diseases**, v. 12, n. 5, p. e0006505, maio 2018.

ZHANG, Z. et al. Host Lipids in Positive-Strand RNA Virus Genome Replication. **Frontiers in Microbiology**, v. 10, 26 fev. 2019.

CAPÍTULO II

Manuscript:

DEVELOPMENT AND VALIDATION OF MAYARO VIRUS WITH LUCIFERASE REPORTER GENES AS A TOOL FOR ANTIVIRAL ASSAYS

*****Este capítulo está apresentado em formato de manuscrito. O artigo em questão foi publicado na revista **"Heliyon"** da editora Elsevier.

Heliyon 10 (2024) e33885

Contents lists available at ScienceDirect

Heliyon

journal homepage: www.cell.com/heliyon

Research article

Development and validation of Mayaro virus with luciferase reporter genes as a tool for antiviral assays

Mikaela dos Santos Marinho [a,1], Ya-Nan Zhang [b,1], Natasha Marques Cassani [a], Igor Andrade Santos [a], Ana Laura Costa Oliveira [a], Anna Karla dos Santos Pereira [c], Pedro Paulo Corbi [c], Bo Zhang [b,**], Ana Carolina Gomes Jardim [a,d,*]

[a] Laboratory of Antiviral Research, Institute of Biomedical Science, Federal University of Uberlândia (UFU), Uberlândia, MG, Brazil
[b] Key Laboratory of Virology and Biosafety, Wuhan Institute of Virology, Chinese Academy of Sciences, Wuhan, 430071, China
[c] Institute of Chemistry, University of Campinas (UNICAMP), Campinas, SP, Brazil
[d] Institute of Biosciences, Humanities, and Exact Sciences, São Paulo State University (UNESP), Campus, São José do Rio Preto, SP, Brazil

ARTICLE INFO

Keywords:
Mayaro virus
Reporter virus
Zika virus
Antiviral
Rimantadine hydrochloride

ABSTRACT

Arboviruses are etiological agents in an extensive group of emerging diseases with great clinical relevance in Brazil, due to the wide distribution of their vectors and the favorable environmental conditions. Among them, the Mayaro virus (MAYV) has drawn attention since its emergence as the etiologic agent of Mayaro fever, a highly debilitating disease. To study viral replication and identify new drug candidates, traditional antiviral assays based on viral antigens and/or plaque assays have been demonstrating low throughput, making it difficult to carry out larger-scale assays. Therefore, we developed and characterized two DNA-launched infectious clones reporter viruses based on the MAYV strain BeAr 20290 containing the reporter genes of *firefly luciferase (FLuc)* and *nanoluciferase (NLuc)*, designated as MAYV-*firefly* and MAYV-*nanoluc*, respectively. The viruses replicated efficiently with similar properties to the parental wild-type MAYV, and luminescence expression levels reflected viral replication. Reporter genes were also preserved during passage in cell culture, remaining stably expressed for one round of passage for MAYV-*firefly* and three rounds for MAYV-*nanoluc*. Employing the infectious clone, we described the effect of Rimantadine, an FDA-approved Alzheimer's drug, as a repurposing agent for MAYV but with a broad-spectrum activity against Zika virus infection. Additionally, we validated MAYV-*nanoluc* as a tool for antiviral drug screening using the compound EIDD-2749 (4′-Fluorouridine), which acts as an inhibitor of alphavirus RNA-dependent RNA polymerase.

1. Introduction

Arboviruses make up an extensive group of emerging pathogens of great clinical relevance in Brazil, due to the wide distribution of their vectors, mediated by favorable environmental conditions [1]. Although their circulation is geographically restricted by vectors

* Corresponding author. Institute of Biomedical Science, ICBIM/UFU, Avenida Amazonas, Bloco 4C – sala 216, Umuarama, Uberlandia, MG, CEP: 38405-302, Brazil.
** Corresponding author.
E-mail addresses: zhangbo@wh.iov.cn (B. Zhang), jardim@ufu.br (A.C.G. Jardim).
[1] These authors contributed equally to this work.

https://doi.org/10.1016/j.heliyon.2024.e33885
Received 12 June 2024; Accepted 28 June 2024
Available online 2 July 2024
2405-8440/© 2024 The Authors. Published by Elsevier Ltd. This is an open access article under the CC BY-NC license (http://creativecommons.org/licenses/by-nc/4.0/).

and reservoir hosts, arboviruses have the potential to adapt to infect new organisms, spreading beyond the endemic areas [2]. In this sense, the global emergence and resurgence of those pathogens lead to management and preparedness efforts for possible new outbreaks, including the search for antivirals against them [3].

Mayaro virus (MAYV; specie *Alphavirus mayaro*) is a single-stranded positive-sense RNA (ssRNA+) arbovirus, that belongs to the *Togaviridae* family and the genus *Alphavirus* [4]. The viral genome encodes MAYV structural proteins (CP, E3, E2, 6k/TF, E1) and non-structural proteins (nsP1, nsP2, nsP3, nsP4), which are involved in virus replication and pathogenesis [5]. It was first described in Trinidad in 1954 [6], and since then, several localized outbreaks of MAYV have been reported, especially in northern region of Brazil, due to increased trade and climate changes [1].

MAYV is the etiologic agent of Mayaro fever, a disease characterized by joint inflammation and arthralgias, which can progress to a chronic condition and cause clinical complications [7]. As an aggravating factor, there is no approved antiviral drug to treat Mayaro fever, and the treatment for the disease is based on controlling symptoms [4]. Another fact is that the virus is maintained in a wild enzootic cycle and the occurrence of spillover into the urban environment has drawn attention due to the potential to remain in an urban cycle [8,9].

On this basis, the emerging character of MAYV combined with the lack of antivirals to control infections caused by this pathogen demonstrates the need to search for molecules with the potential to treat the disease. In this context, drug repurposing can be an effective and rapid strategy to identify new indications of existing drugs to control virus spreading [10]. Rimantadine is an approved antiviral drug, which exhibits structural stability, good thermal and oxidative stability, extreme lipophilicity, and low consumption of energy [11]. In addition, it inhibits the influenza A virus by blocking the M2 ion channel, preventing viral uncoating, and its antiviral profile makes rimantadine an attractive candidate for drug repurposing [12].

Nevertheless, traditional antiviral assays based on viral antigens and/or plaque assays demonstrate low throughput, making it difficult to carry out larger-scale assays [13]. As a response, reporter viruses are an alternative system for high-throughput antiviral assays since the insertion of a specific reporter gene into the viral genome facilitates and provides a more efficient way of measuring viral replication, pathogenesis, and/or dissemination in infected cells and animals [14].

Previous investigations described the development and applicability of several viruses inserted with reporter genes, such as the Dengue virus [15], Influenza virus [16], Hepatitis C virus [17], Poxviruses [18], Sindbis virus, Chikungunya virus [19], and more recently, SARS-CoV-2 [20]. In a previous study, we also developed and characterized a stable enhanced green fluorescent protein (eGFP) reporter virus for the MAYV strain BeAr 20290, providing an interesting tool for antiviral screening assays [21]. Alternatively, Ramjag and coworkers described and characterized the MAYV expressing *nanoluciferase* (MAYV E2^{nLuc}) [22].However, both of these systems are based on the bacteriophage T7 and SP6 promoter, respectively [21,22], and therefore, depends on the transcription of backbone plasmid into infectious RNA to produce virions in eukaryotic cells [23,24]. This is an interesting technique; however, it presents limitations due to the instability of the RNA transfection into host cells, making it susceptible to degradation [25] In addition, the viral RNA can induce cellular immune response, compromising the efficient production of recombinant viruses and stimulating undesired mutations [26]. In contrast, cytomegalovirus (CMV) promoter-driven systems exhibit a less laborious and more efficient rescue process in eukaryotic cells, allowing transcription of the cDNA clone to be initiated directly by cellular RNA polymerase II (Chey et al., 2021). This system exhibits robust activity in mammalian cells, resulting in high levels of gene expression and increased production of viral particles [27]. In addition, it also presents higher accessibility, cost-effectiveness, and production speed than bacteriophage-driven systems, which makes it ideal for the efficient and economical production of viral vectors in research [28].

In this sense, we developed and characterized two stable infectious clones harbouring the *luciferase* reporters under the CMV promoter for antiviral screening assays, based on the strain BeAr 20290 of MAYV, Brazil [29]. The inserted reporter genes of *firefly luciferase (FLuc)* and *nanoluciferase (Nluc)* were designated as MAYV-*firefly* and MAYV-*nanoluc*, respectively. Additionally, we employed the system to identify Rimantadine hydrochloride (rtdH) as a repurposing drug, as well as validated MAYV-*nanoluc* as a tool as a powerful tool for high-throughput antiviral screening by using the compound EIDD-2749 (4′-Fluorouridine), which acts as an inhibitor of alphavirus RNA-dependent RNA polymerase [30]. Furthermore, rtdH presented a potential broad-spectrum activity by inhibiting the Zika virus (ZIKV).

2. Methods

2.1. Cells and compound

Vero E6 cells (kidney tissue derived from a normal adult African green monkey, ATCC E6) were cultivated on Dulbecco's Modified Essential Medium (DMEM, GIBCO) supplemented with 100 U/mL penicillin (Sigma-Aldrich), 100 mg/mL streptomycin (Sigma-Aldrich), 1 % (v/v) non-essential amino acids (Sigma-Aldrich) and 10 % (v/v) fetal bovine serum (FBS; Hyclone) at 37 °C in a humidified 5 % CO_2 incubator. Cell line was monthly tested to avoid mycoplasma infection.

The Rimantadine hydrochloride (rtdH, C12H22NCl, 99 %) was purchased from Sigma-Aldrich Laboratories and 4′-Fluorouridine (EIDD-2749, 98 %) was purchased from Cayman Chemical. The compounds were dissolved in DMSO (dimethyl sulfoxide), stored at −20 °C, and diluted in media at time of the assay.

2.2. Generation of the MAYV reporter construct

Using the previously constructed infectious cDNA clone of MAYV with the T7 promotor (termed as T7-MAYV) as a backbone (Li et al., 2019), the CMV-MAYV-*nanoluc* and CMV-MAYV-*firefly* were constructed under the control of the CMV promoter, in which a

cassette expressing the *NLuc* or/*FLuc* gene and a repeated sub-genomic (sg) promoter was inserted between the nonstructural nsP4 gene and the 5′-terminal of structural genes (Fig. 1). To achieve this, T7-MAYV-*nanoluc* was initially constructed and details for construction were as follows. Three individual fragments, respectively encompassing the sequences from part of nsp4 to the first sg promotor of the *NLuc* gene, and from the second sg promotor to the most of E1, were amplified and fused followed by pasting into the T7-MAYV backbone at *Eco*R I and Rsr II restriction sites to generate T7-MAYV-*nanoluc* clones. To facilitate the construction of the firefly reporter clone, *Asc*I and *Pac*I restriction sites were introduced at both ends of the *NLuc* gene, and the T7-MAYV-*firefly* clone was generated by replacing the *NLuc* gene of the T7-MAYV-*nanoluc* clone with *FLuc* through *Asc*I and *Pac*I sites. Then, the fragment encompassing the sequences from CMV promotor to nsp2 was obtained by fusion PCR and replace the corresponding part of T7-MAYV-*nanoluc* and T7-MAYV-*firefly* clones by *Bam*H I and Mlu restriction sites. The resulting plasmids were confirmed by sequencing and named as CMV-MAYV-*nanoluc* and CMV-MAYV-*firefly*. All primers used for PCRs were listed in Table 1, and the full-length sequences of the clones are available in Supplementary Material 1.

2.3. MAYV plasmids amplification and purification

Initially, 1 μg of the plasmids CMV-MAYV-*nanoluc* or CMV-MAYV-*firefly* was added to 200 μL of competent DH5-α Escheria coli and incubated on ice for 30 min. Subsequently, the bacteria were submitted to a thermal shock at 42 °C for 45 s, returned to ice for 2 min, and incubated with SOC medium at 37 °C for 1 h 200 rpm. Then, the DH5-α cells were streaked for isolation in solid Luria Berthani (LB) medium supplemented or not with Ampicillin (Sigma-Aldrich) at 50 μg/mL, for control based on the antibiotic resistance gene inserted in the plasmids. Afterward, the transformed bacteria were grown for 24 h and lysed to obtain the amplified plasmids. The purification process was performed by Plasmid Maxi kit (QUIAGEN) protocol, and the amount of DNA extracted was quantified through Nanodrop (Thermo Fisher).

2.4. MAYV infectious clone rescue

To produce the MAYV-*nanoluc* and MAYV-*firefly* virions, 1×10^6 BHK-21 cells/well seeded in 6 well plates were transfected with 5 μg of CMV-MAYV-*nanoluc* or CMV-MAYV-*firefly* plasmids using the LipofectamineTM LTX Reagent with PLUS Reagent (Thermo Fisher Scientific) and Optimem Medium following the manufacturer's instructions. After 48 h, the supernatant was collected and stored at −80 °C. The expression of *NLuc* and *FLuc* genes were assessed by luminescence reading on Glomax microplate reader (Promega), through the Renilla luciferase Assay System (Promega) or Luciferase Assay System (Promega), respectively, at different time-points post-transfection.

To determine viral titers, 8×10^4 Vero E6 cells/well were seeded in 24 wells plate, and 24 h later, the cells were infected with ten-fold serial dilutions of each MAYV infectious clone. Cells were incubated with viruses for 1 h at 37 °C and 5 % CO_2, followed by the inoculum removal, washes with PBS to remove the unbound virus, and addition of fresh medium supplemented with 1 % dilution of stock of penicillin and streptomycin, 2 % FBS, and 1 % carboxymethyl cellulose (CMC). Infected cells were incubated for 2 days in a humidified 5 % CO2 incubator at 37 °C, followed by fixation with 4 % formaldehyde and staining with 0.5 % violet crystal. The viral foci were visualized to determine plaque morphology. Images were analyzed at EVOs M5000 Cell Imaging Systems (Thermo Fisher Scientific).

All work was performed at biosafety level 2 under the authorization number SEI: 01245.006267/2022-14 CBQ: 163/02 from the CTNBio — National Technical Commission for Biosecurity from Brazil.

2.5. MAYV-nanoluc and -firefly growth kinetics

To assess the growth kinetics of both MAYV-*nanoluc* and MAYV-*firefly*, 1×10^5 Vero E6 cells were seeded in 12 well plates 24 h before infection. Later, cells were infected with MAYV wild-type strain BeAr 20290 ($MAYV_{WT}$), MAYV-*nanoluc*, or MAYV-*firefly* at the MOIs of 0.01, 0.05, and 0.1. After 2 h of incubation, the supernatants were removed, and cells were washed with PBS (1x) three times and replaced with fresh medium supplemented with 2 % FBS. At different time-points post-infection (4, 6, 12, 24, 36, and 48 h.p.i.), the culture medium was collected and stored at −80 °C.

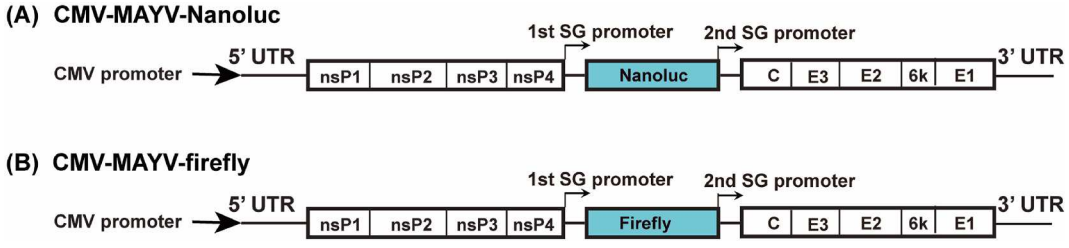

Fig. 1. Scheme of plasmid construction of MAYV-*nanoluc* and –*firefly*. The constructions were developed based on the sequence of MAYV BeAr 20290 strain, isolated in Brazil in 1960 from *Haemagogus* mosquitoes, belonging to genotype L. The marker genes that express the protein *Nano-luciferase* **(A)** and *Firefly luciferase* **(B)** were inserted in the viral genetic sequence between the non-structural proteins and capsid encoding genes.

Table 1
Primers used for construction of infectious MAYV reporter clones.

Primer	Sequence
*Eco*RI-MAYV nsp4-F	CCGGAATTCACAGAGAGCTGGTTCGCCGCC
Nanoluc-F	CTACACGACACCTATTCCACCCGGCGCGCCATGGTCTTCACACTCGAAGATTTC
Nanoluc-R	GGCGCGCCGGGTGGAATAGGTGTCGTGTAGAGCACCTATTTAGGACCGCC
MAYV-*Nanoluc*-Sg-Linker-F	ACGCATTCTGGCGTAATTAATTAATGTCATACATCTGTACGGCGGTCC
MAYV-*Nanoluc*-Sg-Linker-R	GTATGACATTAATTAATTACGCCAGAATGCGTTCGCACAGCCGCCAGCCGG
MAYV-E1-*Rsr*II	GGTCGGACCGGATTTGTCTGGATTATG
*Asc*I-*Firefly*-F	TTGGCGCGCCATGGAAGACGCCAAAAACATAAAG
*Pac*I-*Firefly*-R	TCCTTAATTAATTACACGGCGATCTTTCCGCCCTTC
CMV promoter-5′UTR-F	GCTCGTTTAGTGAACCGTATGGCGGGCAAGTGACAC
5′UTR + MAYV-nsp2-Mlu I–R	CG ACGCGTCAATAGGACATTGACGTGTT
*Bam*H I - CMV promoter-F	CGCGGATCC CATTGATTATTGACTAGTTA
CMV promoter-5′UTR-R	GTGTCACTTGCCCGCCATACGGTTCACTAAACGAGC

The viral titer of each time-point was determined by TCID50 (Median Tissue Culture Infectious Dose). To this, 5×10^3 Vero E6 cells were seeded in each well of a 96 well plate, were infected with ten-fold serial dilutions of the viral stocks, and incubated for 72 h at 37 °C, with 5 % CO2. Subsequently, viral titers were calculated according to the Spearman-Kärber algorithm as described by Killington and Hierholzer [31,32].

2.6. Stability of the reporter viruses in cell culture

To analyze whether the *FLuc* and *NLuc* reporter genes can be stably maintained after cell culture passaging, MAYV-*firefly* and MAYV-*nanoluc* were serially passaged in Vero E6 cells. For this, 1×10^6 cells were seeded in a T25 cm2 and infected with each MAYV infectious clone at an MOI of 0.1. Virus supernatant was stored at −80 °C, titrated through plaque reduction assay, and used to infect a new T25 cm2 flask using the same MOI. The cell passaging was performed 5 times. Additionally, the plaque focus was captured at EVOs M5000 Cell Imaging Systems (Thermo Fisher Scientific), and the morphology was compared among viruses.

To access the *luciferase* level expression during each passage, Vero E6 cells were seeded in a 48-well plate at a density of 2×10^4 cells per well and infected with each passage of the virus at an MOI of 0.1 for 24h. Afterward, cells were washed with PBS [1x] and harvested using Renilla-luciferase lysis buffer (Promega). Virus replication levels were quantified by measuring *NLuc* or *FLuc* activity through the Renilla luciferase assay system (Promega) or the Luciferase Assay System (Promega), respectively.

2.7. Determination of cytotoxic concentration of 50 % (CC_{50})

Cell viability was measured by the MTT [3-(4,5-dimethylthiazol-2-yl)-2,5-diphenyl tetrazolium bromide] (Sigma-Aldrich) assay as previously described [33,34]. Briefly, Vero E6 cells were plated to 24 well plates at a density of 8×10^4 cells/well for MAYV assays, or 5×10^3 cells/well in 96 well plate for ZIKV assays and incubated at 37 °C and 5 % CO_2. After 24h, medium containing two-fold serial dilutions of rtdH or EIDD-2749 (4′-Fluorouridine) was added to cells in concentrations ranging from 1.6 to 400 μM 1.56–200 μM, respectively. Since the CC50 was performed simultaneously with viral infection, the analysis for ZIKV was conducted after 72 h, and MAYV after 48 h. Then, the medium was replaced by MTT solution at 1 mg/mL for 30 min and replaced by 100 μL of DMSO (dimethyl sulfoxide) to solubilize the formazan crystals. The absorbance was measured at 490 nm on the Glomax microplate reader (Promega). Cell viability was calculated according to equation (T/C) × 100 %, where T and C represent the mean optical density of the treated and untreated control groups, respectively. The cytotoxic concentration of 50 % (CC_{50}) was calculated using GraphPad Prism 8.0.

2.8. Determination of effective concentration of 50 % (EC_{50}) using MAYV-nanoluc

To identify the effect of Rimantadine hydrochloride (rtdH) in MAYV replication, the MAYV-*nanoluc* was employed. To this, Vero E6 cells were plated in microplates of 48 wells at a concentration of 2×10^4 cells/well and incubated at 37 °C and 5 % CO_2 for 24 h. RtdH was diluted in a two-fold serial dilution following the concentrations of 1.6–400 μM, in the presence of the virus in a MOI of 0.1. The dose-response assay was also performed with EIDD-2749, a broad-spectrum inhibitor of alphaviruses (positive control) [30] in a two-fold serial dilution from 1.56 to 200 μM. After 24 h of incubation, the supernatant was removed, cells washed and lysed according to the Renilla Luciferase Assay System (Promega) kit protocol, and subsequently submitted to a luminescence analysis on the GloMax (Promega) plate reader. The effective concentration of 50 % inhibition (EC_{50}) was calculated using GraphPad Prism 8.0 software.

2.9. ZIKV assays

A wild-type ZIKV isolate from a clinical sample of a patient in Brazil ($ZIKV_{PE243}$) [35] was amplified employing infected Vero E6 cells in a 75 cm^2 flask for 3 days. It was produced, rescued, and titrated as previously described [34].

For determination of the EC50 using $ZIKV_{PE243}$, Vero E6 cells were seeded at a density of 5×10^3 cells per well into 96 well plates, infected with $ZIKV_{PE243}$ at a MOI of 0.01 and simultaneously treated with rtdH at concentrations ranging from 1.6 to 400 μM. For EC_{50},

cells were also. After 72 h, cells were fixed with 4 % formaldehyde, washed with PBS, and added of blocking buffer (BB) to perform an immunofluorescence assay [34]. The same protocol was performed in parallel in the absence of $ZIKV_{PE243}$ to determine CC50. The CC_{50} and EC_{50} were calculated using GraphPad Prism 8.0 software. These values were used to calculate the selectivity index ($SI = CC_{50}/EC_{50}$).

All work was performed at biosafety level 2 under the authorization number SEI: 01245.006267/2022-14 CBQ: 163/02 from the CTNBio — National Technical Commission for Biosecurity from Brazil.

2.10. Statistical analysis

Individual experiments were conducted in triplicates and all assays were performed a minimum of three times to confirm the reproducibility of the results. All data were normalized and expressed as mean and standard deviation. Differences between mean readings were compared using analysis of variance (one-way and two-way ANOVA) or Student's *t*-test, with p values < 0.05 considered

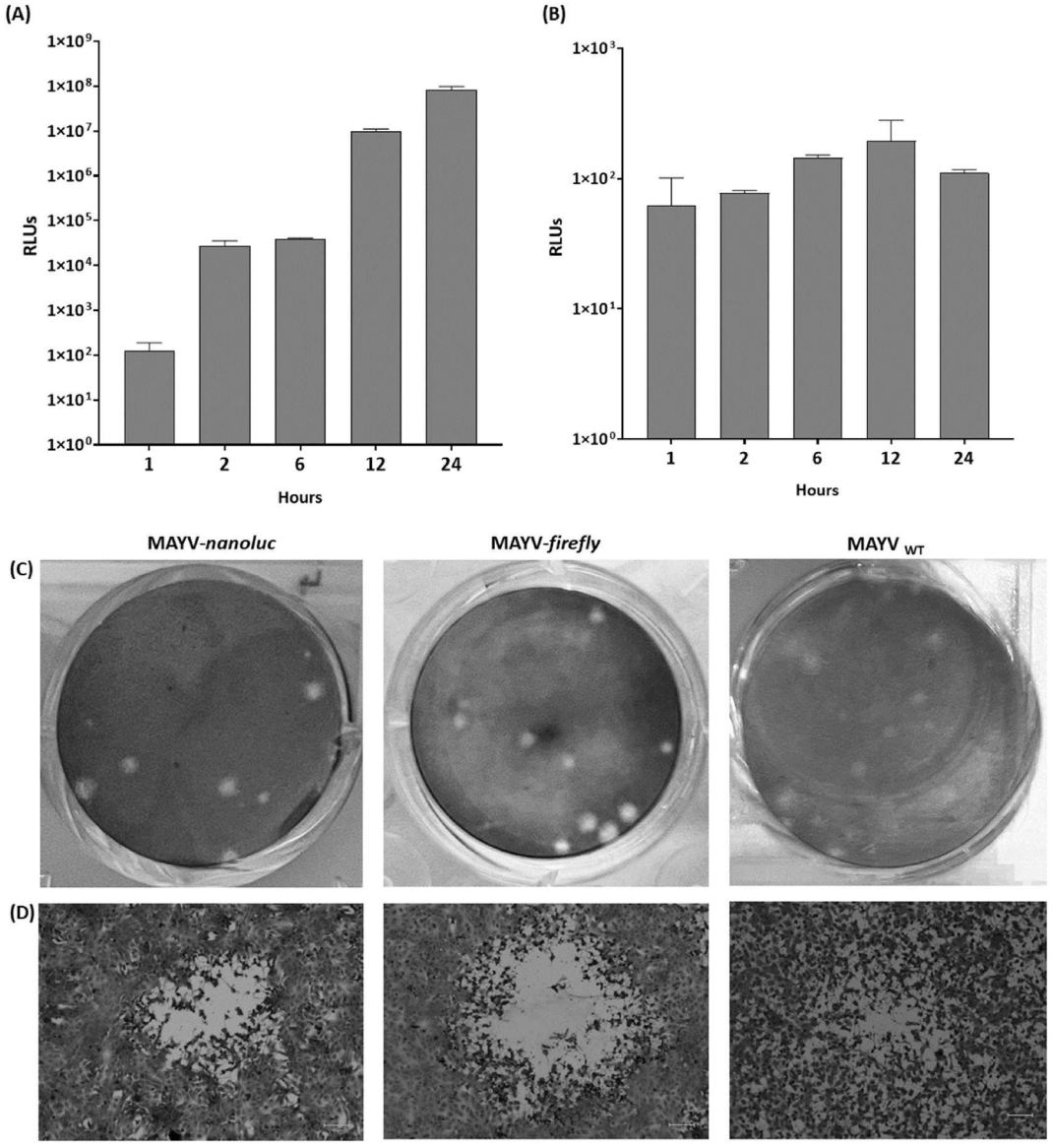

Fig. 2. Characterization of MAYV infectious clones. Analysis of luminescence expression in Vero E6 cells transfected with CMV-MAYV-*nanoluc* and CMV-MAYV-*firefly* and. Vero E6 cells were transfected with 1 μg of each plasmid and the expression of *Nanoluciferase* (A) and *Firefly luciferase* (B) were detected through Luciferase and *Renilla* luciferase assay system after transfection, respectively. (C) Plaque morphology of the recombinant viruses MAYV-*nanoluc* and MAYV-*firefly*, and the wild type. (D) Focus morphology of each virus in Vero E6 cells. Images were analyzed at EVOs M5000 cell imaging systems (Thermo Fisher Scientific). Scale bar 100 nm.

significant. GraphPad Prism 8.0 software was used to assess statistical differences of means of readings using a non-linear regression.

3. Results

3.1. Construction of MAYV-nanoluc and –firefly

To construct the cDNA clones of MAYV reporter viruses, we utilized the protocol reported to the construction of an eGFP Chikungunya reported in our previous study [36]. Briefly, a cassette expressing the *NLuc* or/*FLuc* gene and a repeated sub-genomic (sg) promoter was inserted between the nonstructural nsP4 gene and the 5′-terminal of structural genes. In addition, to avoid steps such as transcription to obtain viral RNAs in vitro, the reporter cDNA clones were placed under the control of CMV promotor (Fig. 1). The resulting plasmids were confirmed by sequencing and named as CMV-MAYV-*nanoluc* and CMV-MAYV-*firefly*.

3.2. Characterization and growth kinetics of MAYV-nanoluc and -firefly

The plasmids of CMV-MAYV-*nanoluc* and CMV-MAYV-*firefly* were transfected into Vero E6 cells to evaluate the efficacy of the infectious clone in producing an infectious particle. At different time points post-transfection, supernatants were collected and subjected to plaque assay to determine plaque morphology and virus production (Fig. 2). As shown in Fig. 2A, Relative Light Units (RLUs) were detectable at 1 h post-transfection (h.p.t.) for MAYV-*nanoluc* and increased until 24 h.p.t., reaching 1×10^8 RLUs (Fig. 2A). Alternatively, luminescence levels in cells transfected with MAYV-*firefly* were also detected 1 h.p.i., however, RLU values were maintained in about 1×10^2 RLUs until 24 h.p.t. (Fig. 2B).

After 48h, the supernatant of transfected cells was titrated employing the plaque formation assay, and as a result, the viral plaque morphology was homogeneously between $MAYV_{WT}$, MAYV-*nanoluc*, and *–firefly* (Fig. 2C). Visualization at a digital inverted microscope demonstrated that the MAYV-*nanoluc* and MAYV-*firefly* presented similar foci morphology, being those larger foci and with rounded edges when compared to $MAYV_{WT}$, which presented smaller and not defined foci (Fig. 2D).

Given the high stability and expression level of *luciferase* protein for both viruses at the first passage, we performed a growth kinetics comparison curve of the P1 from MAYV-*nanoluc*, *-firefly*, and $MAYV_{WT}$. To this, Vero E6 cells were infected with these three viruses at MOIs of 0.1, 0.05, and 0.01, and viral supernatant was collected at the time points 4, 6, 12, 24, 36, and 48 h.p.i. and titrated

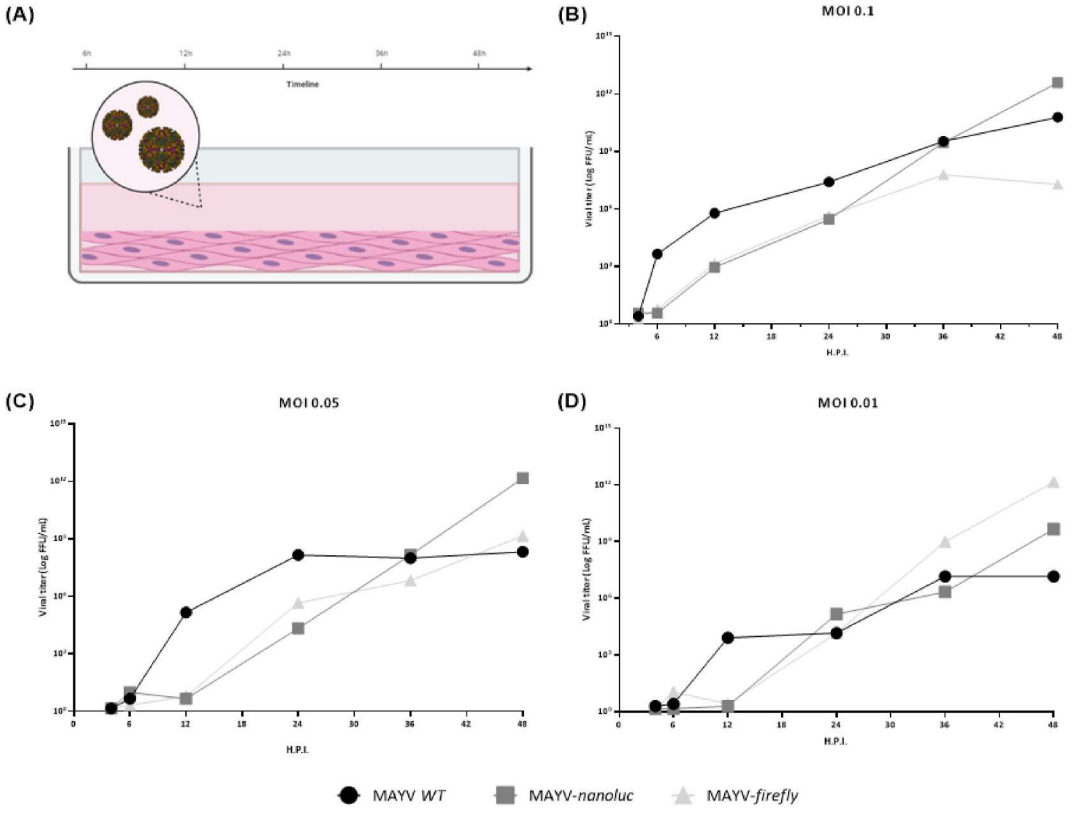

Fig. 3. Replication kinetics of MAYV in cell culture. (A) Schematic representation of replication kinetics assay. Growth kinetics of the wild type MAYV (indicated by ●), MAYV-*nanoluc* (indicated by ■), and MAYV-*firefly* (indicated by ▲). Vero E6 cells were infected with the three viruses at MOIs of 0.01 **(B)**, 0.05 **(C)**, and 0.1 **(D)**, viral supernatant was collected at different time points up to 48 h.p.i. and titrated by $TCID_{50}$.

by TCID50. As an outcome, the viral titers increased in a dose- and time-dependent manner (Fig. 3A). At all MOIs, both reporter viruses and $MAYV_{WT}$ presented low titers at 4 h.p.i., ranging between 1.45 and 3.88 pfu/mL (Fig. 3). At the MOIs of 0.1 (Figs. 3B) and 0.05 (Fig. 3C), the reporter viruses presented lower titers than the $MAYV_{WT}$ until 24h.p.i. However, MAYV-*nanoluc* reached a similar titer to $MAYV_{WT}$ at 36 h.p.i, presenting even higher titers than $MAYV_{WT}$ and MAYV-*firefly* at 48h.p.i. (Fig. 3B and C). Additionally, MAYV-*firefly* presented slightly higher titers than $MAYV_{WT}$ at the MOI of 0.05 at 48 h.p.i. (Fig. 3C). At the lowest MOI, MAYV-*nanoluc* presented higher titers than both MAYV-*firefly* and $MAYV_{WT}$ 24h.p.i., while MAYV-*nanoluc* and MAYV-*firefly* overcame $MAYV_{WT}$ titers at 48 h.p.i (Fig. 3D). These results demonstrated that the reporter viruses could efficiently replicate in Vero E6 cells, reaching similar growth rates to $MAYV_{WT}$.

3.3. *Nluc and Fluc reporter genes present different stability and luminescence expression levels in cell culture*

To analyze the in vitro stability and expression of the *FLuc* and *NLuc* genes, the viruses were serially passaged on Vero E6 cells for five times at an MOI of 0.1 for 48 h (Fig. 4A). The passages were titrated by plaque-forming assay, and the *luciferase* expression of each passage was measured by infecting Vero E6 cells with -*nanoluc*, at an MOI of 0.1 and MAYV-*firefly* at an MOI of 1, due to the contrast in the luminescence activity among the constructs. As an outcome, MAYV-*nanoluc* showed strong and consistent luminescence signals until the third passage, indicating the *NLuc* gene was stable for a minimum of three passages of infectious virus (Fig. 4B). Differently, MAYV-*firefly* presented a significant decrease in luminescence signal from the first to the second passage, indicating the loss of the *FLuc* gene probably due to selective pressure (Fig. 4C). Despite the gradual loss of reporter gene expression, viral titers were stable during passaging, varying from 2.67×10^6 to 2×10^8 PFU/mL.

3.4. *Employing MAYV-nanoluc reporter virus to identify rtdH as a drug candidate to be repurposed against MAYV infections*

In order to validate the employment of MAYV reporter viruses as tools for antiviral screening, and considering the high stability and sensibility of *NLuc* for in vitro assays, we used this reporter virus to analyze the antiviral activity of rtdH on MAYV replication. Additionally, the potential of MAYV-*nanoluc* as a powerful tool for antiviral screening was validated by treating infected cells with EIDD-2749.

To this, Vero E6 cells were infected with MAYV-*nanoluc* and treated with rtdH or EIDD-2749 for 24h. Afterward, the cells were lysed and subjected to a luminescence analysis to evaluate the reporter gene expression. Cell viability assay was performed in parallel. As a result, rtdH had an EC_{50} of 88.5 μM and a CC_{50} of 291.9 μM. Further, EIDD-2749 inhibited MAYV-*nanoluc* replication with an EC_{50} of 2.76 μM and CC_{50} of 4.99×10^7 μM. The calculated selectivity index ($SI = CC_{50}/EC_{50}$) for rtdH and EIDD-2749 were 2.3 and 1.8×10^7, respectively (Fig. 5). These results indicated that the MAYV-*nanoluc* reporter virus could be a useful tool for the evaluation of compounds presenting an anti-MAYV activity.

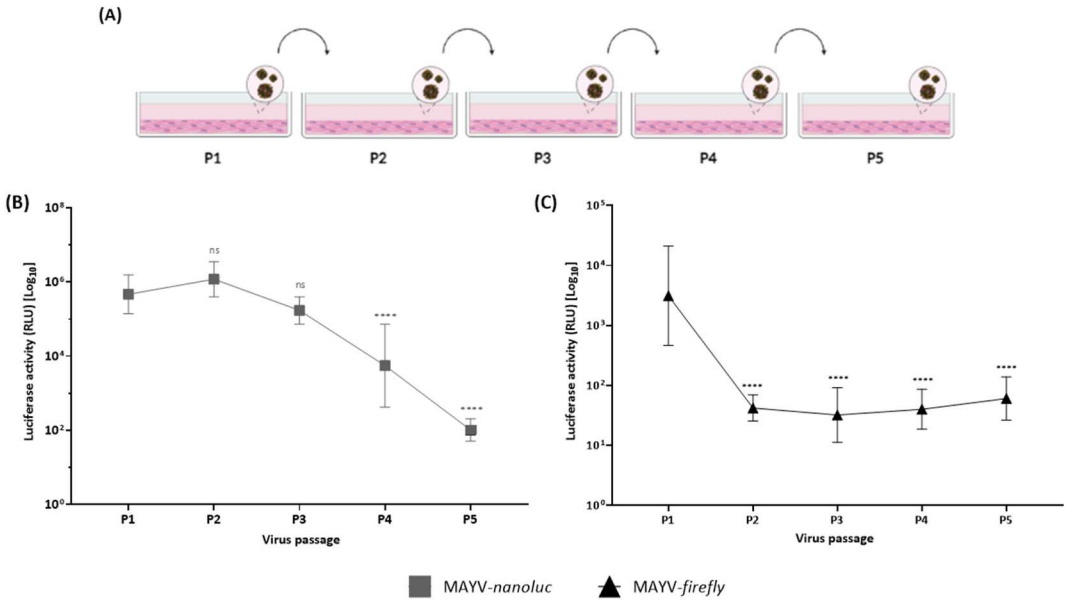

Fig. 4. Stability of the MAYV-*nanoluc* and -*firefly* viruses in cell culture. The *luciferase* expression of the different passages of MAYV-*nanoluc* **(A)** and –*firefly* **(B)** in Vero E6 cells. Vero E6 cells were serially infected with viruses for five passages. Viruses from each passage (P1–P5) were used to infect 1×10^5 Vero E6 cells at an MOI of 0.1, and the expression of *luciferase* proteins were detected 48 h.p.i. through *Luciferase* and *Renilla luciferase* assays, respectively. Mean values of three independent experiments each measured in triplicate including the standard deviation are shown. P values < 0.05 were considered significant. (**) $P < 0.01$, (***) $P < 0.001$ and (****) $P < 0.0001$.

3.5. RtdH also presents antiviral activity against ZIKV

The results presented here suggested that rtdH exerts its antiviral function against MAYV with a SI of 2.3, and, recently, it was described to possess activity against CHIKV [37]. Therefore, this drug could also present an antiviral activity on other arboviruses. To further investigate its broad-spectrum activity, we evaluated the inhibitory effects of rtdH on ZIKV replication. To this, Vero E6 cells were treated with the compound in a two-fold serial dilution ranging from 1.5 to 400 μM, along with the infection with $ZIKV_{PE243}$ at an MOI of 0.01 for 72h, when immunofluorescence assay was performed [34] (Fig. 6A). The results demonstrated that rtdH was able to inhibit ZIKV infection in a dose-dependent manner. The EC_{50} calculated by fluorescence value reduction was 80.3 μM and the CC_{50} of 194.3 μM, with an SI of 2.4 (Fig. 6B). Taken together, our findings demonstrate that rtdH presented an interesting antiviral effect against MAYV and ZIKV infections in vitro.

4. Discussion

The use of infectious clones of emergent viruses has been increasing in the past few years [13]. The insertion of specific reporter genes into the viral genome is a powerful tool to monitor the viral replication into infected mammalian cells, for applications such as high-throughput screening (HTS) for antiviral drug discovery [38]. Traditional plaque reduction assay for antiviral screening requires weeks to complete, while infectious clones expressing reporter genes can be done in days [39].

Here, we described the development of two DNA-launched replicative efficient MAYV-*luciferase* systems, expressing *NLuc* and *FLuc* genes. The *NLuc* or *FLuc* gene was inserted between the nonstructural nsP4 gene and the 5′-terminal of structural genes, and expressed under the control of sg promotor. Transfection of Vero E6 cells with the CMV-MAYV-*nanoluc* and –*firefly* plasmids resulted in detecting luminescence from the l*uciferase* reporters. The reporter viruses were infectious to Vero E6 cells, with robust *luciferase* levels production. While MAYV-*nanoluc* maintained the *NLuc* gene expression for three passages, MAYV-*firefly* was able to maintain the reporter gene for only one passage. Compared with the wild-type virus, the viral-growth kinetics were similar for both clones, showing indistinguishable replication efficiency. Additionally, we confirmed the usefulness of the MAYV-*nanoluc* for rapid antiviral screening assay using the Rimantadine hydrochloride, a well-known antiviral agent against the Influenza A virus. The broad-spectrum antiviral properties of rtdH were also demonstrated against ZIKV.

While the *FLuc* gene has more than 1.6 kb and encodes a 61 kDa protein, the *nLuc* gene has about three times fewer base pairs that encode a 19 kDa protein, being considered to present higher sensitivity and luminescent signal than *FLuc* [40]. In previous studies,

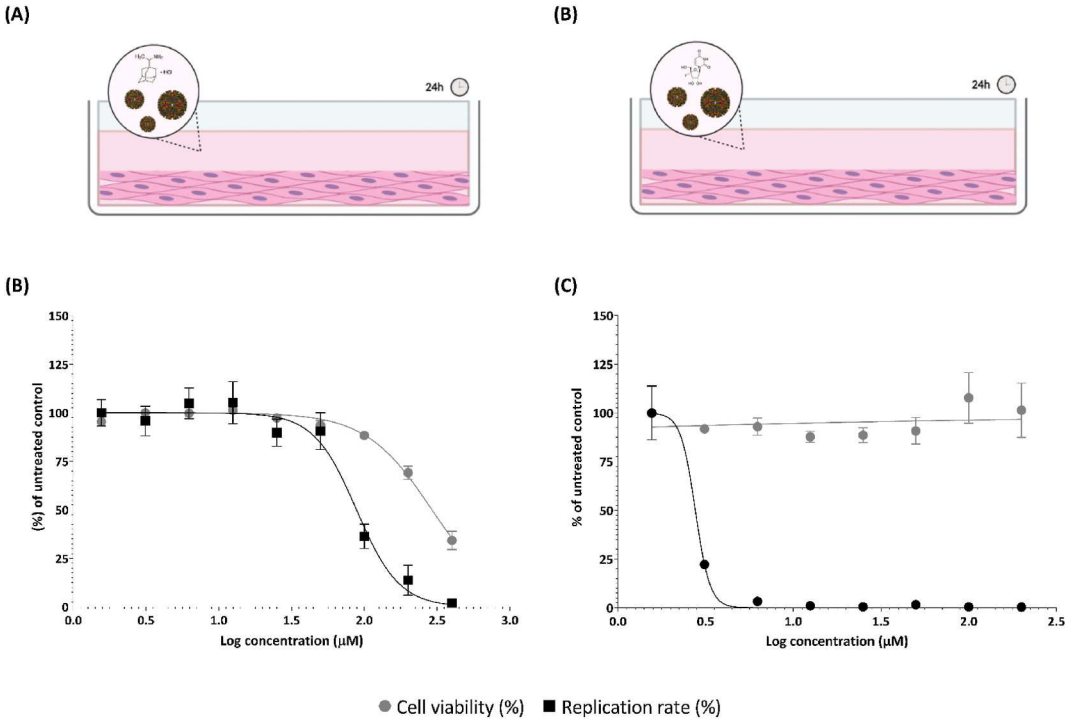

Fig. 5. Antiviral activity of Rimantadine hydrochloride on MAYV infectious clone. (A) Schematic representation of MAYV-*nanoluc* assay. Vero E6 cells were infected with MAYV-*nanoluc* at a MOI of 0.01 and treated with two-fold serial dilutionss of rtdH (1.6–400 μM) **(B)** or EIDD-2749 (1.56–200 μM) **(C)** for 24 h, when luminescence levels were measured by *Renilla* luciferase assay (indicated by ■) and cellular viability measured using MTT assay (indicated by ●). The effective concentration of 50 % (EC_{50}) and cytotoxic concentration of 50 % (CC_{50}) were determined. Mean values of three independent experiments each measured in quadruplicate including the standard deviation are shown.

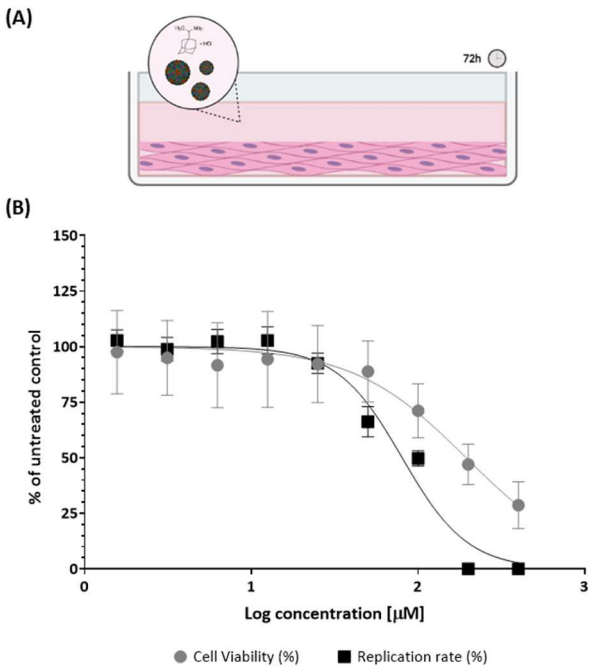

Fig. 6. Anti-ZIKV activity of Rimantadine hydrochloride. (A) Schematic representation of $ZIKV_{PE243}$ assay. **(B)** Vero E6 cells were treated with rtdH at concentrations ranging from 1.6 to 400 μM and the effective concentration of 50 % (EC_{50}) and cytotoxic concentration of 50 % (CC_{50}) were determined. ZIKV replication was measured by FFU/mL (indicated by ■) and cellular viability measured using MTT assay (indicated by ●). Mean values of three independent experiments each measured in triplicate including the standard deviation are shown.

constructs of the Sindbis virus (SINV) that presented the insertion of *FLuc* or *NLuc* genes, demonstrated different stability after cell passaging. In agreement with our data, the *NLuc* gene presented gene stability in SINV for ten passaging rounds, while the *FLuc* gene expression was only detected until the third passage [19]. Furthermore, in our study, the virus passages were performed in Vero E6 cells, which lack innate immune defenses and offer the potential for virus genetic drift, which possibly could also favor the loss of reporter genes during passaging [41].

Nevertheless, the *FLuc* system is applied *in vivo* due to the free diffusion of Firefly *luciferase* protein across the cell membrane [42]. *FLuc* possesses stable glow kinetics in the presence of its substrate and presents longer periods of photon emission than the *nano-luciferase* protein [43]. However, the *Fluc* gene presented low stability in MAYV infectious clones and was lost after the first passage, equivalent to about 4–6 rounds of virus infection [44]. This instability limits the utility of the *FLuc* marker for long-term studies or multiple rounds of viral replication, making it unsuitable for antiviral screening assays. Additionally, the bioluminescent activity of *FLuc* and *NLuc* originated through the reaction with different substrates that do not show cross-reactivity. In this sense, the systems can be applied concurrently for *in vivo* and in vitro dual bioluminescence analyses, allowing the simultaneous characterization of two different organisms or two separate biological processes [45].

Recently, our group pointed out rtdH as an inhibitor of CHIKV, an arbovirus that belongs to the same family and genus as MAYV, demonstrating promising results [37]. We proposed that the compound exhibits multiple effects on CHIKV, impairing mostly the early stages of the viral cycle, due to a virucidal action that involves viroporin blocking and interaction with the virus envelope [37]. Here, we described the antiviral properties of rtdH on both MAYV and ZIKV infections, presenting a SI of 2.3 and 2.4, respectively. In this sense, considering that rtdH has a known pharmacological profile and is an approved drug to treat Influenza A infection, it could be further evaluated in pre-clinical studies as a drug to be repurposed against MAYV, CHIKV and ZIKV infections, being applied more quickly than novel antivirals. Additionally, it could be used as a template to develop more potent drugs against MAYV, CHIKV and ZIKV infections. However, further studies are necessary to elucidate the mechanism of action on MAYV and ZIKV viroporins, which can be hypothesized by the differences between their structure and distribution in host cells. In addition, the compound EIDD-2749, previously described as RNA-dependent RNA polymerase (RdRp) inhibitor against MAYV [30] was used to validate MAYV-*nanoluc* as a potent tool for antiviral screening, presenting a SI of 1.8×10^7, in agreement with the previously published data. In summary, the results with rtdH and EIDD-2749 demonstrate that MAYV-*nanoluc* is a useful tool for HTS assays to detect inhibitors in different compound libraries for future antiviral research.

5. Conclusion

Considering the data described here, the reverse genetic system for MAYV employing DNA-launched plasmids containing *NLuc* and *FLuc* reporter genes were efficiently rescued and presented efficient replication as the wild-type virus in Vero E6 cells. Due to the high

stability of MAYV-*nanoluc* activity, which accurately represents virus replication rates, it is an applicable tool for antiviral assays that could facilitate the antiviral screening for novel anti-MAYV agents. Furthermore, we highlight the repurposing potential of Rimantadine hydrochloride as a broad-spectrum antiviral drug against MAYV and ZIKV.

Data availability statement

All data generated or analyzed during this study are included in this article.

CRediT authorship contribution statement

Mikaela dos Santos Marinho: Formal analysis, Investigation, Methodology, Validation, Writing – original draft. **Ya-Nan Zhang:** Investigation, Methodology, Writing – original draft. **Natasha Marques Cassani:** Investigation, Methodology, Writing – original draft, Writing – review & editing. **Igor Andrade Santos:** Investigation, Methodology, Writing – original draft, Writing – review & editing. **Ana Laura Costa Oliveira:** Investigation. **Anna Karla dos Santos Pereira:** Resources, Writing – review & editing. **Pedro Paulo Corbi:** Resources, Writing – review & editing. **Bo Zhang:** Methodology, Resources, Writing – review & editing. **Ana Carolina Gomes Jardim:** Funding acquisition, Supervision, Writing – review & editing.

Declaration of competing interest

The authors declare that they have no known competing financial interests or personal relationships that could have appeared to influence the work reported in this paper.

Acknowledgments

ACGJ is grateful to FAPEMIG (Fundação de Amparo à Pesquisa do Estado de Minas Gerais — Minas Gerais Research Foundation APQ-01487-22 and APQ-04686-22), and CAPES (Coordenação de Aperfeiçoamento de Pessoal de Nível Superior — Coordination of Superior Level Staff Improvement — Brasil —Prevention and Combat of Outbreaks, Endemics, Epidemics and Pandemics — Finance Code #88881.506794/2020-01 and — Finance Code 001). MDSM is grateful to FAPEMIG for scholarship #12152. NMC is grateful to CAPES for scholarship #88887.703845/2022-00. IAS thanks CNPq (Conselho Nacional de Desenvolvimento Científico e Tecnológico — National Council for Scientific and Technological Development 409187/2023-2) for scholarship #142495/2020-4, as well as for the CAPES.PrInt-UFU sandwich scholarship #88887.700246/2022-00 and FAPEMIG for scholarship #67355. PPC thanks to FAPESP (Fundação de Amparo à Pesquisa do Estado de São Paulo — São Paulo Research Foundation 2018/12062-4 and 2021/10265-8) and to Cancer Theranostics Innovation Center, CancerThera, Centros de Pesquisa, Inovação e Difusão-CEPID.

Appendix A. Supplementary data

Supplementary data to this article can be found online at https://doi.org/10.1016/j.heliyon.2024.e33885.

References

[1] J.C. Semenza, J. Rocklöv, K.L. Ebi, Climate change and cascading risks from infectious disease, Infect. Dis. Ther. (2022), https://doi.org/10.1007/S40121-022-00647-3.
[2] A. Zaid, F.J. Burt, X. Liu, Y.S. Poo, K. Zandi, A. Suhrbier, S.C. Weaver, M.M. Texeira, S. Mahalingam, Arthritogenic alphaviruses: epidemiological and clinical perspective on emerging arboviruses, Lancet Infect. Dis. 21 (2021) e123–e133, https://doi.org/10.1016/S1473-3099(20)30491-6.
[3] T.C. Pierson, M.S. Diamond, The continued threat of emerging flaviviruses, Nat Microbiol 5 (2020) 796–812, https://doi.org/10.1038/S41564-020-0714-0.
[4] R. Abdelnabi, S. Jacobs, L. Delang, J. Neyts, Antiviral drug discovery against arthritogenic alphaviruses: tools and molecular targets, Biochem. Pharmacol. 174 (2020), https://doi.org/10.1016/J.BCP.2019.113777.
[5] M. Bengue, A.R. Pintong, F. Liegeois, A. Nougairède, R. Hamel, J. Pompon, X. de Lamballerie, P. Roques, V. Choumet, D. Missé, Favipiravir inhibits mayaro virus infection in mice, Viruses 13 (2021) 2213, https://doi.org/10.3390/V13112213, 2213 13 (2021).
[6] C.R. Anderson, W.G. Downs, G.H. Wattley, N.W. Ahin, A.A. Reese, Mayaro virus: a new human disease agent. II. Isolation from blood of patients in Trinidad, B. W.I, Am. J. Trop. Med. Hyg. 6 (1957) 1012–1016, https://doi.org/10.4269/AJTMH.1957.6.1012.
[7] C.T. Diagne, M. Bengue, V. Choumet, R. Hamel, J. Pompon, D. Missé, Mayaro virus pathogenesis and transmission mechanisms, Pathogens 9 (2020) 738, https://doi.org/10.3390/PATHOGENS9090738, 738 9 (2020).
[8] Y. Acosta-Ampudia, D.M. Monsalve, Y. Rodríguez, Y. Pacheco, J.M. Anaya, C. Ramírez-Santana, Mayaro: an emerging viral threat? Emerg. Microb. Infect. 7 (2018) https://doi.org/10.1038/s41426-018-0163-5.
[9] S. Masmejan, D. Musso, M. Vouga, L. Pomar, P. Dashraath, M. Stojanov, A. Panchaud, D. Baud, Zika virus, Pathogens 9 (2020), https://doi.org/10.3390/pathogens9110898.
[10] L. Langendries, R. Abdelnabi, J. Neyts, L. Delang, Repurposing drugs for mayaro virus: identification of EIDD-1931, favipiravir and suramin as mayaro virus inhibitors, Microorganisms 9 (2021) 734, https://doi.org/10.3390/microorganisms9040734.
[11] K. Spilovska, F. Zemek, J. Korabecny, E. Nepovimova, O. Soukup, M. Windisch, K. Kuca, Adamantane – a lead structure for drugs in clinical practice, Curr. Med. Chem. 23 (2016) 3245–3266, https://doi.org/10.2174/0929867323666160525114026.
[12] J.C. Garcia, J.F. Justo, W.V.M. Machado, L.V.C. Assali, Structural, electronic, and vibrational properties of amino-adamantane and rimantadine isomers, J. Phys. Chem. A 114 (2010) 11977–11983, https://doi.org/10.1021/jp107496b.

[13] R.S. Fernandes, M.C.L.C. Freire, R. V Bueno, A.S. Godoy, L.H.V.G. Gil, G. Oliva, Reporter replicons for antiviral drug discovery against positive single-stranded RNA viruses, Viruses 12 (2020), https://doi.org/10.3390/v12060598.
[14] F. Kato, T. Hishiki, Dengue virus reporter replicon is a valuable tool for antiviral drug discovery and analysis of virus replication mechanisms, Viruses 8 (2016) 122, https://doi.org/10.3390/V8050122, 122 8 (2016).
[15] F. Pahmeier, C.J. Neufeldt, B. Cerikan, V. Prasad, C. Pape, V. Laketa, A. Ruggieri, R. Bartenschlager, M. Cortese, A versatile reporter system to monitor virus-infected cells and its application to Dengue virus and SARS-CoV-2, J. Virol. 95 (2021), https://doi.org/10.1128/JVI.01715-20/SUPPL_FILE/JVI.01715-20-S0003.MP4.
[16] A. Creanga, R.A. Gillespie, B.E. Fisher, S.F. Andrews, J. Lederhofer, C. Yap, L. Hatch, T. Stephens, Y. Tsybovsky, M.C. Crank, J.E. Ledgerwood, A.B. McDermott, J.R. Mascola, B.S. Graham, M. Kanekiyo, A comprehensive influenza reporter virus panel for high-throughput deep profiling of neutralizing antibodies, Nat. Commun. 12 (2021) 1–12, https://doi.org/10.1038/s41467-021-21954-2, 1 12 (2021).
[17] N.S. Eyre, A.L. Aloia, M.A. Joyce, M. Chulanetra, D.L. Tyrrell, M.R. Beard, Sensitive luminescent reporter viruses reveal appreciable release of hepatitis C virus NS5A protein into the extracellular environment, Virology 507 (2017) 20–31, https://doi.org/10.1016/J.VIROL.2017.04.003.
[18] Z. Bengali, P.S. Satheshkumar, B. Moss, Orthopoxvirus species and strain differences in cell entry, Virology 433 (2012) 506–512, https://doi.org/10.1016/J.VIROL.2012.08.044.
[19] C. Sun, C.L. Gardner, A.M. Watson, K.D. Ryman, W.B. Klimstra, Stable, high-level expression of reporter proteins from improved alphavirus expression vectors to track replication and dissemination during encephalitic and arthritogenic disease, J. Virol. 88 (2014) 2035–2046, https://doi.org/10.1128/JVI.02990-13/ASSET/FF4B8F21-19F2-4B43-95D3-6055AF65DF93/ASSETS/GRAPHIC/ZJV9990986550009. JPEG.
[20] K. Chiem, J.-G. Park, D. Morales Vasquez, R.K. Plemper, J.B. Torrelles, J.J. Kobie, M.R. Walter, C. Ye, L. Martinez-Sobrido, Monitoring SARS-CoV-2 infection using a double reporter-expressing virus, Microbiol. Spectr. 10 (2022), https://doi.org/10.1128/SPECTRUM.02379-22/SUPPL_FILE/REVIEWER-COMMENTS.PDF.
[21] X. Li, H. Zhang, Y. Zhang, J. Li, Z. Wang, C. Deng, A.C.G. Jardim, A.C.B. Terzian, M.L. Nogueira, B. Zhang, Development of a rapid antiviral screening assay based on eGFP reporter virus of Mayaro virus, Antivir. Res. 168 (2019) 82–90, https://doi.org/10.1016/J.ANTIVIRAL.2019.05.013.
[22] A. Ramjag, S. Cutrone, K. Lu, C. Crasto, J. Jin, S. Bakkour, C.V.F. Carrington, G. Simmons, A high-throughput screening assay to identify inhibitory antibodies targeting alphavirus release, Virol. J. 19 (2022) 170, https://doi.org/10.1186/s12985-022-01906-y.
[23] D. Fan, C. Hu, X. Yang, X. Yang, Y. Chen, J. Lin, Generation of a DNA-launched classical swine fever virus infectious clone packaged in bacterial artificial chromosome, Virus Res. 323 (2023) 198961, https://doi.org/10.1016/J.VIRUSRES.2022.198961.
[24] B.M. Kümmerer, in: Establishment and Application of Flavivirus Replicons, 2018, pp. 165–173, https://doi.org/10.1007/978-981-10-8727-1_12.
[25] G. Ávila-Pérez, A. Nogales, V. Martín, F. Almazán, L. Martínez-Sobrido, Reverse genetic approaches for the generation of recombinant Zika virus, Viruses 10 (2018) 597, https://doi.org/10.3390/v10110597.
[26] H. Zhang, D.K. Fischer, M. Shuda, P.S. Moore, S. Gao, Z. Ambrose, H. Guo, Construction and characterization of two SARS-CoV-2 minigenome replicon systems, J. Med. Virol. 94 (2022) 2438–2452, https://doi.org/10.1002/jmv.27650.
[27] T. Kurosaki, H. Nakamura, H. Sasaki, Y. Kodama, Suitable promoter for DNA vaccination using a pDNA ternary complex, Pharmaceutics 16 (2024) 679, https://doi.org/10.3390/pharmaceutics16050679.
[28] C.W. Tan, H.K. Tee, M.H.P. Lee, I.-C. Sam, Y.F. Chan, Enterovirus A71 DNA-launched infectious clone as a robust reverse genetic tool, PLoS One 11 (2016) e0162771, https://doi.org/10.1371/journal.pone.0162771.
[29] D.L.A. Espósito, B.A.L. da Fonseca, Complete genome sequence of mayaro virus (Togaviridae, alphavirus) strain BeAr 20290 from Brazil, Genome Announc. 3 (2015), https://doi.org/10.1128/genomeA.01372-15.
[30] P. Yin, N.A. May, L.S. Lello, A. Fayed, M.G. Parks, A.M. Drobish, S. Wang, M. Andrews, Z. Sticher, A.A. Kolykhalov, M.G. Natchus, G.R. Painter, A. Merits, M. Kielian, T.E. Morrison, 4′-Fluorouridine inhibits alphavirus replication and infection *in vitro* and *in vivo*, mBio (2024), https://doi.org/10.1128/mbio.00420-24.
[31] J. Hierholzer, R. Killington, Virology Methods Manual, 1996.
[32] J.F. Shimizu, S. Feferbaum-Leite, I.A. Santos, D.O.S. Martins, N.J. Kingston, M. Shegdar, C. Zothner, S.V. Sampaio, M. Harris, N.J. Stonehouse, A.C.G. Jardim, Effect of proteins isolated from Brazilian snakes on enterovirus A71 replication cycle: an approach against hand, foot and mouth disease, Int. J. Biol. Macromol. 241 (2023) 124519, https://doi.org/10.1016/J.IJBIOMAC.2023.124519.
[33] I.A. Santos, J.F. Shimizu, D.M. de Oliveira, D.O.S. Martins, L. Cardoso-Sousa, A.C.O. Cintra, V.H. Aquino, S.V. Sampaio, N. Nicolau-Junior, R. Sabino-Silva, A. Merits, M. Harris, A.C.G. Jardim, Chikungunya virus entry is strongly inhibited by phospholipase A2 isolated from the venom of Crotalus durissus terrificus, Sci. Rep. 11 (2021) 1–12, https://doi.org/10.1038/s41598-021-88039-4.
[34] N.M. Cassani, I.A. Santos, V.R. Grosche, G.M. Ferreira, M. Guevara-Vega, R.B. Rosa, L.J. Pena, N. Nicolau-Junior, A.C.O. Cintra, T.P. Mineo, R. Sabino-Silva, S. V. Sampaio, A.C.G. Jardim, Roles of Bothrops jararacussu toxins I and II: antiviral findings against Zika virus, Int. J. Biol. Macromol. 227 (2023) 630–640, https://doi.org/10.1016/j.ijbiomac.2022.12.102.
[35] C.L. Donald, B. Brennan, S.L. Cumberworth, V.V. Rezelj, J.J. Clark, M.T. Cordeiro, R. Freitas de Oliveira França, L.J. Pena, G.S. Wilkie, A. Da Silva Filipe, C. Davis, J. Hughes, M. Varjak, M. Selinger, L. Zuvanov, A.M. Owsianka, A.H. Patel, J. McLauchlan, B.D. Lindenbach, G. Fall, A.A. Sall, R. Biek, J. Rehwinkel, E. Schnettler, A. Kohl, Full genome sequence and sfRNA interferon antagonist activity of Zika virus from recife, Brazil, PLoS Neglected Trop. Dis. 10 (2016) e0005048, https://doi.org/10.1371/JOURNAL.PNTD.0005048.
[36] C.-L. Deng, S.-Q. Liu, D.-G. Zhou, L.-L. Xu, X.-D. Li, P.-T. Zhang, P.-H. Li, H.-Q. Ye, H.-P. Wei, Z.-M. Yuan, C.-F. Qin, B. Zhang, Development of neutralization assay using an eGFP Chikungunya virus, Viruses 8 (2016) 181, https://doi.org/10.3390/v8070181.
[37] I.A. Santos, A.K. dos S. Pereira, M. Guevara-Vega, R.E.F. de Paiva, R. Sabino-Silva, F.R.G. Bergamini, P.P. Corbi, A.C.G. Jardim, Repurposing potential of rimantadine hydrochloride and development of a promising platinum(II)-rimantadine metallodrug for the treatment of Chikungunya virus infection, Acta Trop. 227 (2022) 106300, https://doi.org/10.1016/j.actatropica.2021.106300.
[38] M.P. Jadhav, High-throughput screening (HTS) for the identification of novel antiviral scaffolds, Clin Pharmacol Drug Dev 3 (2014) 79–83, https://doi.org/10.1002/CPDD.99.
[39] J.Q. Li, C.L. Deng, D. Gu, X. Li, L. Shi, J. He, Q.Y. Zhang, B. Zhang, H.Q. Ye, Development of a replicon cell line-based high throughput antiviral assay for screening inhibitors of Zika virus, Antivir. Res. 150 (2018) 148–154, https://doi.org/10.1016/J.ANTIVIRAL.2017.12.017.
[40] C.G. England, E.B. Ehlerding, W. Cai, NanoLuc: a small luciferase is brightening up the field of bioluminescence, Bioconjugate Chem. 27 (2016) 1175–1187, https://doi.org/10.1021/ACS.BIOCONJCHEM.6B00112/ASSET/IMAGES/MEDIUM/BC-2016-00112G_0011.GIF.
[41] C. V Kuny, C.D. Bowen, D.W. Renner, C.M. Johnston, M.L. Szpara, In vitro evolution of herpes simplex virus 1 (HSV-1) reveals selection for syncytia and other minor variants in cell culture, Virus Evol 6 (2020), https://doi.org/10.1093/VE/VEAA013.
[42] J.E. Kim, S. Kalimuthu, B.C. Ahn, In vivo cell tracking with bioluminescence imaging, Nucl Med Mol Imaging 49 (2015) 3–10, https://doi.org/10.1007/S13139-014-0309-X/FIGURES/2.
[43] Y. Liang, P. Walczak, J.W.M. Bulte, Comparison of Red-Shifted Firefly Luciferase Ppy RE9 and Conventional Luc2 as Bioluminescence Imaging Reporter Genes for in Vivo Imaging of Stem Cells, 2012 016004, https://doi.org/10.1117/1.JBO.17.1.016004, 10.1117/1.JBO.17.1.016004 17.
[44] D.C. Mendonça, ErikV.S. Reis, NídiaE.C. Arias, H.J. Valencia, C.A. Bonjardim, A study of the MAYV replication cycle: correlation between the kinetics of viral multiplication and viral morphogenesis, Virus Res. 323 (2023) 199002, https://doi.org/10.1016/j.virusres.2022.199002.
[45] J. Czupryna, A. Tsourkas, Firefly luciferase and Rluc8 exhibit differential sensitivity to oxidative stress in apoptotic cells, PLoS One 6 (2011) e20073, https://doi.org/10.1371/JOURNAL.PONE.0020073.

CAPÍTULO III

Considerações Finais

Considerações Finais

Os resultados do estudo mostraram que MAYV-*nanoluc* e MAYV-*firefly* puderam ser produzidos com eficiência em células eucarióticas, expressando os seus respectivos genes repórter. Adicionalmente, ambos os clones apresentaram taxas de replicação similares ao vírus selvagem.

Tendo em vista a maior estabilidade do gene repórter no clone MAYV-*nanoluc*, esta construção viral representa uma ferramenta relevante para a pesquisa de compostos anti-MAYV. Neste sentido, foi possível observar que a expressão do gene *nanoluc* refletiu com precisão as taxas de replicação viral. MAYV-*nanoluc* apresentou alta sensibilidade para a realização de ensaios antivirais, sendo possível obter valores precisos de EC_{50} e SI para rtdH e para o controle positivo EIDD-2749.

O fármaco reposicionado rtdH demonstrou atividade antiviral promissora contra o MAYV, indicando seu potencial como base para estudos futuros e desenvolvimento de novos antivirais. No entanto, são necessários estudos adicionais para elucidar o mecanismo de ação do fármaco e avaliar sua eficácia como tratamento para a febre do Mayaro.

ANEXOS

Artigos Publicados

viruses

MDPI

Article

Evolutionary Profile of Mayaro Virus in the Americas: An Update into Genome Variability

Mikaela dos Santos Marinho [1], Giulia Magalhães Ferreira [1], Victória Riquena Grosche [1,2], Nilson Nicolau-Junior [3], Túlio de Lima Campos [4], Igor Andrade Santos [1,*] and Ana Carolina Gomes Jardim [1,2,*]

1 Institute of Biomedical Sciences, ICBIM, Federal University of Uberlândia, Avenida Amazonas, 4C- Room 216, Umuarama, Uberlândia 38405-319, MG, Brazil; mikaelamarinho@ufu.br (M.d.S.M.); giumferreira95@gmail.com (G.M.F.); victoriagrosche@gmail.com (V.R.G.)
2 Institute of Biosciences, Humanities and Exact Sciences (Ibilce), São Paulo State University (Unesp), Campus São José do Rio Preto, São José do Rio Preto 15054-000, SP, Brazil
3 Institute of Biotechnology, Federal University of Uberlândia, Uberlândia 38405-319, MG, Brazil; nicolaujr@ufu.br
4 Aggeu Magalhães Institute (Fiocruz), Bioinformatics Core Facility, Recife 50740-465, PE, Brazil; tulio.campos@fiocruz.br
* Correspondence: igorsantos_12@ufu.br (I.A.S.); jardim@ufu.br (A.C.G.J.); Tel.: +55-(34)-3225-8682 (A.C.G.J.)

Abstract: The Mayaro virus (MAYV) is an arbovirus with emerging potential, though with a limited understanding of its epidemiology and evolution due to the lack of studies and surveillance. Here, we investigated 71 MAYV genome sequences from the Americas available at GenBank and characterized the phylogenetic relationship among virus strains. A phylogenetic analysis showed that sequences were grouped according to the genotypes L, D, and N. Genotype D sequences were closely related to sequences collected in adjacent years and from their respective countries, suggesting that isolates may have originated from circulating lineages. The coalescent analysis demonstrated similar results, indicating the continuous circulation of the virus between countries as well. An unidentified sequence from the USA was grouped with genotype D, suggesting the insertion of this genotype in the country. Furthermore, the recombination analysis detected homologous and three heterologous hybrids which presented an insertion into the nsP3 protein. Amino acid substitutions among sequences indicated selective pressure sites, suggesting viral adaptability. This also impacted the binding affinity between the E1–E2 protein complex and the Mxra8 receptor, associated with MAYV entry into human cells. These results provide information for a better understanding of genotypes circulating in the Americas.

Keywords: arboviruses; genomic variability; phylogenetic analysis; Mayaro virus; Mayaro fever

check for updates

Citation: Marinho, M.d.S.; Ferreira, G.M.; Grosche, V.R.; Nicolau-Junior, N.; Campos, T.d.L.; Santos, I.A.; Jardim, A.C.G. Evolutionary Profile of Mayaro Virus in the Americas: An Update into Genome Variability. *Viruses* **2024**, *16*, 809. https://doi.org/10.3390/v16050809

Academic Editor: Rollie J. Clem

Received: 30 April 2024
Revised: 15 May 2024
Accepted: 19 May 2024
Published: 20 May 2024

Copyright: © 2024 by the authors. Licensee MDPI, Basel, Switzerland. This article is an open access article distributed under the terms and conditions of the Creative Commons Attribution (CC BY) license (https://creativecommons.org/licenses/by/4.0/).

1. Introduction

The Mayaro virus (MAYV) was first identified in 1954 in Trinidad and Tobago, in samples of febrile forest workers [1], later described as the etiologic agent of Mayaro fever. This disease is characterized by fever, headache, vomit, diarrhea, muscle pain, skin rashes, and long-lasting arthralgia [2]. In severe cases, MAYV infection can result in chronic polyarthritis, neurological complications, hemorrhage, and myocarditis, which can lead to death [3].

Mayaro fever in humans is mainly observed in Central and South Americas, predominantly in the Amazon Forest, Atlantic Forest, and nearby regions; however, it was also reported in subtropical regions [2]. Additionally, the disease presents dengue-like symptoms and it is present in endemic areas common to other arboviruses [4]; therefore, the differential diagnosis is difficult, which also contributes to the underreporting of Mayaro fever cases and genome sequences available in databanks [5]. Furthermore, there is no data about the circulating virus in other tropical regions, such as Africa and Asia [1].

The main vector for MAYV transmission is *Haemagogus* sp. mosquitoes [1]. However, the virus was also isolated from different nonurban arthropod genera such as the *Culex*,

Mansonia, *Psorophora*, and *Sabethes*, as well as *Aedes albopictus* and *Aedes aegypti* species, demonstrating a high susceptibility to MAYV transmission, indicating an intense viral adaptability to new vectors [6]. Further, the distribution of these species in tropical and subtropical countries associated with globalization, climatic anomalies, deforestation, and the growing contact of humans with animal reservoirs/vectors is an aggravating factor, increasing the risk of MAYV dissemination [1,4]

The MAYV is a member of the *Togaviridae* family and *Alphavirus* genus and is classified into the genotypes D (widely dispersed), L (limited), and N (new), the latest being represented by a single sequence isolated in Peru [7]. The virion particle possesses a positive single-stranded RNA of approximately 11.5 kb, associated with a capsid protein (C), and involved in a host–lipid membrane envelope inserted of the E1 and E2 glycoproteins [8] (Figure 1). The MAYV genome is constituted of two open reading frames (ORFs), one in the 5′ UTR region, responsible for encoding the non-structural proteins (nsP1, nsP2, nsP3, and nsP4), and the second ORF after the nsP4 gene, which encodes the structural proteins (CP, E3, E2, TF, 6k, and E1) [3] (Figure 1).

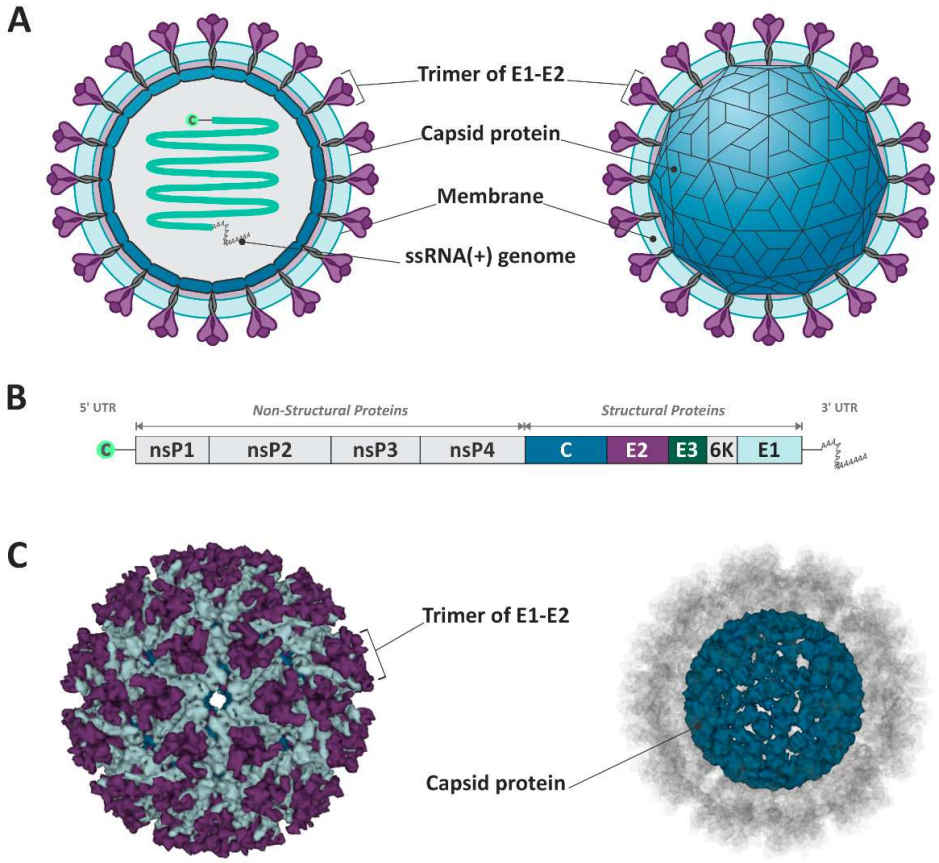

Figure 1. Schematic representation of Mayaro virus structure and genome. (**A**,**C**) The virion is composed of the E1–E2 trimmer, the capsid protein, and the ssRNA+. (**B**) The viral genome encodes structural and non-structural proteins. The figure design was based on Cryo-EM structure of mature MAYV. (PDB ID: 7KO8) [9].

It is also important to emphasize the higher rates of mutations within RNA viruses, which leads to an intra-host variability of the viral population [10]. Therefore, phylogenetic analyses represent important methodologies for developing epidemiological studies, allowing the correlation of data derived from different regions and presuming the history of the dissemination of viral variants [11]. Currently, only a few epidemiological studies on MAYV are reported, with a limited number of genome sequences available in databanks. Considering the severe symptoms caused by MAYV, and that this virus is responsible for a

neglecting disease, allied with the possibility of the emergence of new variants, or additional transmitting vectors, the study of the viral genome variability represents an essential tool to investigate the virulence and transmissibility of the different viral genotypes [11].

In this context, genetic and phylogenetic analyses of MAYV complete-genome sequences were carried out here to investigate genomic variations and the phylogenetic relationships among the MAYV strains from samples collected in the Americas. Thus, an overview of the main features of the MAYV genomic variability was obtained, indicating evolutionary forces that could drive the evolution of the viral genome, and possibly contribute to viral adaptation.

2. Materials and Methods

2.1. Collection and Alignment of MAYV Genome Sequences

Sequences of the complete genome and complete CDS of MAYV (about 11,147 nucleotides) were collected from the GenBank database, and organized according to the year of collection, origin, genotype, host, length of the sequenced genetic material, article of reference, and reference of the genotype identification (Supplementary Table S1). The dataset containing all 71 sequences was submitted to alignment by the ClustalW multiple alignment method, using the program Bioedit 7.2 [12]. The NCBI sequence NC_003417.1 was used as a reference sequence, and the parameters of alignment used were defined by the program's default configuration.

2.2. Detection of Individual Recombination Events

Due to the identification of MAYV sequences initially classified as genotype L as L/D hybrids by previous studies, KY985361.1 (Haiti, 2014) [13] KX496990.1 (Haiti, 2015), and KT818520.1 (Brazil, 2014) [14], the 71 genome sequences of MAYV were evaluated for potential recombination events using Recombination Detection Program 4 (RDP4) [15]. RDP4 was used with the default parameters, applying all available methods through the full exploratory recombination scan (Recombination Detection Program, Bootscan, MaxChi, GENECONV, Chimaera, SiScan, 3Seq, LARD, and Phylpro). The recombination breakpoints suggested by RPD4 were used to identify the potential recombinant sequences.

2.3. Phylogenetic Analysis of MAYV Genomic Sequences

To this, the recombinant regions of MAYV strains were removed and the phylogenetic tree was reconstructed employing PhyML 3.0 through the ATGC- Montpellier Bioinformatics Platform [16]. The method employed was maximum-likelihood analysis (ML), and the GTR + G model of substitution, as determined by the Smart Model Selection in PhyML [17]. A thousand replicates were used to test the support given by the data to the clusters of the tree topology, and bootstrap values > 70 were considered significant (McCormack & Clewley, 2002). The phylogenetic tree was edited using the program FigTree v.1 4.4 [12].

2.4. Coalescent Analysis

The optimal substitution model for the alignment was assessed using ModelFinder in IQ-TREE v2.1.4-beta (GTR + F + I + G4), generating a maximum likelihood tree. Root-to-tip correlation (>0.8) for the consensus tree was inspected in TempEst v1.5.3 with best-fitting root and residual mean square function, suggesting a strict molecular clock. The alignment was then imported into BEAUti v1.10.4 using tip dates parsed (year only) from the sequence names. The GTR substitution model was selected with empirical base frequencies and gamma (4 categories) plus invariant sites. We selected a strict clock type and a coalescent tree, previously, with constant size, and a random starting tree. Other parameters remained unchanged. Further, a Markov chain Monte Carlo with 100 million interactions using BEAST v1.10.4 was performed, logging the results at every 1000 interactions. The convergence of the model parameters was inspected using Tracer v1.7.2, confirming that the ESS for each statistic was >400 at the end of the runs. Tree annotator v1.10.4 was then employed to generate a maximum clade credibility tree with median heights for all trees

generated, following the removal of the first 10% as burn-in. The final tree was inspected, and a figure was generated using IcyTree [18].

2.5. Analysis of Amino Acid Substitutions and Selection Pressure

Sequences were aligned according to their genotype, resulting in two datasets: (1) sequences identified as genotype D, using DQ001069.1 as the reference sequence, and (2) sequences identified as genotypes L and L/D, employing as reference the genotype L sequence NC_003417.1. The alignments were edited according to the protein-coding regions and the translation was performed. Amino acid substitutions were analyzed in comparison to the reference sequence. The selective pressure analysis was performed on MAYV protein-coding sequence subsets through the Datamonkey Adaptive Evolution Server [19], to identify and localize statistically supported positive and negative selective pressure sites, as previously described [20]. To predict the impact of each substitution in protein selection, the fast unconstrained Bayesian approximation (FUBAR) model was used, which applies a maximum-likelihood (ML) approach to infer nonsynonymous (dN) and synonymous (dS) substitution rates on a per-site basis for a given coding alignment and corresponding phylogeny [21]. In addition, the fixed effects likelihood (FEL) model was employed to compare the results obtained. The selection pressure for each site was considered constant throughout the entire phylogeny. The statistically supported selective pressure sites considering Bayes factor (BF) > 30 and p value < 0.05 were reported.

2.6. Protein Modeling and Docking

The structure of the E1 and E2 from MAYV from different isolates were modeled together with its human natural ligand Mxra8 using SWISS-MODEL server [22]. In order to construct the complexes, a template from an electron cryo-microscopy of Chikungunya virus spike protein in complex with mouse Mxra8 receptor (PDB id:6NK7) was used. After the complexes' generation, the results and the template structure (6NK7) were submitted to two servers, PRODIGY [23] for binding affinity prediction and PLIP [24] for hydrophobic, hydrogen bond, and salt bridge interactions. The best E1E2-Mxra8 binding affinity complex was presented in a 3D view using ChimeraX [25].

3. Results

3.1. Epidemiological Features of MAYV in the Americas

The 71 complete genome sequences obtained from GenBank were collected between 1954 and 2016, in Brazil, Trinidad and Tobago, Haiti, United States of America (USA), Bolivia, Peru, French Guiana, and Venezuela (Figure 2). All MAYV sequences and the related data employed in this study are shown in Supplementary Table S1.

3.2. Individual Recombination Events Detected among MAYV Sequences

The submission of the complete alignment with all analyzed sequences from genotypes D, L, and L/D on RDP4 showed evidence of a heterologous recombination among the sequences KY985361.1 (Haiti, 2014), KX496990.1 (Haiti, 2015), and KT818520.1 (Brazil, 2014) (Figure 3). The recombination event was positive in all seven methods listed above ($p < 0.05$), being inconclusive only for LARD and Phylpro, also used in the analysis of the sequences (Supplementary Table S2).

Furthermore, the sequence MK288026.1 (Venezuela, 2016) was identified as a homologous hybrid between DQ001069.1 (genotype D, French Guiana, 1998) and KY618134.1 (genotype D, Brazil, 1991) (Figure 3). The isolate DQ001069.1 was the most closely related to the likely hybrid, being a major parent, and KY618134.1 was identified as the minor parent. In addition, the sequence KT818520.1 (Brasil, 2014) was identified as an L/D hybrid, with supported evidence of a similar origin or same recombination event as KX496990.1 (Haiti, 2015) (Figure 3), as previously described by Mavian and collaborators [14]. Additionally, KY985361.1 (Haiti, 2014), also previously reported as genotype L [2], and subsequently identified as a hybrid [13], was also identified here as an L/D hybrid by all RDP4 conclusive

analyses. The sequence was identified as originating from the major parent KY618133.1 (Genotype L, Brazil, 1988) and the minor parent KY618131.1 (Genotype D, Brazil, 1978) (Figure 3). Interestingly, as with the other sequences, KY985361.1 (Haiti, 2014) also showed a higher similarity to its major parent of genotype L. All the recombination events mentioned presented p-values $\leq 4523 \times 10^{-2}$ (Supplementary Table S2), being considered potential recombinant events.

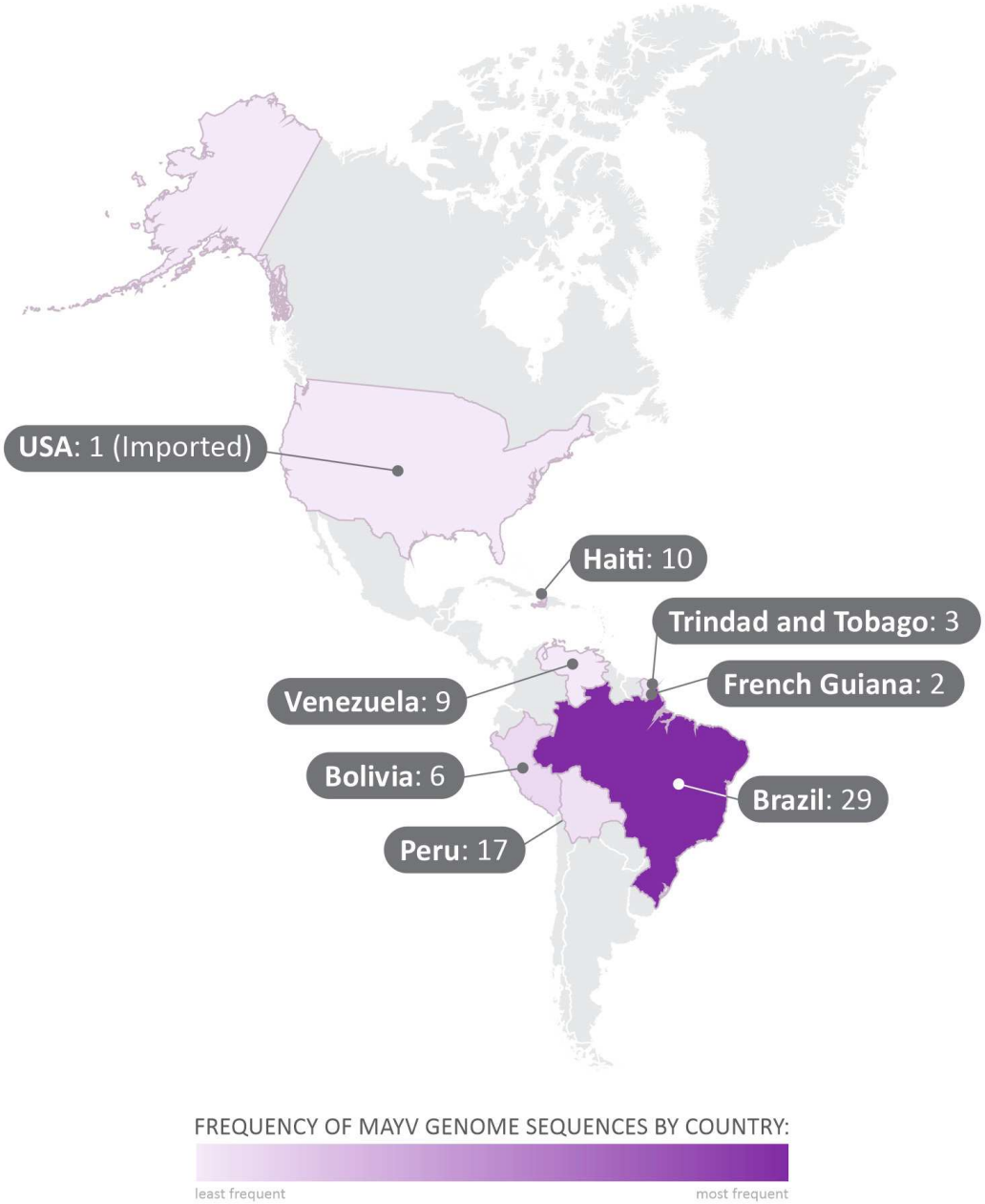

Figure 2. Geographical distribution of the analyzed sequences collected from GenBank. The 71 complete-genome sequences selected in the study were collected between 1954 and 2015, in Brazil, Trinidad and Tobago, Haiti, United States of America (USA), Bolivia, Peru, French Guiana, and Venezuela.

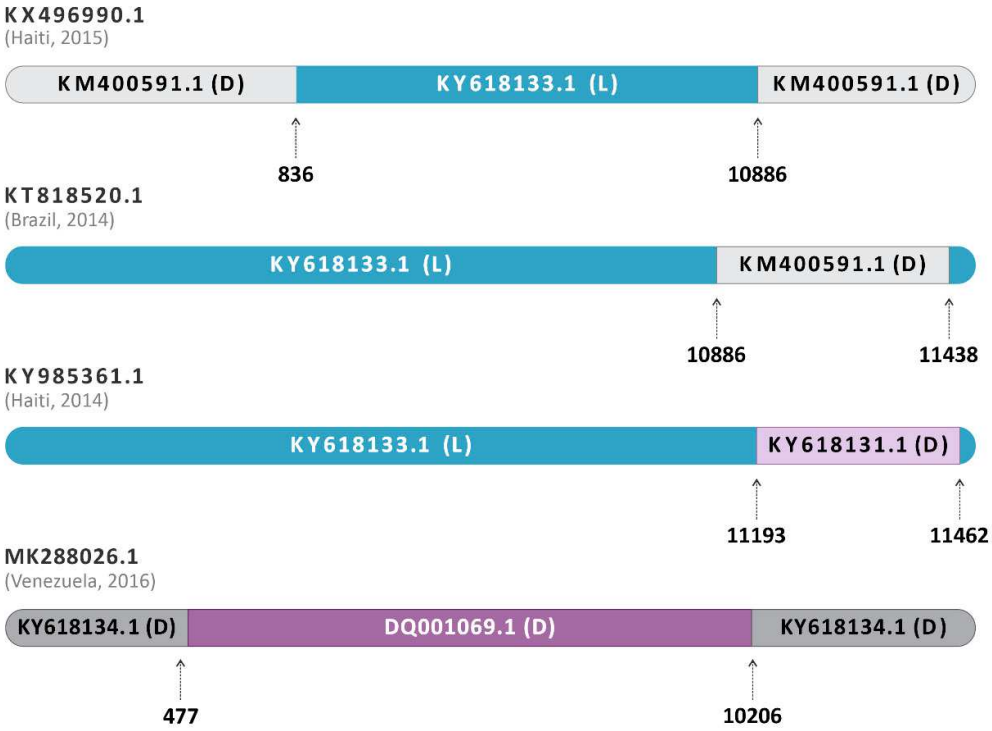

Figure 3. Schematic representation of the recombination event in sequences classified as hybrids. The dataset containing the 71 sequences was submitted to the RDP4 software program v.4.101. KY985361.1, from Haiti, 2014, was identified as an L/D hybrid between the major parent KY618133.1 of Genotype L, Brazil, 1988 (blue) and the minor parent KY618131.1 of Genotype D, Brazil, 1978 (purple). The other hybrids, KX496990.1 (Haiti, 2015) and KT818520.1 (Brazil, 2014), have their L major parents represented in blue and the D minor parents represented in grey. The homologous hybrid MK288026.1 (Venezuela, 2016) had DQ001069.1 (genotype D, French Guiana, 1998) as a major parent and KY618134.1 (genotype D, Brazil, 1991) as a minor parent.

3.3. Phylogenetic Relationships and Coalescent Analysis of MAYV Complete Genomic Sequences

The phylogenetic analysis revealed that sequences were grouped according to the MAYV genotypes (D, L, and N) (Figure 4). Twelve sequences were identified as genotype L, fifty-five as genotype D, and, as previously reported, one was identified as genotype N and three as hybrids L/D [13,14]. Furthermore, in both coalescent and phylogenetic trees, the characterized sequences exhibited a closer grouping with those isolated in the same country and in proximate years (Figures 4 and 5). It suggests that the clustered sequences may have originated from circulating lineages due to the phylogenetic and genomic similarity among the isolates. In this sense, the biggest clade comprehending sequences isolated from Brazil (1981–2011) also present phylogenetic similarity (bootstrap of 94.8) and share the same ancestry, with a time to the most recent common ancestor (tMRCA of 143.75 and posterior probability of 1), indicating the persistent circulation of the virus. Intriguingly, certain groupings within the clusters were associated with notable outbreaks, such as those in Venezuela (2010) and Peru (2010–2013) [26]. It is noteworthy that these strains share a common ancestry with a tMRCA of 73.713 and a high posterior probability of 99.97%. Similarly, six sequences isolated in Brazil (1978) and one from French Guiana (2013) were grouped in the same clade (bootstrap of 100%) and had the same ancestor with a tMRCA of 136.76 and posterior probability of 1, which could indicate the continuous circulation of the virus between countries (Figures 4 and 5).

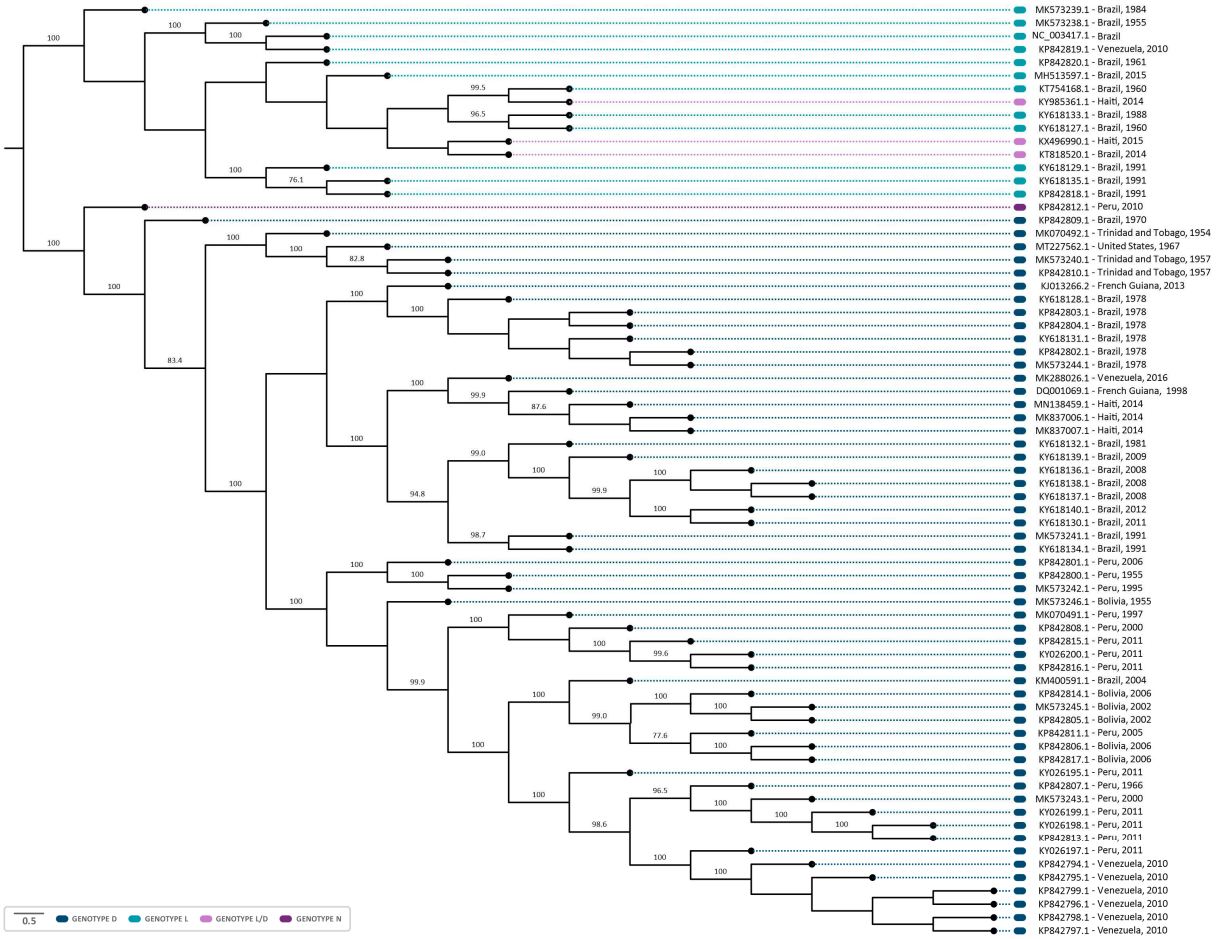

Figure 4. Midpoint-rooted phylogenetic tree reconstruction using 71 sequences of the MAYV complete genome. The sequences were aligned employing the ClustalW multiple alignment method and the phylogenetic tree was reconstructed employing PhyML 3.0, through the ATGC- Montpellier Bioinformatics Platform, using maximum-likelihood analysis (ML), and the GTR + G + I model of substitution, as determined by the Smart Model Selection in PhyML. The NCBI reference sequence NC_003417 (Genotype L) was used as the reference sequence. The sequences from the genotypes D, L, L/D, and N are highlighted in blue, light blue, lilac, and purple, respectively. A thousand replicates were used to test the support given by the data to the clusters of the tree topology, and bootstrap values > 70 were considered significant.

Furthermore, the sequence MT227562.1, isolated from a sample of an allochthonous case in Louisiana (USA), which had no previous description regarding its genotype, formed a cluster with sequences of the genotype D (Figure 4), suggesting this sequence as belonging to this genotype. This strain was closely related to isolates MK070492.1 (1954), MK573240.1 (1957), and MK5732402.1 (1957) from Trinidad and Tobago in the phylogenetic tree, supported by a bootstrap of 100%. The same outcome was observed in a coalescent analysis, with a tMRCA of 71.663 and a posterior probability of 1, indicating that the sequences share the same origin (Figure 5).

Regarding the analysis of genotypes L and N, the lack of sequencing data hindered the undertaking of a coalescent analysis for these specific sequences. The topology of the phylogenetic tree demonstrated that L/D sequences formed a cluster with sequences of the L genotype, suggesting a higher genomic similarity. The sequence KX496990.1–Haiti, 2015 (L/D) showed a phylogenetic proximity with one of the L/D sequences from Brazil (KT818520.1, 2014), (Figure 4). Interestingly, these sequences were collected in subsequent years (2014–2015), which may suggest a possible route of transmission of MAYV.

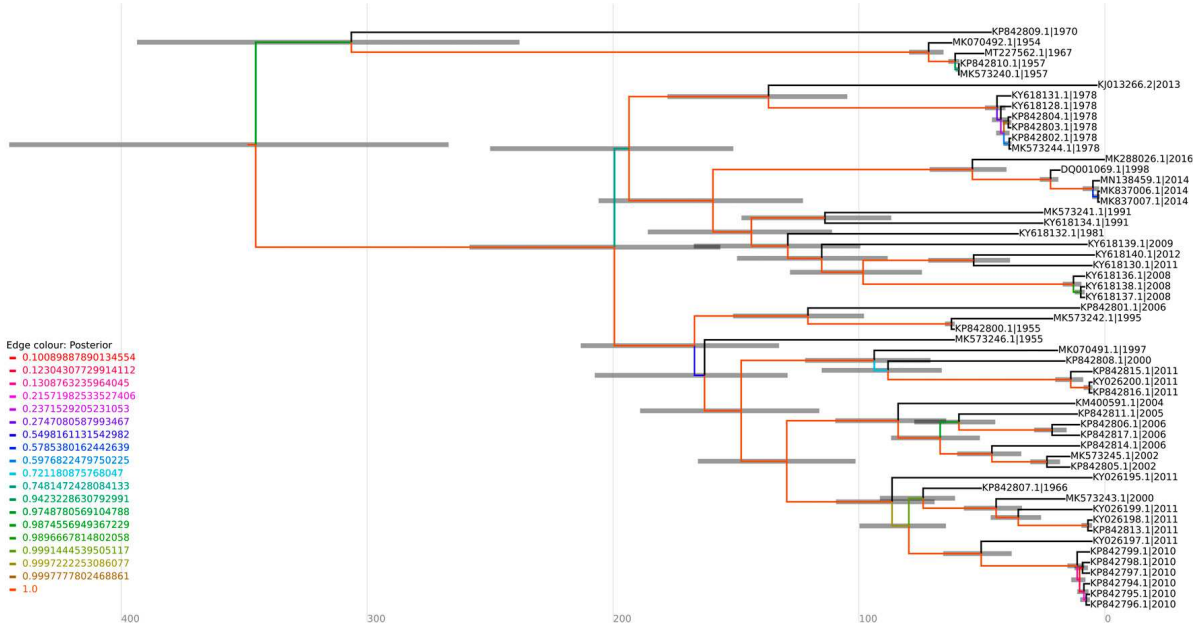

Figure 5. Coalescent analysis of genotype D sequences. The sequences were aligned employing the ClustalW multiple alignment method, and the optimal substitution model for the alignment was assessed using ModelFinder in IQ-TREE v2.1.4-beta (GTR + F + I + G4), generating a maximum likelihood tree. The sequences were submitted to a strict molecular clock using the GTR substitution model.

3.4. Follow-Up of the Amino Acid Substitutions and Selection Pressure among MAYV Sequences

The analysis of the amino acid substitutions and their effects on viral protein structures was performed using the fixed effects likelihood (FEL) and fast unconstrained Bayesian approximation (FUBAR) DataMonkey softwares v. 2.0 to detect the presence of neutral (synonymous), adaptative (non-synonymous), and purifying (non-synonymous) substitutions, under a p-value < 0.05 (Table 1; Figure 6). Additionally, the Bayes factor (BF) was also employed to measure the relative evidence of substitutions, with values higher than 30 characterized as very strong evidence of the positive selection pressure hypothesis at the site [27]. As a result, several substitutions were identified among the MAYV sequences with three of those sites identified to be under positive/adaptative selection (two in genotype D and one in genotype L–L/D) (Table 1; Figure 6). For genotype D, the amino acid substitutions V89M and S190G were observed in nsP1, with a Bayes factor (BF) of 10.065 and 489.759, respectively (Table 1; Figure 6). On the other hand, genotype L demonstrated amino acid substitution in the E1 protein (T300A: BF of 36.041) (Table 1; Figure 3).

Table 1. Sites of the MAYV genome under positive selection pressure based on FUBAR and FEL that presented amino acid substitutions.

Genotype	Protein	Site	Method	Alpha	Beta	Bayes Factor	*p*-Value
D	nsp1	89	FUBAR	0.992	11.058	10.065	<0.05
			FEL	-	-	-	-
		190	FUBAR	0.619	15.575	489.759	<0.05
			FEL	0.000	8.352	n/a	0.0144
L	E1	300	FUBAR	2.252	28.971	36.041	<0.05
			FEL	-	-	-	-

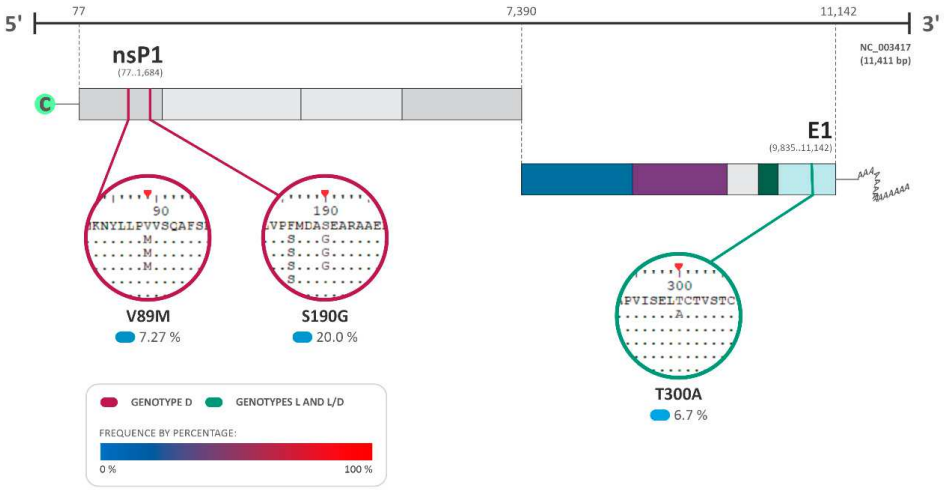

Figure 6. Amino acid substitutions and selection pressure among MAYV sequences. The most relevant amino acid substitutions among the sequences of the complete genome of MAYV that presented positive selection pressure with a *p*-value under 0.05 and a Bayes factor (BF) > 30 are shown (BF of 30–100: very strong evidence for positive selection pressure). DQ001069.1 isolated from a sample of *Homo sapiens* in French Guiana was used as the reference sequence for genotype D. The NCBI reference sequence NC_003417.1 isolated from Brazil was used for genotype L and L/D. The frequency of the substitutions is presented as a percentage, where 0% is represented in light blue and 100% in red.

The sequences of the MAYV genome also presented amino acid substitutions characterized as neutral or under negative selection pressure in all viral proteins. The prevalence of amino acid substitutions was high across most MAYV proteins, particularly within sequences belonging to genotype D, which outnumbered those of genotype L and L/D with 55 sequences compared to 12 sequences, respectively.

The insertion of the amino acids ACQDT (nucleotide sequence: AGCGTGCCAAGACAC) between the amino acid positions 443–444 of the nsP3 was found in three sequences already described as L/D (KX496990.1—Haiti, 2015; KT818520.1—Brazil, 2014; and KY985361.1—Haiti, 2014) (Figure 7). Interestingly, the isolate KM400591.1 (Brazil, 2014), classified as MAYV genotype D, also presented the same insertion and was identified as a minor parent for the heterologous hybrid KX496990.1 (Haiti, 2015), which also presented this characteristic.

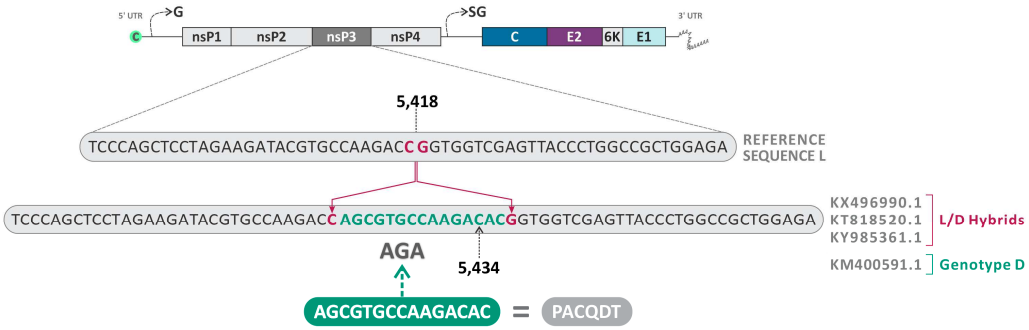

Figure 7. Schematic representation of the nucleotide insertion in the nsP3 observed in the sequences KY985361.1 (Haiti, 2014), KX496990.1 (Haiti, 2015), KT818520.1 (Brazil, 2014), and KM400591.1 (Brazil, 2014).

3.5. Molecular Modeling and Docking

Binding affinity predictions showed that the isolate KT818520.1 (Figure 8) presented the best binding affinity (lowest energy) result among the complexes; however, the reference sequence NC_003417.1 presented the highest number of interactions overall (Table 2).

Interestingly, the sequence MK573239.1, featuring a positive selection site (T300A) on the E1 protein, displayed a binding energy slightly lower than the reference sequence. Another finding was the lower binding affinity observed in the MAYV heterologous hybrids KT818520.1 and KX496990.1, originating from the same parental strains. This affinity was notably lower than that of KY985361.1, which stemmed from the same parental strain of genotype L but was a distinct strain from genotype D. Additionally, the complex of Chikungunya virus E1–E2 and mouse Mxra8 obtained from the protein data bank, used as template in the modeling phase, showed the worst binding affinity (highest energy) and a small number of salt bridges when compared to the human complexes (Table 2).

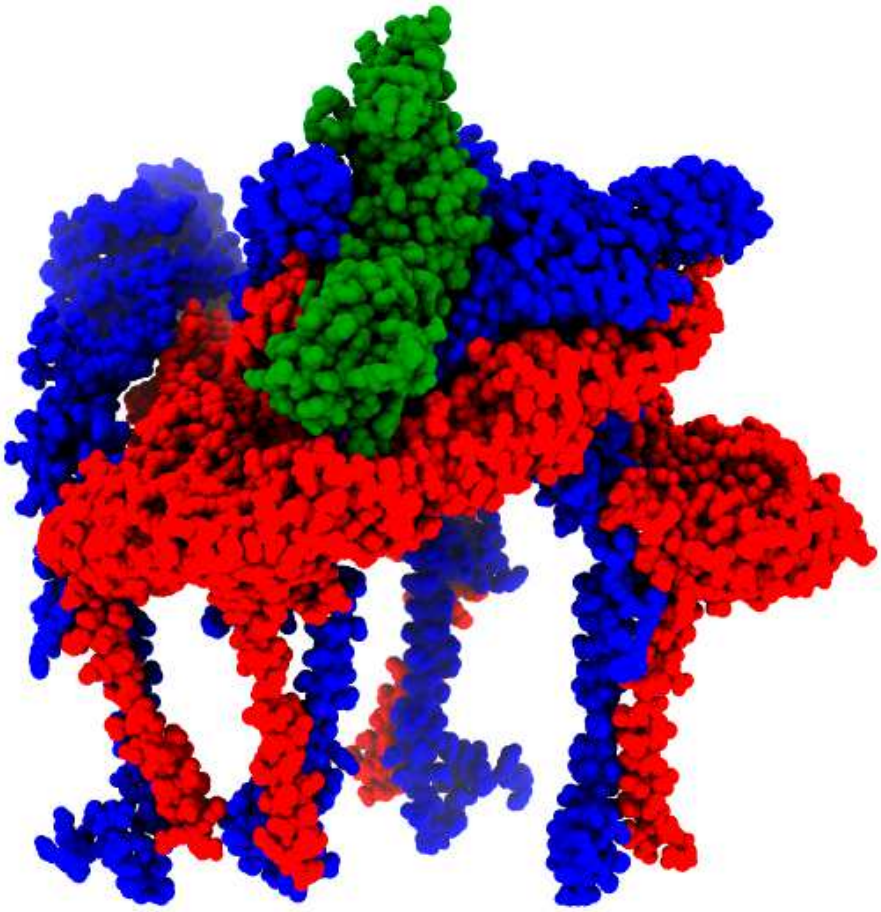

Figure 8. MAYV E1 (red) and E2 (blue) octamer complexed with human Mxra8 (green). The result was generated by MAYV isolate KT818520.1 modeling.

Table 2. E1E2-Mxra8 binding affinity and number of interactions from the different complexes.

Genbank ID	Binding Affinity ΔG (kcal mol^{-1})	Hydrophobic Interaction	Hydrogen Bond	Salt Bridge
KT818520.1	−13.2	8	11	6
KX496990.1	−13.1	9	10	7
MT227562.1	−13.1	9	11	7
MK573239.1	−13.1	9	11	7
NC_003417.1	−13.0	9	12	7
KY985361.1	12.9	9	12	6
DQ001069.1	−12.9	8	10	7
PDB: 6NK7	−11.2	9	12	1

4. Discussion

The incidence of MAYV infections has been mainly described in Latin America, with most Mayaro fever cases reported in Brazil [6]. In agreement with these data, the majority of genomic sequences analyzed here were obtained from samples collected in Brazil, which included MAYV isolates of the genotypes L, D, and L/D. Although most cases of Mayaro fever have been observed in South America, there are reports of outbreaks in Haiti, indicating that the virus is also circulating in Central America [28]. Mayaro fever was likewise reported in Europe [3]; however, there are no epidemiological studies that describe the introduction of the genotypes in the region, or whether the infection has spread by local vectors. Furthermore, to the best of our knowledge, there is no current data on the circulation of MAYV in Africa and Asia, due to the lack of data reported on these continents [1]. It is also observed that there is poorly described information concerning the MAYV strains, such as the N genotype, isolated in Peru in 2010, with no current description of its dissemination degree [2]. Therefore, studies that aim to investigate the epidemiological characteristics of MAYV worldwide, as well as the genetic and phylogenetic relationship among circulating viral strains, are essential.

Here, we analyzed the MAYV genomic variations in sequences from different regions of America and characterized the phylogenetic relationship among these virus strains, to investigate the main evolutionary forces driving the evolution of the viral genome and their possible effect on viral activity, associating them with the dissemination of MAYV. Concerning the genetic variability among the viral genome sequences, it is important to emphasize the higher genetic plasticity and mutational rate of RNA viruses, which leads to an intra-host variability of the viral population, as well as the emergence of new species, genera, and/or new viral families [10,29]. Moreover, arboviruses exhibit bottleneck-mediated drift due to constriction points during vector infection and transmission, as well as within the transmission cycle itself [30]. This dynamic can significantly impact the future of arboviral epidemics and disease outcomes. Herein, a high incidence of polymorphisms was found in MAYV sequences, with several of those substitutions classified within purifying selection sites, which demonstrates mechanisms to eliminate deleterious mutations and maintain the accumulated characteristics of the virus [31]. These polymorphisms were widely observed when the genomic regions related to most viral proteins were evaluated, some of them directly involved in viral replication. This demonstrates an attempt to constrain the variability at the protein level since the negative selection tends to conserve the sequence and the structural characteristics of active motifs of the proteins [32]. The proteins from the replicative complex as well as the structural proteins were found under negative pressure in several positions in almost all analyzed sequences, which may suggest that the circulating genotypes have an adapted fitness. The genetic variability and the evolution potential within a population are the product of a balance of selection and genetic drift [32], and, therefore, further analysis regarding the up and down fluctuation of viral fitness is necessary to achieve knowledge of the gain or loss of function due to substitutions observed over the viral genome. However, the restricted number of sequences of MAYV poses a delay in the analyses of the persistence and disappearance of polymorphisms over time, as well as the difficulty in the suggestion of adaptability to the host, higher transmissibility, or immune escape [33].

Alternatively, we also identified positive selection pressure sites, which drives the accumulation of mutations or genetic variations that confer advantages in the viral population, such as immune evasion and host-jumps [34]. Among the sequences of the genotype L, it was observed only in the sequence MK573239.1 (Brazil, 1984) at the E1 protein. Interestingly, the substitution into the E1 (T300L) protein was not identified by FEL, which utilizes a maximum-likelihood (ML) method to spot genetic variations [21]. In contrast, the polymorphism was identified through the analysis carried out with FUBAR, which produces similar information to FEL but employs a Bayesian approach to infer nonsynonymous (dN) and synonymous (dS) substitution rates [21]. Interestingly, a single mutation in the CHIKV E1 protein (A226V) allowed the virus to infect a new vector species, *Aedes albopictus* [35,36],

facilitating the spread of the virus and leading to outbreaks in non-endemic areas [35]. In this context, given the susceptibility of *Aedes albopictus* and other mosquito species to MAYV infection, coupled with this new mutation found in MAYV E1 protein, it is possible to suggest that a similar outcome might be expected. In addition, the molecular modeling indicated that this positive selection site induced a slightly lower binding energy between the E1–E2 trimmer and the receptor Mxra8, resulting in a higher affinity. However, this polymorphism was not found in other isolates, which may suggest that these substitutions did not sustain their circulation at low frequency. In this sense, these mutations can also be associated with immune response escape, as demonstrated by Earnest and colleagues [37]. Their study evaluated different monoclonal IgG antibodies against the MAYV strain containing substitutions on the E1 protein and only 4 of 18 antibodies demonstrated elite neutralizing activity against this virus [37]. Similarly, Rangel and colleagues pointed out that the single mutations V156A and K211T can influence antibody neutralization against CHIKV and increase virus replication and virulence in mice, emphasizing the role of the mutation in escaping immune response and infectivity increase [36].

In addition, amino acid substitutions identified in the genomic regions of the nsP1 of sequences of genotype D were found to be under positive selection pressure (Figure 2, Supplementary Table S2), suggesting the possible viral adaptability and improvement of fitness during viral replication. The nsP1 protein is directly involved in the initiation of virus replication, responsible for interacting with the inner face of the plasma membrane and promoting the formation of the spherules, which are vesicles where the replicative process initiates [38]. Even though the presence of polymorphisms by positive selective pressure is relevant due to its impact on virus evolution, the low level of positive selection suggests that the amino acid changes have been a result of random genetic drift. Interestingly, the same pattern was seen in other RNA viruses such as the West Nile virus and Hepatitis C virus [39].

Another finding was the insertion of the amino acids ACQDT into nsP3 found in three sequences identified as L/D hybrids (KX496990.1—Haiti, 2015; KT818520.1—Brazil, 2014; and KY985361.1—Haiti, 2014) and one genotype D strain (KM400591.1—Brazil, 2014). A study conducted by Neyret and colleagues demonstrated that the deletion of an upstream FGAP sequence in the G3BP binding sequence present in nsP3 damages the nsP3/G3BP interaction and infectivity of MAYV, resulting in lower rates of viral replication [40]. Differently, in our study, we observed insertions in nsP3 located between positions 443–444, close to the canonical binding site of nsP3 G3BP (associated with residues between 456–478). In this sense, considering that nsP3 plays a critical role in the infectivity of alphaviruses, this insertion may favor the replication of the L/D strains or make them unfeasible.

Our phylogenetic analysis demonstrated that the sequence MT227562.1 was classified as genotype D. This sequence was obtained from a sample of an allochthonous case in Louisiana (USA), isolated from *Icterus spurius*, a bird with a migratory route between Central America, Colombia/Venezuela, and the USA [41]. Furthermore, within the phylogenetic tree, this sequence exhibits a close grouping with sequences isolated in Trinidad and Tobago between 1954 and 1957. Remarkably, our coalescent analysis indicated that these sequences also present a common ancestral source. Therefore, it is possible to infer that the bird was infected in nearby regions of Trinidad and Tobago, and, during its migration to the USA, this led to the insertion of the genotype in the region, given the predominance of genotype D in the Americas.

Furthermore, the L/D sequences were phylogenetically closer to the sequences of genotype L, demonstrating a higher genomic similarity with the L genotype sequences, as indicated by previous studies [13,14]. It is important to emphasize that L/D hybrids were initially classified as members of the L genotype, prior to the recognition of the L/D recombination [42,43]. Among these, KT818520.1 (Brazil, 2014) and KX496990.1 (Haiti, 2015) were identified by RDP4 as potentially originating from the same recombination event, which may suggest a possible route of dissemination of MAYV. Furthermore, the emergence of MAYV recombinants/hybrids demonstrates the potential for the emergence of a future

new genotype and its dissemination, highlighting the need for genomic surveillance for this pathogen. It has also been described for other RNA viruses, such as in Chikungunya virus (CHIKV), that homologous recombination resulted in cross-species transmission, and, therefore, impacted virus evolution, emergence, and epidemiology [44]. In addition, the interspecies recombination was also identified in other types of Alphavirus, such as Eastern equine encephalitis virus (EEEV) and Sindbis-like virus (SIN), originating from the Western equine encephalitis virus (WEEV), Highlands J virus (HJV), and Fort Morgan virus (FMV) [45]. In this context, MAYV recombinants could emerge and spread as new strains with an increased fitness in human and *Haemagogus* vector hosts, as well as adapt to new hosts.

5. Conclusions

In conclusion, the data presented here demonstrate that sequences of the complete genome of MAYV are under negative and positive selection pressures, emphasized by the high number of purifying selection sites, that might result in the emergence of new strains. Moreover, the study highlights the concerning absence of surveillance efforts for MAYV. Despite sequences being collected across decades, they share common ancestors and exhibit phylogenetic proximity, suggesting the sustained circulation of the virus. In this sense, it is essential to diagnose and sequence the MAYV genome to characterize the virus adaptation and transmissibility. Therefore, these data can be used to define the degree of MAYV dissemination and implement protective measures to manage Mayaro fever.

Supplementary Materials: The following supporting information can be downloaded at: https://www.mdpi.com/article/10.3390/v16050809/s1, Table S1: MAYV sequence data from the analyzed sequences. Contains year of collection, origin, genotype, host, size of the sequenced genetic material, reference article for sequencing, and reference of genotype identification.; Table S2: Recombination confirmation provided by RDP4. Presents the recombination event, methods applied, and *p*-value.

Author Contributions: Collation of data and results analysis: M.d.S.M., I.A.S., G.M.F., N.N.-J. and T.d.L.C.; drafting of the manuscript: M.d.S.M., I.A.S., G.M.F.; V.R.G., N.N.-J. and T.d.L.C.; figures: V.R.G.; dtudy design, supervision, and critical revision: I.A.S., G.M.F. and A.C.G.J. All authors have read and agreed to the published version of the manuscript.

Funding: This research received no external funding.

Institutional Review Board Statement: Ethical review and approval were waived for this study due to the absence of the participation of humans and animals.

Informed Consent Statement: Not applicable.

Data Availability Statement: All the sequencing data used in this article can be found at PubMed Genbank database.

Acknowledgments: ACGJ is grateful to Coordenação de Aperfeiçoamento de Pessoal de Nível Superior (CAPES)—Brasil—Prevention and Combat of Outbreaks, Endemics, Epidemics, and Pandemics—Finance Code #88881.506794/2020-01, and to FAPEMIG (Minas Gerais Research Foundation APQ-03385-18). MDSM thanks FAPEMIG for scholarship # 12152. IAS thanks CNPq for scholarship # 142495/2020-4, FAPEMIG # 67355, and CAPES. Print scholarship # 88887.700246/2022-00.4. GMF and VRG thanks CAPES for scholarships # 88887.571465./2020-00 and # 88887.505971/2020–00.

Conflicts of Interest: The authors declare no conflicts of interest.

References

1. Diagne, C.T.; Bengue, M.; Choumet, V.; Hamel, R.; Pompon, J.; Missé, D. Mayaro Virus Pathogenesis and Transmission Mechanisms. *Pathogens* **2020**, *9*, 738. [CrossRef] [PubMed]
2. Caicedo, E.-Y.; Charniga, K.; Rueda, A.; Dorigatti, I.; Mendez, Y.; Hamlet, A.; Carrera, J.-P.; Cucunubá, Z.M. The Epidemiology of Mayaro Virus in the Americas: A Systematic Review and Key Parameter Estimates for Outbreak Modelling. *PLoS Negl. Trop. Dis.* **2021**, *15*, e0009418. [CrossRef] [PubMed]
3. Acosta-Ampudia, Y.; Monsalve, D.M.; Rodríguez, Y.; Pacheco, Y.; Anaya, J.-M.; Ramírez-Santana, C. Mayaro: An Emerging Viral Threat? *Emerg. Microbes Infect.* **2018**, *7*, 1–11. [CrossRef] [PubMed]

4. Lorenz, C.; Freitas Ribeiro, A.; Chiaravalloti-Neto, F. Mayaro Virus Distribution in South America. *Acta Trop.* **2019**, *198*, 105093. [CrossRef] [PubMed]
5. Vieira, C.J.d.S.P.; da Silva, D.J.F.; Barreto, E.S.; Siqueira, C.E.H.; Colombo, T.E.; Ozanic, K.; Schmidt, D.J.; Drumond, B.P.; Mondini, A.; Nogueira, M.L.; et al. Detection of Mayaro Virus Infections during a Dengue Outbreak in Mato Grosso, Brazil. *Acta Trop.* **2015**, *147*, 12–16. [CrossRef] [PubMed]
6. Ganjian, N.; Riviere-Cinnamond, A. Mayaro Virus in Latin America and the Caribbean. *Rev. Panam. Salud Pública* **2020**, *44*, 1. [CrossRef]
7. Diop, F.; Alout, H.; Diagne, C.T.; Bengue, M.; Baronti, C.; Hamel, R.; Talignani, L.; Liegeois, F.; Pompon, J.; Morales Vargas, R.E.; et al. Differential Susceptibility and Innate Immune Response of Aedes Aegypti and Aedes Albopictus to the Haitian Strain of the Mayaro Virus. *Viruses* **2019**, *11*, 924. [CrossRef]
8. Choi, H.; Kudchodkar, S.B.; Reuschel, E.L.; Asija, K.; Borole, P.; Ho, M.; Wojtak, K.; Reed, C.; Ramos, S.; Bopp, N.E.; et al. Protective Immunity by an Engineered DNA Vaccine for Mayaro Virus. *PLoS Negl. Trop. Dis.* **2019**, *13*, e0007042. [CrossRef]
9. Ribeiro-Filho, H.V.; Coimbra, L.D.; Cassago, A.; Rocha, R.P.F.; Guerra, J.V.d.S.; de Felicio, R.; Carnieli, C.M.; Leme, L.; Padilha, A.C.; Paes Leme, A.F.; et al. Cryo-EM Structure of the Mature and Infective Mayaro Virus at 4.4 Å Resolution Reveals Features of Arthritogenic Alphaviruses. *Nat. Commun.* **2021**, *12*, 3038. [CrossRef]
10. Duffy, S. Why Are RNA Virus Mutation Rates so Damn High? *PLoS Biol.* **2018**, *16*, e3000003. [CrossRef]
11. Chesnut, M.; Muñoz, L.S.; Harris, G.; Freeman, D.; Gama, L.; Pardo, C.A.; Pamies, D. In Vitro and In Silico Models to Study Mosquito-Borne Flavivirus Neuropathogenesis, Prevention, and Treatment. *Front. Cell. Infect. Microbiol.* **2019**, *9*, 223. [CrossRef] [PubMed]
12. Hall, T.A. BioEdit: A user-friendly biological sequence alignment editor and analysis program for Windows 95/98/NT. *Nucl. Acids. Symp. Ser.* **1999**, *41*, 95–98.
13. White, S.K.; Mavian, C.; Elbadry, M.A.; Beau De Rochars, V.M.; Paisie, T.; Telisma, T.; Salemi, M.; Lednicky, J.A.; Morris, J.G. Detection and Phylogenetic Characterization of Arbovirus Dual-Infections among Persons during a Chikungunya Fever Outbreak, Haiti 2014. *PLoS Negl. Trop. Dis.* **2018**, *12*, e0006505. [CrossRef] [PubMed]
14. Mavian, C.; Rife, B.D.; Dollar, J.J.; Cella, E.; Ciccozzi, M.; Prosperi, M.C.F.; Lednicky, J.; Morris, J.G.; Capua, I.; Salemi, M. Emergence of Recombinant Mayaro Virus Strains from the Amazon Basin. *Sci. Rep.* **2017**, *7*, 8718. [CrossRef] [PubMed]
15. Martin, D.P.; Murrell, B.; Golden, M.; Khoosal, A.; Muhire, B. RDP4: Detection and Analysis of Recombination Patterns in Virus Genomes. *Virus Evol.* **2015**, *1*, vev003. [CrossRef] [PubMed]
16. Guindon, S.; Dufayard, J.-F.; Lefort, V.; Anisimova, M.; Hordijk, W.; Gascuel, O. New Algorithms and Methods to Estimate Maximum-Likelihood Phylogenies: Assessing the Performance of PhyML 3.0. *Syst. Biol.* **2010**, *59*, 307–321. [CrossRef] [PubMed]
17. Lefort, V.; Longueville, J.-E.; Gascuel, O. SMS: Smart Model Selection in PhyML. *Mol. Biol. Evol.* **2017**, *34*, 2422–2424. [CrossRef] [PubMed]
18. Vaughan, T.G. IcyTree: Rapid Browser-Based Visualization for Phylogenetic Trees and Networks. *Bioinformatics* **2017**, *33*, 2392–2394. [CrossRef]
19. Delport, W.; Poon, A.F.Y.; Frost, S.D.W.; Kosakovsky Pond, S.L. Datamonkey 2010: A Suite of Phylogenetic Analysis Tools for Evolutionary Biology. *Bioinformatics* **2010**, *26*, 2455–2457. [CrossRef]
20. Grosche, V.R.; Santos, I.A.; Ferreira, G.M.; Dutra, J.V.R.; Costa, L.C.; Nicolau-Junior, N.; Queiroz, A.T.L.; José, D.P.; Jardim, A.C.G. Insights on the SARS-CoV-2 Genome Variability: The Lesson Learned in Brazil and Its Impacts on the Future of Pandemics. *Microb. Genom.* **2021**, *7*, 000656. [CrossRef]
21. Murrell, B.; Moola, S.; Mabona, A.; Weighill, T.; Sheward, D.; Kosakovsky Pond, S.L.; Scheffler, K. FUBAR: A Fast, Unconstrained Bayesian AppRoximation for Inferring Selection. *Mol. Biol. Evol.* **2013**, *30*, 1196–1205. [CrossRef] [PubMed]
22. Waterhouse, A.; Bertoni, M.; Bienert, S.; Studer, G.; Tauriello, G.; Gumienny, R.; Heer, F.T.; de Beer, T.A.P.; Rempfer, C.; Bordoli, L.; et al. SWISS-MODEL: Homology Modelling of Protein Structures and Complexes. *Nucleic Acids Res.* **2018**, *46*, W296–W303. [CrossRef] [PubMed]
23. Xue, L.C.; Rodrigues, J.P.; Kastritis, P.L.; Bonvin, A.M.; Vangone, A. PRODIGY: A Web Server for Predicting the Binding Affinity of Protein–Protein Complexes. *Bioinformatics* **2016**, *32*, 3676–3678. [CrossRef] [PubMed]
24. Adasme, M.F.; Linnemann, K.L.; Bolz, S.N.; Kaiser, F.; Salentin, S.; Haupt, V.J.; Schroeder, M. PLIP 2021: Expanding the Scope of the Protein–Ligand Interaction Profiler to DNA and RNA. *Nucleic Acids Res* **2021**, *49*, W530–W534. [CrossRef] [PubMed]
25. Pettersen, E.F.; Goddard, T.D.; Huang, C.C.; Meng, E.C.; Couch, G.S.; Croll, T.I.; Morris, J.H.; Ferrin, T.E. UCSF ChimeraX: Structure Visualization for Researchers, Educators, and Developers. *Protein Sci.* **2021**, *30*, 70–82. [CrossRef] [PubMed]
26. Pezzi, L.; Rodriguez-Morales, A.J.; Reusken, C.B.; Ribeiro, G.S.; LaBeaud, A.D.; Lourenço-de-Oliveira, R.; Brasil, P.; Lecuit, M.; Failloux, A.B.; Gallian, P.; et al. GloPID-R Report on Chikungunya, o'nyong-Nyong and Mayaro Virus, Part 3: Epidemiological Distribution of Mayaro Virus. *Antivir. Res.* **2019**, *172*, 104610. [CrossRef] [PubMed]
27. Dittrich, D.; Leenders, R.T.A.J.; Mulder, J. Network Autocorrelation Modeling: A Bayes Factor Approach for Testing (Multiple) Precise and Interval Hypotheses. *Sociol. Methods Res.* **2019**, *48*, 642–676. [CrossRef]
28. Blohm, G.; Elbadry, M.A.; Mavian, C.; Stephenson, C.; Loeb, J.; White, S.; Telisma, T.; Chavannes, S.; Beau De Rochar, V.M.; Salemi, M.; et al. Mayaro as a Caribbean Traveler: Evidence for Multiple Introductions and Transmission of the Virus into Haiti. *Int. J. Infect. Dis.* **2019**, *87*, 151–153. [CrossRef] [PubMed]

29. Higuera, A.; Ramírez, J.D. Molecular Epidemiology of Dengue, Yellow Fever, Zika and Chikungunya Arboviruses: An Update. *Acta Trop.* **2019**, *190*, 99–111. [CrossRef]
30. Weaver, S.C.; Forrester, N.L.; Liu, J.; Vasilakis, N. Population Bottlenecks and Founder Effects: Implications for Mosquito-Borne Arboviral Emergence. *Nat. Rev. Microbiol.* **2021**, *19*, 184–195. [CrossRef]
31. Lin, J.-J.; Bhattacharjee, M.J.; Yu, C.-P.; Tseng, Y.Y.; Li, W.-H. Many Human RNA Viruses Show Extraordinarily Stringent Selective Constraints on Protein Evolution. *Proc. Natl. Acad. Sci. USA* **2019**, *116*, 19009–19018. [CrossRef] [PubMed]
32. Domingo, E.; Escarmís, C.; Sevilla, N.; Baranowski, E. Population Dynamics in the Evolution of RNA Viruses. In *Coronaviruses and Arteriviruses. Advances in Experimental Medicine and Biology*; Springer: Boston, MA, USA, 1998; pp. 721–727.
33. Cong, M.; Heneine, W.; García-Lerma, J.G. The Fitness Cost of Mutations Associated with Human Immunodeficiency Virus Type 1 Drug Resistance Is Modulated by Mutational Interactions. *J. Virol.* **2007**, *81*, 3037–3041. [CrossRef] [PubMed]
34. Poirier, E.Z.; Vignuzzi, M. Virus Population Dynamics during Infection. *Curr. Opin. Virol.* **2017**, *23*, 82–87. [CrossRef] [PubMed]
35. Tsetsarkin, K.A.; Vanlandingham, D.L.; McGee, C.E.; Higgs, S. A Single Mutation in Chikungunya Virus Affects Vector Specificity and Epidemic Potential. *PLoS Pathog.* **2007**, *3*, e201. [CrossRef] [PubMed]
36. Rangel, M.V.; McAllister, N.; Dancel-Manning, K.; Noval, M.G.; Silva, L.A.; Stapleford, K.A. Emerging Chikungunya Virus Variants at the E1-E1 Interglycoprotein Spike Interface Impact Virus Attachment and Inflammation. *J. Virol.* **2022**, *96*, e0158621. [CrossRef] [PubMed]
37. Earnest, J.T.; Basore, K.; Roy, V.; Bailey, A.L.; Wang, D.; Alter, G.; Fremont, D.H.; Diamond, M.S. Neutralizing Antibodies against Mayaro Virus Require Fc Effector Functions for Protective Activity. *J. Exp. Med.* **2019**, *216*, 2282–2301. [CrossRef]
38. Zhang, K.; Law, Y.-S.; Law, M.C.Y.; Tan, Y.B.; Wirawan, M.; Luo, D. Structural Insights into Viral RNA Capping and Plasma Membrane Targeting by Chikungunya Virus Nonstructural Protein 1. *Cell Host Microbe* **2021**, *29*, 757–764.e3. [CrossRef] [PubMed]
39. Beasley, D.W.C.; Davis, C.T.; Guzman, H.; Vanlandingham, D.L.; Travassos da Rosa, A.P.A.; Parsons, R.E.; Higgs, S.; Tesh, R.B.; Barrett, A.D.T. Limited Evolution of West Nile Virus Has Occurred during Its Southwesterly Spread in the United States. *Virology* **2003**, *309*, 190–195. [CrossRef]
40. Neyret, A.; Bernard, E.; Aïqui-Reboul-Paviet, O.; Bakhache, W.; Eldin, P.; Chaloin, L.; Briant, L. Identification of a Non-Canonical G3BP-Binding Sequence in a Mayaro Virus NsP3 Hypervariable Domain. *Front. Cell. Infect. Microbiol.* **2022**, *12*, 958176. [CrossRef]
41. DeBrock, S.; Cohen, E.; Balasubramanian, S.; Marra, P.P.; Hamer, S.A. Characterization of the Plasmodium and Haemoproteus Parasite Community in Temperate-Tropical Birds during Spring Migration. *Int. J. Parasitol. Parasites Wildl.* **2021**, *15*, 12–21. [CrossRef]
42. Lednicky, J.; de Rochars, V.M.B.; Elbadry, M.; Loeb, J.; Telisma, T.; Chavannes, S.; Anilis, G.; Cella, E.; Ciccozzi, M.; Okech, B.; et al. Mayaro Virus in Child with Acute Febrile Illness, Haiti, 2015. *Emerg. Infect. Dis.* **2016**, *22*, 2000–2002. [CrossRef] [PubMed]
43. Mota, M.T.O.; Vedovello, D.; Estofolete, C.; Malossi, C.D.; Araújo, J.P.; Nogueira, M.L. Complete Genome Sequence of Mayaro Virus Imported from the Amazon Basin to São Paulo State, Brazil. *Genome Announc.* **2015**, *3*, e01341-15. [CrossRef] [PubMed]
44. Casal, P.E.; Chouhy, D.; Bolatti, E.M.; Perez, G.R.; Stella, E.J.; Giri, A.A. Evidence for Homologous Recombination in Chikungunya Virus. *Mol. Phylogenet. Evol.* **2015**, *85*, 68–75. [CrossRef] [PubMed]
45. Allison, A.B.; Stallknecht, D.E.; Holmes, E.C. Evolutionary Genetics and Vector Adaptation of Recombinant Viruses of the Western Equine Encephalitis Antigenic Complex Provides New Insights into Alphavirus Diversity and Host Switching. *Virology* **2015**, *474*, 154–162. [CrossRef] [PubMed]

Disclaimer/Publisher's Note: The statements, opinions and data contained in all publications are solely those of the individual author(s) and contributor(s) and not of MDPI and/or the editor(s). MDPI and/or the editor(s) disclaim responsibility for any injury to people or property resulting from any ideas, methods, instructions or products referred to in the content.

Archives of Microbiology (2023) 205:106
https://doi.org/10.1007/s00203-023-03441-y

MINI REVIEW

An update on the development of antiviral against Mayaro virus: from molecules to potential viral targets

Marina Paschoalino[1] · Mikaela dos Santos Marinho[1] · Igor Andrade Santos[1] · Victória Riquena Grosche[1,2] · Daniel Oliveira Silva Martins[1,2] · Rafael Borges Rosa[3,4] · Ana Carolina Gomes Jardim[1,2]

Received: 19 November 2022 / Revised: 16 January 2023 / Accepted: 15 February 2023 / Published online: 7 March 2023
© The Author(s), under exclusive licence to Springer-Verlag GmbH Germany, part of Springer Nature 2023

Abstract

Mayaro virus (MAYV), first isolated in 1954 in Trinidad and Tobago islands, is the causative agent of Mayaro fever, a disease characterized by fever, rashes, headaches, myalgia, and arthralgia. The infection can progress to a chronic condition in over 50% of cases, with persistent arthralgia, which can lead to the disability of the infected individuals. MAYV is mainly transmitted through the bite of the female *Haemagogus* spp. mosquito genus. However, studies demonstrate that *Aedes aegypti* is also a vector, contributing to the spread of MAYV beyond endemic areas, given the vast geographical distribution of the mosquito. Besides, the similarity of antigenic sites with other *Alphavirus* complicates the diagnoses of MAYV, contributing to underreporting of the disease. Nowadays, there are no antiviral drugs available to treat infected patients, being the clinical management based on analgesics and non-steroidal anti-inflammatory drugs. In this context, this review aims to summarize compounds that have demonstrated antiviral activity against MAYV in vitro, as well as discuss the potentiality of viral proteins as targets for the development of antiviral drugs against MAYV. Finally, through rationalization of the data presented herein, we wish to encourage further research encompassing these compounds as potential anti-MAYV drug candidates.

Keywords Mayaro fever · Mayaro virus · Antiviral · Natural and synthetic compounds · Viral targets

Introduction

The Mayaro virus (MAYV) belongs to the *Togaviridae* family and *Alphavirus* genus, which is composed of a positive single-stranded RNA of 11,5 kb in length, covered by an icosahedral capsid and viral envelope (Fig. 1) (Diagne et al. 2020). It was first isolated in 1954 in Trinidad and Tobago islands from the blood of five febrile rural workers (Anderson et al. 1957). Since then, sporadic outbreaks have been identified in countries with tropical forests, including Brazil, Bolivia, Suriname, Peru, Equator, Venezuela, and recently Haiti (Aguilar-Luis et al. 2020). In addition, cases in North America (Taylor et al. 2005) and Europe (Theilacker et al. 2013) were reported in citizens who traveled to South America.

MAYV belongs to the Semliki Complex, a subgroup of the *Alphavirus* genus that includes Bebaru virus, Chikungunya virus (CHIKV), Getah virus, Una Forest virus (UNAV), O'nyong-nyong virus, among others. Viruses from this complex are classified into the same serological group, sharing common antigenic sites, resulting in cross-reactivity in conventional serological tests, complicating the accurate diagnosis of MAYV infections and the underreporting of the disease (Acosta-Ampudia et al. 2018).

MAYV infection is the causative agent of the Mayaro Fever, a disease characterized by acute fever, rashes, headache, retro-orbital pain, nausea, diarrhea, myalgia, and arthralgia (Acosta-Ampudia et al. 2018) that remain for months or years in over 50% of cases (Mackay and Arden

Marina Paschoalino and Mikaela dos Santos Marinho contributed equally to this work.

✉ Ana Carolina Gomes Jardim
jardim@ufu.br

[1] Institute of Biomedical Science, Federal University of Uberlândia, Uberlândia, Minas Gerais, Brazil

[2] Institute of Biosciences, Humanities and Exact Sciences, São Paulo State University, São José do Rio Preto, São Paulo, Brazil

[3] Institute Aggeu Magalhães, Fiocruz Pernambuco, Recife, Pernambuco, Brazil

[4] Rodents Animal Facilities Complex, Federal University of Uberlândia, Uberlândia, Minas Gerais, Brazil

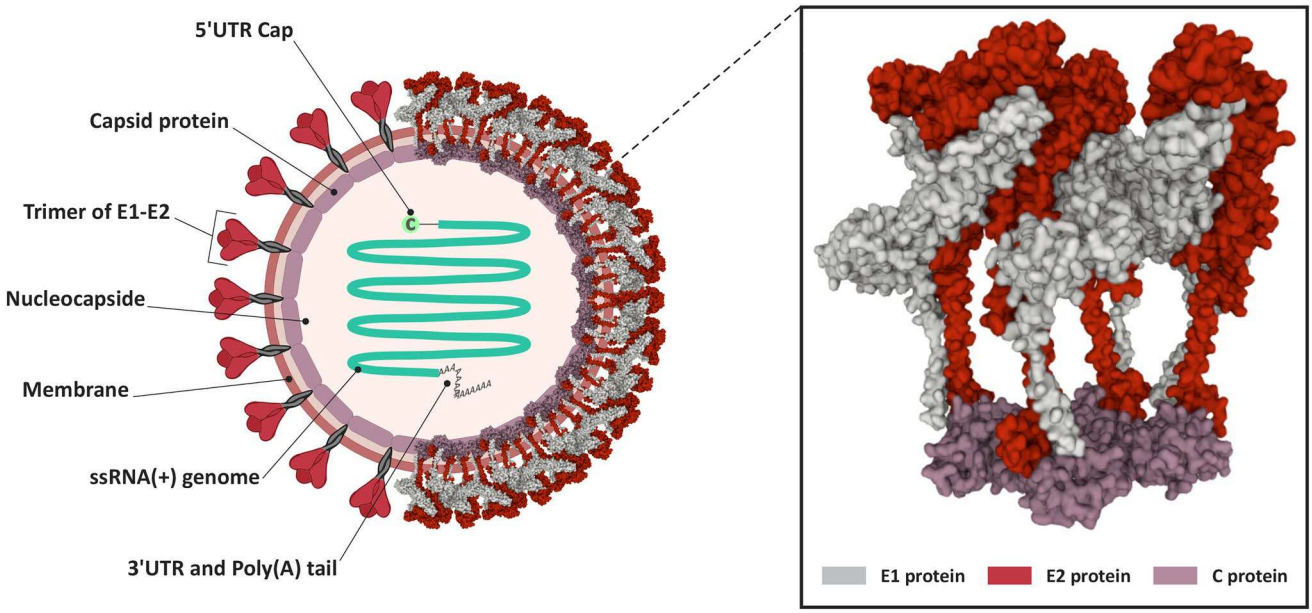

Fig. 1 Schematic structure of MAYV virion. Electron microscopy data show that the viral particle is about 70 nm in diameter. The virion is composed of a positive single-stranded RNA with an icosahedral capsid formed by the capsid protein (C), covered by an envelope membrane inserted of the E1, E2, and E3 glycoproteins. The E3 protein is not shown since it detaches from the E2 protein at the viral surface during maturation (Ribeiro-Filho et al. 2021). Viral structure was based on Cryo-EM structure of mature MAYV (PDB ID: 7KO8) (Ribeiro-Filho et al. 2021)

2016; Li et al. 2019), culminating in physical disability (Ferreira et al. 2018). In severe cases, Mayaro fever can cause intermittent fever, neurological complications, myocarditis, and ultimately death (Acosta-Ampudia et al. 2018).

MAYV is transmitted through the bite of the *Haemagogus* spp. mosquito, usually from infected non-human primates, birds, rodents, and small mammals to susceptible humans (Esposito and Fonseca 2017). The vector competence of Aedes aegypti mosquitoes in the transmission of MAYV is also known, and considering the wide geographic distribution of the Aedes genus, there is a concern about virus spread beyond endemic areas (Long et al. 2011; Choi et al. 2019).

The MAYV replication begins with virus entry into the host cells via specific receptors on the cell surface, such as MXRA8, triggering clathrin-mediated endocytosis or, alternatively, through a caveolin-coated pit (Carvalho et al. 2017; Zhang et al. 2018). Through pH changes in the endosome, the interaction between the endosome membrane and the viral envelope leads to the viral RNA release into the cytoplasm. MAYV RNA is composed of two open reading frames (ORFs). The first ORF is translated in the non-structural viral proteins (nsP) nsP1, nsP2, nsP3, and nsP4, which form the replicative complex (RC), responsible to produce a negative strand from the viral genome, that serves as templates for the synthesis of new positive-sense strands, besides the sub-genomic 26S RNA (Diagne et al. 2020). The other ORF is transcribed from the negative strand, and translated into a polyprotein which is cleaved to the structural proteins C, E1, E2, E3, and 6K (viroporin). Additionally, a frameshift event occurs during translation of the 6K gene, yielding the production of the transframe (TF) protein, comprised of a C-terminal extension of the 6K protein in the −1 ORF. TF protein has been associated with *alphavirus* budding efficiency and/or assembly (Firth et al. 2008; Snyder et al. 2013). The replication process is followed by the assembling of the viral components and virus release through budding in mammalian cells membrane (Jose et al. 2017; Brown et al. 2018) (Fig. 2), or through an alternative exocytosis pathway in insect cells (Acosta-Ampudia et al. 2018).

Despite the chronic condition of a high number of MAYV infections, there is no licensed antiviral against Mayaro fever. The treatment is palliative and consists in managing the symptoms using analgesics and/or non-steroidal anti-inflammatory drugs (Sun and Wu 2019). Therefore, research data have been produced on the potential of natural and synthetic molecules against MAYV. Here we summarize the natural and synthetic compounds previously described to possess antiviral activity against MAYV (Table 1). Thus, we critically compare molecules that could be further investigated in vivo and suggest protein targets to be further evaluated as anti-MAYV molecules. Finally, we aim to encourage further research encompassing these compounds as potential anti-MAYV drug candidates to treat infected patients.

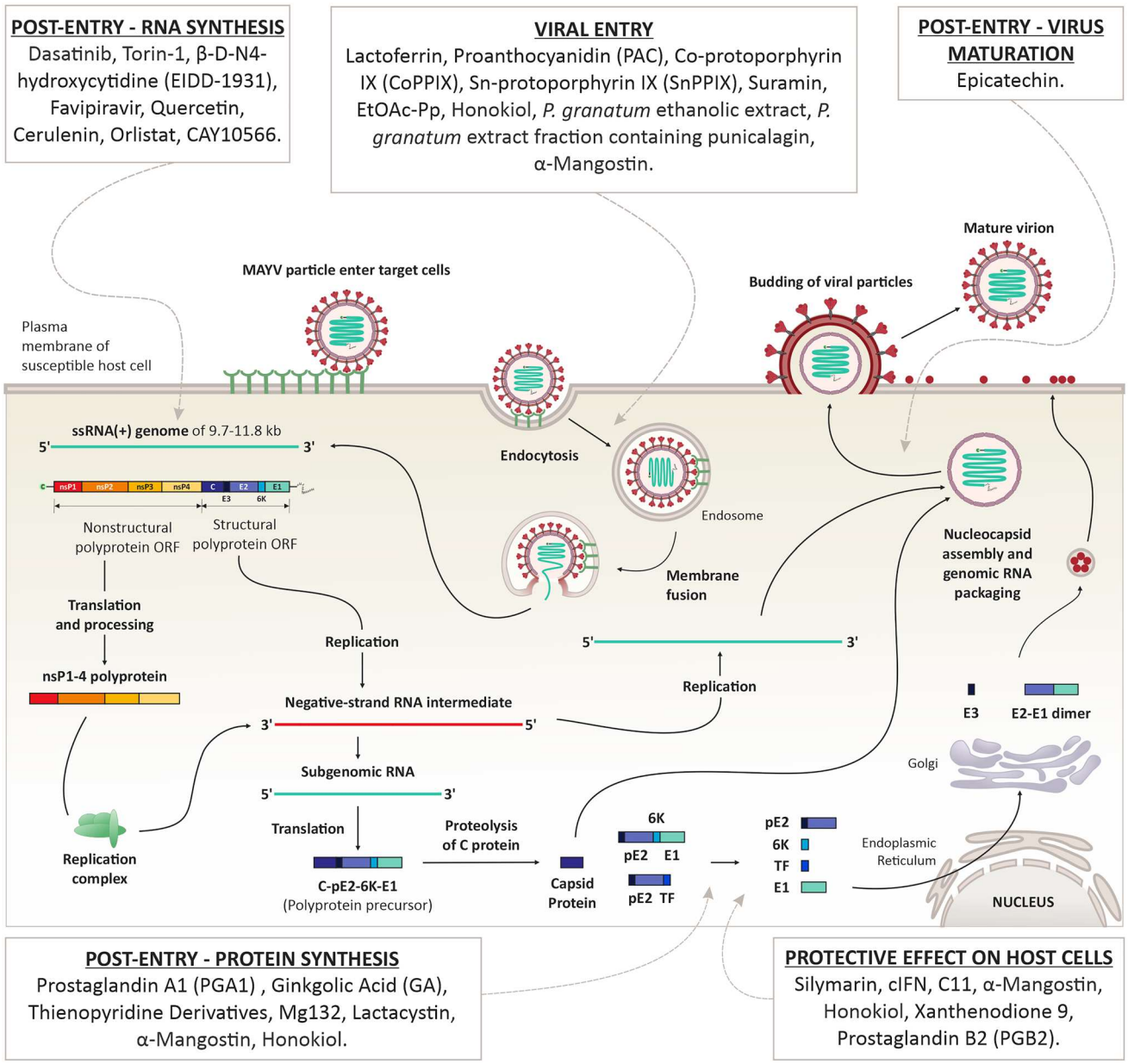

Fig. 2 Schematic representation of MAYV replicative cycle. The replicative cycle and genomic structure of MAYV. *E* envelope, *nsP* nonstructural protein, *UTR* untranslated region, *nt* nucleotides. MAYV attaches to the host cells through the interaction between the host receptors and glycoproteins. Endocytosis occurs through a clathrin-coated pit or, alternatively, a caveolin-coated pit; virus internalization starts after interaction with host cell receptors; the low pH in the endosome leads to structural modifications in the viral envelope that reveal the E1. The latter mediates cell membrane-virus fusion, and later, endosomal cell membrane-virus fusion. Viral uncoating results in the release of the viral genome, and the replication stage occurs (translation and transcription). From the RNA of the virus, nsP precursors are generated; the replication complex is obtained from nsP proteins. This complex thus allows the synthesis of a minus-strand RNA, and it is used as the template to generate both genomic and subgenomic RNAs. Polyprotein precursor is cleaved by an autoproteolytic serine protease; and genomic RNA involved in nucleocapsid core assembly and genomic RNA packaging. Maturation of glycoproteins pE2 and E1 occurs. In the Golgi, processed glycoproteins are associated. Then they are transported into the cell membrane. At the cell membrane, the pE2 is split into E2 and E3; there is also the association of the viral RNA with the capsid C and the recruitment of E1 allows viral assembly. Last, particles of MAYV associated with the core are released outside of the host cell through the membrane. Compounds with antiviral activity against MAYV are indicated in each step of the virus replication cycle: (i) Viral Entry; (ii) Post-Entry (Maturation, RNA and Protein Synthesis); and (iii) Protective Effect on Host Cells. Viral cycle was based on the work of Diagne and colleagues (Diagne et al. 2020)

Table 1 Compounds with antiviral activity against MAYV

Compound*	Chemical Structure	Structure Reference	Antiviral activity Reference	Inhibition	Mechanism	EC_{50}	CC_{50}	Cell lineage
Prostaglandin A1 (PGA1)	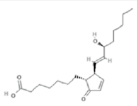	PubChem CID: 5281912 (Kim et al. 2021)	(Ishimaru et al. 1998; Burlandy and Rebello 2001; Caldas et al. 2018)	Post-entry	Reduction in the synthesis of E1, E2, C, and in the precursors of virus proteins	3 µg/mL	ND	Vero
						1 µg/mL	ND	Hep-2
						3 µg/mL	ND	Vero
Prostaglandin B2 (PGB2)	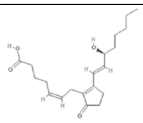	PubChem CID: 5280881 (Kim et al. 2021)	(Ishimaru et al. 1998)	Host cells	ND	8 µg/mL	ND	Vero
Lactoferrin	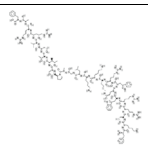	PubChem CID: 126456119 (Kim et al. 2021)	(Carvalho et al. 2014)	Viral Entry	Prevents the viral entrance	ND	ND	Vero
Proanthocyanidin (PAC)	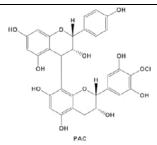	(Ferraz et al. 2019)	(Ferraz et al. 2019)	Viral Entry	Interacts with proanthocyanins on the envelope glycoproteins, preventing viral entry	37.9 µM	> 1640 µM	Vero
Ginkgolic Acid (GA)	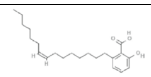	PubChem CID: 5281858 (Kim et al. 2021)	(Campos et al. 2020)	Post-entry	Inhibits the initial stages of the viral cycle, and suppresses the expression of E1 and E2 viral proteins	ND	ND	Vero, HeLa
Silymarin	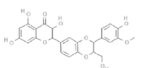	PubChem CID: 5213 (Kim et al. 2021)	(Camini et al. 2018)	Host cells	Decreases virus-induced oxidative stress on host cells associated with the antiviral activity	3.58 µg/ml	103.5 µg/mL	HepG2
Thienopyridine Derivative 104	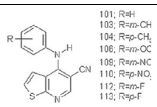	(Amorim et al. 2017)	(Amorim et al. 2017)	Post-entry	Decreases viral protein synthesis	20.0 µM	2500 µM	Vero
Co-protoporphyrin IX (CoPPIX)	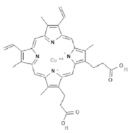	PubChem CID: 3000479 (Kim et al. 2021)	(Neris et al. 2018)	Viral Entry	Impairs viral entry and adsorption	5.94 µM - without light	762.3 µM - without light	BHK-21, Vero
						7.48 µM - with light	1018 µM - with light	
Sn-protoporphyrin IX (SnPPIX)	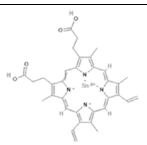	PubChem CID: 3000478 (Kim et al. 2021)	(Neris et al. 2018)	Viral Entry	Impairs viral entry and adsorption	5.99 µM - without light	816 µM - without light	BHK-21, Vero
					Generates ROS	0.09 µM - with light	20.7 µM - with light	
Dasatinib	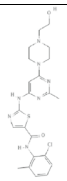	PubChem CID: 3062316 (Kim et al. 2021)	(Broeckel et al. 2019)	Post-entry	Blocks the subgenomic RNA translation, impairing viral replication	ND	ND	ND

Natural compounds as inhibitors of the replicative cycle of MAYV

Some of the first natural molecules tested for their potential to inhibit MAYV replication in vitro were Prostaglandin A1 (PGA1) and Prostaglandin B2 (PGB2) (Ishimaru et al. 1998). PGA1, a natural molecule that possesses a hormone-like lipid structure, is produced by cells in the presence of injury and/or inflammation (Caldas et al. 2018). Alternatively, PGB2 is a lipid mediator

Table 1 (continued)

Torin-1	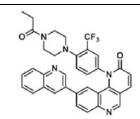	(Sun et al. 2015)	(Broeckel et al. 2019)	Post-entry	Blocks the subgenomic RNA translation, impairing viral replication	ND	ND	ND
β-D-N4-hydroxycytidine (EIDD-1931)	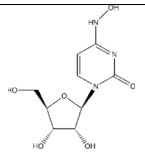	(Agostini et al. 2019)	(Langendries et al. 2021)	Post-entry	Impairs viral RNA synthesis, resulting in non-functional copied viruses	1.6 µM	> 100 µM	Vero
Favipiravir	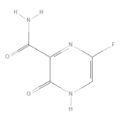	PubChem CID: 492405 (Kim et al. 2021)	(Langendries et al. 2021)	Post-entry	Impairs viral RNA synthesis, resulting in non-functional copied viruses	79 µM	2837 µM	Vero
Suramin	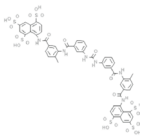	PubChem CID: 5361 (Kim et al. 2021)	(Langendries et al. 2021)	Viral Entry	Inhibits viral entry	124 µM	> 2000 µM	Vero
9-(5-(4-chlorophenyl]furan-2-yl)-3,6-dimethyl-3,4,5,6,7,9-hexahydro-1H-xanthene-1,8(2))-dione (Xantenedione)	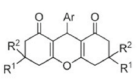	(Fernandes et al. 2021)	(Fernandes et al. 2021)	Host Cells and post-entry	Inhibits viral in pretreatment and post-entry assay.	21,5 µM	338.8 µM	Vero
Quercetin	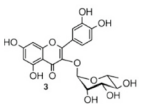	(dos Santos et al. 2014)	(dos Santos et al. 2014)	Post-entry	Binds to viral RNA, inhibition RNA metabolism	10 µM ND	941 µM ND	Vero HEK293T
***n*-BuOH**	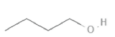	PubChem CID: 263 (Kim et al. 2021)	(dos Santos et al. 2014)	ND	ND	7.1 µM 3.0 µM	2614 µM 418 µM	Vero Vero
EtOAc	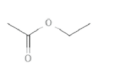	PubChem CID: 8857 (Kim et al. 2021)	(dos Santos et al. 2014)	ND	ND	8.2 µM 5.0 µM	457.7 µM 3116 µM	Vero Vero
EtOAc-Pp	NA	NA	(dos Santos et al. 2014)	Viral Entry	Impairs viral entry and adsorption	2.5 µM	324.1 µM	Vero
cIFN	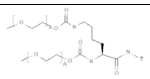	PubChem SID: 135347948 (Kim et al. 2021)	(Grabarz et al 2021)	Host cells	ND	3,57 X 10^{-7} µg/mL	ND	Vero
MG132	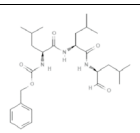	PubChem CID: 462382 (Kim et al. 2021)	(Llamas-González et al. 2019)	Post entry	Reduces the expression of viral proteins nsP1 and E1	ND	ND	Vero-E6, HeLa
Lactacystin	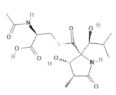	PubChem CID: 6610292 (Kim et al. 2021)	(Llamas-González et al. 2019)	Post entry	Reduces the expression of viral proteins nsP1 and E1	ND	ND	Vero-E6, HeLa
Cerulenin	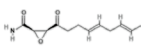	PubChem CID: 5282054 (Kim et al. 2021)	(Bakhache et al. 2019)	Post entry	Decreases genome replication due to manipulation of FASN enzymatic activity.	ND	ND	HEK293T

Table 1 (continued)

Orlistat	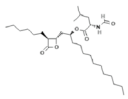	PubChem CID: 3034010 (Kim et al. 2021)	(Bakhache et al. 2019)	Post entry	Decreases genome replication due to manipulation of FASN enzymatic activity.	ND	ND	HEK29 3T
CAY10566	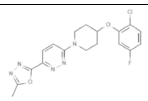	PubChem CID: 16732433 (Kim et al. 2021)	(Bakhache et al. 2019)	Post entry	Decreases genome replication due to manipulation of SCD1 enzymatic activity.	ND	ND	HEK29 3T
Epicatechin	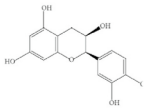	(Hosseinimehr et al. 2013)	Ferreira et al. 2018)	Post entry	Binds to mature virions released into the extracellular environment	0.247 µM	> 1.723 µM	Vero
C11	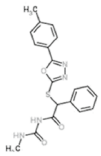	(Gall et al. 2018)	(Gall et al. 2018)	Host cells	Acts as an agonist of the STING Pathway	ND	ND	THF, MM6
α-punicalagin (*P. granatum* extract fraction containing punicalagin)	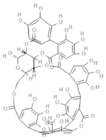	PubChem CID:16149716 (Kim et al. 2021)	(Salles et al. 2021)	Viral Entry	ND	523.1 µg/ml	62.5 µg/ml	Vero
***P. granatum* ethanolic extract**	NA	NA	(Salles et al. 2021)	Viral Entry	Virucidal	590.8 µg/ml	12.3 µg/ml	Vero
Honokiol	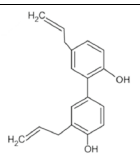	(Valdés-Torres et al. 2022)	(Valdés-Torres et al. 2022)	Host cells and post-entry	Downmodulates the expression of E1 and nsP1 proteins decreases viral RNA and increases type I interferon cellular response	ND	ND	Vero-E6, HeLa
α--Mangostin	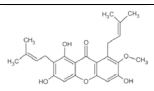	(Valdés-Torres et al. 2022)	(Valdés-Torres et al. 2022)	Host cells, Viral Entry and Post-entry	Downmodulates the expression of E1 and nsP1 proteins decreases viral RNA and increases type I interferon cellular response	ND	ND	Vero-E6, HeLa

ND not described, EC_{50} effective concentration of 50%, CC_{50} cytotoxic concentration of 50%, *NA* not applicable

*A list of abbreviations was provided as supplementary material

that acts as an auxiliary signal to T lymphocyte activation (Ishimaru et al. 1998; Raulin 2002). The antiviral effects of PGA1 and PGB2 against MAYV were investigated by using the plaque reduction assay in infected green monkey kidney cells (Vero cells) (Ishimaru et al. 1998). Cells were infected with MAYV at a concentration of 1 plaque-forming unit (pfu) per cell for 1 h, followed by the administration of PGs at concentrations ranging from 0 to 10 µg/ml for 1 h. The EC_{50} was observed with doses of 3 µg/ml for PGA1 and 8 µg/ml for PGB2. A higher antiviral effect was observed when compounds were added up to 2 h post-infection (h.p.i.) (Ishimaru et al. 1998). PGA1 was more effective than PGB2, being able to inhibit the production of glycoproteins E1 and E2 by over 50% at 10 µg/ml, resulting in a decrease of infectious particles (Ishimaru et al. 1998).

Later, Burlandy and Rebello corroborated the anti-MAYV activity of PGA1 that reduced 99% of MAYV replication in vitro at 10 µg/mL through a reduction plaque assay (Burlandy and Rebello 2001). Moreover, to suggest which stage of the replicative cycle was affected, a time-of-drug addition assay was performed. The results showed that PGA1 possesses the strongest effect when added to the cells simultaneously to the virus. The authors also identified a reduction in the synthesis of E1, E2, and C, and in the precursors of virus proteins, which suggests the effect in the early stages of viral replication. Additionally, an increase in the heat shock protein 70 (HSP70) was detected, and since this molecule is

responsible for protein folding, disaggregation, and degradation to ensure proper cell function (Holbrook et al. 1992), it is possible to suggest a mode of action for PGA1(Burlandy and Rebello 2001). Caldas and coworkers also assessed the effect of PGA1 on MAYV replication and the relevance of HSP70 in this process (Caldas et al. 2018). Human cervix carcinoma cells (Hep-2 cells) were infected with MAYV with a multiplicity of infection (MOI) of 1 for 1 h and treated with different concentrations of the compound. According to the authors, the PGA1 was not cytotoxic, presented an EC_{50} of 1 µg/mL, and inhibited up to 95% of viral production at 6 µg/mL. In agreement with the previous studies, PGA1 impaired p110, p62, E1/E2, and C synthesis, as well as a significantly increased HSP70 expression (Ishimaru et al. 1998; Caldas et al. 2018). The HSP70 increase seems to be related to the PGA1 antiviral effect since the inhibition of viral replication was only observed in PGA1 concentrations that induced the production of this HSP. In this context, the authors proposed that PGA1 may act in different stages of viral replication due to the different strategies presented by the molecule.

Alternatively, Carvalho and colleagues proposed the natural macromolecule Lactoferrin, a globular glycoprotein, as a candidate for treatment against MAYV (Carvalho et al. 2014). This molecule is produced by exocrine glands, such as mammary and lacrimal glands (Kell et al. 2020) and has been used as apolactoferrin, its apo form found in bovine whey (bLf). To assess the effect of Lactoferrin against MAYV, Vero cells were infected with viral particles labeled with DiD (1,1′-dioctadecyl-3,3,3′,3′-tetramethylindodicarbo cyanine,4-chlorobenzenesulfonate salt), a lipophilic carbocyanine marker that expresses red fluorescence, and then incubated with bLf at concentrations ranging from 0.2 to 1.0 mg/mL. BLf inhibited viral replication in a dose-dependent manner, with 1 mg/mL being able to inhibit 85% of viral infection. Furthermore, a time-of-drug addition assay was also carried out to investigate which stage of the replication cycle was affected (Carvalho et al. 2014). The bLf mainly acted on virus entry, suggesting that this molecule may interact with the sulfate groups of the glycosaminoglycans layer (GAGs) of the host cells, preventing the attachment of the virus. However, since the specific MAYV receptor at the time of the study was unknown (Carvalho et al. 2014), further studies involving the Mrxa8 are needed to corroborate this mechanism of action.

Other potential antiviral candidates tested against MAYV were the flavonoids 4′-*O*-methylepigallocatechin (MEP) and the proanthocyanidin [(−)-epicatechin-(4β → 8)-(−)-4′-methylepigallocatechin] (PAC), an MEP dimerized with the epicatechin, isolated from *Maytenus imbricata* roots (Ferraz et al. 2019). The viability of MEP and PAC was evaluated through an MTT ([(3-(4,5-dimethylthiazol-2-yl)-2,5-diphenyltetrazolium Bromide)] assay using Vero cells, and both demonstrated no cytotoxic effect, with CC_{50} over 1640 µM. To assess the antiviral effect, cells were infected with MAYV and treated with concentrations of MEP and PAC. No activity was observed against MAYV with MEP, even at the highest tested concentration (1000 µM). However, the treatment of MAYV-infected cells with PAC resulted in EC_{50} of 37.9 µM and a SI (selectivity index) higher than 43. The treatment at different stages of the virus cycle demonstrated the virucidal activity of PAC, which was confirmed by a dialysis membrane assay. The authors proposed that the mechanism of action may be related to the interaction of proanthocyanins with the envelope glycoproteins, decreasing the infectivity of viral particles (Ferraz et al. 2019).

The antiviral effect of the flavonoid Quercetin, as well as the EtOAc, and n-BuOH fractions, isolated from *Bauhinia longifólia,* was investigated by employing the viral yield inhibition assay. Vero cells with MAYV (MOI of 0.1) for 1 h, and then treated for 24 h with the substances (0–100 µg/ml). Subsequently, the culture supernatants were recovered and tittered to calculate the extracellular infectious viral particles using the plaque reduction assay. Among the tested compounds, quercetin and the fractions of EtOAc, and n-BuOH had an EC_{50} of 10 µM, 5 µM, and 3 µM, respectively. EtOAc had the highest SI (623), followed by n-BuOH (208) and quercetin (94). The mechanisms of action of these substances still need to be elucidated. It has been suggested that quercetin may act inhibiting viral RNA polymerase (dos Santos et al. 2014).

The antiviral activity of Quercetin against MAYV was also studied by Bakhache and coworkers, in addition to the compounds Cerulenin, Orlistat, and CAY10566 (Bakhache et al. 2019). These molecules are known to interfere with fatty acid synthase (FASN) or stearoyl-CoA desaturase (SCD1), cofactors of MAYV infection. To assess the their antiviral activity, human embryonic epithelial kidney cells (HEK293T) were infected with the MAYV-Luc reporter virus in an MOI of 1, and Quercetin, Cerulenin, Orlistat, and CAY10566 were added 1.5 h before or 1.5 h after the cell infection at concentrations of 0–150 µM, 0–25 µM, 0–100 µM, and 0–7.5 µM, respectively. Luciferase activity was then monitored for 6, 16, and 24 h.p.i.. As an outcome, the inhibitors induced a dose-dependent inhibitory effect on MAYV, when added before or after the infection. Among the tested drugs, Cerulenin presented the highest antiviral activity, demonstrating an increased ability to inhibit MAYV infectivity when added before the viral infection. The authors also screened these molecules against CHIKV, which demonstrated to decrease CHIKV genome replication due to the interference with FASN or SCD1 enzymatic activity, proposing that these compounds act in a similar mechanism against MAYV.

Similarly, the antiviral activity of EtOAc, n-BuOH, and EtOAc-Pp, extracted from *Cassia australis*, against MAYV were evaluated (Spindola et al. 2014). The production of MAYV in Vero cells decreased by about 70% and 85% in the presence of EtOAc and n-BuOH at 25 µg/mL, respectively, while EtOAc-Pp at 10 µg/mL decreased 90% the viral progeny production. The authors proposed that the highest antiviral effect of EtOAc-Pp may be due to the condensed tannins, which are present only in this substance. Tannins are a class of polyphenols, characterized by having different molecular sizes and degrees of polymerization, which affect their pharmacokinetics and antiviral activity (Maugeri et al. 2022). Condensed tannins have previously demonstrated antiviral activity against other viruses, such as the respiratory syncytial virus (RSV), influenza A virus (FLU-A), and parainfluenza virus (PIV) (Bruyne et al. 1999). The authors suggested that the mechanism of action of EtOAc-Pp is related to the binding of tannins with viral envelope proteins, resulting in the inhibition of viral binding and penetration into host cells.

What is more, the EtOH fruit extract from *Punica granatum* (Pomegranate), and its two main fractions, one containing the α and β anomers of Punicalagin and another the Pomegranate ethanol extract, were assessed by their anti-MAYV activity (Salles et al. 2021). To this, Vero cells were infected with MAYV at an MOI of 0.1 for 1 h, and then added of medium-containing substances at concentrations of 12.5, 25, 50, and 100 µg/ml. Virus was titrated 24 h.p.i. and titrated by the $TCID_{50}$. As a result, *P. granatum* ethanolic extract demonstrated strong antiviral activity against MAYV infection, with a CC_{50} of 590.8 µg/mL and an EC_{50} of 12.3 µg/mL. The fraction containing punicalagin as the main component also showed strong antiviral activity, with a CC_{50} of 523.1 µg/mL and an EC_{50} of 62.5 µg/mL. The authors performed a virucidal assay, incubating the virus with each substance at 200 µg/mL for 1 h at 37 °C. Pomegranate ethanol extract showed 98% virucidal activity against MAYV particles, and punicalagin showed no visible virucidal activity, being the results confirmed by immunofluorescence microscopy.

Another natural compound identified to possess anti-MAYV activity is Epicatechin, isolated from extracts of *Salacia crassifolia*, which belongs to a genus of plants known by its use against diabetes, and as an anti-inflammatory, in folk medicine (Ferreira et al. 2018). Ferreira and coworkers selected Epicatechin for in vitro analysis after performing in silico screening tests that suggested a potential binding interaction with MAYV C protein. To assess the in vitro antiviral activity, cells were pretreated for 30 min with dilutions of the compound (0.013 to 0.574 µmol/mL), and then infected with MAYV at an MOI of 0.1 or 5 for 48 h. Epicatechin presented EC_{50} of 0.247 µmol/mL, and prevented approximately 100% of the cytopathic effect in MAYV-infected cells at 0.430 µmol/mL. A time-of-drug addition assay was also performed, and when added after infection, epicatechin reduced virus production by two logs in the first 12 h. The authors suggested that the compound acts in the second cycle of infection, when mature virions are released into the extracellular environment, but did not exclude an intracellular action in the late stages of viral replication, considering the MOI used in the assay, concluding that epicatechin acts by binding to components of the viral particle, but not to cellular components.

Ginkgolic Acid (GA), a compound isolated from *Ginkgo biloba*, is widely used in traditional Chinese medicine (Campos et al. 2020), reported to possess biological activities, such as anti-tumor (Ma et al. 2015; Qiao et al. 2017), antibacterial (Hua et al. 2017), anti-parasitic (Chen et al. 2008), and antiviral (Lü et al. 2012). Campos and colleagues evaluated the effects of GA on CHIKV, MAYV, and UNAV replication. Through a plaque reduction assay using epithelial cervical cancer cells (HeLa cells), it was found that GA at 10 µM reduced the MAYV viral progeny in almost 2 log_{10} at 16 h.p.i.. To confirm these results, an immunofluorescence assay was performed, demonstrating that treated cells presented a decrease in viral antigens. Additionally, a time-of-drug-addition assay was performed by adding GA to the cells hourly after adsorption, and supernatants were collected 24 h.p.i. to measure viral progeny yields. As a result, the compound was able to mainly inhibit the initial stages of the viral cycle, which was confirmed by the suppression of E1 and E2 viral proteins in western blot (Campos et al. 2020). Despite the promising effects of GA against MAYV in vitro, the molecule demonstrated to be toxic in other cell lines and animal studies (Berg et al. 2015; Qian et al. 2017). Therefore, the authors suggest that further investigations are needed to confirm the safety of the treatment, and the antiviral activity against MAYV.

Another promising inhibitor of MAYV is Silymarin, a compound extracted from *Silybum marianum*. This molecule is widely used for the treatment of liver disorders (Camini et al. 2018), and was described to have antiviral activity against the Hepatitis C virus (Wagoner et al. 2010) and CHIKV (Lani et al. 2015). Camini and coworkers assessed the effects of Silymarin using hepatocarcinoma cells (HepG2 cells), which resulted in CC_{50} of 103.5 µg/mL and EC_{50} of 3.58 µg/mL. Then, HepG2 cells were treated with 25 µg/mL of Silymarin and simultaneously infected with MAYV at an MOI of 5. Supernatants were collected 48 h.p.i. and used to infect naïve Vero cells. The results demonstrated a reduction of up to two logs in MAYV replication, inhibiting almost 100% of the cytopathic effect. The production of reactive species of oxygen (ROS) was measured by employing infected HepG2 cells with a fluorogenic marker, confirming that MAYV infection increased ROS generation in a time-dependent curve. Other oxidative stress biomarkers were quantified, such as malondialdehyde (MDA) and

carbonyl protein, in the presence of MAYV and Silymarin, which culminated in a drop of these biomarkers, suggesting a protective effect on host cells, associated with the antiviral activity (Camini et al. 2018).

Finally, Valdés-Torres and collaborators investigated the potential of Honokiol and α-Mangostin against MAYV (Valdés-Torres et al. 2022). Primary human dermal fibroblasts (HDFs), Vero-E6, and HeLa cells were infected with MAYV at an MOI of 1 for 1 h, and then treated with Honokiol (5 to 10 µM) or α-Mangostin (1 to 5 µM) for 24 h. Honokiol and α-Mangostin reduced MAYV-induced cytopathic effects in a dose-dependent manner and inhibited the production of viral progeny in pretreatment assay. MAYV-infected HDFs revealed that α-Mangostin at 1 µM affected MAYV binding to the host cells, while Honokiol showed a modest effect at 10 µM. The viral entry was partially disturbed by α-Mangostin, but not by Honokiol. Both compounds affected the post-entry stage of MAYV infection. The authors also evaluated the expression of Interferon (IFN) type I and specific genes stimulated by IFN in treated or untreated HeLa cells through quantitative RT-PCR. As an outcome, treatment with Honokiol and α-Mangostin promoted a significant increase in IFN type I and interferon-stimulated genes. In addition, the compounds decreased the expression of MAYV E1 and nsP1, and affected viral RNA replication. The authors pointed out that Honokiol and α-Mangostin are post-entry inhibitors impairing MAYV replication through different mechanisms of action, and may act as potential broad-spectrum antivirals, also inhibiting UNAV, CHIKV, and Zika virus (ZIKV).

Synthetic and semi-synthetic inhibitors of MAYV replicative cycle

Natural compounds may present limitations in terms of large-scale production and patentability, and therefore, the production of synthetic and semi-synthetic compounds is an alternative and attractive approach to the development of antiviral candidates (Ortholand and Ganesan 2004).

Among the synthetic molecules, the Thienopyridine derivatives were described as antimicrobial agents against bacteria (Aly et al. 2011), protozoa (Pinheiro 2012), viruses (Bernardino et al. 2004), and parasites (Rolim Bernardino et al. 2006). In this context, Amorim and coworkers conducted a study based on the antiviral activity of thieno[2,3-b]pyridine derivatives 101 to 113 on the MAYV replicative cycle in vitro, using Vero cells (Amorim et al. 2017). Among the non-cytotoxic compounds, molecule 104 was the most viable compound, presenting CC_{50} of 2500 µM, EC_{50} of 20.0 µM, and an SI of 125. To further assess the effect of molecule 104 on viral protein synthesis, Vero cells were infected with MAYV at an MOI of 0.05 and treated with 100 µM of the compound in a time-of-drug addition assay. Through the quantification of the plaque-forming assay, it was observed that 104 presented a higher effect when added prior or during the virus infection. Therefore, a virucidal assay was performed by incubating the virus and the compound for 1 h prior to the infection, confirming the virucidal effect of 104 at concentrations higher than 25 µM. The authors also showed a decrease in protein synthesis in the presence of 104, by labeling viral proteins with 35S-methionine, confirmed by transmission electron microscopy, which demonstrated a reduction in the number of intracytoplasmic nucleocapsids and mature virus particles in treated cells.

Porphyrins are organic molecules that can bear a metal ion in the center of their tetrapyrrolic structure (Assunção-Miranda et al. 2016). These molecules are capable of absorbing light and are widely used in photodynamic therapies. The porphyrins have also been shown to inactivate viral particles by targeting the viral envelope of Dengue virus (DENV) and Yellow Fever virus (YFV) (Neris et al. 2018). Neris and coworkers evaluated the antiviral potential of the heme porphyrins Co-protoporphyrin IX (CoPPIX) and Sn-protoporphyrin IX (SnPPIX) in the presence or absence of light against MAYV using Baby Hamster Kidney Fibroblast (BHK-21) or Vero cells (Neris et al. 2018). With no light stimulation, CoPPIX and SnPPIX presented a CC_{50} of 762.3 µM and 816 µM, respectively, while in the presence of light, the compounds demonstrated a CC_{50} of 1018 µM and 20.7 µM, respectively. Later, 10^7 PFU of viruses were pre-incubated with different concentrations of each compound in the absence of light for 1 h at 37 °C, and then used to infect the cells with an MOI of 0.1. CoPPIX and SnPPIX at 300 µM were able to completely inactivate MAYV, with an EC_{50} of 5.94 µM and 5.99 µM, respectively. Additionally, light-stimulated for 10 min before incubation for 1 h in the dark resulted in EC_{50} of 0.09 µM for SnPPIX and 7.48 µM for CoPPIX. To further investigate the CoPPIX and SnPPIX inhibition, MAYV was labeled with DiD to follow fusion between virus and endosomal membranes during endocytosis. After treatment with CoPPIX or SnPPIX at 300 µM with no light stimulation, and SnPPIX at 10 µM with light stimulation, MAYV was unable to efficiently fuse with the endosomal membrane. The authors highlighted that the porphyrins are hydrophobic molecules, that might interact with viral envelope lipids, impairing the attachment and entry of the virus into the cells. Furthermore, the photoactivation of SnPPIX generates ROS, which can modify viral proteins in the envelope environment, producing an antiviral activity. The authors emphasized that a single intensity of light stimulation was performed and suggested that an increase in luminous intensity might increase SnPPIX virucidal efficiency (Neris et al. 2018).

Another promising compound is β-D-N4-hydroxycytidine (EIDD-1931), a ribonucleoside analogue which previously

demonstrated antiviral activity against RNA viruses, such as SARS-COV-2, Equine Encephalitis Virus, and CHIKV (Yousefi et al. 2021; Langendries et al. 2021). EIDD-1931 can rapidly reach plasma, is efficiently distributed in mice organs, and also presents a high genetic barrier for the development of viral resistance (Painter et al. 2019; Yousefi et al. 2021). A study conducted by Langendries and coworkers screened compounds with previously reported antiviral activity against other arboviruses, such as EIDD-1931, Favipiravir, and Suramin, against MAYV (strain TC625, MOI of 0.01), using Vero cells (Langendries et al. 2021). The experiments demonstrated CC_{50} of > 100 µM, > 2000 µM, and 2837 µM, and EC_{50} of 1.6 µM, 124 µM, and 79 µM for EIDD-1931, Suramin, and Favipiravir, respectively. To evaluate which stage of the replicative cycle was affected by these compounds, a time-of-drug-addition assay was carried out. Vero cells were incubated with 300 µM Favipiravir, 500 µM Suramin, and 25 µM EIDD-1931 2 h before infection, and 0, 2, 4, 6, and 8 h.p.i. at an MOI of 1. Through end-point titration at 10 h.p.i and qRT-PCR quantification, the authors demonstrated that EIDD-1931 impaired viral replication when added at 0, 2, and 4 h.p.i., with a moderated effect if added at 6 h.p.i. Differently, Suramin and Favipiravir reduced viral titers at 0 and 2 h.p.i., respectively. From the results and previous data in the literature, the authors suggested that EIDD-1931 and Favipiravir impair viral RNA synthesis, resulting in non-functional copied viruses due to a large number of mutations in the viral genome (Joshi et al. 2021; Langendries et al. 2021). It was also proposed that Suramin acts during the early steps of the MAYV replicative cycle, more specifically in the viral entry, in a similar mechanism demonstrated by studies with CHIKV (Albulescu et al. 2020) and SARS-CoV-2 (Salgado-Benvindo et al. 2020).

Cyclic ketones are natural and synthetic compounds with antiviral (Sivropoulou et al. 1997; Chung 2017), antioxidant (Pombal et al. 2017), and antifungal (Pizzolitto et al. 2015) properties. The antiviral activity of 24 cyclic ketones was assessed by Fernandes and coworkers, by screening these compounds, using MAYV-infected Vero cells (MOI 1), treated with each compound at concentrations ranging from 1 to 100 µM for 24 h. Among them, 8 compounds showed viability ≥ 50% and were selected for viral inhibition assay. A plaque-forming assay was performed, and among the 8 compounds, the Xanthenodione 9-(5-(4-chlorophenyl]furan-2-yl)-3,6-dimethyl-3,4,5,6,7,9-hexahydro-1H-xanthene-1,8(2))-dione inhibited the MAYV with EC_{50} of 21.5 µM and SI of 15.8. The authors also performed a time-of-drug addition assay and found that the compound inhibits viral replication in the prior and post-treatment assays (Fernandes et al. 2021).

The Proteasome inhibitors MG132 and Lactacystin are also antiviral candidates against MAYV (Llamas-González et al. 2019). MG132 acts as a reversible inhibitor of the chymotryptic activity of the proteasome, and Lactacystin is an irreversible inhibitor capable of binding to the catalytic β subunits of the 20S proteasome (Llamas-González et al. 2019). The anti-MAYV activity of these compounds was evaluated by Llamas-González and colleagues. Vero-E6 or HeLa cells were treated with MG132 at 10 µM or Lactacystin at 25 µM for 1 h, and then infected with MAYV (MOI of 1 or 10) for 1 h, when the inoculum was replaced by fresh medium-containing compounds. Viruses were titrated by plaque-forming assay 24 h.p.i.. MG132 and Lactacystin low cytotoxicity and significant antiviral effect using either cell lines. The authors also performed immunofluorescence of MAYV-infected HeLa cells, which demonstrated a significant reduction in the percentage of MAYV-positive cells under treatment, resulting in < 5% for MG132 and < 10% for Lactacystin, versus > 20% in the untreated control group. Viral titers were lower when compounds were added in the early stages of infection, and the treatment with MG132 or Lactacystin affected the production of viral proteins nsP1 and E1, showed by the reduced expression of MAYV proteins under the treatment with these proteasome inhibitors.

Exploiting host factors, the Src family of protein tyrosine kinases (SFK) are involved in intracellular signaling pathways related to virus elimination (Broeckel et al. 2019). However, during infection, the virus can interact with kinases favoring viral replication. Therefore, cell signaling inhibitors, including SFK inhibitors, have been tested for their antiviral activity against *Alphavirus* in human fibroblasts (Broeckel et al. 2019). Since the knowledge of the signaling profile of SFK during *Alphavirus* is limited, the authors carried out a range of experiments using CHIKV infection, as a base to identify the kinase pathways involved in this genus infection. The SFK-phosphatidylinositol 3-kinase (PI3K)-Akt-mTOR signaling was demonstrated to be the main pathway during CHIKV infection. Then, the authors evaluate the effects of dasatinib and Torin, inhibitors of this pathway, on fibroblasts infected with MAYV. Through the viral titration of the supernatant collected from infected and treated cells, it was shown that MAYV was significantly reduced by these inhibitors. The authors demonstrated that the SFK inhibitors blocked the subgenomic RNA translation, resulting in the impairment of *Alphaviruses* replication (Broeckel et al. 2019).

A non-natural interferon (cIFN) that was designed according to the analysis of the amino acid sequences present in several subtypes of IFN-α was investigated by its anti-MAYV activity by Grabarz et al. (2021). Vero cells were treated with increasing concentrations of cIFN for two hours and then infected with MAYV (MOI = 0.1) for 48 h. MAYV infection was inhibited by cIFN inhibited, with EC50 of 35.7 fg/mL, being possible to obtain about 80% and 100% cell confluency with concentrations of 81.4 fg/mL, and 162.8 fg/mL of the compound, respectively. In comparison,

untreated cells showed almost complete destruction of the cell monolayer 24 h.p.i. with MAYV. In this study, cIFN was also able to inhibit the cytopathic effect of other viruses, such as ZIKV, CHIKV, and SARS-CoV-2.

Another promising compound is N-(methylcarbamoyl)-2-{[5-(4-methylphenyl)-1,3,4-oxadiazol-2-yl]sulfanyl}-2-phenylacetamide (known as C11), a molecule that induces type I IFN-dependent activity in human cell lines (Gall et al. 2018). In this context, Gall and collaborators produced THF cells and MM6 cells with deletion of the stimulator of interferon genes (STING), such as the RIG-1 mitochondrial antiviral signaling (MAVS) and the TIR-domain-containing adapter-inducing interferon-β gene (TRIF), related to the activation of the immune response. To assess the antiviral activity of C11, these cells were treated for 2 h with C11, IFN-β, or DMSO at non-cytotoxic concentrations and then infected with MAYV at an MOI of 1. The results demonstrated that C11 had an effective concentration of 90% (EC_{90}) of 25.19 µM against MAYV. STING-deleted cells showed no inhibition of virus replication in the presence of the compound. C11 was also evaluated against CHIKV, VEEV, and RRV viruses in human cells, resulting in reductions in the virus titer, but when evaluated using non-human cells (RAW264.7 monocytic cells), a lack of antiviral activity in the murine RAW264.7 cell line was noticed. The authors proposed that C11 acts by activating specifically the human type I IFN response through a STING-dependent process, leading to the generation of an IFNAR-mediated antiviral cellular state.

Molecular target to drug development against MAYV

Drug development can be a time-consuming process, which can result in unexpected outcomes (Adamson et al. 2021). Additionally, the lack of treatment against viral infections, mainly for neglected diseases, may jeopardize the control of the disease, as well as its consequences, such as the loss of human lives (Young et al. 2019). In this context, several strategies can be applied to accelerate the progress toward the development of novel molecules. Therefore, this section focuses on the MAYV proteins which could be exploited as a target for antiviral development, considering the factors: (i) previously described compounds with antiviral activity against MAYV and/or other *Alphaviruses*, (ii) resolved structure of viral proteins deposited in databanks, and (iii) structural similarity and conservation among viruses.

The glycoprotein E1 possesses an ectodomain, subdivided into subdomains I, II, and III, and a transmembrane subdomain (TM). Similarly, the E2 ectodomain is composed of subdomains A, B, C, and D, and a TM portion (Filho et al. 2020). The ectodomains of E1 and E2 interact with each other to form a portion of the spike structure outside the envelope: the glycoproteins E1 and E2 interact forming a dimeric unit (Fig. 3A) that is further associated with additional two dimers to form the spike (Fig. 3B–D). The TM portions of E1/E2 bind the spike to the lipid membrane, while E2 C-terminal connects the spike to the capsid protein, through a well-described TPY consensus motif (West et al. 2006; Ribeiro-Filho et al. 2021), forming an E1–E2-capsid unit (Fig. 3C, E). As observed for other *Alphaviruses*, MAYV possesses an asymmetric unit formed by the assembling of four E1–E2-capsid units resulting in 80 spikes (Filho et al. 2020). MAYV belongs to the arthritogenic class of viruses, and, therefore, it is possible to suggest that Mxra8 is the main receptor related to the MAYV entry into host cells (Fig. 3E) (Powell et al. 2020). In this context, considering that the glycoprotein protein complex interacts with Mxra8, mainly through E2, this interaction could be impaired by active molecules through interference or destabilization of E2 binding sites (Zhang et al. 2018; Filho et al. 2020). Molecules were previously described to bind to viral glycoproteins of other arthritogenic viruses, such as CHIKV, consequently inhibiting viral entry to the host cells. For instance, Oliveira and coworkers described the in vitro virucidal activity of a coordinated organic compound against CHIKV, and demonstrated that in silico analysis suggested interactions between the compound and CHIKV E2 domain (Oliveira et al. 2020). Additionally, studies encompassing the compounds PAC (Ferraz et al. 2019), bLf (Carvalho et al. 2014), CoPPIX, and SnPPIX (Neris et al. 2018), which are discussed here, also demonstrated a virucidal activity against MAYV infection. Even though these molecules were not rationally designed for specific targets, further studies could investigate whether their mode of action is related to these hint targets.

Another spot protein in MAYV replication is the nsp4, an RNA-dependent RNA polymerase (RdRp) essential to the viral replication (Rubach et al. 2009). Therefore, it is an attractive target to the development of antiviral drugs. To the best of our knowledge, the RdRp crystal structure of MAYV has not been determined and characterized yet, which might postpone drug design applied to this target. Regardless, the RdRp amino acid sequence is commonly conserved among viruses from the A*lphaviruses* genus, and especially between the Semliki Forest serocomplex members (Rupp et al. 2015). Therefore, the RdRp structure from the Ross River virus (RRV) (Fig. 4), another member of the *Alphavirus* genus might be employed as a template for drug development. Its structure is composed of fingers, the palm containing the GDD active site, and thumb domains (Rubach et al. 2009). Therefore, it is possible to hypothesize that compounds with antiviral activity described against the RdRp of other viruses could act against MAYV infection (Chen et al. 2017). Indeed, most of the described and approved drugs are

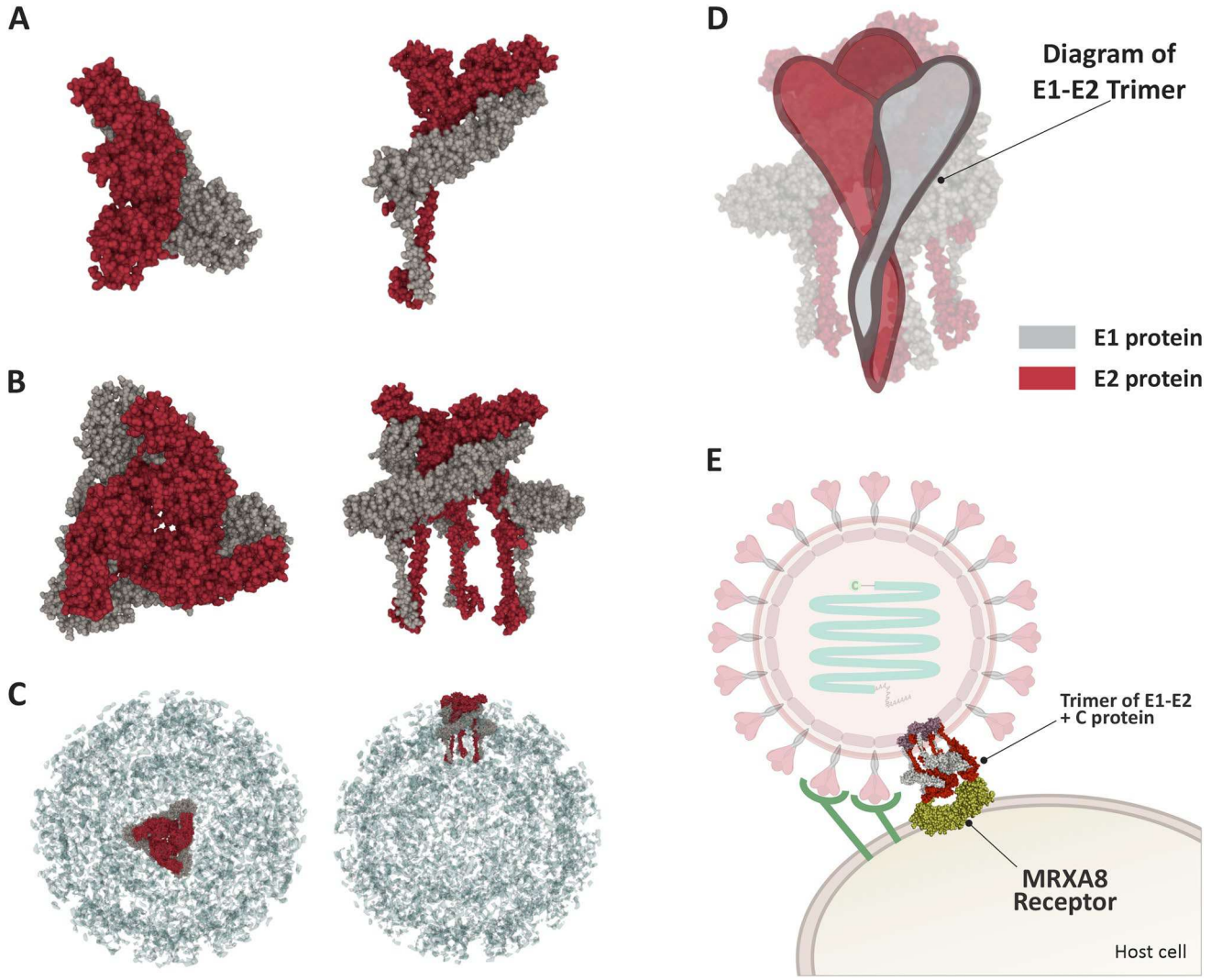

Fig. 3 Schematic structure of MAYV glycoprotein. The glycoproteins E1 and E2 interact forming a dimeric unit (**A**), that is further associated to two additional dimeric units to form a trimer (**B**). The localization of the trimers is demonstrated in (**C**), and a diagram of the E1–E2 trimer is shown in (**D**). The interaction between the glycoproteins and the MRXA8 receptor in host cells is demonstrated in **E**. MAYV E1 and E2 structure were based on Cryo-EM structure of mature MAYV (PDB ID: 7KO8) (Ribeiro-Filho et al. 2021), and the receptor was based on human MXRA8 (PDB ID: 6JO8) (Powell et al. 2020)

nucleoside and non-nucleoside inhibitors that impair viral infections through RNA synthesis inhibition. Among them, Remdesivir, Azidothymidine (AZT), Sofosbuvir, and Lopinavir/Ritonavir, are licensed antivirals used to treat Ebola virus, Hepatitis C virus, and Human immunodeficiency virus infections (Tian et al. 2021).

The MAYV nsP3 is another protein that represent a target for antiviral development (Tsika et al. 2019). It is a modular protein with three domains: the N-terminal macro domain, a central zinc-binding domain, and the C-terminal hypervariable domain (Fig. 4) (Götte et al. 2018). Each domain plays a different role in viral replication and interferes with the virulence among Old and New World Alphaviruses, being necessary for RNA synthesis (Rupp et al. 2015). The MAYV macro domain possesses four alpha-helices and six beta-strands (Malet et al. 2009; Melekis et al. 2015). On the other hand, the central zinc-binding domain plays an undefined, but essential role in minus-strand RNA synthesis, through an association with the macro domain, forming a ring-like structure to RNA binding (Shin et al. 2012). Alternatively, the hypervariable domain is a large protein that upholds several insertions and deletions, and is responsible for interactions with multiple host proteins during viral replication, probably favoring virulence (Davis et al. 1989; Dé et al. 2003; Uversky 2013). However, the macro domain is the most conserved site in the protein structure and could be exploited for drug development, particularly as a broad-spectrum antiviral. The macro domain site binds to ADP-ribose,

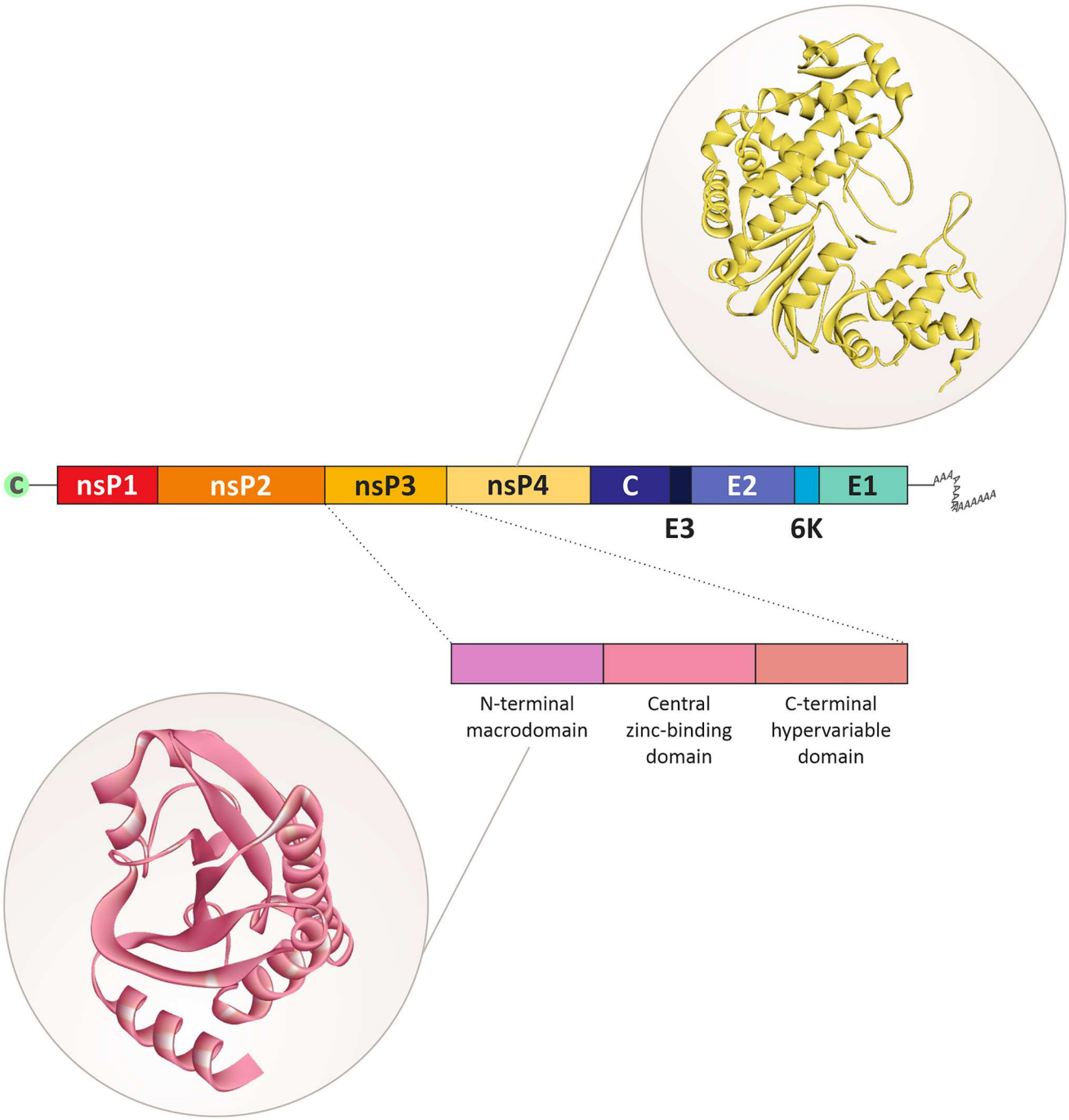

Fig. 4 Schematic structure of MAYV genome and the crystal structure of nsP3 macrodomain and nsP4. Nsp3 is a modular protein with three domains: the N-terminal macro domain, a central zinc-binding domain, and the C-terminal hypervariable domain, being the macro domain constituted by four alpha-helices and six beta-strands. The nsP4 protein acts as an RNA-dependent RNA polymerase (RdRp), and its structure is composed of fingers, the palm containing the GDD active site, and thumb domains. Since RdRp crystal structure of MAYV has not been determined and characterized yet, the template used in the figure was obtained from Ross River virus RdRp (PDB ID: 7F0S) (Tan et al. 2022). The nsP3 structure was based on MAYV macro domain structure (PDB ID: 5IQ5) (Tsika et al. 2019)

dephosphorylate ADP-ribose-1′-phosphate, and possesses a de-ADP-ribose hydrolase activity, which is essential to viral replication (McPherson et al. 2017). Several compounds were virtually screened employing the nsP3 macrodomain of CHIKV (Nguyen et al. 2014; Shimizu et al. 2020; Subudhi et al. 2018), SARS-CoV-2 (Jung et al. 2020), and the Venezuelan equine encephalitis virus (VEEV) (Atasheva et al. 2014) as targets. Shimizu and collaborators selected

compounds that targeted the nsP3 macro domain of CHIKV by in silico analysis, and validated their antiviral activity performing in vitro assays (Shimizu et al. 2020). Therefore, it is possible to suggest the nsP3 macrodomain of MAYV as a relevant target for future antiviral discovery.

Furthermore, components of virus lipidic membrane are also potential targets yet to be explored. Among membrane components, the cholesterol is an important molecule related to *alphavirus* stability, infectivity, and assembly (Sousa et al. 2020). This molecule was recently associated with the successful infection in several viruses (Sun and Whittaker 2003; Huang et al. 2006), being also modulated to increase the infection efficiency (Zhang et al. 2019). Cholesterol can be found in increased proportions in MAYV viral particles isolated from vertebrate cells, being associated with the lateral organization of the viral envelope and binding to the host membrane (Sousa et al. 2020). Additionally, a decrease in *alphavirus* infectivity is observed when the arrangement of the viral envelope is disturbed, suggesting that the lateral membrane organization is important for the physical stability of the viral particle and, consequently, for virus-cell interactions (Kielian et al. 2010). Cholesterol is also associated with MAYV entry, being used as an alternative pathway for its entry through cholesterol-enriched caveolae-derived vesicles and release (Carvalho et al. 2017). Therefore, targeting cholesterol from the viral lipidic membrane represent an interesting approach for antiviral drug development. However, designing and identifying active compounds focusing on these components can be challenging, due to their similarity to the host cell membrane (Sousa et al. 2020). Interestingly, the compound 25-hydroxycholesterol (25HC), a reactive oxysterol catalyzed by cholesterol-25-hydroxylase, is a promising molecule that can interact with lipids on viral membrane, and demonstrated broad-spectrum antiviral activity, low toxicity, and ability to reduce viremia and protect embryonic mice against ZIKV in vivo (Li et al. 2017; Mao et al. 2022). In this context, molecules focused on interacting with cholesterol could be employed to drug development against MAYV. ed to drug development against MAYV.

Perspectives

MAYV infection can impact the quality of life of infected patients, due to the chronic condition that can result in progressive arthralgia and disabling disease. Besides that, the lack of approved antiviral treatment and vaccines against MAYV, associated with the presence of susceptible vectors in tropical and subtropical countries, can lead to future outbreaks.

In this context, this review summarized and discussed the literature concerning the compounds with anti-MAYV activity, as well as presented possible viral proteins that could be further exploited as targets for drug development. To the best of our knowledge, only the studies described here reported antiviral activity against MAYV infection, demonstrating that further research on treatments against Mayaro fever is urgent. It is important to emphasize that the data presented here employed different methodologies, including cell lines, MOI for infection assays, and the design of the assays. However, these studies present relevant information on the antiviral activity of a range of molecules (natural and synthetic) against MAYV, and suggested possible mechanisms of action (MOA) related to each compound. The characterization of the MOA of these molecules represents an advance for further studies, providing information concerning the interactions among host cells, viruses, and compounds (Iorio et al. 2010; Salters-Pedneault 2014). Besides, the MOA of several compounds against MAYV are still unknown (Figueiredo et al. 2019). From the compounds discussed here, Lactoferrin, molecule 104 (thienopyridine derivative), and Silymarin presented significant antiviral activity against MAYV in vitro, with low or no cytotoxicity. The repurposing antiviral agent EIDD-1931 is also a promising treatment since it was able to completely inhibit MAYV replication in vitro. However, these compounds need to be further investigated in vivo against MAYV. Ginkgolic Acid (GA) was one of the most active compounds, and the only molecule tested in vivo, however demonstrating hepatotoxicity and nephrotoxicity effects, as well cytotoxicity in different cell lines. Qian and collaborators also observed that rats treated with either, high or low doses of GA, showed histopathological changes in the liver and kidneys. In addition, the serum levels of urea nitrogen and creatinine increased in the blood, and total protein and albumin decreased, indicating kidney dysfunction and liver damage (Qian et al. 2017). On the other hand, the genotoxicity evaluation of GA evidenced a low risk of genotoxicity in vivo (Berg et al. 2015). Therefore, more studies in human cells and animal models are necessary to analyze the safety of this compound.

Furthermore, we discussed and highlighted MAYV proteins that could represent relevant targets for drug development, acknowledging that focusing on host factors might produce cytotoxicity in vitro, and adverse effects in vivo. Here, we suggested the glycoproteins complex, the nsP4 (RdRp), and the nsP3 macro domain as targets. The lack of resolved structures of several MAYV proteins, such as nsP1, nsP2, C, and E, invalidate them as targets for drug development.

Finally, licensed drugs employed in the treatment of several diseases have the potential to be repurposed to target the viral molecules underlined here. In this sense, Langendries and colleagues identified EIDD-1931, favipiravir, and suramin, three licensed antivirals, with activity against MAYV (Langendries et al. 2021). Additionally, the

potential of Lactacystin (Llamas-González et al. 2019), Cerulenin, Orlistat (Bakhache et al. 2019), and Quercetin (dos Santos et al. 2014), as repurposing therapy against MAYV was also discussed. The compounds were active with low EC_{50} and low cytotoxicity, and showed potential to be applied as antiviral therapy in the treatment of infections caused by this pathogen, being a prospective target for further research. The use of approved drugs as repurposing therapy may favor patient access to drugs due to the potential to result in shorter clinical studies, since these molecules have their pharmacological profile and adverse effects already described (Santos et al. 2022). Bearing that in mind, it is an inconsistency that repurposing drugs against MAYV have been understudied. Therefore, we further emphasize and encourage researchers to screen licensed drugs against MAYV.

Conclusions

The spread of MAYV infections in tropical and subtropical regions represents a threat to developing countries. Additionally, the lack of epidemiological data on Mayaro fever might underestimate the importance of this disease and its consequences. There is an urgent need for studies to understand the biology of the virus, thus creating paths to combat future outbreaks. In this context, the compounds described to possess anti-MAYV activity, and the possible targets discussed herein, may contribute to the future development of antiviral drugs against MAYV.

Supplementary Information The online version contains supplementary material available at https://doi.org/10.1007/s00203-023-03441-y.

Acknowledgements ACGJ is grateful to FAPEMIG (Minas Gerais Research Foundation APQ-01487-22 and APQ-04686-22), and to Coordenação de Aperfeiçoamento de Pessoal de Nível Superior (CAPES)-Brasil-Prevention and Combat of Outbreaks, Endemics, Epidemics and Pandemics-Finance Code #88881.506794/2020-01. MP thanks Conselho Nacional de Desenvolvimento Científico e Tecnológico (CNPq) for the scholarship # 23117.018764/2020-00. MSM thanks CNPq and FAPEMIG for the scholarships # 129422/2021-5 and # 12152. IAS thanks to CNPq for the scholarship # 142495/2020-4 and CAPES.Print scholarship # 88887.700246/2022-00. VRG and DOSM thanks to CAPES for the scholarships # 88887.505971/2020–00 and # 88887.505880/2020-00, respectively.

Authors contribution Literature research: MP, MdSM, IAS, VRG, and DOSM. Drafting of the manuscript: MP, MdSM, and DOSM. Figures: VRG. Design and Critical revision: IAS, RBR, and ACGJ. All authors reviewed the manuscript.

Data availability statement All data generated or analysed during this study are included in this published article (and its supplementary information files).

Declarations

Conflict of interest The authors declare that the research was conducted in the absence of any commercial or financial relationships that could be construed as a potential direct or indirect conflict of interest.

References

Acosta-Ampudia Y, Monsalve DM, Rodríguez Y et al (2018) Mayaro: an emerging viral threat? Emerg Microbes Infect 7:1–11

Adamson CS, Chibale K, Goss RJM et al (2021) Antiviral drug discovery: preparing for the next pandemic. Chem Soc Rev 50:3647. https://doi.org/10.1039/d0cs01118e

Agostini ML, Pruijssers AJ, Chappell JD et al (2019) Small-molecule antiviral β-hydroxycytidine inhibits a proofreading-intact coronavirus with a high genetic barrier to resistance. J Virol. https://doi.org/10.1128/JVI.01348-19

Aguilar-Luis MA, del Valle-Mendoza J, Silva-Caso W et al (2020) An emerging public health threat: Mayaro virus increases its distribution in Peru. Int J Infect Dis 92:253–258. https://doi.org/10.1016/j.ijid.2020.01.024

Albulescu IC, White-Scholten L, Tas A et al (2020) Suramin inhibits chikungunya virus replication by interacting with virions and blocking the early steps of infection. Viruses. https://doi.org/10.3390/v12030314

Aly HM, Saleh NM, Elhady HA (2011) Design and synthesis of some new thiophene, thienopyrimidine and thienothiadiazine derivatives of antipyrine as potential antimicrobial agents. Eur J Med Chem 46:4566–4572. https://doi.org/10.1016/j.ejmech.2011.07.035

Amorim R, de Meneses MDF, Borges JC et al (2017) Thieno[2,3-b]pyridine derivatives: a new class of antiviral drugs against Mayaro virus. Arch Virol 162:1577–1587. https://doi.org/10.1007/s00705-017-3261-0

Anderson CR, Wattley GH, Ahin NW et al (1957) Mayaro virus: a new human disease agent. Am J Trop Med Hyg 6:1012–1016. https://doi.org/10.4269/ajtmh.1957.6.1012

Arias-Arias JL, Vega-Aguilar F, Picado-Soto D et al (2021) In vitro inhibition of Zika virus replication with amantadine and rimantadine hydrochlorides. Microbiol Res (pavia) 12:727–738. https://doi.org/10.3390/microbiolres12030052

Assunção-Miranda I, Cruz-Oliveira C, Neris RLS et al (2016) Inactivation of dengue and yellow fever viruses by heme, cobalt-protoporphyrin IX and tin-protoporphyrin IX. J Appl Microbiol 120:790–804. https://doi.org/10.1111/jam.13038

Atasheva S, Frolova EI, Frolov I (2014) Interferon-stimulated poly(ADP-ribose) polymerases are potent inhibitors of cellular translation and virus replication. J Virol 88:2116–2130. https://doi.org/10.1128/jvi.03443-13

Bakhache W, Neyret A, McKellar J et al (2019) Fatty acid synthase and stearoyl-CoA desaturase-1 are conserved druggable cofactors of Old World Alphavirus genome replication. Antiviral Res 172:104642. https://doi.org/10.1016/j.antiviral.2019.104642

Berg K, Braun C, Krug I, Schrenk D (2015) Evaluation of the cytotoxic and mutagenic potential of three ginkgolic acids. Toxicology 327:47–52. https://doi.org/10.1016/j.tox.2014.10.001

Bernardino AMR, Pinheiro LCS, Ferreira VF, Azevedo AR (2004) Synthesis and antiviral activity of new 4-(phenylamino) thieno[2,3-b]pyridine derivatives. Heterocycl Comm. https://doi.org/10.1515/HC.2004.10.6.407

Broeckel R, Sarkar S, May NA et al (2019) Src family kinase inhibitors block translation of alphavirus subgenomic mRNAs. Antimicrob Agents Chemother. https://doi.org/10.1128/AAC.02325-18

Brown R, Wan J, Kielian M (2018) The alphavirus exit pathway: what we know and what we wish we knew. Viruses 10:89. https://doi.org/10.3390/v10020089

Burlandy FM, Rebello MA (2001) Inhibition of Mayaro virus replication by prostaglandin A1 in Vero cells. Intervirology 44:344–349. https://doi.org/10.1159/000050069

Caldas LA, Ferreira DF, Freitas TRP (2018) Prostaglandin A1 triggers Mayaro virus inhibition and heat shock protein 70 expression in an epithelial cell model. Rev Soc Bras Med Trop 51:584–590. https://doi.org/10.1590/0037-8682-0235-2018

Camini FC, da Silva TF, da Silva Caetano CC et al (2018) Antiviral activity of silymarin against Mayaro virus and protective effect in virus-induced oxidative stress. Antiviral Res 158:8–12. https://doi.org/10.1016/j.antiviral.2018.07.023

Campos D, Navarro S, Llamas-González YY et al (2020) Broad antiviral activity of ginkgolic acid against chikungunya, Mayaro, una, and Zika viruses. Viruses. https://doi.org/10.3390/v12040449

Carvalho CAM, Sousa IP, Silva JL et al (2014) Inhibition of Mayaro virus infection by bovine lactoferrin. Virology 452–453:297–302. https://doi.org/10.1016/j.virol.2014.01.022

Carvalho CAM, Silva JL, Oliveira AC, Gomes AMO (2017) On the entry of an emerging arbovirus into host cells: Mayaro virus takes the highway to the cytoplasm through fusion with early endosomes and caveolae- derived vesicles. PeerJ. https://doi.org/10.7717/peerj.3245

Chen SX, Wu L, Jiang XG et al (2008) Anti-toxoplasma gondii activity of GAS in vitro. J Ethnopharmacol 118:503–507. https://doi.org/10.1016/j.jep.2008.05.023

Chen MW, Tan YB, Zheng J et al (2017) Chikungunya virus nsP4 RNA-dependent RNA polymerase core domain displays detergent-sensitive primer extension and terminal adenylyltransferase activities. Antiviral Res 143:38–47. https://doi.org/10.1016/j.antiviral.2017.04.001

Choi H, Kudchodkar SB, Reuschel EL et al (2019) Protective immunity by an engineered DNA vaccine for mayaro virus. PLoS Negl Trop Dis 13:1–21. https://doi.org/10.1371/journal.pntd.0007042

Chung MS (2017) Antiviral activities of Artemisia princeps var. orientalis essential oil and its α-thujone against norovirus surrogates. Food Sci Biotechnol 26:1457. https://doi.org/10.1007/S10068-017-0158-3

Davis NL, Willis LV, Smitht JF, Johnston RE (1989) In vitro synthesis of infectious venezuelan equine encephalitis virus RNA from a cDNA clone: analysis of a viable deletion mutant. Virology 171:189–204. https://doi.org/10.1016/0042-6822(89)90526-6

Dé I, Fata-Hartley C, Sawicki SG, Sawicki DL (2003) Functional analysis of nsP3 phosphoprotein mutants of Sindbis virus. J Virol 77:13106–13116. https://doi.org/10.1128/jvi.77.24.13106-13116.2003

de Bruyne T, Pieters L, Deelstra H, Vlietinck A (1999) Condensed vegetable tannins: biodiversity in structure and biological activities. Biochem Syst Ecol 27:445–459. https://doi.org/10.1016/S0305-1978(98)00101-X

de Oliveira DM, de Santos IA, Martins DOS et al (2020) Organometallic complex strongly impairs Chikungunya virus entry to the host cells. Front Microbiol. https://doi.org/10.3389/fmicb.2020.608924

Diagne CT, Bengue M, Choumet V et al (2020) Mayaro virus pathogenesis and transmission mechanisms. Pathogens 9:1–23

dos Santos AE, Kuster RM, Yamamoto KA et al (2014) Quercetin and quercetin 3-O-glycosides from Bauhinia longifolia (Bong.) Steud. show anti-Mayaro virus activity. Parasit Vectors 7:130. https://doi.org/10.1186/1756-3305-7-130

Elm JL, Halstead SB, Koff WC (1981) Suppression of dengue virus replication in vitro by rimantadine hydrochloride *. Am J Trop Med Hyg 30:184–189. https://doi.org/10.4269/ajtmh.1981.30.184

Esposito DLA, da Fonseca BAL (2017) Will Mayaro virus be responsible for the next outbreak of an arthropod-borne virus in Brazil? Brazil J Infect Dis 21:540–544

Fernandes LS, da Silva ML, Dias RS et al (2021) Evaluation of antiviral activity of cyclic ketones against Mayaro virus. Viruses 13:2123. https://doi.org/10.3390/V13112123

Ferraz AC, de Moraes T, FS, Nizer WS da C, et al (2019) Virucidal activity of proanthocyanidin against Mayaro virus. Antiviral Res 168:76–81. https://doi.org/10.1016/j.antiviral.2019.05.008

Ferreira PG, Ferraz AC, Figueiredo JE et al (2018) Detection of the antiviral activity of epicatechin isolated from Salacia crassifolia (Celastraceae) against Mayaro virus based on protein C homology modelling and virtual screening. Arch Virol 163:1567–1576. https://doi.org/10.1007/s00705-018-3774-1

Figueiredo CM, da Neris RLS, Gavino-Leopoldino D et al (2019) Mayaro virus replication restriction and induction of muscular inflammation in mice are dependent on age, type-I interferon response, and adaptive immunity. Front Microbiol 10:1–11. https://doi.org/10.3389/fmicb.2019.02246

Filho HR, Coimbra LD, Cassago A et al (2020) Cryo-EM structure of the mature and infective Mayaro virus at 44 Å resolution reveals new features of arthritogenic alphaviruses. bioRxiv. https://doi.org/10.1101/2020.11.06.371773

Firth AE, Chung BY, Fleeton MN, Atkins JF (2008) Discovery of frameshifting in alphavirus 6K resolves a 20-year enigma. Virol J 5:108. https://doi.org/10.1186/1743-422X-5-108

Gall B, Pryke K, Abraham J et al (2018) Emerging alphaviruses are sensitive to cellular states induced by a novel small-molecule agonist of the STING pathway. J Virol. https://doi.org/10.1128/JVI.01913-17

Gescher K, Hensel A, Hafezi W et al (2011) Oligomeric proanthocyanidins from *Rumex acetosa* L. inhibit the attachment of herpes simplex virus type-1. Antiviral Res 89:9–18. https://doi.org/10.1016/j.antiviral.2010.10.007

Götte B, Liu L, McInerney GM (2018) The enigmatic alphavirus nonstructural protein 3 (nsP3) revealing its secrets at last. Viruses. https://doi.org/10.3390/v10030105

Grabarz F, Lopes APY, Barbosa FF et al (2021) Strategies for the Production of Soluble Interferon-Alpha Consensus and Potential Application in Arboviruses and SARS-CoV-2. Life 11:460. https://doi.org/10.3390/life11060460

Holbrook NJ, Carlson SG, Choi AM, Fargnoli J (1992) Induction of HSP70 gene expression by the antiproliferative prostaglandin PGA2: a growth-dependent response mediated by activation of heat shock transcription factor. Mol Cell Biol 12:1528–1534. https://doi.org/10.1128/mcb.12.4.1528

Hosseinimehr SJ, Rostamnejad M, Ghaffari-rad V (2013) Epicatechin enhances anti-proliferative effect of bleomycin in ovarian cancer cell. Res Mol Med 1:25–28. https://doi.org/10.18869/acadpub.rmm.1.3.25

Hua Z, Wu C, Fan G et al (2017) The antibacterial activity and mechanism of ginkgolic acid C15:1. BMC Biotechnol 17:1–12. https://doi.org/10.1186/s12896-016-0324-3

Huang H, Li Y, Sadaoka T et al (2006) Human herpesvirus 6 envelope cholesterol is required for virus entry. J Gen Virol 87:277–285. https://doi.org/10.1099/vir.0.81551-0

Iorio F, Bosotti R, Scacheri E et al (2010) Discovery of drug mode of action and drug repositioning from transcriptional responses. Proc Natl Acad Sci 107:14621–14626. https://doi.org/10.1073/pnas.1000138107

Ishida YI, Takeshita M, Kataoka H (2014) Functional foods effective for hepatitis C: identification of oligomeric proanthocyanidin and its action mechanism. World J Hepatol 6:870–879. https://doi.org/10.4254/wjh.v6.i12.870

Ishimaru D, Marcicano FGP, Rebello MA (1998) Inhibition of Mayaro virus replication by prostaglandin A1 and B2 in Vero cells. Braz J Med Biol Res 31:1119–1123. https://doi.org/10.1590/S0100-879X1998000900003

Jose J, Taylor AB, Kuhn RJ (2017) Spatial and temporal analysis of alphavirus replication and assembly in mammalian and mosquito cells. Mbio. https://doi.org/10.1128/mBio.02294-16

Joshi S, Parkar J, Ansari A et al (2021) Role of favipiravir in the treatment of COVID-19. Int J Infect Dis 102:501–508

Jung LS, Gund TM, Narayan M (2020) Comparison of binding site of remdesivir and its metabolites with NSP12-NSP7-NSP8, and NSP3 of SARS CoV-2 virus and alternative potential drugs for COVID-19 treatment. Protein J 39:619–630. https://doi.org/10.1007/s10930-020-09942-9

Karupiah G, Xie QW, Buller RML et al (1993) Inhibition of viral replication by interferon-γ-induced nitric oxide synthase. Science (1979) 261:1445–1448. https://doi.org/10.1126/science.7690156

Kell DB, Heyden EL, Pretorius E (2020) The biology of lactoferrin, an iron-binding protein that can help defend against viruses and bacteria. Front Immunol 11:1–15. https://doi.org/10.3389/fimmu.2020.01221

Kielian M, Chanel-Vos C, Liao M (2010) Alphavirus entry and membrane fusion. Viruses 2:796–825. https://doi.org/10.3390/v2040796

Kim S, Chen J, Cheng T et al (2021) PubChem in 2021: new data content and improved web interfaces. Nucleic Acids Res 49:D1388–D1395. https://doi.org/10.1093/nar/gkaa971

Langendries L, Abdelnabi R, Neyts J, Delang L (2021) Repurposing drugs for Mayaro virus: Identification of eidd-1931, favipiravir and suramin as Mayaro virus inhibitors. Microorganisms. https://doi.org/10.3390/microorganisms9040734

Lani R, Hassandarvish P, Chiam CW et al (2015) Antiviral activity of silymarin against chikungunya virus. Sci Rep 5:11421. https://doi.org/10.1038/srep11421

Li C, Deng Y-Q, Wang S et al (2017) 25-hydroxycholesterol protects host against Zika virus infection and its associated microcephaly in a mouse model. Immunity 46:446–456. https://doi.org/10.1016/j.immuni.2017.02.012

Li X, Zhang H, Zhang Y et al (2019) Development of a rapid antiviral screening assay based on eGFP reporter virus of Mayaro virus. Antiviral Res 168:82–90. https://doi.org/10.1016/j.antiviral.2019.05.013

Llamas-González YY, Campos D, Pascale JM et al (2019) A functional ubiquitin-proteasome system is required for efficient replication of new world Mayaro and Una alphaviruses. Viruses 11:370. https://doi.org/10.3390/v11040370

Long KC, Ziegler SA, Thangamani S et al (2011) Experimental transmission of Mayaro virus by Aedes aegypti. Am J Trop Med Hyg 85:750–757. https://doi.org/10.4269/ajtmh.2011.11-0359

Lü JM, Yan S, Jamaluddin S et al (2012) Ginkgolic acid inhibits HIV protease activity and HIV infection in vitro. Med Sci Monit 18:293–298. https://doi.org/10.12659/MSM.883261

Ma J, Duan W, Han S et al (2015) Ginkgolic acid suppresses the development of pancreatic cancer by inhibiting pathways driving lipogenesis. Oncotarget 6:20993–21003. https://doi.org/10.18632/oncotarget.3663

Mackay IM, Arden KE (2016) Mayaro virus: a forest virus primed for a trip to the city? Microbes Infect 18:724–734

Malet H, Coutard B, Jamal S et al (2009) The crystal structures of chikungunya and Venezuelan equine encephalitis virus nsP3 Macro domains define a conserved adenosine binding pocket. J Virol 83:6534–6545. https://doi.org/10.1128/jvi.00189-09

Mao S, Ren J, Xu Y et al (2022) Studies in the antiviral molecular mechanisms of 25-hydroxycholesterol: disturbing cholesterol homeostasis and post-translational modification of proteins. Eur J Pharmacol 926:175033. https://doi.org/10.1016/j.ejphar.2022.175033

Maugeri A, Lombardo GE, Cirmi S et al (2022) Pharmacology and toxicology of tannins. Arch Toxicol 96:1257–1277. https://doi.org/10.1007/s00204-022-03250-0

McPherson RL, Abraham R, Sreekumar E et al (2017) ADP-ribosylhydrolase activity of Chikungunya virus macrodomain is critical for virus replication and virulence. Proc Natl Acad Sci USA 114:1666–1671. https://doi.org/10.1073/pnas.1621485114

Melekis E, Tsika AC, Lichière J et al (2015) NMR study of non-structural proteins—part I: 1H, 13C, 15N backbone and side-chain resonance assignment of macro domain from Mayaro virus (MAYV). Biomol NMR Assign 9:191–195. https://doi.org/10.1007/s12104-014-9572-0

Neris RLS, Figueiredo CM, Higa LM et al (2018) Co-protoporphyrin IX and Sn-protoporphyrin IX inactivate Zika, Chikungunya and other arboviruses by targeting the viral envelope. Sci Rep 8:1–13. https://doi.org/10.1038/s41598-018-27855-7

Nguyen PTV, Yu H, Keller PA (2014) Discovery of in silico hits targeting the nsP3 macro domain of chikungunya virus. J Mol Model. https://doi.org/10.1007/s00894-014-2216-6

Ortholand JY, Ganesan A (2004) Natural products and combinatorial chemistry: back to the future. Curr Opin Chem Biol 8:271–280

Painter GR, Bowen RA, Bluemling GR et al (2019) The prophylactic and therapeutic activity of a broadly active ribonucleoside analog in a murine model of intranasal Venezuelan equine encephalitis virus infection. Antiviral Res. https://doi.org/10.1016/j.antiviral.2019.104597

Pinheiro LCS (2012) Searching for new antileishmanial lead drug candidates: synthesis, biological and theoretical evaluations of promising thieno[2,3-b] pyridine derivatives. J Microbiol Antimicrob. https://doi.org/10.5897/JMA11.109

Pizzolitto RP, Herrera JM, Zaio YP et al (2015) Bioactivities of ketones terpenes: antifungal effect on *F. verticillioides* and repellents to control insect fungal vector, *S. Zeamais*. Microorganisms 3:851–865. https://doi.org/10.3390/MICROORGANISMS3040851

Pombal S, Hernández Y, Diez D et al (2017) Antioxidant activity of carvone and derivatives against superoxide ion. Nat Prod Commun 12:653–655. https://doi.org/10.1177/1934578X1701200502

Powell LA, Miller A, Fox JM et al (2020) Human mAbs broadly protect against arthritogenic alphaviruses by recognizing conserved elements of the Mxra8 receptor-binding site. Cell Host Microbe 28:699-711.e7. https://doi.org/10.1016/j.chom.2020.07.008

Qian Y, Peng Y, Shang E et al (2017) Metabolic profiling of the hepatotoxicity and nephrotoxicity of Ginkgolic acids in rats using ultra-performance liquid chromatography-high-definition mass spectrometry. Chem Biol Interact 273:11–17. https://doi.org/10.1016/j.cbi.2017.05.020

Qiao L, Zheng J, Jin X et al (2017) Ginkgolic acid inhibits the invasiveness of colon cancer cells through AMPK activation. Oncol Lett 14:5831–5838. https://doi.org/10.3892/ol.2017.6967

Raulin J (2002) Human immunodeficiency virus and host cell lipids. Interesting pathways in research for a new HIV therapy. Prog Lipid Res 41:27–65. https://doi.org/10.1016/S0163-7827(01)00019-4

Ribeiro-Filho HV, Coimbra LD, Cassago A et al (2021) Cryo-EM structure of the mature and infective Mayaro virus at 4.4 Å resolution reveals features of arthritogenic alphaviruses. Nat Commun 12:3038. https://doi.org/10.1038/s41467-021-23400-9

Rolim Bernardino AM, da Silva Pinheiro LC, Rodrigues CR et al (2006) Design, synthesis, SAR, and biological evaluation of new 4-(phenylamino)thieno[2,3-b]pyridine derivatives. Bioorg Med Chem 14:5765–5770. https://doi.org/10.1016/j.bmc.2006.03.013

Rubach JK, Wasik BR, Rupp JC et al (2009) Characterization of purified Sindbis virus nsP4 RNA-dependent RNA polymerase

activity in vitro. Virology 384:201–208. https://doi.org/10.1016/j.virol.2008.10.030
Rupp JC, Sokoloski KJ, Gebhart NN, Hardy RW (2015) Alphavirus RNA synthesis and non-structural protein functions. J Gen Virol 96:2483–2500. https://doi.org/10.1099/jgv.0.000249
Salgado-Benvindo C, Thaler M, Tas A et al (2020) Suramin inhibits SARS-CoV-2 infection in cell culture by interfering with early steps of the replication cycle. Antimicrob Agents Chemother. https://doi.org/10.1128/AAC.00900-20
Salles TS, Meneses MDF, Caldas LA et al (2021) Virucidal and antiviral activities of pomegranate (Punica granatum) extract against the mosquito-borne Mayaro virus. Parasit Vectors 14:443. https://doi.org/10.1186/s13071-021-04955-4
Salters-Pedneault K (2014) Definition of Mechanism of Action. In: About Health. https://www.cancer.gov/publications/dictionaries/cancer-terms/def/mechanism-of-action
Santos IA, dos Pereira AKS, Guevara-Vega M et al (2022) Repurposing potential of rimantadine hydrochloride and development of a promising platinum(II)-rimantadine metallodrug for the treatment of Chikungunya virus infection. Acta Trop 227:106300. https://doi.org/10.1016/j.actatropica.2021.106300
Shimizu JF, Martins DOS, McPhillie MJ et al (2020) Is the ADP ribose site of the Chikungunya virus NSP3 Macro domain a target for antiviral approaches? Acta Trop 207:105490. https://doi.org/10.1016/j.actatropica.2020.105490
Shin G, Yost SA, Miller MT et al (2012) Structural and functional insights into alphavirus polyprotein processing and pathogenesis. Proc Natl Acad Sci USA 109:16534–16539. https://doi.org/10.1073/pnas.1210418109
Sivropoulou A, Nikolaou C, Papanikolaou E et al (1997) Antimicrobial, cytotoxic, and antiviral activities of *Salvia fructicosa* essential oil. J Agric Food Chem 45:3197–3201. https://doi.org/10.1021/JF970031M
Snyder JE, Kulcsar KA, Schultz KLW et al (2013) Functional characterization of the alphavirus TF protein. J Virol 87:8511–8523. https://doi.org/10.1128/JVI.00449-13
Sousa IP, Carvalho CAM, Gomes AMO (2020) Current understanding of the role of cholesterol in the life cycle of alphaviruses. Viruses 13:35. https://doi.org/10.3390/v13010035
Spindola KCW, Simas NK, Salles TS et al (2014) Anti-Mayaro virus activity of Cassia australis extracts (Fabaceae, Leguminosae). Parasit Vectors 7:537. https://doi.org/10.1186/s13071-014-0537-z
Subudhi B, Chattopadhyay S, Mishra P, Kumar A (2018) Current strategies for inhibition of chikungunya infection. Viruses 10:235. https://doi.org/10.3390/v10050235
Sun X, Whittaker GR (2003) Role for influenza virus envelope cholesterol in virus entry and infection. J Virol 77:12543–12551. https://doi.org/10.1128/JVI.77.23.12543-12551.2003
Sun J, Wu D (2019) Mayaro virus, a regional or global threat? Travel Med Infect Dis 32:101462
Sun W, Tanaka TQ, Magle CT et al (2015) Chemical signatures and new drug targets for gametocytocidal drug development. Sci Rep 4:3743. https://doi.org/10.1038/srep03743
Tan YB, Lello LS, Liu X et al (2022) Crystal structures of alphavirus nonstructural protein 4 (nsP4) reveal an intrinsically dynamic RNA-dependent RNA polymerase fold. Nucleic Acids Res 50:1000–1016. https://doi.org/10.1093/nar/gkab1302
Taylor SF, Patel PR, Herold TJS (2005) Recurrent arthralgias in a patient with previous mayaro fever infection. South Med J 98:484–485. https://doi.org/10.1097/01.SMJ.0000145879.14102.F4
Terlizzi ME, Occhipinti A, Luganini A et al (2016) Inhibition of herpes simplex type 1 and type 2 infections by Oximacro®, a cranberry extract with a high content of A-type proanthocyanidins (PACs-A). Antiviral Res 132:154–164. https://doi.org/10.1016/j.antiviral.2016.06.006
Theilacker C, Held J, Allering L et al (2013) Prolonged polyarthralgia in a German traveller with Mayaro virus infection without inflammatory correlates. BMC Infect Dis 13:2011–2014. https://doi.org/10.1186/1471-2334-13-369
Tian L, Qiang T, Liang C et al (2021) RNA-dependent RNA polymerase (RdRp) inhibitors: The current landscape and repurposing for the COVID-19 pandemic. Eur J Med Chem 213:113201
Tsika AC, Melekis E, Tsatsouli SA et al (2019) Deciphering the nucleotide and RNA binding selectivity of the Mayaro virus macro domain. J Mol Biol 431:2283–2297. https://doi.org/10.1016/j.jmb.2019.04.013
Tsukuda S, Watashi K, Hojima T et al (2017) A new class of hepatitis B and D virus entry inhibitors, proanthocyanidin and its analogs, that directly act on the viral large surface proteins. Hepatology 65:1104–1116. https://doi.org/10.1002/hep.28952
Uversky VN (2013) Intrinsic disorder-based protein interactions and their modulators. Curr Pharm Des 19:4191–4213. https://doi.org/10.2174/1381612811319230005
Valdés-Torres P, Campos D, Bhakta M et al (2022) Honokiol and alpha-Mangostin inhibit Mayaro virus replication through different mechanisms. Molecules 27:7362. https://doi.org/10.3390/molecules27217362
Wagoner J, Negash A, Kane OJ et al (2010) Multiple effects of silymarin on the hepatitis C virus lifecycle. Hepatology 51:1912–1921. https://doi.org/10.1002/hep.23587
West J, Hernandez R, Ferreira D, Brown DT (2006) Mutations in the endodomain of Sindbis virus glycoprotein E2 define sequences critical for virus assembly. J Virol 80:4458–4468. https://doi.org/10.1128/JVI.80.9.4458-4468.2006
Young LS, Ruschel S, Yanchuk S, Pereira T (2019) Consequences of delays and imperfect implementation of isolation in epidemic control. Sci Rep 9:1–9. https://doi.org/10.1038/s41598-019-39714-0
Yousefi H, Mashouri L, Okpechi SC et al (2021) Repurposing existing drugs for the treatment of COVID-19/SARS-CoV-2 infection: a review describing drug mechanisms of action. Biochem Pharmacol 183:114269
Zhang R, Kim AS, Fox JM et al (2018) Mxra8 is a receptor for multiple arthritogenic alphaviruses. Nature 557:570–574. https://doi.org/10.1038/s41586-018-0121-3
Zhang Z, He G, Filipowicz NA et al (2019) Host lipids in positive-strand RNA virus genome replication. Front Microbiol. https://doi.org/10.3389/fmicb.2019.00286

Publisher's Note Springer Nature remains neutral with regard to jurisdictional claims in published maps and institutional affiliations.

Springer Nature or its licensor (e.g. a society or other partner) holds exclusive rights to this article under a publishing agreement with the author(s) or other rightsholder(s); author self-archiving of the accepted manuscript version of this article is solely governed by the terms of such publishing agreement and applicable law.

iScience

CellPress
OPEN ACCESS

Review

In vitro and *in vivo* models for monkeypox

Rafael Borges Rosa,[1,2] Emilene Ferreira de Castro,[2] Murilo Vieira da Silva,[2] Denise Caroline Paiva Ferreira,[2] Ana Carolina Gomes Jardim,[3] Igor Andrade Santos,[3] Mikaela dos Santos Marinho,[3] Flávia Batista Ferreira França,[4] and Lindomar José Pena[1,*]

SUMMARY

The emergence and rapid spread outside of monkeypox virus (MPXV) to non-endemic areas has led to another global health emergency in the midst of the COVID-19 pandemic. The scientific community has sought to rapidly develop *in vitro* and *in vivo* models that could be applied in research with MPXV. *In vitro* models include two-dimensional (2D) cultures of immortalized cell lines or primary cells and three-dimensional (3D) cultures. *In vitro* models are considered cost-effective and can be done in highly controlled conditions; however, they do not always resemble physiological conditions. In this way, several *in vivo* models are being characterized to meet the growing demand for new studies related to MPXV. In this review, we summarize the main MPXV models that have already been developed and discuss how they can contribute to advance the understanding of its pathogenesis, replication, and transmission, as well as identifying antivirals to treat infected patients.

INTRODUCTION

The etiologic agent of zoonotic monkeypox disease (MPX) is the monkeypox virus (MPXV). Belonging to the family Poxviridae and the genus *Orthopoxvirus*, this virus was isolated for the first time in 1958 from vesicopustular lesions of infected cynomolgus monkeys kept for research.[1] The virus can be divided into two viral clades: the Congo Basin (clade I) and the West African (clade II). The Congo Basin viruses are more virulent, with human case fatality rates during outbreaks in parts of Africa estimated to be around 10%. Although monkeypox is so named because researchers first detected it in monkeys, the virus is believed to be transmitted by wild animals such as rodents or infected people.[2] These animals can transmit the disease to humans and secondarily the disease is limited through person-to-person transmission.[3]

Patients affected by the disease may initially present with fever, headache, back pain, asthenia, myalgia, rash, and lymphadenopathy. Lymphadenopathy is a distinctive feature of the disease that can be used to differentiate it from other infections that have similar clinical presentation at onset (chickenpox, measles, smallpox).[3] In more severe cases, monkeypox complications can cause pneumonitis, encephalitis, vision hazard keratitis, and secondary bacterial infections.[4,5] Previous studies show that mortality rates vary substantially and are vulnerable to case finding bias.[6] Historically, the case fatality rate of monkeypox ranges from 0% to 11%, with young children being the most vulnerable group. In the recent epidemics, the case fatality ratio has varied from 3% to 6%.[3]

Since the first human monkeypox infection was reported in 1970, most outbreaks have been confined to central Africa. The first significant outbreak outside Africa occurred in 2003 in the U.S. and was epidemiologically linked to imported exotic pets (Gambian pouched rats and dormice) from Ghana that spread the virus to pet prairie dogs and from them to humans.[7] In recent years, both travel-related and non-travel-related cases have been reported outside of West and Central Africa, which are considered endemic areas. Europe, North America, Australia, and Asia had records of the disease.[8] However, the number of cases registered outside endemic areas has increased considerably. As of November 7, 2022, more than 78 thousand cases of monkeypox with 43 fatalities have been reported in a total of 109 countries (102 non-endemic and 7 endemic countries).[9] On July 23, 2022, World Health Organization (WHO) declared the current monkeypox epidemic represents a Public Health Emergency of International Concern (PHEIC).[10]

Since its discovery to date, several research models have already been developed mimicking the pathophysiology of the disease. In this review, we summarize the main models *in vitro* (2D and 3D cell culture)

[1]Department of Virology and Experimental Therapy (LAVITE), Aggeu Magalhães Institute (IAM), Oswaldo Cruz Foundation (Fiocruz), Recife 50740-465, Brazil

[2]Rodents Animal Facilities Complex, Federal University of Uberlândia (REBIR-UFU), Uberlândia 38400-902, Brazil

[3]Institute of Biomedical Sciences, Federal University of Uberlândia, Uberlândia 38405-302, Brazil

[4]Institute of Biomedical Sciences, Federal University of Uberlândia, Uberlândia 38405-318, Brazil

*Correspondence: lindomar.pena@fiocruz.br, lindomarfiocruz@gmail.com

https://doi.org/10.1016/j.isci.2022.105702

This is an open access article under the CC BY-NC-ND license (http://creativecommons.org/licenses/by-nc-nd/4.0/).

and *in vivo* developed to study monkeypox biology and discuss its advantages, disadvantages, and how these models can contribute to coping with the disease.

IN VITRO MODELS

In order to study viral infections, tools rather than the natural host are needed due to the impact and lethality of the disease caused by viruses.[11] As a solution, Renato Dulbecco and Marguerite Vogt proposed the use of cell lineages in viral research in late 1950, which revolutionized how knowledge is acquired by facilitating the study of viral infection and its replication kinetics.[12,13] It also resulted in the evolution of the previous time-consumption drug discovery process to an optimized and high selective one,[14] added to the alignment with the ethical desire for reducing animal use.[15] In this context, it is possible to hypothesize the importance of knowing the most suitable cell culture model to be applied in the studying of the MPXV pathogenesis or to the screening and identification of active molecules that might be capitalized into the clinical treatment of the disease. The *in vitro* assays have shown that the cells Vero, Vero 76, Vero E6, LLC-MK2, BSC-40, BSC-1, PEK, HEP-2, HeLa, MA-104, HFF, and Balb/3T3 clone A31 are susceptible and capable of maintaining the MPXV replication, resulting in a high titer stock of virus, added of interested applicability into antiviral identification. The cell culture models, their characteristics, as well as their advantages and disadvantages are detailed below and summarized in Table 1.

CELL LINEAGES DIRECTLY EMPLOYED IN THE MPXV STUDY

MPXV was isolated in non-human primates in 1958 from pustules present on cynomolgus monkeys.[1] For this, HeLa, monkey kidney, and human amnion cells were incubated with the supernatant of the emulsified pustules. The presence of cytopathic effect was observed 2–3 days after infection. The three types of infected cells were characterized by presenting alterations in their morphological structure.[1]

In humans the MPXV was first isolated from a human host in 1970 in the Democratic Republic of the Congo by material collected from skin lesions.[16] The isolation and characterization of the cytopathic effect were performed by infecting four immortalized cell lines Vero (African green monkey kidney), PEK (pig embryonic kidney cells), and HEP-2 (*Homo sapiens* epithelial carcinoma cells) with a 10-fold $TCID_{50}$ serial dilution of MPXV and analyzed up to 7 days post-infection (d.p.i.). In Vero cells, the MPXV formed larger plates than the variola virus with a pattern of internal structure characteristic of other MPXV isolated from monkeys. In addition, when comparing all cell lines, Vero cells were more sensitive to MPXV when compared with HEP-2, and PEK, producing higher titers (about 10^7 to 10^8 $TCID_{50}$). The MPXV can be distinguished from variola and vaccinia viruses in PEK cells by its lower replication and the lack of hemadsorption phenomena.

In the attempt to identify antiviral molecules capable of inhibiting the MPXV replication cycle as well as understanding its replication mechanism, several methodologies were employed throughout the literature. Baker and coworkers used Vero 76 (African green monkey kidney), Vero E6 (African green monkey kidney deficient in type I interferon [IFN-I]), LLC-MK2 (Rhesus monkey kidney cells), and BSC-40 cells. The BSC-40 is a continuous cell line derived from BSC-1 cells (Vervet monkey kidney cell)[18,31] and is suitable for amplification and isolation of large viruses such as the poxviruses due to their resemblance with the natural host. Therefore, this cell lineage was used by the authors for inoculation and amplification for 5 days and collected by centrifugation associated with freeze-thaw cycles. As for the title of the MPXV, Vero E6 cells were employed because it is deficient in an IFN-I pathway and might favor viral replication.[32] The protocol used by the authors was based on incubating the virus with cells for 2 h, adding a medium with carboxymethyl cellulose (CMC), analyzed for up to 3 or 5 days p.i. through fixation with crystal violet staining solution (1.3 mg/mL crystal violet, 5% ethanol, 30% formalin), and plaques counted visually. For antiviral assays, the authors employed the neutral red uptake assay, an absorbance technique to assess cell viability where healthy, uninfected cells will take up neutral red dye through pinocytosis, whereas cells infected with a cytopathic virus will not. The Vero 76 and LLC-MK2 cell lines were infected with MOI of 0.01, 0.1, and 1 in the presence of serial dilutions of each one of the 24 compounds analyzed in 96 well plates. The incubation period was related to the presence of CPE in virus-infected and untreated cell control, and the assessment of the potential compounds by IC_{50} values was better visualized in 5-day incubation and MOI of 0.1. Alternatively, the plaque-forming assay was also used, and the MPXV took 4–5 days to produce plaques of similar size in Vero 76, Vero E6, or BSC-40 cells, whereas other poxviruses produced small plaques after 5–6 days with lower cytopathic effect. Following the technical protocol of plaque reduction assay, Rogers and collaborators (2008) evaluated the effect of silver nanoparticles against MPXV, however employing only

Table 1. Cells models used in the study of MPXV

Cell/tissue type	Virus strain	Viral cultivation	Main applications	Reference
Vero	Congo-8 virus; VARV-UK-60/Ind-3a, MPXV-Copenhagen/Z79-I-005, VACV- Copenhagen, CPXV-Grishak, and ECTV-K-1	Cells were cultured in RPMI-1640 or MEM supplemented with 2–10% fetal bovine serum, at 37°C in a 5% CO2 atmosphere. Some authors mentioned the use of antibiotics and antimycotics	Virus isolation, plaque-forming assay, virus amplification, infection characterization, evaluation of host responses, and evaluation of antiviral activity	(Marennikova et al.[16]; Rogers et al.[17])
PEK, and HEP-2	Congo-8 virus; VARV-UK-60, MPXV-Copenhagen/ Liberia-1/Liberia-2/V-70 1 266	[a]	Cell susceptibility	(Marennikova et al.[16])
LLC-MK2	MPXV-V79-1-005-Scab/ Katako Kombe and MPXV-GFP	Cells were cultured in RPMI-1640 or OPTI-MEM-I supplemented with 2-10% fetal bovine serum, with antibiotics and antimycotics, at 37°C in a 5% CO2 atmosphere. Cells were infected with an MOI of 0.001, 0.01, 0.1, or 1 and incubated for 1–8 days	Plaque-forming assay, neutral red uptake assay, MTT assay, virus amplification, virus isolation, infection characterization, evaluation of host responses, evaluation of antiviral activity, and siRNA transfection	(Baker et al.[18]; Alkhalil et al.[19])
Vero 76	MPXV-V79-1-005-Scab, VACV-Elstree/ Copenhagen, CPXV-Marina/Brighton, and CMLV-Somalia	Cells were cultured in RPMI-1640 supplemented with 2 or 10% fetal bovine serum or Eagle's EMEM with Hanks' salts and 5% fetal calf serum, supplemented with antibiotics and antimycotics, at 37°C in a 5% CO2 atmosphere. Cells were infected with an MOI of 0.01–1 or with 100 plaque-forming units (p.f.u) of virus/well and incubated for 3–6 days	Plaque-forming assay, neutral red uptake assay, virus amplification, virus isolation, infection characterization, evaluation of host responses, and evaluation of antiviral activity	(Baker et al.[18]; Yang and Schneller,[20]; Smee et al.,[21])
Vero E6	MPXV-V79-1-005-Scab, MPXV-GFP-tdTR, Katako Kombe and MPXV-GFP	Cells were cultured in RPMI-1640, EMEM, or DMEM supplemented with 2%–10% fetal bovine serum, with antibiotics and antimycotics, at 37°C in a 5% CO2 atmosphere. Cells were infected with an MOI of 0.1 or 5 and incubated for 1–5 days	Plaque-forming assay, neutral red uptake assay, virus amplification, virus isolation, infection characterization, evaluation of host responses, evaluation of antiviral activity, and transfection	(Baker et al.[18]; Johnston et al.[22]; Alkhalil et al.[19])
MA-104	MPXV-GFP-tdTR/Z79-I-005	Cells were cultured in MEM supplemented with 10% fetal bovine serum, with antibiotics and antimycotics, at 37°C in a 5% CO2 atmosphere. Cells were infected with an MOI	Infection characterization, evaluation of host responses, evaluation of antiviral activity	(Johnston et al.[22])

(*Continued on next page*)

Table 1. *Continued*

Cell/tissue type	Virus strain	Viral cultivation	Main applications	Reference
		of 0.01 or 5 and incubated for 24 h		
HeLa	MPXV-GFP-tdTR/Z79-I-005 CPXV-Brighton Red, VACV-WR-GFP/NLS/WR-A4-YFP/LUC and AKMV	Cells were cultured in DMEM supplemented with 2%–10% fetal bovine serum or calf serum, at 37°C in a 5% CO2 atmosphere. Some authors mentioned the use of antibiotics and antimycotics. Cells were infected with an MOI of 0.01 or 5 and incubated for 16–24 h	MPXV isolation, plaque-forming assay, infection characterization, evaluation of host responses, evaluation of antiviral activity, immunofluorescent cell staining, transfection, IFN I response analysis	(Magnus et al.[1]; Johnston et al.[22]; Priyamvada et al.[23]; Fernández de Marco et al.[24])
Balb/3T3 clone A31	MPXV-Z79-I005, VARV-Copenhagen, CPXV-Brighton, and CMLV-Somalia	Cells were cultured in medium supplemented with 2% serum and infected with 100 plaque-forming units (p.f.u) of virus/well and incubated for 3–6 days	Plaque-forming assay, neutral red uptake assay, infection characterization, evaluation of host responses, evaluation of antiviral activity	(Smee et al.[21])
BSC-40	MPXV-V79-1-005-Scab)/V70-I-266/V78-I-3945/V81-I-179/V77-I-823/V1979-I-005/2003-RCG-358/2003-USA-039/2003-USA-044/RCG2003-RCG-358, VARV-SOM77-ali/NEP73-175/BSH74-sol/SUD47-juba/SLN68-258/BRZ66-39, CPXV-Brighton Red, VACV-WR-GFP/NLS/WR-A4-YFP/LUC, and AKMV	Cells were cultured at 37°C in a 5% CO2 atmosphere, in Opti-MEM (Invitrogen) or DMEM/RPMI-1640 supplemented with 2%–10% fetal bovine serum, antibiotics, and antimycotics. Cells were infected with an MOI of 0.1 or 10 PFU/cell and incubated for 2–5 days	Plaque-forming assay, neutral red uptake assay, virus amplification, infection characterization, evaluation of host responses, evaluation of antiviral activity, transfection	(Baker et al.[18]; Smith et al.[25]; Priyamvada et al.[23]; Fernández de Marco et al.[24]; Fogg et al.[26])
BSC-1	CPXV-Brighton/GER_1990_2/GER_1991_3/GER_2002_MKY/CPXV-Br (ATCC VR-302)/CPXV-GFP, MPXV-Z76/Z79-I-005/MSF6 B16R, VACV -WR (ATCC VR-1354)/IHD-J/MVA (ATCC VR-1508)/WR B18, VARV-BSH1975 B17R	DMEM, RPMI supplemented with 2%–10% fetal bovine Serum or with 5%–10% fetal calf serum. Cells were infected with an MOI of 0.01 or 1	Plaque-forming assay, infection characterization, analysis of the virus-cell fusion process, evaluation of host responses, evaluation of antiviral activity, and yield reduction assay	(Altmann et al.[27,28]; Bengali et al.[29]; Fernández de Marco et al.[24])
A549	MPXV 2003-USA-044/RCG2003-RCG-358	DMEM with 5%–10% fetal calf serum	Transfection, IFN-III response analysis	(Fernández de Marco et al.[24])
RK 13	MPXV WR-7-61	Cells were maintained in MEM supplemented with 5% fetal bovine serum, at 37°C with 5% CO2	Plaque-forming assay	(Arndt et al.[30])

[a]Not reported; VARV: variola virus; MPXV: monkeypox virus; VACV: vaccinia virus; CPXV: cowpox virus; ECTV: ectromelia virus; CMLV: camelpox virus; AKMV: Akhmeta virus; MOI: MOI; p.f.u: plaque formation unit.

the Vero cells in 12 well plates. The cells were infected with 50 p.f.u/well for 1 h and further treated with a serial dilution of the compound diluted into the medium with methylcellulose for 72 h.[17]

In another study, BSC-40 cells were also infected with MPXV V70-I-266 (Sierra Leone) to propagation finality, but also for the antiviral screening protocols. The cells were seeded in 96 well plates, infected with MOI of 0.1 for 1 h, removed, and replaced with ST-246 in 8 concentrations. After 3 days, the plate was stained with 2x crystal violet, and absorbance was measured at 570 nm, where the intensity of treatment was compared with the virus-infected control.[25] Alternatively, the plaque reduction assay was performed by infecting BSC-40 cells in six-well plates with 25 p.f.u for 1 h, added of media with CMC with the compound in five concentrations for 3 days, fixed with 10% formalin, and submitted to immunohistochemistry polyclonal rabbit anti-variola virus antibody and goat anti-rabbit immunoglobulin G-horseradish peroxidase conjugate. The effect of the compound ST-246 was observed by the protection of reducing the CPE, which was seen even in low concentrations (0.015 μM). The BSC-40 was also employed by the authors in further studies to confirm and evaluate results encountered *in vivo* and in clinical trials to find viral titer, evaluate drug resistance, and perform serological analysis following the same protocols cited earlier.[33,34]

Differently, other authors employed the original BSC-1 cell line instead of the BSC-40 with interesting results. The BSC-1 cells seeded in 24 well plates were infected with 100 PFU for 1 h, overlaid with agarose 2% in the presence or absence of EB peptide (NH_2- RRKKAAVALLPAVLLALLAP-COOH) to assess the reduction effect on plaque formation. To this, BSC-1 cells were infected at an MOI of 0.01 with the MPXV or with an inoculum containing the virus pre-treated with EB. Three days post-infection, cells were harvested by scraping, lysed by repeated cycles of freezing and thawing, and tittered on BSC-1 cells. As a result, the MXPV infectivity was significantly inhibited by the EB peptide, mainly in its attachment stage.[27] To confirm, the authors based on the fact orthopoxvirus cores are only accessible to antibodies after being released into the cytoplasm, which allows the differentiation between attached and entered viruses using virion-specific or core-specific antibodies, respectively.[35] To examine whether EB was disrupting virus attachment or entry into the cells, the number of attached and entered viruses per cell for 100 cells in the absence or presence of EB at 100 μM was quantified in a fluorescence microscope. Samples for attachment staining were fixed with 4% paraformaldehyde, quenched for 5 min with 100 mM glycine, blocked with 10% FBS in PBS, and stained with 1:200 anti-VACPXV antibody. Even if the compound is not capitalized in the clinic, it possesses the greatest potential as a novel *in vitro* tool to study the poorly characterized early steps in infection with poxviruses.

Further studies conducted by Altmann and collaborators also employed the BSC-1 cells in the assays with MPXV.[28] Because the MXN is an intercalating agent and inhibits topoisomerase II function resulting in impaired cellular DNA replication and RNA synthesis,[36] the authors suggested the possibility of inhibiting MPXV replication. Interestingly, to identify the activity of the MXN, a growth curve with MPXV at an MOI of 3 in the presence of the mitoxantrone (MXN) at 1 μM was generated. The supernatant was collected in time intervals of 1, 2, 6, 12, 24, and 36 h post-infection (h.p.i.). The authors also used an MPXV containing a GFP marker with MOI 1 in the presence of the serial dilutions of the MXN, which resulted in inhibition of MPXV replication with a low EC_{50} (0.25 μM). In addition, Bengali et al. (2012) used BSC-1 cells to analyze and compare characteristics involved in the cellular invasion of some orthopoxviruses strains *in vitro*, including MPXV. For this, MPXV expressing luciferase was constructed, and its expression was measured during the entry of the virus into the cell, using a luminometer. The authors observed that MPXV utilizes a low pH-dependent endocytic pathway during cell invasion.[29]

Johnston and coworkers took a different approach and employed several cell lineages: Vero-E6, HeLa, and MA-104. The Vero E6 cells were infected with MPXV and then transfected with a DNA plasmid containing the GFP from the early viral synthetic E/L promoter and tandem dimer Tomato Red (TR). The assay resulted in the production of MPXV-GFP-tdTR. After harvesting, the virus was amplified in MA-104 cells. These are non-human primate cells isolated from a pure cell population of African green monkey kidneys, which are also derived from the MPXV's natural host. Further, the HeLa cells, naturally non-producing IFN-β cells[37,38] were pre-treated with IFN-β in serial dilutions and then infected with the MPXV-GFP-tdTR in high (5) or low (0.01) MOIs. The effect was assessed by titration in a plaque reduction assay and resulted in the identification that MPXV is susceptible to IFN-β, even in low concentrations.[22]

In an attempt to identify antiviral molecules capable of inhibiting the MPXV replication cycle, Alkhalil and coworkers evaluated the RNAi pathway as a new approach in drug discovery against poxviruses. For

antiviral screening, siRNAs targeted against various monkeypox viral proteins were developed and transfected into LLC-MK2 cells. The morphology of the transfected cells was analyzed with phase-contrast light microscopy after transfection, and no signs of cytotoxicity were observed in cells treated with the siRNA pools. The antiviral properties of the most potent siRNA constructs were characterized by transfecting LLC-MK2 cells with a single serial dilution of each construct at six concentrations between 40 and 1.25 nM. Later, the transfected cells were infected with 100 p.f.u/well of MPXV, and viral replication was examined at 48 h.p.i. The siA6-a siRNA was able to inhibit completely the MPXV infection at concentrations of $\geq$20 nM. The antiviral effects of siA6-a target the virus directly, silencing gene expression or interfering with vDNA replication without disrupting host cell biology. The study of chemical modification and the development of a siRNA delivery system are necessary before the evaluation of siA6-a in animal models.[19]

Yang and Schneller (2005) investigated the antiviral potential of S-adenosyl-L-hemocosteine (AdoHcy) hydrolase inhibitors, important for interrupting methylation reaction processes essential for viral replication. The experiments were performed using Vero 76 cells, MPXV, and 5'Homoaristeromycin inhibitor. The authors observed that the use of 5'homoaristeromycin 0.12 μg/mL showed satisfactory results against MPXV replication.[20]

To assess the antiviral activity of ribavirin and mycophenolic acid, Vero 76 and Balb/3T3 clone A31 cells were infected with MPXV (Zaire strain). The reduction effect on plaque formation was observed from cells infected with 100 plaque-forming units (p.f.u) of virus per well incubated for 1.5–2 h. Antivirals were incubated for 6 days, and plate sizes were analyzed.[21] In addition, Priyamvada et al. (2021) used HeLa cells to test the antiviral effects of methylene blue derivatives against orthopoxviruses, including the MPXV WA clade. For the plaque reduction assay, HeLa cells were incubated with MPXV and treated with PAV-164 derived from PAV-866, a methylene blue analog, for 24 h. PAV-164 demonstrated efficiency in inhibiting viral replication at concentrations of 5 μM and 1.6 μM.[23]

It has been reported that poxvirus evades the immune response through the expression of secreted interferon (IFN) decoy receptors such as IFNα/β-binding protein (IFNα/βBP). These proteins prevent the interaction of IFN with cell receptors. Thus, de Marco et al. (2009) investigated the expression of IFNα/βBP in MPXV, using BSC-1 cells. For this analysis, BSC-1 cells were infected with RCG or USA MPXV strains, and after 40 h of incubation, their supernatant was collected and analyzed using the western blotting technique. It was observed that MPXV secretes proteins with type I IFN inhibitory activity, which leads to a failure in the antiviral response and disease progression. Furthermore, the antiviral activity induced by hIFNα-2b, hIFNα-A, or hIFNβ was inhibited.[24] In addition, Arndt et al. (2015) observed that in RK13 (rabbit kidney cells) and BSC-40 cells treated with IFN-α A/D and infected with MPXV, viral replication was not affected. Similar result was found in cells treated and infected with VACV.[30]

BSC-40 cells were used in a study to investigate the neutralizing potential of monkey sera previously immunized with recombinant VACV protein. The results showed that MPXV incubated with monkey serum were neutralized and had their ability to spread prevented.[26]

From what has been presented here, it is possible to suggest that MPXV can infect several mammalian cell lineages independently of being a primate or non-primate host. This agrees with previous data described in literature because poxviruses do not need specific receptors for attaching and entering the cells,[39] as they can interact with glycosaminoglycans or components of the extracellular matrix,[40–43] and thus cytokine receptors may favor the infection.[39] In this context, poxviruses can enter permissive and restrictive cells, but what will differentiate the establishment of infection will be the presence of machinery that can control downstream intracellular events to favor or abort viral replication. It was demonstrated by Marennikova and coworkers that HEP-2 and PEK cells produced low viral titer when compared with Vero cells, confirming that those would not be a good fit for viral isolation, amplification, or research purposes.[16] What is more interesting is that a tissue-cell lineage is permissible and has the machinery needed for viral replication, which can result in a good fit for *in vitro* infection; however, in normal conditions, the vertebrate species might not be considered a permissive host.[39] Therefore, the appropriated cell choice will be dependent on the purpose and/or hypothesis to be evaluated. Given the continuous accelerated evolution of MPXV, new studies with the currently circulating strains will contribute to understanding of viral infection mechanism.

IN VIVO MODELS

What is expected of an ideal animal model is that it can develop the viral infection in a similar way to what occurs in humans, taking into account the pathogenesis of the disease and the clinical signs presented by patients. It is possible to elucidate virus biology and the mechanisms of infection using *in vivo* approaches; such findings are important for the definition of a suitable animal model for the development of studies aimed at the search for new preventive and therapeutic therapies. Although each animal species has some limitations as to inoculation route, dose, and age, *in vivo* experimental studies have demonstrated a wide variety of species capable of efficiently modeling the cycle of infection caused by MPXV.[44,45] The main animal models already used in monkeypox studies will be detailed below, and their main characteristics are summarized in Tables 2, 3, 4, 5, and 6. Because some of these studies were done with past MPXV strains, these data should be interpreted with caution in the context of emerging viral lineages and strains.

MURINES

The mouse (*Mus musculus*) has been a widely used model since the discovery of MPXV. The pathogenesis of the disease has been modeled largely from animal studies, with mice initially used in the evaluation of ectromelia infection and to make kinetic observations of the spread of some viruses.[98]

Initial studies were devoted to investigating the susceptibility of mice to MPXV. In these tests, adult mice were inoculated intracerebrally with MPXV recovered from infected monkeys. After infection, the animals showed signs of encephalitis followed by 100% lethality. The brains of the animals were collected, processed, and the supernatant reinoculated into a new group of animals, and all these succumbed to infection. A group of two-day-old suckling mice was also evaluated in this study. The animals were inoculated intranasally. Both the virus passed into monkeys, and the virus passed into mice killed 100% of the animals.[1] Mortality rates related to contemporary strains of MPXV are low compared with data with past strains.[99] Lethal models certainly helped to elucidate the mechanisms that lead patients to death and contributed to the prophylactic measures that are available. It should also be considered that the current mortality rate may be underestimated considering the lack of adequate surveillance in some countries, in addition to the possibility of new, more virulent variants as the virus circulates. For all these possibilities, lethal models may contribute to further investigations on MPXV. Still, there is a need to develop new non-lethal characterized models for studies of current circulating strains. Recently, Warner and coworkers demonstrated that CAST/EiJ mice, a wild-derived inbred strain, does not succumb to infection with the 2022 circulating strain following intranasal exposure, although they are highly susceptive to clade 1 and 2 MPXV and developed fatal disease upon challenge.[55]

The subcutaneous paw pad inoculation route in adult mice was not efficient in infecting the A129, C57BL/6, DBA, A/Ncr, C3HeJ, IFN$\gamma R^{-/-}$, and IFN-$\alpha/\beta R^{-/-}$ strains. In animals characterized as not responding to IFN-1-dependent or type 2 signaling pathways, on the other hand, infection occurred satisfactorily induced by strain line 1 in C57BL/6 stat1$^{-/-}$ and 129 stat1$^{-/-}$ mice. Twenty-five percent death was observed in female C57BL/6 stat1$^{-/-}$ mice 21 days post-infection, whereas 50% death was observed in male mice 12 days post-infection. When infected at the higher dose (4,700 p.f.u), all animals died within 9 days post-infection showing high viral titers in the lung. The immunodeficient SCID (severe combined immunodeficient) strain was susceptible to an intranasal MPXV infection, as were C57BL/6 and 129 stat1$^{-/-}$, which are due to their failure to respond to STAT1 induced by IFN type 1 and 2 pathway signaling. Overall, high mortality was a feature observed in STAT1-deficient mice, in addition to weight loss and viral presence in internal organs.[46] Stabenow et al. (2010) showed a gender effect on MPXV-induced mortality in STAT1-deficient C57BL/6 mouse, with males showing higher mortality rate than females. New studies are needed to assess the role of sex in monkeypox susceptibility and may elucidate mechanisms of host-pathogen interaction.

The importance of IFN in protection against MPXV infection has also been demonstrated by intranasal administration of the cytokine in CAST/EiJ mice, which led to protection against MPXV. In addition, C57BL/6 mice with inactivation of the IFN gene or the IFN receptor gene show increased sensitivity to the disease.[47] Interferon knockout mice are historically known as suitable models in studies of viral infections. Many viruses have infection mechanisms that can be easily interrupted by the natural defense of mice with an intact immune system; this can be considered one of the reasons why the characterization of immunocompetent models for studies on the development of antivirals and vaccines is still a difficult task. For this reason, knockout models and/or immunocompetent mice at an age when the immune system

Table 2. Mice used in the study of MPXV

Animal species	Strain	Age	Viral strain	Route of infection/ dose	Major findings	Reference
Mouse (*Mus muscullus*)	[a]	Adults and 2-day-old	Egg passage material of the monkey agent	Intracerebral and intranasal/agent diluted 10^4	Adult mice inoculated intracerebrally showed signs of encephalitis followed by 100% lethality. Two-day-old infant mice inoculated intranasally showed 100% lethality	(Magnus et al.[1])
	C57BL/6, SCID, DBA, A/Ncr, C3HeJ, IFN-γR−/−, BALB/c, IFN-α/βR−/−, 129 stat1−/−, C57BL/6 stat1−/−	6- to 12-week-old	MPXV-ZAI-79	Intranasal/[a] and footpad 10^2–10^4 p.f.u/mL	Footpad inoculation in adult mice was not efficient in infecting strains characterized as not responding to IFN-1 or type-2-dependent signaling pathways, on the other hand, infection occurred satisfactorily in C57BL/6 stat1−/− and 129 stat1−/− mice. In contrast, the immunodeficient SCID strain was susceptible to an intranasal MPXV infection, as were C57BL/− and 129 stat1−/− 129 stat1−/−. Overall, high mortality was a feature observed in STAT1-deficient mice, in addition to weight loss and viral presence in internal organs	(Stabenow et al.[46])
	CAST/EiJ, C57BL/6, B6.129S7-IFNγ, BALB/c	[a]	MPXV-Z79-I-005 and MPXV-Z79-CB2	Intranasal10^2–10^6 p.f.u/mL	MPXV replicated in the lungs to previous titers from other sites in CAST/EiJ mice. Surprisingly, lung titers	(Earl et al.[47])

(*Continued on next page*)

Table 2. *Continued*

Animal species	Strain	Age	Viral strain	Route of infection/ dose	Major findings	Reference
					in dose-infected BALB/ c mice were similar to titers in CAST/EiJ mice, although all mice survived. Animals without IFN-γ, treated by gravity, or left by weight presented an upright posture and became moribund. In contrast, similar disease symptoms were delayed and markedly less pronounced in the animals that received IFN-γ, and these animals fully recovered. Inoculation of IFN in CAST/EiJ mice led to protection against MPXV. In addition, C57BL/6 mice with inactivation of the IFN gene or the IFN receptor gene are more sensitive to the disease	
	[a]	2-, 8-, 12-, and 15-day-old	Copenhagen	Intraperitoneal and intranasal/1,2x10^6 p.f.u/mL, footpad/ 6x10^2 p.f.u/mL and oral/[a]	When inoculated intraperitoneally, all animals showed similar symptoms and occurred as a result of infection, whereas 50% died infected via the footpad and 40% died orally. Sequential evaluations showed that the virus can be	(Marennikova and Seluhina,[48])

(*Continued on next page*)

Table 2. *Continued*

Animal species	Strain	Age	Viral strain	Route of infection/ dose	Major findings	Reference
					found in the blood, lungs, liver, spleen, and kidneys, with considerable amounts of virus detected in the lungs and other organs in the acute phase of the disease	
	BALB/c and SCID	3- to 4-week-old	MPXV-2003-USA-044 and MPXV-Congo-Luc+	Intraperitoneal/[a]	In BALB/c mice, the luminescent signal had the highest peaks between 96 and 120 h. Greater replication and faster dissemination were observed mainly to organs of the peritoneal cavity, with eventual dissemination to axillary lymph. In SCID mice, a more intense luminescent light was observed after 96 h. It was spread to organs and tissues in the regions of the abdominal, thoracic, and axillary lymph nodes, in addition to showing visible signs in the tail, feet, and nasal region. Biophotonic images also revealed the tropism of MPXV for ovarian tissues	(Osorio et al.[49])
	CAST/EiJ and BALB	9-week-old	MPXV-z06 and MPXV-z79-CB2	Intranasal/[a]	High luminescence in the nasal area with a peak between 7 and 12 days after infection was observed in the	(Earl et al.[50])

(*Continued on next page*)

Table 2. *Continued*

Animal species	Strain	Age	Viral strain	Route of infection/ dose	Major findings	Reference
					animals. With the recombinant strain MPXV-z79-CB2, CAST/EiJ mice infected intranasally showed lethargy, hunched posture, ruffled hair, and severe weight loss	
	ICR	8- to 10-day-old	MPXV-Z79-I-005	Intranasal/10^4–10^5 p.f.u/mL	Mice by MPXV accumulations of nasal, lung, and brain pathogens. The presence and replication in primary target cells and traditional observations of MPXV (mononuclear phagocytic cells and tract epitheliocytes) are present, as well as some other cell types (endothelial cells, reticular cells, connective tissue cells) were also observed	(Sergeev et al.[51])
	129S1/SvlmJ, A/J, BALB/cByJ, C3H/HeJ, C57BL/6J, CAST/EiJ (WD), DBA/2J, FVB/NJ, SJL/J, SPRET/EiJ (WD), AKR/J, C57 L/J, C58/J, MOLF/EiJ (WD), NOD/ShiLtJ, NZB/BINJ, PERA/EiJ(WD), PL/J, SM/J, SWR/J, BUB/BnJ, C57BL/10J, C57BLKS/J, CBA/J, CZECHII/EiJ (WD), LP/	4- to 8- week-old and 5- to 11-month- old	MPXV-Z79-I-005 and MPXV-USA-2003-044	Intranasal and intraperitoneal/10^2–10^6 p.f.u/mL	Thirty-eight inbred mouse strains were tested for MPXV susceptibility. Three strains were developed, from which CAST/ were developed. CAST/EiJ exhibit weight loss, morbidity, and death in a dose-dependent manner, whereas there were no deaths of	(Americo et al.[52])

(*Continued on next page*)

Table 2. *Continued*

Animal species	Strain	Age	Viral strain	Route of infection/ dose	Major findings	Reference
	J, RIIIS/J, WSB/EiJ (WD), BTBR T+ tf/J, C57BR/cdJ, CE/J, I/LnJ, MA/MyJ, NON/ ShiLtJ, NZW/LacJ, PWK/PhJ (WD), SEA/ GnJ and BALB/c				BALB/c mice at high doses. Both routes of inoculation resulted in replication in the spleen	
	CAST/EiJ, C57BL/6, B6:129X1-Il15ratm1Ama/J and B6-129X1	9- to 13-week-old	MPXV-z06	Intraperitoneal/[a]	Administration of IL-15 to CAST mice transiently increased NK and $CD8^+$ T cells that could express IFN-γ, indicating that progenitor cells were able to respond to cytokines. However, the number of NK cells rapidly decreased, indicating a defect in their homeostasis. In addition, antibodies to interferon-γ abrogated the protection by activated NK cells. Thus, the inherent susceptibility of CAST mice to orthopoxviruses may be explained by a low level of natural killer (NK) cells	(Earl et al.[53])
	C57BL/6J, CAST/EiJ, MOLF/EiJ, C58/J, NZW/Lacj, CASA/Rkj and BALB/c	[a]	MPXV-Z79-CB2 and MPXV-Z79-005	Intranasal/10^4–10^6 p.f.u/mL	NZW/Lac and C58 mice exhibited more weight loss than other classical inbred strains, but all survived intranasal MPXV challenges. Mice from three naturally derived	(Earl et al.[54])

(*Continued on next page*)

Table 2. *Continued*

Animal species	Strain	Age	Viral strain	Route of infection/ dose	Major findings	Reference
					strains, in addition to CAST, exhibited severe weight loss and died or were euthanized	
	C57BL/6 and BALB/c	6- to 7-week-old	MPXV-2003-044 and MPXV-2003-358	Footpad and intranasal/ 10^5 p.f.u/mL	Mice inoculated on the footpad with the Congo Basin strain showed clinical signs of the disease, with BALB/c mice showing greater edema compared with C57BL/6 mice. One mouse of the BALB/c strain showed weight loss, whereas no mouse of the C57/BL6 strain showed this clinical sign. When inoculation took place intranasally, weight loss was observed in both strains of mice. On the other hand, mice inoculated on the footpad with MPXV from West Africa showed only mild swelling at the inoculation site. None of the mice in the group inoculated with intranasal MPXV from West Africa developed any obvious signs of morbidity	(Hutson et al.[44])
	CAST/EiJ mice	4- to 6-week-old	2022 MPXV isolate (SP2833)	Inhalation/10^4 or 10^6 PFU	Although the virus replicated efficiently in the respiratory tract, mice did not succumb to the infection	(Warner et al.[55])

[a]Not reported; p.f.u: plaque formation unit; mL: milliliter; MPXV: monkeypox virus.

Table 3. Non-human primates used in the study of MPXV

Animal specie	Age	Viral strain	Route of infection/dose	Major findings	Reference
Cynomolgus (*Macaca fascicularis*)	[a]	Virus strain isolated from pustules of naturally infected animals	Intradermally/[a]	The infected animal developed a local pustule surrounded by edema 7 days after inoculation. Body temperature increased slightly between the 5th and 9th day after inoculation, but no propagation of the eruption occurred	(Magnus et al.[1])
	[a]	MPXV- Z79-005	Intravenous/$5x10^6$ and $5x10^7$ p.f.u/mL	Unimmunized monkeys became seriously ill with fever and weight loss, with between 575 and 820 skin lesions. There were fewer lesions in 65–140 immunized monkeys each, and they were generally smaller and atypical, developed less synchronously, and healed quickly	(Fogg et al.[26])
	[a]	Strain recovered from naturally infected monkey (Strain 1744)	Intravenous, intradermally and subcutaneous/[a]	Acute disease was observed, characterized by marked facial swelling that extends to the cervical region. Severe difficulty in breathing, papular eruptions throughout the body, ulcerative lesions of the oral mucous membrane, and generalized lymphadenopathy	(Prier and Sauer,[56]; Prier et al.[57])
	[a]	Strain recovered from the blood of an infected monkey (Strain 10,001)	Intramuscular/10^{-1}–10^{-6}	After inoculation of graduated doses of MPVX, the clinical features emerging from the infection at each dilution were visibly indistinguishable. The mortality rate reached 30%, and a more intense rash was observed in these animals, followed by progressive disease, prostration, hypothermia, and collapse. Severe illness lasted from 4 to 11 days; during this time the	(Wenner et al.[58])

(*Continued on next page*)

Table 3. *Continued*

Animal specie	Age	Viral strain	Route of infection/dose	Major findings	Reference
				animals became progressively dehydrated and lost weight. In some cases, there was evidence of pyoderma	
	[a]	[a]	Intravenous, intramuscular, intradermally or intradermally combined and conjunctival routes/[a]	The main events during the course of the infection were fever and cutaneous and oral mucosal lesions. Some animals developed a generalized smallpox rash, whereas in others only a few scattered pustules were seen	(Wenner et al.[59])
	Immature	[a]	Intramuscular/[a]	The skin lesions progressed rapidly through the papular and vesicular stages. The pustular phase was of short duration with formation of hard crusts. Pustules were observed on the scrotum of males, lesions on the oral mucosa, on the amygdala with histological characteristics similar to those described for the skin and lymph nodes. Generalized lymphadenopathy developed during the first week and lasted until the 3rd week of the disease; there was moderate enlargement of the spleen, histological and cytological changes in a combination of diffuse and follicular hyperplasia, reticular lymphoblast proliferation	(Wenner et al.[60])
	6.2 $\pm$ 0.7 year-old	MPXV- Z79-005	Intravenous/5x10^7 p.f.u/mL	MPXV infection caused a vesiculopustular rash, fever, lymphadenopathy, splenomegaly, pulmonary edema, increased white blood	(Huggins et al.[61])

(*Continued on next page*)

Table 3. *Continued*

Animal specie	Age	Viral strain	Route of infection/dose	Major findings	Reference
				cells, and the death of some animals	
	3- to 6-year-old	MPXV- Z79-005	Intravenous/5x10^7 p.f.u/mL	Infected animals developed severe clinical syndromes consisting of anorexia, extremely low temperature, shock, disseminated intravascular coagulation, or respiratory distress leading to death. Severe pathology was characterized by generalized smallpox lesions on the skin and oral mucosa, notable lymphadenopathy and splenomegaly, and pulmonary congestion/edema with gross lesions	(Wei et al.[62])
	[a]	MPXV- Z79-005	Intravenous/5x10^7 p.f.u/mL	All infected and untreated animals presented skin lesions observed first in the mouth and head that spread to the rest of the body, progressive signs of the disease that led to their death	(Jordan et al.[63])
	[a]	MPXV- Z79-005	Intravenous/5x10^7 p.f.u/mL	Although the PCR data suggested a low viremia, all immunized animals remained clinically well, whereas the non-immunized animals became extremely ill with fever, weight loss, and decreased activity in addition to having a large number of smallpox skin lesions that exhibited a pustular progression	(Earl et al.[64])
	[a]	MPXV- Z79-005	Intravenous/5x10^6 and 5x10^7 p.f.u/mL	A large number of skin lesions appeared in control animals in the first few days, coinciding with high viremia, but disappeared in 4 out of 6	(Earl et al.[65])

(*Continued on next page*)

Table 3. *Continued*

Animal specie	Age	Viral strain	Route of infection/dose	Major findings	Reference
				animals. Four untreated animals had severe illness requiring euthanasia. Although treated animals had a high lesion count, the viral load was much lower than that of unvaccinated animals	
	[a]	MPXV- Z79-005	Intravenous/1 mL $2x10^7$ p.f.u/mL	Clinical symptoms and post-challenge survival, lesion counts, and viral loads were analyzed. Unvaccinated animals exhibited typical signs of the disease, depression, lethargy, pustule lesions, and high peaks of viral load after challenge	(Buchman et al.[66])
	Adults	MPXV- Z79-005	Intravenous/$5x10^7$ p.f.u/mL	Even the vaccinated animals showed signs of the disease. Untreated animals showed increased body temperature, weight loss, and a high number of skin lesions succumbing to the infection	(Denzler et al.[67])
	2- to 8-year-old	MPXV- Z79-005	Intravenous/$1,65x10^7$ and 5, $4x10^7$ p.f.u/mL	After the lethal challenge with MPXV, the unvaccinated control animals succumbed to monkeypox 11 days after the challenge, numerous lesions were observed throughout the body and a weak primary immune response when compared with the treated animals	(Russo et al.[68])
	[a]	[a]	Exposure to aerosols/[a]	The first sign of infection after exposure was a rise in temperature. From the 4th or 5th day after exposure, cough, runny nose, apathy, and loss of appetite were observed. Mild rash with papules or pustules	(Hahon and McGavran,[69])

(*Continued on next page*)

Table 3. *Continued*

Animal specie	Age	Viral strain	Route of infection/dose	Major findings	Reference
				limited to face and hands is observed. Histologically, ulcerative bronchiolitis, bronchitis, and peribronchitis were observed; in addition, fibrinous necrosis was found in the bronchial walls, peribronchial lymphoid tissues, and bronchopulmonary lymph nodes	
	2-4 years-old	MPXV- Z79-005	Exposure to aerosols/2,6x10^5 p.f.u/mL	Untreated animals showed severe infection, weight decline, progressive depression, dyspnea, and nasal discharge. Skin lesions, first appearing on day 6 after challenge, live virus, and viral DNA were detected in the throats of all challenged animals. Most of the tissues analyzed were positive for the virus, and there were histological changes consistent with focal acute necrotizing bronchitis and bronchopneumonia; focal, fibrinous necrotizing alveolitis often accompanied by edema; and acute focal vasculitis, sometimes accompanied by thrombosis and perivascular edema	(Hatch et al.[70])
	Youth to adults	MPXV- Z79-005	Exposure to aerosols/[a]	The animals presented exanthema, enanthema, mild anorexia, fever, cough, nasal secretion, cutaneous, oral, and gastrointestinal lesions. Dyspnea, depression, severe anorexia, and signs of weakness were evident in all	(Zaucha et al.[71])

(*Continued on next page*)

Table 3. *Continued*

Animal specie	Age	Viral strain	Route of infection/dose	Major findings	Reference
				animals. Clinical signs progressed to the animals' natural death or euthanasia	
	[a]	MPXV- Z79-005	Intratracheal/3,42×10^6, 8, 37×10^6 and 3,53×10^7 p.f.u/mL	Animals challenged with the lowest dose had fever, weight loss, pustular skin lesions, and lymphadenopathy. Animals exposed to the 8.37 × 106 p.f.u dose showed similar clear signs but with some animals dying and animals exposed to the higher dose had a similar disease course but with an accelerated progression to death	(Goff et al.[72])
	2- to 4-year-old	MPXV-MSF#6 (Isolated human)	Intratracheal/10^7 p.f.u i/5 mL	Severe morbidity, extensive skin lesions, dyspnea, and low saturation were observed in all control animals. Treated animals showed mild morbidity despite the typical signs of the disease	(Stittelaar et al.[73])
	[a]	MPXV- Z79-005	Exposure to aerosols/3×10^4, 1×10^5, 3×10^5 and 9×10^5 p.f.u/mL	Lesions appeared 6 days after exposure in two animals at the highest dose. One animal succumbed with no apparent injury and a single animal had severe injuries. Another animal that died presented histopathologically with pneumonia and intranuclear inclusion bodies consistent with smallpox infection. Discoloration of the lung and enlargement of the bronchial lymph nodes were also observed	(Barnewall et al.[74])
	[a]	MPXV- Z79-005	Exposure to aerosols/4×10^4, 1×10^5, 4×10^5 and 1×10^6 p.f.u/mL	Clinical signs observed were fever, decreased appetite and activity, drowsiness,	(Nalca et al.[75])

(*Continued on next page*)

Table 3. *Continued*

Animal specie	Age	Viral strain	Route of infection/dose	Major findings	Reference
				depression, inguinal and axillary lymphadenopathy, and macules that progressed to pustules. Necrotizing lesions were also present on the skin, gastrointestinal tract, mucosal surfaces, and gonads. The histological findings of animals sacrificed during acute illness were similar to those previously reported for aerosolized MPXV	
	2- to 7-year-old	MPXV- Z79-005	Exposure to aerosols/1×10^5 p.f.u/mL	Challenged animals showed typical signs of the disease, fever, weight loss, papules and pustules, weight loss, and viremia detected in the first day's post infection. When treated, they have a greater survival with rapid improvement of clinical signs	(Russo et al.[76])
	2-year-old	MPXV- Z79-005	Exposure to aerosols/1×10^5 p.f.u/mL	Typical signs of the disease were observed, which included increased weight loss, dyspnea, anorexia and a spike in body temperature. Viral RNA was also identified in body tissues such as lungs, spleen, amygdala, tongue, kidney, heart, cerebrospinal fluid, and mediastinal lymph nodes. Histological changes were restricted to the respiratory bronchioles in the lungs	(Tree et al.[77])
	[a]	MPXV- Z79-005	Intravenous/$5x10^4$ to $5x10^7$ p.f.u/mL and Intrabronchial/$5x10^4$ to $5x10^6$ p.f.u/mL	Both routes of inoculation resulted in a rapid spread of the virus; typical signs of the disease from moderate to severe were observed. Disease progression was twice as rapid for animals infected via the	(Johnson et al.[78])

(*Continued on next page*)

Table 3. *Continued*

Animal specie	Age	Viral strain	Route of infection/dose	Major findings	Reference
				intravenous route compared with those infected via the intrabronchial route. All challenged animals resolved the infection	
Rhesus (*Macaca mullata*)	[a]	Virus strain isolated from pustules of naturally infected animals	Intradermally/[a]	After inoculation none of the challenged animals developed any signs of disease	(Magnus et al.[1])
	[a]	Strain recovered from naturally infected monkey (Strain 1744)	Intravenous, Intradermally and Subcutaneous/[a]	Intravenous infection resulted in generalized rashes, the subcutaneous one produced a similar granuloma, and the intracutaneous one caused local lesions without spreading to other parts of the body	(Prier and Sauer,[56]; Prier et al.[57])
	[a]	[a]	Intramuscular/[a]	Signs of typical disease in cynomolgus were much less pronounced in rhesus; however, rash, dermal lesions, and short-lived exanthema were observed. None of the animals looked remarkably sick, and none specifically died of the disease, but all developed antibodies against the virus	(Wenner et al.[59])
	2-5 years-old	MPXV- Z79-005	Intravenous/1,65x10^7 and 5, 4x10^7 p.f.u/mL	Lethally challenged with MPXV, the animals showed the typical clinical signs of the disease, skin lesions, strong anamnestic responses to the challenge, and a weak primary immune response when compared with treated animals. Treated animals were protected from lethal challenge with MPXV	(Russo et al.[68])
	4- to 9-year old	MPXV- Z79-005	Intrabronchial/2×10^5 p.f.u/mL	The challenge resulted in the appearance of numerous disseminated lesions, initially	(Estep et al.[79])

(*Continued on next page*)

Table 3. *Continued*

Animal specie	Age	Viral strain	Route of infection/dose	Major findings	Reference
				as pustules on the skin and oral mucosa and then progressing from pustular stages to crusts. The animals also developed coughing, symptoms of labored breathing, and fever	
Sagui (*Callithrix jacchus*)	Adults	MPXV- Z79-005	Intravenous/2,4x10,^{7} 9,5 x 10^{5}, 7,8 x 10^{4}, 5x10,^{3} 510 or 48 p.f.u/mL	All animals developed a similar disease course and died or were sacrificed. The different doses also showed different clinical progression, mainly the temporal onset of the disease and the phenotypic presentation of rash. In general, all animals had a skin rash, significant lymphadenopathy, and pronounced lethargy, some of which needed to be euthanized	(Mucker et al.[80])
	Adults	MPXV- Z79-005	Intranasal/100, 1000, 5000 p.f.u/mL	The disease progressed in all animals; the animals became increasingly unresponsive and lay down until they were sacrificed or succumbed to the disease. Other signs included light sensitivity, swelling, runny nose, swelling around the eyes, skin lesions, papules, petechiae, and crusts. They also showed an increase in white blood cells, a decrease in platelets, lymphocytes, and very high neutrophils	(Mucker et al.[81])

[a]Not reported; p.f.u: plaque formation unit; mL: milliliter; MPXV: Monkeypox virus.

Table 4. Prairie dogs used in the study of MPXV

Animal specie	Age	Viral strain	Route of infection/dose	Major findings	Reference
Prairie dog (*Cynomys ludovicianus*)	3-year-old	MPXV ROC-2003-358	Intranasal/10^5 p.f.u/mL	Infected and untreated group: facial swelling, nasal discharge, nasal crust, bloody nose, inappetence, weight loss, pustular lesions, petechial rash, mouth breathing. The treated groups: prophylaxis (0) and post-infection (3) did not present symptoms of the disease, whereas the therapeutic group (after the appearance of lesions) presented facial swelling, nasal discharge, nasal crust, bloody nose, lack of appetite, weight loss, pustular lesions	(Smith et al.[33])
	Adults	MPXV-USA-2003-044	Intraperitoneal/$10x^{1,5}$ p.f.u/mL and intranasal/$10x^{6.1}$ p.f.u/mL	Animals infected by the intraperitoneal route died approximately 8–11 days after infection and no mucosal or cutaneous lesions were observed. Via the intranasal route, 60% died similarly to the animals in the intraperitoneal group, and the survivors had vesicular lesions on the lips and tongue, along with nasal congestion and mucopurulent nasal secretion, but recovered	(Xiao et al.[82])
	3-year-old	MPXV-USA-2003-044 and MPXV-ROC-2003-358	Intranasal/10^4, 10^5, and 10^6 p.f.u/mL	Clinical signs were dose dependent, ranging from inappetence, facial edema, forced breathing, nasal pus, crusty nose, nasal blood, swollen paws, crusted lesion on the face, and death	(Hutson et al.[83])
	2-year-old	MPXV-USA-2003-044 and MPXV-ROC-2003-358	Intranasal and intradermal by scarification/$10^{4,5}$ p.f.u/mL	The animals presented skin lesions on the head, limbs, and trunk. Animals infected with the Congo strain showed a greater	(Hutson et al.[84])

(*Continued on next page*)

Table 4. *Continued*

Animal specie	Age	Viral strain	Route of infection/dose	Major findings	Reference
				increase in temperature and a tendency to lose weight compared with the African strain	
	2- to 4- year-old	MPXV-USA-2003-044	Intranasal/8,8x10^5 p.f.u/mL	It was observed that animals from all groups began to show clinical signs about 8 days after infection; among these signs are inappetence, decreased activity with recumbency and reluctance to move, as well as skin lesions; in addition, some animals needed to be euthanized due to clinical condition. The survival rate of the animals varied according to the time of initiation of treatment; the earlier it was started, the greater the effectiveness	(Hutson et al.[85])
	2-year-old	MPXV-USA-2003-044	Intranasal/5x10^4 p.f.u/mL (actual dose confirmed by 5.9x10^4 p.f.u/10 μL of WT and 4.3x10^4 p.f.u/10 μL of luc+ MPXV)	West African (WA) MPXV can be visualized using *in vivo* imaging in the nose, lymph nodes, intestines, heart, lung, kidneys, and liver at day 6 post-infection. On day 9, lesions became visible on the skin and, in some cases, the spleen. After day 9 post-infection, the luminescent signal representing replication either increased, indicating a progression to what would be a fatal infection, or decreased as the infection resolved	(Weiner et al.[86])
	20-month-old	MPXV-USA-2003-044	Intranasal/9x10^3 p.f.u/mL	Sharing contaminated bedding led to all healthy animals developing the disease. In the group in which healthy animals were in contact with the	(Hutson et al.[87])

(*Continued on next page*)

Table 4. *Continued*

Animal specie	Age	Viral strain	Route of infection/dose	Major findings	Reference
				challenged animal, clinical signs of the disease also developed. All four animals that were experimentally challenged recovered from the infection. The euthanized animals had severe diarrhea and countless skin lesions	
	2-3-years-old	MPXV-USA-2003-044 and MPXV-ROC-2003-358	Intranasal/$6x10^3$ and $5x10^3$ p.f.u/mL	Animals challenged with the West African strain developed skin lesions, crusty noses, dehydration, and inappetence. In the group challenged with Congo Basin, all animals showed inappetence, dehydration, nasal congestion, pus/blood in the mouth, breathing difficulties, facial edema, pus in the genitals, and swollen paws, in addition to skin lesions	(Hutson et al.[88])
	10-month-old	MPXV-USA-2003-044 and MPXV-ROC-2003-358	Intranasal/$8x10^3$ p.f.u/mL	Animals infected with the Congo Basin (CB) strain had virus recovered from the nasal mucosa, oropharyngeal lymph nodes, and spleen in animals challenged with on day 4 and in animals challenged with the West African (WA) strain on day 6. For In both groups, primary viremia was observed from days 6–9 to day 17. The CB strain spread faster and accumulated at higher levels, causing greater morbidity in the animals when compared with the WA strain. The viral antigen was abundant in all organs tested, except for the brain. Splenocytes were	(Hutson et al.[89])

(*Continued on next page*)

Table 4. ***Continued***

Animal specie	Age	Viral strain	Route of infection/dose	Major findings	Reference
				labeled positive for apoptosis more often than hepatocytes in both groups	
	Adults	MPXV-ROC-2003-358	Intranasal/4,3x10^6 and 2, 25x10^4 p.f.u/mL	The incubation period presented by prairie dogs were similar to that observed in humans with systemic orthopoxvirus infection. Regarding the clinical signs observed in the animals, the occurrence of inappetence and weight loss, as well as cutaneous and mucosal lesions, varying in degree of intensity, stands out	(Shannon Keckler et al.[90])

Not reported; p.f.u: plaque formation unit; mL: milliliter; MPXV: monkeypox virus.

Table 5. Squirrels used in the study of MPXV

Animal specie	Age	Viral strain	Route of infection/dose	Major findings	Reference
Squirrel (*S. tridecemlineatus*)	Adults	MPXV-USA-2003-044	Intraperitoneal/$10^{5,1}$ and intranasal/$10^{6,1}$ p.f.u/mL	The infection caused severe and fatal disease in all animals in both inoculation routes. High rate of viral load and wide distribution of the virus through the organs. The squirrels were lethargic and anorexic within 4 or 5 days, with death within 9 days. No apparent skin lesions were observed; however, severe liver and spleen lesions were seen in both groups; in addition, necrosis of peribronchial lymphoid tissue and lymph nodes from other sites was also observed in the group challenged by the intranasal route	(Tesh et al.[91])
	[a]	MPXV-ZAI-1979-005 and MPXV-USA-2003-044	Subcutaneous/$3{,}7x10^4$ and $1{,}8x10^4$ p.f.u/mL	Clinical symptoms were earlier and more severe in animals that received strain Z79 and mortality in these animals occurred between days 6 and 11; on the other hand, despite presenting a milder symptomatology, death in animals that received strain US03 occurred in a very similar period. Animals infected with the Z79 virus strain showed consistently higher viral titer in blood and lung tissue compared with those infected with US03 virus alone, but it was also possible to identify virus titers in the spleen and liver of these animals	(Sbrana et al.[92])
	[a]	MPXV-ZAI-1979-005	Subcutaneous/$10^{6,3}$ p.f.u/mL	Infected and untreated animals show signs of disease on day 4 post-infection, and all died between 6 and 9 days post-infection. The animals had a high viral load; however, none of the challenged and treated squirrels developed detectable viremia	(Sbrana et al.[93])

(*Continued on next page*)

Table 5. *Continued*

Animal specie	Age	Viral strain	Route of infection/dose	Major findings	Reference
Squirrel (*Marmota bobak*)	1–2-year-old	MPXV-ZAI-1979-005	Subcutaneous/2.6, 4.1, 5.6, 7.1 log10 p.f.u/mL and intranasal/1.8, 0.2, 2.2, 3.7, 4.2, 5.0, 6.6 and 7.8 log10 p.f.u/mL	Virus was recovered from nasal mucosa, oropharyngeal lymph nodes, and spleen in animals challenged by MPXV Congo Basin (CB) on day 4 and in animals challenged with the West African (WA) strain on day 6. For both groups, viremia primary was seen from days 6–9 through day 17. Although the histopathology and immunohistochemistry findings were similar, CB MPXV spread faster and accumulated to higher levels, causing greater morbidity in animals when compared to WA MPXV. Two animals that succumbed to the disease showed abundant viral antigen in all organs tested, except the brain. Interestingly, splenocytes were labeled positive for apoptosis more often than hepatocytes in both MPXV groups	(Sergeev et al.[94])
Squirrel (*Funisciurus anerythrus*)	[a]	Congo Basin MPXV/Luc+	Intranasal and intradermal/10^6 p.f.u/mL	MPXV infection in these animals caused moderate to severe morbidity and mortality, with clinical signs including smallpox lesions on the skin, eyes, mouth, and nose, dyspnea, and profuse nasal discharge. Both intranasal and intradermal exposures induced high levels of viremia, rapid systemic spread, and long periods of viral shedding. The sentinel animal showed clinical signs of infection including increased respiratory rate, nasal discharge and mouth lesions, respiratory problems, weight loss, and severe lethargy	(Falendysz et al.[95])

[a]Not reported; p.f.u: plaque formation unit; mL: milliliter; MPXV: Monkeypox virus.

Table 6. Rabbits used in the study of MPXV

Animal species	Age	Viral strain	Route of infection/ dose	Major findings	Reference
Rabbit (*Oryctolagus cuniculus*)	Adults and 2-day -old	Serial dilutions of virus recovered from infected monkeys	Intradermal, scarification, and intracutaneous/[a]	Intradermal inoculation led to severe hemorrhagic reactions, but unlike what is observed with the vaccinia virus, pustules followed by necrosis were also observed. Lesions and pustules were also observed by scarification. Infection was fatal for two-day-old rabbits after scarification or intracutaneous inoculation	(Magnus et al.[1])
	[a]	[a]	Scarification, intravenous, intradermally, and subcutaneous/[a]	Scarification produced confluent lesions according to the concentration used. The virus was also infectious by the intravenous, intradermal, and subcutaneous routes. The intradermal rout caused after pulse lesions followed by secondary pustules and the intravenous route resulted in generalized disease although the animals recovered	(Prier and Sauer,[56]; Prier et al.[57])
	Adults	[a]	Intradermally/[a]	Intradermal infection led to hemorrhagic-necrotic lesion in rabbits	(Gispen and Brand-Saathof,[96])
	Adults and 2-day-old	Copenhagen and MPXV-6-7255	Intracerebral and intradermally/[a]	All strains caused hemorrhagic necrotic skin lesions. Intracerebral infections in adult and 2-day-old rabbits were fatal with the development of adult meningoencephalitis	(Gispen et al.[97])

(*Continued on next page*)

Table 6. *Continued*

Animal species	Age	Viral strain	Route of infection/ dose	Major findings	Reference
Rabbit (*Oryctolagus cuniculus domesticus*)	10-day-old	Copenhagen	Intravenous/10^7 p.f.u and scarification/10^5 and 10^6 p.f.u/0, 1 mL. Oral route/1,4 x 10^6; 10^7; 10^8; 10^9 p.f.u/ 2 mL.	Animals inoculated with MPXV generally had a generalized process of fever, conjunctivitis, rhinitis, rash on the skin and mucous membranes, and weight loss. Papules also appeared that developed into pustules and in some cases became hemorrhagic, with younger animals being more susceptible than adults	(Marennikova and Seluhina,[48])

[a]Not reported; p.f.u: plaque formation unit; mL: milliliter; MPXV: monkeypox virus.

is still immature are well accepted. However, the use of these models increases the chances that the tests were underestimated due to the absence of the antiviral defense of the model.

To address the limitation of using immunocompetent mice and to allow assessment of susceptibility and the course of infection in this model, S. S. Marennikova and E. M. Seluhina, inoculated 1-, 2-, 8-, 12-, and 15-day-old mice with the Copenhagen strain of MPXV. The 8-day-old animals showed clinical signs such as asthenia and loss of appetite when inoculated intraperitoneally or intranasally. Besides these signs, the animals inoculated via plantar cushion showed edema in the foot. In these inoculation routes, all animals died as a result of infection, whereas the intradermal route resulted in the death of 50% of the inoculated animals. Mice inoculated orally became flabby and lost their appetite, leading to a 40% mortality rate in the infected group. For 12-day-old mice, mortality occurred in only 14% of cases. On the other hand, 100% mortality was observed in 15-day-old animals after intranasal inoculation. Sequential evaluations showed that the virus could be found in the blood, lungs, liver, spleen, and kidneys, with a considerable amount of virus detected in the lungs and other organs in the acute phase of the disease.[48] The fact that young mice succumb to the disease caused by MPXV suggests the possibility of using this model for viral adaptation, which would allow the development of an immunocompetent adult mouse capable of modeling the disease. Serial passage studies of MPXV in young mice with intact immune system could result in selection of an adapted strain that would cause disease in adult animals, considering the high rate of viral mutation and adaptation by natural selection. These studies will be useful for the development of challenge models for antivirals and vaccines testing using contemporary strain of MPXV.

The progression of infection caused by MPXV was also compared in mice with an intact immune system and in immunodeficient mice using viruses with MPXV engineered to express luminescent markers. Viral infection of Balb/c (immunocompetent) and SCID (immunodeficient) mice was monitored using biophoton imaging. In BALB/c mice, the luminescent signal was visualized in the first 24 h extending to 96–120 h, where higher peaks were detected. Higher replication and faster dissemination were observed mainly to organs in the peritoneal cavity, with eventual dissemination to axillary lymph. After 240 h, the animals were able to clear the infection. Balb/c mice have an immune response skewed toward a Th2 profile that not only negatively regulates the secretion of Th1 cytokines but also inhibits and counteracts the activating actions of IFNγ and tumor necrosis factor alpha (TNF-α), deactivating the transcription and translation of several genes in macrophages. Furthermore, interleukin-10 (IL-10) acts by negatively controlling the immune response in general and mainly the inflammatory response and tissue damage.[100,101] Therefore, although they are immunocompetent mice, it is possible to observe the infection cycle with the appearance of some disease phenotypes. In SCID mice, luminescence indicative of MPXV infection was also visible at 24 h and limited to the peritoneal cavity. A more intense luminescent light was observed, and after 96 h it had

already spread to other organs and tissues in the abdominal, thoracic, and axillary lymph node regions, in addition to showing visible signs in the tail, feet, and nasal region when the evaluation reached 264 h. At 168 h after inoculation the animals died, biophotonics images also revealed the tropism of MPXV for ovarian tissues.[49]

A study by Duggal and collaborators demonstrated the presence of MPXV in the interstitial cells and seminiferous tubules of the testes, as well as in the lumen of the epididymis, which are the sites of sperm production and maturation, in non-human primates.[102] These findings, together with the work of Osorio et al. (2009), support the potential sexual transmission of MPXV. New studies addressing the questions are urgently needed. Studies carried out with Zika virus, a virus known to be sexually transmitted, can help as a basis for investigations for MPXV. Viral load should be quantified in vaginal washes and semen from male testes to have a better understanding of viral tropism for cells of the genitourinary system. Once this potential has been identified, crossovers between infected and healthy mice should be performed to determine the possibility and rates of sexual transmission. Vertical transmission also deserves attention. Murine models may also help to discover whether contemporary strains of MPXV can infect fetuses and what the consequences of infection to the offspring are.

Also using bioluminescence imaging, Earl et al. found high luminescence in the nasal area peaking between 7 and 12 days post-infection, moving on to the lung. Using the recombinant strain MPXV-z79-CB2, the study also demonstrated that CAST/EiJ mice infected intranasally showed lethargy, arched posture, raised hairs, and severe weight loss.[50]

Intact 8- to 10-day-old male and female ICR mice were also challenged intranasally with MPXV showing no lethality; however, after day 7 post-infection, clinical signs of disease such as purulent conjunctivitis, blepharitis, and raised hairs were observed, which disappeared after 11–13 days.[51]

The CAST/EiJ mouse also proved to be an efficient model of MPXV infection, among 37 mouse strains evaluated. In addition to CAST/Eij, MOLF/EiJ and PERA/EiJ also succumbed to the disease. Females between 5 and 11 weeks of age inoculated intranasally showed weight loss and lethality of 100%, 75%, and 40%, respectively. CAST/EiJ mice showed greater sensitivity to MPXV when infected intraperitoneally. Both routes of inoculation resulted in MPXV replication in the lung, spleen, and liver of the infected animals.[52] Intranasal infection in CAST/EiJ mice also led to viral replication in lungs and dissemination to other organs (liver, spleen, kidneys, and brain).[47]

The inherent susceptibility of CAST/EiJ mice can be explained by a low level of NK cells.[53] Crossing of CAST/EiJ mice with C57BL/6 or BALB/c was performed to investigate whether resistance or sensitivity to MPXV is a dominant factor. The F1 progeny was relatively resistant to MPXV. However, there was a sex difference; some crossbred male mice succumbed to the disease, whereas all females survived.[54]

Mice were also models used in evaluations of phylogenetically distinct strains of MPXV. Hutson and coworkers infected 6- to 7-week-old mice subcutaneously in the footpad or intranasally with a dose of 10.5 West African or Congo Basin MPXV strain. Mice inoculated in the footpad with the Congo Basin strain showed edema in the inoculation region, which led to impaired locomotion of some animals, and BALB/c mice had greater edema compared with C57BL/6 mice. BALB/c mice showed weight loss, whereas no mice from the C57/BL6 strain showed this clinical sign. In general, 13 days after infection, the animals had already recovered from the disease. When inoculation took place intranasally, weight loss was observed in both strains of mice. Although weight loss has been verified, no obvious signs of morbidity (ie, lesions) were observed, and all mice survived. On the other hand, mice inoculated in the footpad with MPXV from West Africa showed mild swelling in the inoculation site. None of the animals lost weight over the course of the study or developed some lesion, and all animals in this group survived the infection. None of the mice in the group inoculated with intranasal MPXV from West Africa developed any obvious signs of morbidity.[103]

NON-HUMAN PRIMATE MODELS

Reports of MXPV infection in non-human primates (NHPs) have been described in several studies, most of which were carried out in cynomolgus (*Macaca fascicularis*) and rhesus (*M. mulatta*) monkeys,[1,56] but there are studies with *Macaca philippinensis*[104] and *Callithrix jacchus*.[80,81]

MPXV was first identified and isolated in 1958 in Copenhagen, Denmark, following the observation of two non-fatal outbreaks of a disease in Asian macaques (mainly *M. fascicularis*) that had come from Singapore for research of polio vaccines. The infected animals presented generalized petechial eruption in the skin that quickly evolved to a maculopapular eruption, with lesions observed throughout the body, particularly abundant and developed on the palms of the hands and soles of the feet.[1] Magnus et al. (1959), after isolating the virus from these animals, intradermally inoculated the palm of *M. fascicularis* with 0.2 mL of tissue culture material from the pustules, which developed a local pustule surrounded by edema 7 days after inoculation and elevation of body temperature between the fifth and the ninth day, but without propagation of the rash.

In 1960, Prier et al. confirmed the findings of Magnus et al. by performing challenges through the intradermal, subcutaneous, and intravenous routes and demonstrated again the susceptibility of cynomolgus monkeys to MXPV infection. Intravenous inoculation resulted in generalized eruptions; the subcutaneous one developed a granuloma and the intracutaneous one generated only local lesions.[56,57,105]

Subsequently, a series of experiments with non-human primate models were conducted. In the first experiment, immature cynomolgus monkeys (*M. fascicularis*) were inoculated by the intravenous, intramuscular, intradermal, or intradermal combined and conjunctival routes, and in the second experiment the monkeys were inoculated by the intramuscular route. Assessed daily, the animals developed a typical papular rash observed throughout the body, buccal mucosa, and soft palate.[58–60]

Cynomolgus monkeys infected with MPXV intravenously developed a uniformly lethal disease and had lesions like what is seen in human infection. After challenge, the animals developed a generalized vesiculopustular eruption including fever, elevated white blood cell count, lymphadenopathy, splenomegaly, and pulmonary edema that led to death between 7 and 15 days after infection.[61] Severe pathology characterized by disseminated lesions, lymphadenopathy, pulmonary edema, and splenomegaly was also observed in vaccine studies performed.[62] In a drug trial in cynomolgus monkeys, similar results were found; untreated infected animals had disease progression presenting the main phenotypes and a high mortality rate.[63]

In human smallpox vaccine research, non-human primates are often challenged for MPXV, and cynomolgus are the most used animal model. In the studies carried out, the animals were infected by the intravenous route; those previously immunized were healthy without the appearance of lesions or with the appearance of few and small lesions of rapid healing, unlike the non-immunized monkeys (control), which became seriously ill with depression, lethargy, fever, weight loss, high number of lesions, high viremia, lymphadenopathy, even death.[26,64–68]

In studies carried out with aerosolized virus, these animals showed clinical signs of the disease and elevation of body temperature, cough, coryza, anorexia, eruptions, papules, and deaths in addition to histological changes such as focal acute necrotizing bronchitis and bronchopneumonia; focal, fibrinous necrotizing alveolitis often accompanied by edema; and acute focal vasculitis, sometimes accompanied by thrombosis and perivascular edema.[69,70] Animals also showed exanthema and enanthema, depression, and anorexia in addition to weakness and progression to natural death or euthanasia.[71]

Because of the efficiency of MPXV infection by aerosol exposure, new studies were carried out. In one of the studies, the virus was deposited directly in the tracheal carina of the animals, whereas in others, aerosol exposure systems were used for infection. In general, cynomolgus of both sexes with different ages and weights succumb to the disease and develop similar signs such as decreased appetite and activity, elevation of body temperature, respiratory stress followed by bronchopneumonia, vesiculopustular lesions, crusted skin lesions, oral ulcers, enlarged and proliferative peripheral lymph nodes, and necrotizing or ulcerative lesions in the esophagus, stomach, and urinary bladder. In addition, some animals still presented subpleural hemorrhage and testicular hemorrhage, reaching death. In all animals, the presence of MPXV was identified in blood, tissues, and mucosal smears.[72–77]

A comparison of the disease course after an intravenous and intrabronchial inoculation in cynomolgus monkeys was performed using serial doses of MPXV. In both inoculation routes, a classic smallpox-like disease was observed. Animals infected by the intravenous route showed fever, appearance of lesions, peak viremia, and viral shedding in nasal and oral smears while intrabronchial exposure beyond typical signs led to the development of pneumonia and increased disease progression. The development of cutaneous

lesions in relation to viremia also demonstrated that both routes of inoculation resulted in a rapid spread of the virus to surrounding tissues, resulting in moderate to severe lesional disease.[78]

As identified in cynomolgus, Magnus et al. (1959) also observed a generalized picture of the disease in rhesus monkeys. These animals showed the same signs, petechial eruption with evolution to maculopapular eruption and lesions throughout the body, but when performing the same challenge intradermally inoculating the palm of two rhesus monkeys with 0.2 mL of tissue culture material from the pustules, the animals did not develop any signs of the disease.[1]

Rhesus monkeys challenged by inoculating the virus by intradermal, subcutaneous, and intravenous routes resulted in generalized and/or local rashes and granulomas.[56,57,105] In intramuscular inoculations, after daily evaluation, it was observed that the animals developed less evident cutaneous eruptions along the body and oral mucosa and short-lived exanthema. Although apparently healthy, all animals developed antibodies against the virus.[59]

When inoculated intravenously, rhesus monkeys challenged with MPXV were shown to be highly susceptible to the disease. The animals presented a severe condition with all the typical signs and progressive death. Viral titers were detected in the blood of all animals.[68]

To understand the differences in pathogenicity of Congo Basin (clade I) and the West African (clade II) viruses, Estep and collaborators deleted the MPXV inhibitor of complement enzymes (MOPICE) from the MPXV-Zaire strain, which is not expressed by viruses of the West African clade and infected rhesus monkeys (n = 4) with wild type and a virus lacing MOPICE through the intrabronchial route. Typical signs of the disease were observed in both groups and, in general, the disease manifestations associated with both viruses were similar. However, infection with the recombinant MPXV lacking MOPICE resulted in lethal disease in one animal, and all animals in the wild type group survived infection. Analysis of viral loads in infected animals showed similar patterns between bronchial alveolar lavage and whole blood samples, but viral load levels were higher in animals infected with the virus lacking, suggesting that this protein is not the sole virulence factor of clade I viruses.[79]

Another animal model of non-human primates is the marmoset (*C. jacchus*). Adult males infected intravenously through the tail vein, or through the saphenous vein, develop the normal course of the disease caused by MPXV and died 15 days post-infection. Marmosets that receive higher doses show definable clinical signs already on the second day post-infection in addition to decreased activity. Rash, significant lymphadenopathy and pronounced lethargy were also observed in marmosets experimentally infected with MPXV. In contrast, lymphadenopathy and rash in the lower-dose infected group were not observed. Lesions in this group were much more discrete and were flat, well-defined lesions and never progressed through the typical stages of the disease. In addition, later examinations showed high viremia, decreased platelets, and an abbreviated acute phase, reflecting early type hemorrhagic smallpox.[80]

New experiments by Mucker et al. (2018) with adult male and female marmosets infected via the intranasal route were performed. All animals showed signs of disease and were euthanized or succumbed to the disease 15 days after exposure. The only animal that was exposed to a dose of 5,000 p.f.u had dyspnea, a runny nose, and a temperature rise of about 0.5°C above the pre-exposure temperature. Animals that received doses of 1,000 p.f.u had different degrees of dyspnea. In general, all animals, regardless of the dose received, showed other signs such as sensitivity to light, swelling around the eyes, some signs of photophobia, and skin lesions. Subsequent immunological evaluations revealed an increase in white blood cells and a decrease in platelet counts, in addition to the presence of the virus in the oral cavity of all animals from the 15th day after infection, and the animal with the highest dose was identified as having the virus on the sixth day post-infection.[81]

The evolutionary kinship of non-human primates with humans makes them effective models for comparative studies. A great example of this is the fact that in the studies carried out so far, mice do not present one of the main characteristics of the disease caused by MPXV—the formation of pustules, which is seen only in non-human primates.

PRAIRIE DOGS

Prairie dogs (PD) (*Cynomys ludovicianus*) are highly susceptible to monkeypox virus (MPXV) infection, and the pathogenesis and severity of the disease vary according to the route of infection, being 100% fatal by

the intraperitoneal route, whereas the intranasal route had a mortality of 60%,[82] being the main route of choice for further studies. This animal species is an important model for the study of virulence factors, pathogenesis, transmission routes, and elimination of the MPXV virus, in view of its ability to mimic the way the disease occurs in humans, including the different manifestations caused by different strains of the virus.[83,84] It has also been a widely used model for testing new prophylactic and therapeutic measures.[33,85]

A study using two groups of animals, males and females approximately 2 years old, inoculated intranasally with the West African strain, helped to understand the pathogenesis of the disease, and showed that both showed similar symptoms, despite the difference when different doses were used. The results showed that West African MPXV could be visualized using *in vivo* imaging in the nose, lymph nodes, intestines, heart, lung, kidneys, and liver as early as day six post-infection. By day nine, it was possible to visualize the skin lesions and, in some cases, also the spleen. After day nine, the luminescent signal representing MPXV replication increased in some animals, indicating a progression to what would be a fatal infection, and decreased in others as the infection resolved. The use of recombinant MPXV luc+ allowed for a greater understanding of how MPXV spreads throughout the body in prairie dogs during the course of infection.[86]

Studies on the transmission routes using West African and Congo Basin strains showed that infected animals developed the disease and started shedding the virus at 6 and 10 dpi, through oral, nasal, ocular, and fecal secretions, and that contamination of healthy animals occurred either by sharing bedding, fomites and physical contact, or by respiratory secretion.[84,87] Respiratory transmissibility was questioned in a later study, according to which no healthy animals were infected by the West African MPXV carrier and only 25% of healthy animals became infected from the Congo Basin MPXV carrier, indicating that transmission respiration appears to be less efficient than contact as a transmission mechanism within this model.[88] It is noteworthy that the course of the disease was similar regardless of the transmission route, including weight loss, the development of disseminated skin lesions, and antibody production, among others.[87] In these studies, the age of the animals ranged from 20 to 36 months, and the viral inoculation doses used were $5x10^3$ [96], $9x10^3$ [87] and $10^{4.5}$ [84] p.f.u, demonstrating the ability of the virus to develop disease even at lower doses. Of note, the Congo Basin strain proved to be more pathogenic than the West African strain.[84]

Still on the study that compared the pathogenicity of the Congo Basin strain with that of West Africa, it is noteworthy that the clinical symptoms observed in animals challenged with West African MPXV and that developed the infection (3 out of 5) included skin lesions, crusty nose, dehydration, and inappetence. In the group challenged with Congo Basin MPXV, all animals developed the infection and presented inappetence, dehydration, nasal congestion, pus/blood in the mouth, breathing difficulties, facial edema, pus in the genitals, and swollen paws, in addition to skin lesions. Of this group, 3 of the 5 infected animals were euthanized due to the severity of the degree of morbidity presented, showing once again that Congo Basin MPXV is more pathogenic than West African MPXV.[88]

A study carried out to verify the effectiveness of the antiviral ST-246 in prairie dogs aged approximately 3 years showed that the infected and untreated group had a mortality rate of 75%, in contrast to all animals in the groups treated prophylactically at day 0 and at 3 days post-infection showed no symptoms of the disease and survived, whereas the therapeutic group, although treated after the appearance of lesions, also resulted in a survival rate of 100%. The clinical symptoms observed in the animals that developed the disease were inappetence, facial swelling, nasal discharge, congestion, weight loss, and, to a lesser extent, mucosal and cutaneous lesions in different degrees of severity. The results of this study suggest that this anti-orthopoxvirus compound proved effective for prophylactic treatment, although some viruses were recovered from treated animals, suggesting the possibility of resistant strains. The study was performed with adult animals, inoculated intranasally with the strain from the Congo Basin.[33]

In order to better understand the differences in the pathogenesis of MPXV strains, groups of 10-month-old prairie dogs were infected intranasally with the Congo Basin (CB) strain and the West African MPXV strain (WA), and tissues were collected on days 2, 4, 6, 9, 12, 17, and 24 post-infections. Samples were evaluated for the presence of viruses and macro and microscopic lesions. Virus was recovered from nasal mucosa, oropharyngeal lymph nodes, and spleen in CB-challenged animals on day 4 and in WA-challenged animals on day 6. For both groups, primary viremia was seen on days 6–9 through day 17. Although the histopathology and immunohistochemistry findings were similar, CB MPXV spread faster and accumulated to higher levels, causing greater morbidity in animals when compared with WA MPXV. Two animals that succumbed

to the disease showed abundant viral antigen in all organs tested, except the brain. Interestingly, splenocytes were labeled positive for apoptosis more often than hepatocytes in both MPXV groups. These findings allow further characterization of differences between the pathogenesis of MPXV strains, including the identification of important sites during early viral replication and cellular response to viral infection. Clinical manifestations, when they occurred, were similar in both groups and included inappetence, maculopapular skin lesions, nasal discharge, and respiratory depression under anesthetic effect.[89]

Subsequently, a study was carried out using smallpox vaccines post-monkeypox infection. Dryvax, ACAM2000, and IMVAMUNE vaccines were tested in 2 groups of adult animals infected with the Congo Basin strain intranasally at different doses. The study found that, for high doses of infection, none of the vaccines showed efficacy, culminating in the death of all individuals in the groups tested, but for lower doses of infection, vaccine efficacy is related to the interval of post-infection application and the vaccine applied. The incubation period presented by prairie dogs was like that observed in humans with systemic orthopoxvirus infection. In general, the animals showed prodromal symptoms, such as inappetence and weight loss, in addition to an inflammatory reaction and cutaneous and mucosal lesions such as smallpox. The incubation period presented by prairie dogs was like that observed in humans with systemic orthopoxvirus infection. In general, the animals showed prodromal symptoms, such as inappetence and weight loss, in addition to an inflammatory reaction and cutaneous and mucosal lesions similar to smallpox.[90]

Recently, another study was carried out to test the effectiveness of Brincidofovir (BCV) against monkeypox virus. Adult animals infected with the West African strain intranasally were used. The results showed that the plasma exposure to BCV observed in prairie dogs after 20 or 5 mg/kg was 2–4 times lower than the exposure parameters observed in mice (ectromelia) and rabbits (cotopor) given the same doses. Our findings suggest potentially suboptimal exposure; however, higher doses have been shown to be toxic to prairie dogs. It is possible that the lower plasma exposure is due to the drug metabolization pathway by prairie dogs. It was observed that animals from all groups began to show clinical signs about 8 days after infection; the signs observed were inappetence, decreased activity with recumbency and reluctance to move, as well as cutaneous lesions, which varied in intensity between the animals from each group. Some animals needed to be euthanized due to the clinical condition. The survival rate of the animals varied according to the time of initiation of treatment; the earlier it was started, the greater the effectiveness.[85]

Although prairie dogs show a satisfactory result in modeling MPXV infection; these animals are not considered conventional experimental models. The use of unconventional animals implies specialized labor, differentiated facilities, and compliance with specific environmental legislation for this type of species. Compared with conventional laboratory species, these animals do not have well-characterized genome sequence, neither hematological and biochemical profile, and immunological reagents are very scarce.

SQUIRRELS

The use of ground squirrels (Sciuridae) in studies related to MPXV were considered when natural infections began to be identified in the species, evidencing its importance for the epidemiology of the disease. In addition, the data found suggested that the species has the potential to become a great experimental model aimed at understanding the pathophysiology caused by MPXV and for testing therapeutic and prophylactic countermeasures,[98] such as antiviral medications and vaccines.

In 2004, a study was carried out in order to study the effects of MPXV infection in adult squirrels of the species *S. tridecemlineatus*. Animals were infected with the MPX 2003 strain by the intraperitoneal and intranasal routes with the dose of 10^6 p.f.u/mL. The infection caused severe and fatal illness in all animals in both groups, suggesting that these animals are highly susceptible to the virus. The viral load and the wide distribution of the virus through the organs suggest that the infection was systemic. The squirrels were lethargic and anorexic within 4 or 5 days, with death occurring within 9 days. No apparent skin lesions were observed; however, severe liver and spleen lesions were seen in both groups. In addition, necrosis of peribronchial lymphoid tissue and lymph nodes from other sites were also observed in the group challenged by the intranasal route. It is noteworthy that the pathological features of MPXV in *S. tridecemlineatus* were similar to severe smallpox virus infection in humans.[91]

In 2007, another study using the same species of squirrel was performed comparing the pathogenic effects of two strains of MPXV, MPX Z79 and MPX US03, inoculated subcutaneously at doses of 3.7×10^4

p.f.u/mL and 1 0.8 × 10^4 p.f.u/mL US03, respectively. The research showed that clinical symptoms were earlier and more severe in animals that received the Z79 strain and that mortality in these animals occurred between days 6 and 11; on the other hand, despite presenting a milder symptomatology, death in animals that received the US03 strain occurred in a very similar period, between days 7 and 11 after infection. Animals infected with the Z79 MPX virus strain showed consistently higher viral titer in blood and lung tissue compared with those infected with US03 virus alone, but it was also possible to identify virus titers in the spleen and liver of these animals. Therefore, the results indicate that the US03 virus, belonging to the West African MPX virus family, was less virulent than the Central African MPX virus strains.[93]

In the same year, squirrels (*S. tridecemlineatus*) were used to investigate the efficacy of the antipoxvirus compound ST-246, after infection by the strain MPX-ZAI-1979-005, inoculated by the subcutaneous route. The results showed that all ground squirrels inoculated with the MPX virus and treated with ST-246 at 0, 24, 48, or 72 h after the challenge survived and none of these animals showed any apparent clinical symptoms. However, 33% of the animals that received treatment from 96 h after infection died; the others survived although some of them showed symptoms of the disease. In contrast, all animals infected with the MPX virus and treated with placebo showed clinical symptoms and died. All animals inoculated with MPXV and treated with placebo had a high MPXV load. However, none of the squirrels challenged with MPX virus and treated with ST-246 at 0, 24, 48, and 72 h post-infection developed detectable viremia. Squirrels in the ST-246-96h group that were humanely killed had low-titer viremia. None of the animals in the placebo or ST-246-0h, ST-246-24h, ST-246-48h, and ST-246-72h treatment groups developed detectable antibodies to the MPX virus. However, the two squirrels in the ST-246-96h group that became ill and recovered had detectable MPX virus antibody titers at the end of the experiment.[92]

Subsequently, squirrels of the *Marmota bobak* species were inoculated with the V79-1-005 strain by either subcutaneous or intranasal routes, at different doses, to verify the infective dose (ID_{50}) and the lethal dose (LD_{50}), as well as the effects of antiviral drugsNIOC-14 and ST-246. The study demonstrated that all doses of subcutaneous inoculation of the pathogen caused evident clinical symptoms, such as hyperthermia, skin rash on the body and mucous membranes, serous and purulent rhinitis, conjunctivitis, and incoordination, among others, culminating in the death of all infected animals. Clinical manifestations were similar in both groups. However, the skin and mucosal eruptions were milder and only 41.67% of the sick animals died. In the surviving animals, after the disappearance of clinical signs, scars were formed at the sites of eruptive elements, like smallpox. It is noteworthy that no sign of the disease was recorded in animals from experimental groups treated with NIOC-14 and ST-246 during the entire observation period. In addition, sufficiently high MPXV antibody titers were detected in the neutralization reaction in all animals in the experimental groups and surviving animals in the control group.[94]

In 2017, a study aimed at characterizing the infection by the MPXV/Congo/Luc+ strain in squirrels (*Funisciurus anerythrus*) was carried out. Animals were inoculated by intranasal and intradermal routes at a dose of 1x10^6 p.f.u/mL. MPXV infection caused moderate to severe morbidity and mortality of 75% in the intranasal group and 50% in the intradermal group, with clinical signs including lesions on the skin, eyes, mouth, and nose, as well as dyspnea and profuse nasal discharge. Both intranasal and intradermal exposure induced high levels of viremia, rapid systemic spread, and long periods of viral shedding. Housed in the same room, albeit in a different cage, was the sentinel animal, which showed clinical signs of MPXV infection, including increased respiratory rate, nasal discharge, and oral lesions and needed to be euthanized due to respiratory problems, weight loss, and lethargy. This study suggested that African rope squirrels develop severe pathology when infected with MPXV and that they shed large amounts of virus, evidencing their role as a source of transmission of MPXV to humans and other animals in MPXV endemic regions.[95]

Similar to prairie dogs, squirrels should be considered sparingly a model for MPXV as they are also unconventional species. In addition, there are countries where access to these animals is restricted.

RABBITS

Rabbits (*Oryctolagus cuniculus*) are generally resistant to infection caused by MPXV as adults, except in albino rabbits by inoculations performed by the intracerebral route or by scarification. In contrast, animals

up to 10 days of age can be easily infected by other routes of infection considering the absence of a robust immune system at this stage of life. Intradermally, for example, hemorrhagic conditions, the appearance of pustules, and lesions have already been reported.[1,48,96]

Intracerebral infections in adult and 2-day-old rabbits were fatal with the development of adult meningoencephalitis.[97] Infection by scarification was fatal for 2-day-old rabbits. Albino adults had fever and lesions, but recovered from the disease.[1,48]

Intravenous infection was more efficient in causing severe disease in adult rabbits when compared with the subcutaneous route. When infected subcutaneously, the animals presented generalized smallpox lesions, whereas in the intravenous route, an acute disease was observed with the presentation of papules that later became pustules followed by crusts on the skin and mucous membranes. Although the disease was more severe, the animals recovered.[1,56,57]

Oral infection in 10-day-old rabbits resulted in generalized disease and lesions on the skin, ears, and lips, whereas intranasal infection resulted in weight loss in animals. In both infections the animals died. In adult animals, no clinical signs of the disease were observed.[48]

The intravenous route seems promising for the development of a non-lethal adult model in rabbits. Considering the low lethality of the new circulating strains of MPXV, this animal model has the potential to become a cost-effective option, because it is an animal widely disseminated in animal experimentation units. Depending on the scientific question to be answered, other animal model options should be considered, as adult rabbits, except for the intravenous route, do not present satisfactory answers, requiring the use of animals with an incomplete immune system and/or inoculation routes with greater complexity.

OTHERS ANIMAL MODELS

Guinea pigs (*Cavia porcellus*) infected via the footpad showed swelling and edema at the inoculation site with the development of a granulomatous lesion. The animals showed antibody titers 14 days after infection. No viral titers were found in collected organs. By scarification, a mild inflammatory reaction occurred on the second day after infection and the development of discrete papules on the fourth day, followed by crusting and subsequent healing. Other routes of infection (intravenous, intracerebral, subcutaneous, intraperitoneal, intradermal, and oral) were evaluated, but the animals did not develop the disease.[1,48,56,57,106]

Similar to guinea pigs, hamsters (*Cricetinae*) were also not susceptible to attempts at infection by different routes of inoculation by MPXV, although intraperitoneal and intracardiac infection of the virus was detected in the lungs, liver, and spleen of the animals 7 days after infection. Focal lesions were observed only in the liver, kidney, and brain. The main manifestations were perivascular lymphocytic infiltrate and damage to the endothelial structure of blood vessels.[48,107]

Intravenous inoculation or scarification did not lead to overt in clinical disease in white rats (Rattus sp.) to. However, in newborn rats (1–3 days old) infection reached 100% mortality with virus replication in the lungs and liver after intranasal challenge.[48]

Cotton rats (*Sigmodon sp.*) can be infected intranasally, and these animals develop generalized disease that led the animals to develop difficulty breathing, cough, rhinitis, conjunctivitis, and progressive weight loss, which led to 50% mortality in the experimental group. High concentrations of virus were detected in blood and organs.[108]

The rodent Kellen's dormice (*Graphiurus kelleni*) challenged with MPXV had 100% mortality. In general, the animals showed weight loss, dehydration, conjunctivitis, rhinitis, and lymphadenopathy. Necrosis in the submandibular lymph nodes, spleen, and thymus; hepatocellular necrosis; and hemorrhage in the lungs, stomach, and small intestine were also observed.[109]

Chickens (*Gallus Gallus*) aged 3 to 4 days or 4 to 8 weeks are permissible to infection when inoculated intradermally but develop mild disease phenotypes. Once infected with MPXV, they present vesicles heal 10 days after infection. The same does not occur in adult animals.[1,106]

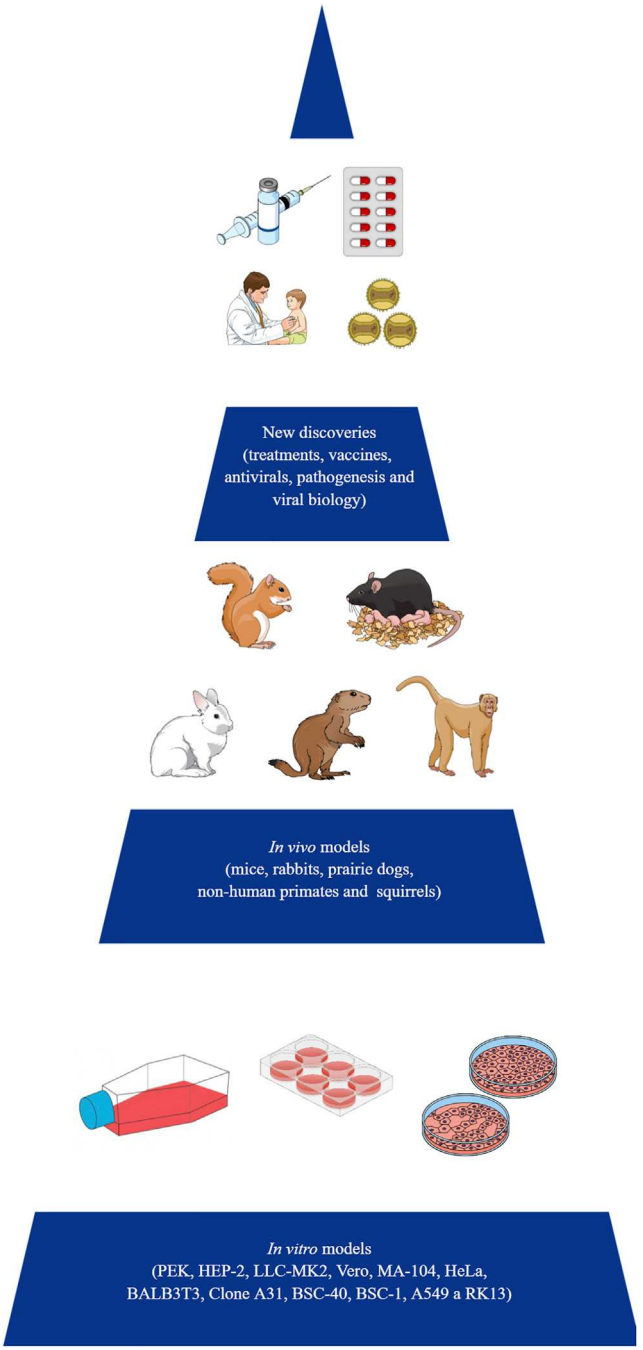

Figure 1. Cellular and animal models for monkeypox studies

In vitro models (PEK, HEP-2, LLC, MK2, Vero, MA-104, HeLa, BALB3T3, Clone A31, BSC-40, BSC-1, A549, and RK13 cells) and *in vivo* models (mice, rabbits, prairie dogs, non-human primates, and squirrels) are the basis for the elucidation the biology of new viral strains and for the discovery of new drugs, treatments, and vaccines. Created with Mindthegraph.com.

Although the findings using guinea pigs, hamsters, rats, Kellen's dormice, and chickens as an experimental model have been limited, further research using the contemporary strain of MPXV may change what we know about infection in these species and therefore further studies should be considered.

Recently, Seang and colleagues described a case of possible human-dog transmission of human MPXV of B.1 lineage, demonstrating the potential of the virus to perform host-jumps. The dog had no contact with other animals, but co-slept with the infected tutors.[110]

CONCLUDING REMARKS

The number of monkeypox cases has increased outside endemic areas putting the world on alert. However, great discoveries have already occurred and through them it was possible to develop new *in vivo* and *in vitro* models capable of mimicking aspects of viral biology and the pathology caused by the disease. Using the models described herein, the characterization of different viral strains and the development of vaccines and antiviral therapies has been successfully achieved. In experimental studies, the most adequate models must provide reliable results that can be extrapolated to humans. Given the rapid evolution that MPXV has undergone over the past few years, care should be taken in translating the findings produced with historical strains to contemporary ones.

Many animal models have been shown to be susceptible to infection and develop clinical disease with varying degrees of severity, including cases of lethality. Each model has its own applicability for virus and disease studies. The choice of model is linked to the question to which one wants to answer, and each species will have an adequate morphological or physiological particularity to contribute to the experimental response. Mice and rabbits, for example, are readily available, easy to handle, have low maintenance costs, and have a widely known genome, unlike unconventional laboratory species such as prairie dogs and squirrels. However, translating knowledge from rodent studies to the clinic can be a challenge. Non-human primates are genetically closer models to humans, but handling these animals can be costly, in addition to having a longer life cycle, which makes the development of the model difficult.

The *in vitro* and *in vivo* models developed so far can contribute to study several aspects of the disease and mechanism of virus-host interactions. These models will be key to the development of new drugs and therapies capable of blocking the advance of MPXV, as the virus is spreading around the world (Figure 1).

ACKNOWLEDGMENTS

The authors thank the postgraduate program in Biosciences and Biotechnology in Health at the Instituto Aggeu Magalhães (FIOCRUZ - PE) for the institutional assistance and support. Dr. Pena's lab is supported by grants APQ-0560-2.12/19 and 441030/2020-3 from the Pernambuco State Foundation for Science and Technology (FACEPE) and National Council for Scientific and Technological Development (CNPq), respectively.

ACGJ is grateful to CAPES (Coordination for the Improvement of Higher Education Personnel)—Brazil, Prevention and Combat of Outbreaks, Endemics, Epidemics and Pandemics-Finance Code #88881.506794/2020-01, and to FAPEMIG (Minas Gerais Research Foundation APQ-03385-18 and APQ-01487-22). MSM thanks FAPEMIG for the scholarship # 12152. IAS thanks CNPq for the scholarship # 142495/2020-4 and CAPES. Print scholarship # 88887.700246/2022-00.

AUTHOR CONTRIBUTIONS

R.B.R., E.F.d.C., D.C.P.V., I.A.S., M.d.S.M., and F.B.F.F participated in the search for articles to be reviewed and carried out the writing of the review. R.B.R. designated graphical abstract. L.J.P. participated in the supervision. L.J.P., M.V.d.S., and A.C.G.J. participated in the writing and review of this paper. All authors have read and agreed to the published version of the manuscript.

DECLARATION OF INTERESTS

The authors declare no conflict of interest.

REFERENCES

1. Magnus, P.v., Andersen, E.K., Petersen, K.B., and Birch-Andersen, A. (1959). A Pox-like disease in Cynomolgus monkeys. Acta Pathol. Microbiol. Scand. *46*, 156–176. https://doi.org/10.1111/j.1699-0463.1959.tb00328.x.

2. Kozlov, M. (2022). Monkeypox goes global: why scientists are on alert. Nature *606*, 15–16. https://doi.org/10.1038/d41586-022-01421-8.

3. World Health Organization (2022). Monkeypox. World Heal. Organ. https://www.who.int/news-room/fact-sheets/detail/monkeypox.

4. Learned, L.A., Reynolds, M.G., Wassa, D.W., Li, Y., Olson, V.A., Karem, K., Stempora, L.L., Braden, Z.H., Kline, R., Likos, A., et al. (2005).

Extended interhuman transmission of monkeypox in a hospital community in the Republic of the Congo, 2003. Am. J. Trop. Med. Hyg. *73*, 428–434. https://doi.org/10.4269/ajtmh.2005.73.428.

5. Jezek, Z., Grab, B., Szczeniowski, M., Paluku, K.M., and Mutombo, M. (1988). Clinico-epidemiological features of monkeypox patients with an animal or human source of infection. Bull. World Health Organ. *66*, 459–464.

6. Beer, E.M., and Rao, V.B. (2019). A systematic review of the epidemiology of human monkeypox outbreaks and implications for outbreak strategy. PLoS Negl. Trop. Dis. *13*, e0007791. https://doi.org/10.1371/journal.pntd.0007791.

7. Bunge, E.M., Hoet, B., Chen, L., Lienert, F., Weidenthaler, H., Baer, L.R., and Steffen, R. (2022). The changing epidemiology of human monkeypox—a potential threat? a systematic review. PLoS Negl. Trop. Dis. *16*, e0010141. https://doi.org/10.1371/journal.pntd.0010141.

8. Yang, Z. (2022). Monkeypox: a potential global threat? J. Med. Virol. *94*, 4034–4036. https://doi.org/10.1002/jmv.27884.

9. Centers for Disease Control and Prevention (2022). Monkeypox Outbreak Global Map. Centers Dis. Control Prev. https://www.cdc.gov/poxvirus/monkeypox/response/2022/world-map.html.

10. World Health Organization (2022). Who Director-General Declares the Ongoing Monkeypox Outbreak a Public Health Emergency of International Concern (World Health Organization). https://www.who.int/europe/news/item/23-07-2022-who-director-general-declares-the-ongoing-monkeypox-outbreak-a-public-health-event-of-international-concern.

11. Goeijenbier, M., van Wissen, M., van de Weg, C., Jong, E., Gerdes, V.E.A., Meijers, J.C.M., Brandjes, D.P.M., and van Gorp, E.C.M. (2012). Modeling human viral diseases: trials and triumphs. J. Med. Virol. *84*, 1680–1696. https://doi.org/10.1002/jmv.23354.

12. Dulbecco, R. (1952). Production of plaques in monolayer tissue cultures by single particles of an animal virus. Proc. Natl. Acad. Sci. USA *38*, 747–752. https://doi.org/10.1073/pnas.38.8.747.

13. Dulbecco, R., and Marguerite Vogt, M.D. (1953). Plaque formation and isolation of pure lines with poliomyelitis viruses. J. Exp. Med. *99*, 167–182.

14. Yao, X., Ye, F., Zhang, M., Cui, C., Huang, B., Niu, P., Liu, X., Zhao, L., Dong, E., Song, C., et al. (2020). In vitro antiviral activity and projection of optimized dosing design of hydroxychloroquine for the treatment of severe acute respiratory syndrome Coronavirus 2 (SARS-CoV-2). Clin. Infect. Dis. *71*, 732–739. https://doi.org/10.1093/cid/ciaa237.

15. Pena, L.J., Miranda Guarines, K., Duarte Silva, A.J., Sales Leal, L.R., Mendes Félix, D., Silva, A., De Oliveira, S.A., Junqueira Ayres, C.F., Júnior, A.S., and De Freitas, A.C. (2018). In vitro and in vivo models for studying Zika virus biology. J. Gen. Virol. *99*, 1529–1550. https://doi.org/10.1099/jgv.0.001153.

16. Marennikova, S.S., Seluhina, E.M., Mal'ceva, N.N., Cimiskjan, K.L., and Macevic, G.R. (1972). Isolation and properties of the causal agent of a new variola-like disease (monkeypox) in man. Bull. World Health Organ. *46*, 599–611.

17. Rogers, J.V., Parkinson, C.V., Choi, Y.W., Speshock, J.L., and Hussain, S.M. (2008). A preliminary assessment of silver nanoparticle inhibition of monkeypox virus plaque formation. Nanoscale Res. Lett. *3*, 129–133. https://doi.org/10.1007/s11671-008-9128-2.

18. Baker, R.O., Bray, M., and Huggins, J.W. (2003). Potential antiviral therapeutics for smallpox, monkeypox and other orthopoxvirus infections. Antiviral Res. *57*, 13–23. https://doi.org/10.1016/S0166-3542(02)00196-1.

19. Alkhalil, A., Strand, S., Mucker, E., Huggins, J.W., Jahrling, P.B., and Ibrahim, S.M. (2009). Inhibition of Monkeypox virus replication by RNA interference. Virol. J. *6*, 188. https://doi.org/10.1186/1743-422X-6-188.

20. Yang, M., and Schneller, S.W. (2005). 5′-Homoaristeromycin. Synthesis and antiviral activity against orthopox viruses. Bioorg. Med. Chem. Lett. *15*, 149–151. https://doi.org/10.1016/j.bmcl.2004.10.019.

21. Smee, D.F., Bray, M., and Huggins, J.W. (2001). Antiviral activity and mode of action studies of ribavirin and mycophenolic acid against orthopoxviruses in vitro. Antivir. Chem. Chemother. *12*, 327–335. https://doi.org/10.1177/095632020101200602.

22. Johnston, S.C., Lin, K.L., Connor, J.H., Ruthel, G., Goff, A., and Hensley, L.E. (2012). In vitro inhibition of monkeypox virus production and spread by Interferon-β. Virol. J. *9*, 5. https://doi.org/10.1186/1743-422X-9-5.

23. Priyamvada, L., Burgado, J., Baker-Wagner, M., Kitaygorodskyy, A., Olson, V., Lingappa, V.R., and Satheshkumar, P.S. (2021). New methylene blue derivatives suggest novel anti-orthopoxviral strategies. Antiviral Res. *191*, 105086. https://doi.org/10.1016/j.antiviral.2021.105086.

24. Fernández de Marco, M.d.M., Alejo, A., Hudson, P., Damon, I.K., and Alcami, A. (2010). The highly virulent variola and monkeypox viruses express secreted inhibitors of type I interferon. FASEB J. *24*, 1479–1488. https://doi.org/10.1096/fj.09-144733.

25. Smith, S.K., Olson, V.A., Karem, K.L., Jordan, R., Hruby, D.E., and Damon, I.K. (2009). In vitro efficacy of ST246 against smallpox and monkeypox. Antimicrob. Agents Chemother. *53*, 1007–1012. https://doi.org/10.1128/AAC.01044-08.

26. Fogg, C.N., Americo, J.L., Lustig, S., Huggins, J.W., Smith, S.K., Damon, I., Resch, W., Earl, P.L., Klinman, D.M., and Moss, B. (2007). Adjuvant-enhanced antibody responses to recombinant proteins correlates with protection of mice and monkeys to orthopoxvirus challenges. Vaccine *25*, 2787–2799. https://doi.org/10.1016/j.vaccine.2006.12.037.

27. Altmann, S.E., Brandt, C.R., Jahrling, P.B., and Blaney, J.E. (2012). Antiviral activity of the EB peptide against zoonotic poxviruses. Virol. J. *9*, 6. https://doi.org/10.1186/1743-422X-9-6.

28. Altmann, S.E., Smith, A.L., Dyall, J., Johnson, R.F., Dodd, L.E., Jahrling, P.B., Paragas, J., and Blaney, J.E. (2012). Inhibition of cowpox virus and monkeypox virus infection by mitoxantrone. Antiviral Res. *93*, 305–308. https://doi.org/10.1016/j.antiviral.2011.12.001.

29. Bengali, Z., Satheshkumar, P.S., and Moss, B. (2012). Orthopoxvirus species and strain differences in cell entry. Virology *433*, 506–512. https://doi.org/10.1016/j.virol.2012.08.044.

30. Arndt, W.D., Cotsmire, S., Trainor, K., Harrington, H., Hauns, K., Kibler, K.V., Huynh, T.P., and Jacobs, B.L. (2015). Evasion of the innate immune type I interferon system by monkeypox virus. J. Virol. *89*, 10489–10499. https://doi.org/10.1128/jvi.00304-15.

31. Brockman, W.W., and Nathans, D. (1974). The isolation of simian virus 40 variants with specifically altered genomes. Proc. Natl. Acad. Sci. USA *71*, 942–946. https://doi.org/10.1073/pnas.71.3.942.

32. Earley, E., and Johnson, K. (1988). The lineage of the Vero, Vero 76 and its clone C1008 in the United States. In Vero Cells : Origin, Properties and Biomedical Applications, pp. 26–29.

33. Smith, S.K., Self, J., Weiss, S., Carroll, D., Braden, Z., Regnery, R.L., Davidson, W., Jordan, R., Hruby, D.E., and Damon, I.K. (2011). Effective antiviral treatment of systemic orthopoxvirus disease: ST-246 treatment of prairie dogs infected with monkeypox virus. J. Virol. *85*, 9176–9187. https://doi.org/10.1128/jvi.02173-10.

34. Berhanu, A., Prigge, J.T., Silvera, P.M., Honeychurch, K.M., Hruby, D.E., and Grosenbach, D.W. (2015). Treatment with the smallpox antiviral tecovirimat (ST-246) alone or in combination with ACAM2000 vaccination is effective as a postsymptomatic therapy for monkeypox virus infection. Antimicrob. Agents Chemother. *59*, 4296–4300. https://doi.org/10.1128/AAC.00208-15.

35. Law, M., and Smith, G.L. (2004). Studying the binding and entry of the intracellular and extracellular enveloped forms of vaccinia virus. Methods Mol. Biol. *269*, 187–204. https://doi.org/10.1385/1-59259-789-0:187.

36. Fox, E.J. (2004). Mechanism of action of mitoxantrone. Neurology *63*, S15–S18.

https://doi.org/10.1212/WNL.63.12_suppl_6.S15.

37. Blach-Olszewska, Z., Halasa, J., Matej, H., and Cembrzyńska-Nowak, M. (1977). Why HeLa cells do not produce interferon? Arch. Immunol. Ther. Exp. *25*, 683–691.

38. Konishi, K., Yamaji, T., Sakuma, C., Kasai, F., Endo, T., Kohara, A., Hanada, K., and Osada, N. (2022). Whole-genome sequencing of Vero E6 (VERO C1008) and comparative analysis of four Vero cell sublines. Front. Genet. *13*, 801382. https://doi.org/10.3389/fgene.2022.801382.

39. Lalani, A.S., Masters, J., Zeng, W., Barrett, J., Pannu, R., Everett, H., Arendt, C.W., and McFadden, G. (1999). Use of chemokine receptors by poxviruses. Science *286*, 1968–1971. https://doi.org/10.1126/science.286.5446.1968.

40. Blasco, R., Sisler, J.R., and Moss, B. (1993). Dissociation of progeny vaccinia virus from the cell membrane is regulated by a viral envelope glycoprotein: effect of a point mutation in the lectin homology domain of the A34R gene. J. Virol. *67*, 3319–3325. https://doi.org/10.1128/jvi.67.6.3319-3325.1993.

41. Lin, C.-L., Chung, C.-S., Heine, H.G., and Chang, W. (2000). Vaccinia virus envelope H3L protein binds to cell surface heparan sulfate and is important for intracellular mature virion morphogenesis and virus infection in vitro and in vivo. J. Virol. *74*, 3353–3365. https://doi.org/10.1128/jvi.74.7.3353-3365.2000.

42. Hsiao, J.-C., Chung, C.-S., and Chang, W. (1999). Vaccinia virus envelope D8L protein binds to cell surface chondroitin sulfate and mediates the adsorption of intracellular mature virions to cells. J. Virol. *73*, 8750–8761. https://doi.org/10.1128/jvi.73.10.8750-8761.1999.

43. Hsiao, J.-C., Chung, C.-S., and Chang, W. (1998). Cell surface proteoglycans are necessary for A27L protein-mediated cell fusion: identification of the N-terminal region of A27L protein as the glycosaminoglycan-binding domain. J. Virol. *72*, 8374–8379. https://doi.org/10.1128/jvi.72.10.8374-8379.1998.

44. Hutson, C.L., and Damon, I.K. (2010). Monkeypox virus infections in small animal models for evaluation of anti-poxvirus agents. Viruses *2*, 2763–2776. https://doi.org/10.3390/v2122763.

45. Rosa, R.B., Dantas, W.M., Do Nascimento, J.C.F., da Silva, M.V., de Oliveira, R.N., and Pena, L.J. (2021). In vitro and in vivo models for studying sars-cov-2, the etiological agent responsible for covid-19 pandemic. Viruses *13*, 379. https://doi.org/10.3390/v13030379.

46. Stabenow, J., Buller, R.M., Schriewer, J., West, C., Sagartz, J.E., and Parker, S. (2010). A mouse model of lethal infection for evaluating prophylactics and therapeutics against monkeypox virus. J. Virol. *84*, 3909–3920. https://doi.org/10.1128/jvi.02012-09.

47. Earl, P.L., Americo, J.L., and Moss, B. (2012). Lethal monkeypox virus infection of CAST/EiJ mice is associated with a deficient gamma interferon response. J. Virol. *86*, 9105–9112. https://doi.org/10.1128/jvi.00162-12.

48. Marennikova, S.S., and Seluhina, E.M. (1976). Susceptibility of some rodent species to monkeypox virus, and course of the infection. Bull. World Health Organ. *53*, 13–20.

49. Osorio, J.E., Iams, K.P., Meteyer, C.U., and Rocke, T.E. (2009). Comparison of monkeypox viruses pathogenesis in mice by in vivo imaging. PLoS One *4*, e6592. https://doi.org/10.1371/journal.pone.0006592.

50. Earl, P.L., Americo, J.L., Cotter, C.A., and Moss, B. (2015). Comparative live bioluminescence imaging of monkeypox virus dissemination in a wild-derived inbred mouse (Mus musculus castaneus) and outbred African dormouse (Graphiurus kelleni). Virology *475*, 150–158. https://doi.org/10.1016/j.virol.2014.11.015.

51. Sergeev, A.A., Kabanov, A.S., Bulychev, L.E., Sergeev, A.A., Pyankov, O.V., Bodnev, S.A., Galahova, D.O., Zamedyanskaya, A.S., Titova, K.A., Glotov, A.G., et al. (2016). The possibility of using the ICR mouse as an animal model to assess antimonkeypox drug efficacy. Transbound. Emerg. Dis. *63*, e419–e430. https://doi.org/10.1111/tbed.12323.

52. Americo, J.L., Moss, B., and Earl, P.L. (2010). Identification of wild-derived inbred mouse strains highly susceptible to monkeypox virus infection for use as small animal models. J. Virol. *84*, 8172–8180. https://doi.org/10.1128/jvi.00621-10.

53. Earl, P.L., Americo, J.L., and Moss, B. (2020). Natural killer cells expanded in vivo or ex vivo with IL-15 overcomes the inherent susceptibility of CAST mice to lethal infection with orthopoxviruses. PLoS Pathog. *16*, e1008505. https://doi.org/10.1371/journal.ppat.1008505.

54. Earl, P.L., Americo, J.L., and Moss, B. (2015). Genetic studies of the susceptibility of classical and wild-derived inbred mouse strains to monkeypox virus. Virology *481*, 161–165. https://doi.org/10.1016/j.virol.2015.02.048.

55. Warner, B.M., Klassen, L., Sloan, A., Deschambault, Y., Soule, G., Banadyga, L., Cao, J., Strong, J.E., Kobasa, D., and Safronetz, D. (2022). In vitro and in vivo efficacy of Tecovirimat against a recently emerged 2022 Monkeypox virus isolate. Sci. Transl. Med. *14*, eade7646.

56. Prier, J.E., and Sauer, R.M. (1960). A pox disease of monkeys. Ann. N. Y. Acad. Sci. *85*, 951–959. https://doi.org/10.1111/j.1749-6632.1960.tb50015.x.

57. Prier, J.E., Sauer, R.M., Malsberger, R.G., and Sillaman, J.M. (1960). Studies on a pox disease of monkeys. II. Isolation of the etiologic agent. Am. J. Vet. Res. *21*, 381–384.

58. Wenner, H.A., Bolano, C.R., Cho, C.T., and Kamitsuka, P.S. (1969). Studies on the pathogenesis of monkey pox - III. Histopathological lesions and sites of immunofluorescence. Arch. Gesamte Virusforsch. *27*, 179–197. https://doi.org/10.1007/BF01249642.

59. Wenner, H.A., Macasaet, F.D., Kamitsuka, P.S., and Kidd, P. (1968). Monkey pox. I. Clinical, virologic and immunologic studies. Am. J. Epidemiol. *87*, 551–566. https://doi.org/10.1093/oxfordjournals.aje.a120846.

60. Wenner, H.A., Bolano, C.R., Cho, C.T., and Kamitsuka, P.S. (1969). Studies on the pathogenesis of monkey pox - II. Dose-Response and Virus Dispersion. Arch. Gesamte Virusforsch. *27*, 179–197. https://doi.org/10.1007/BF01249642.

61. Huggins, J., Goff, A., Hensley, L., Mucker, E., Shamblin, J., Wlazlowski, C., Johnson, W., Chapman, J., Larsen, T., Twenhafel, N., et al. (2009). Nonhuman primates are protected from smallpox virus or monkeypox virus challenges by the antiviral drug ST-246. Antimicrob. Agents Chemother. *53*, 2620–2625. https://doi.org/10.1128/AAC.00021-09.

62. Wei, H., Huang, D., Fortman, J., Wang, R., Shao, L., and Chen, Z.W. (2009). Coadministration of cidofovir and smallpox vaccine reduced vaccination side effects but interfered with vaccine-elicited immune responses and immunity to monkeypox. J. Virol. *83*, 1115–1125. https://doi.org/10.1128/jvi.00984-08.

63. Jordan, R., Goff, A., Frimm, A., Corrado, M.L., Hensley, L.E., Byrd, C.M., Mucker, E., Shamblin, J., Bolken, T.C., Wlazlowski, C., et al. (2009). ST-246 antiviral efficacy in a nonhuman primate monkeypox model: determination of the minimal effective dose and human dose justification. Antimicrob. Agents Chemother. *53*, 1817–1822. https://doi.org/10.1128/AAC.01596-08.

64. Earl, P.L., Americo, J.L., Wyatt, L.S., Eller, L.A., Whitbeck, J.C., Cohen, G.H., Eisenberg, R.J., Hartmann, C.J., Jackson, D.L., Kulesh, D.A., et al. (2004). Immunogenicity of a highly attenuated MVA smallpox vaccine and protection against monkeypox. Nature *428*, 182–185. https://doi.org/10.1038/nature02331.

65. Earl, P.L., Americo, J.L., Wyatt, L.S., Espenshade, O., Bassler, J., Gong, K., Lin, S., Peters, E., Rhodes, L., Spano, Y.E., et al. (2008). Rapid protection in a monkeypox model by a single injection of a replication-deficient vaccinia virus. Proc. Natl. Acad. Sci. USA *105*, 10889–10894. https://doi.org/10.1073/pnas.0804985105.

66. Buchman, G.W., Cohen, M.E., Xiao, Y., Richardson-Harman, N., Silvera, P., DeTolla, L.J., Davis, H.L., Eisenberg, R.J., Cohen, G.H., and Isaacs, S.N. (2010). A protein-based smallpox vaccine protects non-human primates from a lethal monkeypox virus challenge. Vaccine *28*, 6627–6636. https://doi.org/10.1016/j.vaccine.2010.07.030.

67. Denzler, K.L., Babas, T., Rippeon, A., Huynh, T., Fukushima, N., Rhodes, L., Silvera, P.M., and Jacobs, B.L. (2011). Attenuated NYCBH vaccinia virus deleted for the E3L gene confers partial protection against lethal monkeypox virus disease in cynomolgus macaques. Vaccine *29*, 9684–9690. https://doi.org/10.1016/j.vaccine.2011.09.135.

68. Russo, A.T., Berhanu, A., Bigger, C.B., Prigge, J., Silvera, P.M., Grosenbach, D.W., and Hruby, D. (2020). Co-administration of tecovirimat and ACAM2000™ in non-human primates: effect of tecovirimat treatment on ACAM2000 immunogenicity and efficacy versus lethal monkeypox virus challenge. Vaccine *38*, 644–654. https://doi.org/10.1016/j.vaccine.2019.10.049.

69. Hahon, N., and McGavran, M.H. (1961). Airborne infectivity of the variola-vaccinia group of poxviruses for the cynomolgus monkey, macaca irus. J. Infect. Dis. *109*, 294–298. https://doi.org/10.1093/INFDIS/109.3.294.

70. Hatch, G.J., Graham, V.A., Bewley, K.R., Tree, J.A., Dennis, M., Taylor, I., Funnell, S.G.P., Bate, S.R., Steeds, K., Tipton, T., et al. (2013). Assessment of the protective effect of imvamune and Acam2000 vaccines against aerosolized monkeypox virus in cynomolgus macaques. J. Virol. *87*, 7805–7815. https://doi.org/10.1128/jvi.03481-12.

71. Zaucha, G.M., Jahrling, P.B., Geisbert, T.W., Swearengen, J.R., and Hensley, L. (2001). The pathology of experimental aerosolized monkeypox virus infection in cynomolgus monkeys (Macaca fascicularis). Lab. Invest. *81*, 1581–1600. https://doi.org/10.1038/labinvest.3780373.

72. Goff, A.J., Chapman, J., Foster, C., Wlazlowski, C., Shamblin, J., Lin, K., Kreiselmeier, N., Mucker, E., Paragas, J., Lawler, J., et al. (2011). A novel respiratory model of infection with monkeypox virus in cynomolgus macaques. J. Virol. *85*, 4898–4909. https://doi.org/10.1128/jvi.02525-10.

73. Stittelaar, K.J., Neyts, J., Naesens, L., Van Amerongen, G., Van Lavieren, R.F., Holý, A., De Clercq, E., Niesters, H.G.M., Fries, E., Maas, C., et al. (2006). Antiviral treatment is more effective than smallpox vaccination upon lethal monkeypox virus infection. Nature *439*, 745–748. https://doi.org/10.1038/nature04295.

74. Barnewall, R.E., Fisher, D.A., Robertson, A.B., Vales, P.A., Knostman, K.A., and Bigger, J.E. (2012). Inhalational monkeypox virus infection in cynomolgus macaques. Front. Cell. Infect. Microbiol. *2*, 117. https://doi.org/10.3389/fcimb.2012.00117.

75. Nalca, A., Livingston, V.A., Garza, N.L., Zumbrun, E.E., Frick, O.M., Chapman, J.L., and Hartings, J.M. (2010). Experimental infection of cynomolgus macaques (Macaca fascicularis) with aerosolized monkeypox virus. PLoS One *5*, e12880. https://doi.org/10.1371/journal.pone.0012880.

76. Russo, A.T., Grosenbach, D.W., Brasel, T.L., Baker, R.O., Cawthon, A.G., Reynolds, E., Bailey, T., Kuehl, P.J., Sugita, V., Agans, K., et al. (2018). Effects of treatment delay on efficacy of tecovirimat following lethal aerosol monkeypox virus challenge in cynomolgus macaques. J. Infect. Dis. *218*, 1490–1499. https://doi.org/10.1093/infdis/jiy326.

77. Tree, J.A., Hall, G., Pearson, G., Rayner, E., Graham, V.A., Steeds, K., Bewley, K.R., Hatch, G.J., Dennis, M., Taylor, I., et al. (2015). Sequence of pathogenic events in cynomolgus macaques infected with aerosolized monkeypox virus. J. Virol. *89*, 4335–4344. https://doi.org/10.1128/jvi.03029-14.

78. Johnson, R.F., Dyall, J., Ragland, D.R., Huzella, L., Byrum, R., Jett, C., St Claire, M., Smith, A.L., Paragas, J., Blaney, J.E., et al. (2011). Comparative analysis of monkeypox virus infection of cynomolgus macaques by the intravenous or intrabronchial inoculation route. J. Virol. *85*, 2112–2125. https://doi.org/10.1128/jvi.01931-10.

79. Estep, R.D., Messaoudi, I., O'Connor, M.A., Li, H., Sprague, J., Barron, A., Engelmann, F., Yen, B., Powers, M.F., Jones, J.M., et al. (2011). Deletion of the monkeypox virus inhibitor of complement enzymes locus impacts the adaptive immune response to monkeypox virus in a nonhuman primate model of infection. J. Virol. *85*, 9527–9542. https://doi.org/10.1128/jvi.00199-11.

80. Mucker, E.M., Chapman, J., Huzella, L.M., Huggins, J.W., Shamblin, J., Robinson, C.G., and Hensley, L.E. (2015). Susceptibility of marmosets (Callithrix jacchus) to monkeypox virus: a low dose prospective model for monkeypox and smallpox disease. PLoS One *10*, e0131742. https://doi.org/10.1371/journal.pone.0131742.

81. Mucker, E.M., Wollen-Roberts, S.E., Kimmel, A., Shamblin, J., Sampey, D., and Hooper, J.W. (2018). Intranasal monkeypox marmoset model: prophylactic antibody treatment provides benefit against severe monkeypox virus disease. PLoS Negl. Trop. Dis. *12*, e0006581. https://doi.org/10.1371/journal.pntd.0006581.

82. Xiao, S.Y., Sbrana, E., Watts, D.M., Siirin, M., da Rosa, A.P.A.T., and Tesh, R.B. (2005). Experimental infection of prairie dogs with monkeypox virus. Emerg. Infect. Dis. *11*, 539–545. https://doi.org/10.3201/eid1104.040907.

83. Hutson, C.L., Carroll, D.S., Self, J., Weiss, S., Hughes, C.M., Braden, Z., Olson, V.A., Smith, S.K., Karem, K.L., Regnery, R.L., et al. (2010). Dosage comparison of Congo Basin and West African strains of monkeypox virus using a prairie dog animal model of systemic orthopoxvirus disease. Virology *402*, 72–82. https://doi.org/10.1016/j.virol.2010.03.012.

84. Hutson, C.L., Olson, V.A., Carroll, D.S., Abel, J.A., Hughes, C.M., Braden, Z.H., Weiss, S., Self, J., Osorio, J.E., Hudson, P.N., et al. (2009). A prairie dog animal model of systemic orthopoxvirus disease using west African and Congo Basin strains of Monkeypox virus. J. Gen. Virol. *90*, 323–333. https://doi.org/10.1099/vir.0.005108-0.

85. Hutson, C.L., Kondas, A.V., Mauldin, M.R., Doty, J.B., Grossi, I.M., Morgan, C.N., Ostergaard, S.D., Hughes, C.M., Nakazawa, Y., Kling, C., et al. (2021). Pharmacokinetics and efficacy of a potential smallpox therapeutic, Brincidofovir, in a lethal monkeypox virus animal model. mSphere *6*, 009277-20. https://doi.org/10.1128/msphere.00927-20.

86. Weiner, Z.P., Salzer, J.S., LeMasters, E., Ellison, J.A., Kondas, A.V., Morgan, C.N., Doty, J.B., Martin, B.E., Satheshkumar, P.S., Olson, V.A., et al. (2019). Characterization of Monkeypox virus dissemination in the black-tailed prairie dog (Cynomys ludovicianus) through in vivo bioluminescent imaging. PLoS One *14*, e0222612. https://doi.org/10.1371/journal.pone.0222612.

87. Hutson, C.L., Carroll, D.S., Gallardo-Romero, N., Weiss, S., Clemmons, C., Hughes, C.M., Salzer, J.S., Olson, V.A., Abel, J., Karem, K.L., et al. (2011). Monkeypox disease transmission in an experimental setting: prairie dog animal model. PLoS One *6*, e28295. https://doi.org/10.1371/journal.pone.0028295.

88. Hutson, C.L., Gallardo-Romero, N., Carroll, D.S., Clemmons, C., Salzer, J.S., Nagy, T., Hughes, C.M., Olson, V.A., Karem, K.L., and Damon, I.K. (2013). Transmissibility of the monkeypox virus clades via respiratory transmission: investigation using the prairie dog-monkeypox virus challenge system. PLoS One *8*, e55488. https://doi.org/10.1371/journal.pone.0055488.

89. Hutson, C.L., Carroll, D.S., Gallardo-Romero, N., Drew, C., Zaki, S.R., Nagy, T., Hughes, C., Olson, V.A., Sanders, J., Patel, N., et al. (2015). Comparison of monkeypox virus clade kinetics and pathology within the prairie dog animal model using a serial sacrifice study design. Biomed Res. Int. *2015*, 965710. https://doi.org/10.1155/2015/965710.

90. Keckler, M.S., Salzer, J.S., Patel, N., Townsend, M.B., Nakazawa, Y.J., Doty, J.B., Gallardo-Romero, N.F., Satheshkumar, P.S., Carroll, D.S., Karem, K.L., et al. (2020). Imvamune® and acam2000® provide different protection against disease when administered postexposure in an intranasal monkeypox challenge prairie dog model. Vaccines *8*, 396. https://doi.org/10.3390/vaccines8030396.

91. Tesh, R.B., Watts, D.M., Sbrana, E., Siirin, M., Popov, V.L., and Xiao, S.Y. (2004). Experimental infection of ground squirrels with monkeypox virus. Emerg. Infect. Dis. *10*, 1563–1567.

92. Sbrana, E., Jordan, R., Hruby, D.E., Mateo, R.I., Xiao, S.Y., Siirin, M., Newman, P.C., da Rosa, A.P.A.T., and Tesh, R.B. (2007). Efficacy of the antipoxvirus compound ST-246 for treatment of severe orthopoxvirus infection. Am. J. Trop. Med. Hyg. *76*, 768–773. https://doi.org/10.4269/ajtmh.2007.76.768.

93. Sbrana, E., Xiao, S.Y., Newman, P.C., and Tesh, R.B. (2007). Comparative pathology of North American and Central African strains of monkeypox virus in a ground squirrel

model of the disease. Am. J. Trop. Med. Hyg. *76*, 155–164. https://doi.org/10.4269/ajtmh.2007.76.155.

94. Sergeev, A.A., Kabanov, A.S., Bulychev, L.E., Sergeev, A.A., Pyankov, O.V., Bodnev, S.A., Galahova, D.O., Zamedyanskaya, A.S., Titova, K.A., Glotova, T.I., et al. (2017). Using the ground squirrel (Marmota bobak) as an animal model to assess monkeypox drug efficacy. Transbound. Emerg. Dis. *64*, 226–236. https://doi.org/10.1111/tbed.12364.

95. Falendysz, E.A., Lopera, J.G., Doty, J.B., Nakazawa, Y., Crill, C., Lorenzsonn, F., Kalemba, L.N., Ronderos, M.D., Mejia, A., Malekani, J.M., et al. (2017). Characterization of Monkeypox virus infection in African rope squirrels (Funisciurus sp.). PLoS Negl. Trop. Dis. *11*, e0005809. https://doi.org/10.1371/journal.pntd.0005809.

96. Gispen, R., and Brand-Saathof, B. (1972). White" poxvirus strains from monkeys. Bull. World Health Organ. *46*, 585–592.

97. Gispen, R., Verlinde, J.D., and Zwart, P. (1967). Histopathological and virological studies on monkeypox. Arch. Gesamte Virusforsch. *21*, 205–216. https://doi.org/10.1007/BF01241445.

98. Parker, S., and Buller, R.M. (2013). A review of experimental and natural infections of animals with monkeypox virus between 1958 and 2012. Future Virol. *8*, 129–157. https://doi.org/10.2217/fvl.12.130.

99. Kozlov, M. (2022). How deadly is monkeypox? What scientists know. Nature *609*, 663. https://doi.org/10.1038/d41586-022-02931-1.

100. Pereira, V.R.A., Lorena, V.M.B., Nakazawa, M., Luna, C.F., Silva, E.D., Ferreira, A.G.P., Krieger, M.A., Goldenberg, S., Soares, M.B.P., Coutinho, E.M., et al. (2005). Humoral and cellular immune responses in BALB/c and C57BL/6 mice immunized with cytoplasmic (CRA) and flagellar (FRA) recombinant repetitive antigens, in acute experimental Trypanosoma cruzi infection. Parasitol. Res. *96*, 154–161. https://doi.org/10.1007/s00436-005-1336-4.

101. Trunova, G.V., Makarova, O.V., Diatroptov, M.E., Bogdanova, I.M., Mikchailova, L.P., and Abdulaeva, S.O. (2011). Morphofunctional characteristic of the immune system in BALB/c and C57Bl/6 mice. Bull. Exp. Biol. Med. *151*, 99–102. https://doi.org/10.1007/s10517-011-1268-1.

102. Duggal, N.K., Ritter, J.M., Pestorius, S.E., Zaki, S.R., Davis, B.S., Chang, G.J.J., Bowen, R.A., and Brault, A.C. (2017). Frequent Zika virus sexual transmission and prolonged viral RNA shedding in an immunodeficient mouse model. Cell Rep. *18*, 1751–1760. https://doi.org/10.1016/j.celrep.2017.01.056.

103. Hutson, C.L., Abel, J.A., Carroll, D.S., Olson, V.A., Braden, Z.H., Hughes, C.M., Dillon, M., Hopkins, C., Karem, K.L., Damon, I.K., et al. (2010). Comparison of West African and Congo Basin monkeypox viruses in BALB/c and C57BL/6 mice. PLoS One *5*, e8912. https://doi.org/10.1371/journal.pone.0008912.

104. Hahon, N. (1961). Smallpox and related poxvirus infections in the simian host. Bacteriol. Rev. *25*, 459–476. https://doi.org/10.1128/mmbr.25.4.459-476.1961.

105. Sauer, R.M., Prier, J.E., Buchanan, R.S., Creamer, A.A., and Fegley, H.C. (1960). Studies on a pox disease of monkeys. I. Pathology. Am. J. Vet. Res. *21*, 377–380.

106. Sehgal, C.L., and Ray, S.N. (1982). Laboratory studies on monkeypox virus. J. Commun. Dis. *14*, 26–35.

107. Shchelukhina, E.M., and Marennikova, S.S. (1975). [Generalized monkeypox in orally infected rabbits and white mice]. Vopr. Virusol. 703–705.

108. Marennikova, S., Shelukhina, E.M., and Shenkman, L.S. (1998). Cotton rats (Sigmodon hispidus) as an experimental model of monkeypox infection. In Twelfth International Poxvirus Symposium (St. Thomas US Virgin Islands), pp. 6–10.

109. Schultz, D.A., Sagartz, J.E., Huso, D.L., and Buller, R.M.L. (2009). Experimental infection of an African dormouse (Graphiurus kelleni) with monkeypox virus. Virology *383*, 86–92. https://doi.org/10.1016/J.VIROL.2008.09.025.

110. Seang, S., Burrel, S., Todesco, E., Leducq, V., Monsel, G., Le Pluart, D., Cordevant, C., Pourcher, V., and Palich, R. (2022). Evidence of human-to-dog transmission of monkeypox virus. Lancet *400*, 658–659. https://doi.org/10.1016/S0140-6736(22)01487-8.